Mechanisms of interaction of electromagnetic radiation with biological tissues

Peyman, Azadeh

Mechanisms of Interaction of Electromagnetic Radiation with Biological Tissues

by

Azadeh Peyman

Submitted in accordance with the requirement for the degree of Doctor of Philosophy

King's College London
University of London
Department of Electronic Engineering

2002

Abstract

The purpose of the research presented in this thesis is to obtain an up to date account of the interaction mechanisms of electromagnetic radiation with biological tissues by studying their dielectric properties.

This work consists of three independent projects which all have one common goal and that is to investigate the dielectric behaviour of biological tissues and the interaction mechanisms.

The performance of the measurement system used throughout this project has been tested by several dielectric measurements on standard liquids with well known dielectric properties. The results were mathematically analysed and compared to those reported in literature.

The first project investigates the use of dielectric spectroscopy in compositional studies of biological materials. At microwave frequencies the dielectric properties of biological materials are closely related to the composition, particularly the water content and this may provide means to perform some compositional analysis. This approach however, is not sufficiently rigorous for the study of complex biological systems such as foodstuffs where the dielectric data may be influenced by more than one component. Therefore, a multivariate analysis approach is proposed to determine the dependence of the dielectric data on the analytical composition of processed meat samples.

The second project investigates the changes in the dielectric properties of rat tissue as a function of age at microwave frequencies. The extent of the variation of dielectric properties with age is particularly relevant to the rigorous assessment of exposure of experimental animals throughout their lifetime. It gives an indication into the extent to which variations in dielectric properties need to be taken into consideration in the assessment of the exposure of children and adults. The purpose of this work is to provide data for use in the assessment of exposure of animals to electromagnetic radiation at microwave frequencies. It is also aimed to quantify the parameters of the γ dispersion and investigate their correlation with the water content of the tissue.

The third project investigates the changes in the dielectric properties of cellular membrane when electric pulses are applied to the tissue. The dielectric properties of freshly sacrificed animal tissues are measured before and after applying certain electric fields and the results are analysed and studied. In this project the low frequency side of the dielectric spectrum is studied as the main interest is focused on the β dispersion region which is associated with the polarisation of the cellular membrane.

Table of Contents

Acknowledgements

I would like to thank Dr. Camelia Gabriel from Microwave Consultant Ltd. for her constant scientific guidance and moral support throughout my studies. I thank her for all the technical and scientific help and never-ending support in difficult situations. Her company provided me with up to date training and interesting projects which I enjoyed working on very much. I am also grateful as her company partly supported this PhD work financially.

I would also like to thank Dr. Ali Rezazadeh my supervisor and mentor at King's College London for his support and helps throughout this work. I thank him for providing the necessary resources and equipment needed at different stages of the projects.

This work could never be completed without endless support and encouragement I received from my family. I am thankful to my husband Amir, for his help, support and patience during my studies. My parent's constant encouragement made the difficult days easier to cope. During the time this thesis was being written, my father was spending very difficult time in solitary cells of injustice prisons because of his beliefs and his passion for freedom and liberty. I would like to dedicate this thesis to his silent nights. It is also dedicated to my mother because of all the sacrifices she made in her life.

Finally, I would like to acknowledge the financial support from the Engineering and Physical Science Research Council (EPSRC) studentship award.

To mum & Dad

To Amir & Iman

To Faezeh, Ali & Mohammed

List of Publications

[1] Peyman A, Rezazadeh A A and Gabriel C, 2001, "Changes in the dielectric properties of rat tissue as a function of age at microwave frequencies". *Phys. Med. Biol.* 46 No 6, 1617-1629.

[2] Kent M, Peyman A, Gabriel C and Knight A, 2002, " Determination of added water in pork products using microwave dielectric spectroscopy", *Food Control*, Vol. 13, 143-149.

[3] Peyman A, Rezazadeh A A and Gabriel C, "Changes in the dielectric properties of ageing rat tissues", June 2000, BEMS 22nd annual meeting, Munich, Abstract book, 196-197.

[4] Peyman A, Chen X, Woods L, Kent M and Gabriel C, "Dielectric Spectroscopy for Compositional Analysis of Biological Material", Sept. 1999, 7th International Conference on Microwave and High Frequency Heating, Valencia, Spain.
This paper won the best paper prize of the conference.

[5] Gabriel C and Peyman A, "Assessment of the accuracy of dielectric properties measurements, an empirical approach", Eureka SARSYS project 2001, Final technical report.

[6] Gabriel C and Peyman A, "Dielectric properties of human skin in-vivo, a pilot study", Eureka SARSYS project 2001, Final technical report.

[7] Peyman A and Chen X, "The feasibility of using medical imaging modalities for in-vivo detecting of physiological effects of electromagnetic radiation in the human brain during the use of cellular phones", June 1999, IEE Seminar on electromagnetic assessment and antenna design relating to health implications of mobile phones, Savoy Place, London.

Chapter 1- Introduction

1-2 General Introduction

One of the main tools in studying the interaction mechanisms of electromagnetic radiation and biological systems is dielectric spectroscopy. Knowledge of the dielectric properties of tissues is of importance for several reasons. Molecular interactions of electromagnetic fields with matter including biological tissues can be deduced from dielectric data. In addition, dielectric properties provide an insight into the structure and function of molecules, cells and of biological systems such as tissues. Therefore, understanding the interaction mechanisms of electromagnetic fields with biological systems requires proper knowledge of dielectric properties.

On the applied level, information on the dielectric properties of various tissues is needed to determine the specific absorption rate (SAR) in models of animals and human. Also there is a need to study the effect of permittivity on predicted SAR values in biological tissues during the electromagnetic-field exposure [1].

In cancer therapy by RF- induced hyperthermia, the design of effective treatment methods is facilitated when the tissue's dielectric properties are known. Other areas where information on dielectric properties is important are thawing of frozen organs and detection of pathological conditions.

Moreover, the most recent interest in the dielectric properties of biological materials is because of an increasing awareness of the possible physiological effects elicited by the absorption by tissues of electromagnetic radiation specifically those emitted by mobile phones and their base stations [2-4]. People can be exposed to microwaves either from the cellular base stations or from the hand held mobile phones themselves. In the perspective of human health there are public concerns about adverse health effects resulting from these kinds of exposures. Because mobile phone handsets operate in close

proximity to the human body, one particularly important consideration involves the interaction of the radiated electromagnetic fields with the nearby biological tissue. Once a person uses his/her cellular phone a coupling between his/her head and the handset occurs which results in the absorption of the microwave energy emitted from the phone to the head. The coupling of the head and the cellular phone handset can cause some biological effects in the tissues that are in the path of electromagnetic radiation. It seems that the fast growing use of mobile phones will continue on a lifelong basis and this makes it necessary to study the possible health hazards to human body resulted from using them.

Despite large number of studies, details understanding of mechanisms of electromagnetic absorption of biological tissues from various sources are not fully understood and needs further investigation. The main purpose of this project is to study the dielectric properties of biological tissues to obtain an up to date account of the interaction mechanisms of electromagnetic radiation and biological tissues.

This chapter will give a brief background on the subject of dielectric spectroscopy and methods of research in this area. It also explains the structure of the thesis.

1-2 History and background

The study of the dielectric properties of biological materials has a long history. Many textbooks and references give an account of the history of the interest in the electrical properties of biological materials, which began about 100 years ago. Foster and Schwan, 1996 [5] gave a general history of developments in dielectric spectroscopy of biological materials before and after the two World Wars. According to these authors, before the World War I, scientists of the day had gained the following understandings. They recognised that tissue conducts electricity and that its resistance varies with frequency. They also knew that the mechanism for conduction is the movement of ions. The fact

that cellular structure and cell membranes determines the electrical properties of tissues had been recognised. Although not fully understood, the anisotropy of electrical properties of muscle and nerve tissues were addressed. Also, the concept of tissue 'polarisation' which reflects the capacitive properties of tissues as we know them today, was established in that era but its origins remained unknown.

After World War I, more frequency ranges and more variety of materials were included in the dielectric studies. The frequency dependence of the electrical properties of many biological tissues was demonstrated and different types of equivalent circuits proposed to describe this phenomenon. At this time, more attempts were made to understand the underlying mechanisms. Studies carried out on the dielectric properties of aqueous molecular solutions, cell suspensions and on some biological tissues and various cellular systems were successfully characterised.

All the measurements before World War II were performed at frequencies between a few kilohertz and 100 MHz. Because of the rapid developments of microwave technology during the Second World War, including transmission lines, waveguides and oscillators operating at frequencies of up to 10GHz, the frequency range of dielectric measurements was extended to lower and higher frequencies. In that period the relaxation mechanisms responsible for the electrical behaviour were analysed [6-9]. Also, the existence of dispersions at microwave and audio frequencies and below was discovered. As the experimental advances continued, the early theories for the dielectric properties of cell suspensions were further simplified and extended.

More major developments took place in the 1960's and 1970's due to the availability of automated measurement systems and data analysis procedures. By the late 1970s an increased interest in the electrical properties of tissues became evident. There were new reasons for these interests in addition to the ever-present interest for understanding of the basic biophysical interaction mechanisms. This new interest could be attributed to the concern about the health hazards of exposure to electromagnetic fields and to the new

applications of these fields in medicine, particularly in cancer therapy and stimulation of bone growth.

According to Gabriel, 2000 [10], since the 1970's, there have been two main reasons for progress in the dielectric spectroscopy of biological tissues. The first was because of developments in theoretical dosimetry, which have produced numerical procedures capable of estimating the internal electromagnetic field in a full-scale human model with high-resolution anatomical details. For this development, it was essential to obtain detailed and accurate knowledge of the dielectric properties of body tissues. The second reason for significant progress in this area of research was the emergence of swept frequency network analysers and their adaptation for dielectric investigation. The measurement procedures have been greatly simplified because of this and also rapid determination of permittivity and conductivity over a wide frequency range became possible.

Despite all the developments in the field of dielectric spectroscopy of biological materials, many opportunities still exist and problems remain to be solved. Some of the experimentally observed interactions of electromagnetic fields can not be explained on the basis of available knowledge and thus, the field of dielectric properties of biological systems and interaction mechanisms remains open to new theories and experimentation.

1-3 Methods of research

The studies of interaction of electromagnetic radiation with biological systems are carried out with different methods for different purposes. The most common goal of all research techniques is to provide information about the spatial distribution of absorbed energy in the human body resulting from exposure to electromagnetic fields. This is achieved through dosimetry studies, which in turn requires knowledge of the dielectric properties of the different tissues of interest.

Some of these studies are briefly explained as follows:

Human studies

In the *human* studies, human volunteers are subjected to electromagnetic radiation. All the biological and bioelectrical functions of the body can be monitored during the exposure. Possible changes in the normal functions of different organs can be monitored and studied.

The absorption of energy is the important fact of the interaction between the electromagnetic fields and the human body. The result of the distribution of absorbed energy in the body can be a temperature rise (thermal effect) or any other non-thermal changes. If the absorbed energy does not exceed a certain level, the body reacts to the temperature rise through its natural thermoregulatory mechanisms, otherwise it may cause adverse biological effects.

One way of studying the effects of electromagnetic radiation on the human body, is to calculate the amount of energy absorbed by it. This is achieved by calculating the so-called 'specific absorption rate' (SAR). SAR is the rate of energy absorbed per unit body mass expressed in watts per kilogram (W kg^{-1}).

$$SAR = \frac{1}{2}\frac{\sigma}{\rho}|E|^2 \qquad (1.1)$$

where σ and ρ are the conductivity and the density of the tissue at the site of the measurement respectively and $|E|$ is the local electric field. The SAR cannot be measured directly, and the dielectric properties of tissues and electric field values must be provided. Therefore, knowledge of the dielectric properties of different tissues is required in such studies.

In-Vivo (animal) studies

In the *in-vivo* studies the live animal is exposed to the EM radiation and different biological changes can be monitored. It is also possible to carry out dielectric measurements on live animals using appropriate anaesthetic procedures. In most animal investigations, rodents are being used (mainly rats and mice). This is because of the huge experience biologists have with these animals and in view of the wide range of biological tests that can be performed with rodents. This is also due to their moderate size that allows a large number of animals to be exposed at the same time.

In-Vitro (biological tissue) studies

In-vitro studies involve biological tissues outside of the living body. This could be a cell culture or any other tissues dissected from the animal body. These studies are important in the understanding of the interaction mechanisms between the microwave and the biological tissue. *In-vitro* studies play an important role in providing basic information about the electrical properties of tissues such as permittivity and conductivity. *In-vitro* studies require less preparation of animals and the measurement procedures are simpler. However, it is important to consider the possible difference in the dielectric properties of live and dead tissues. Physiological changes that are known to occur as a function of time after death affect mostly the dielectric data at low frequencies which is the site of the α dispersion [11]. Therefore it is important to choose the appropriate method when studying different frequency parts of dielectric spectrum.

All the experiments in this project have been carried out *in-vitro*.

1-4 Scope of the present work

The purpose of the research presented in this thesis is to obtain an up to date account of the interaction mechanisms of electromagnetic radiation with biological tissues by studying their dielectric properties.

The interest in the study of dielectric properties of biological systems in this project has three origins. The first is to use dielectric spectroscopy as an application tool in predicting the composition of biological materials. The second is to obtain necessary dielectric data for the assessment of health hazards associated with electromagnetic radiation emitted from mobile phones. The third aim is to study the effect of physiological and pathological changes of the tissue on its dielectric properties.

While the first two objectives have been obtained by studying the dielectric properties of biological systems at microwave frequencies (300kHz - 20GHz), the third one has been achieved by performing measurements on the lower frequency side of the dielectric spectrum (1kHz - 1MHz).

This work consists of three independent projects, each serving one of the three objectives mentioned above. Together, the projects pursue the same goal which is to obtain an up to date account of our knowledge about dielectric spectroscopy of biological tissues. The details of each project and the order in which this thesis is presented are mentioned in the following.

Chapter 2 gives an overview about the dielectric theory with special reference to biological tissues. Dielectric relaxation and different dispersions are explained. The effect of physiological and pathological changes in the dielectric spectrum of the tissues is discussed. Some experimental results are presented to match the theory where appropriate.

Finally different dielectric measurement techniques are mentioned and those used in this research are addressed in detail. Sources of errors in the measurement and the ways to overcome these are also presented in this chapter.

Chapter 3 contains the result of dielectric measurements on some standard liquids. Although the accuracy of the experimental techniques used throughout this project have been tested before by others [12], it felt essential for the purpose of this project to perform some tests in order to ensure that the uncertainties fall well within the acceptable level. This chapter explains that how, by performing dielectric measurement on standard liquids of well-known dielectric properties, one can assess the accuracy of the techniques used in this project. The obtained dielectric data for the standard liquids were then fitted to well-known mathematical models and the results compared to the literature data.

Chapter 4 contains description and the results of the first main project, which looks at dielectric spectroscopy as an application tool to predict the composition of biological material. In this study foodstuff is used as biological samples. The main goal of the project was to find the extent in which the amount of added water to the foodstuff can be predicted by using a relatively easier and non-destructive method rather than using chemical analysis methods. The idea comes from the fact that at microwave frequencies the dielectric properties of biological materials are closely related to the composition, particularly the water content. Above 1GHz, the spectral dielectric parameters correlate with water content and provide a means to perform some compositional analysis. However, this approach is not sufficiently rigorous for the study of complex biological systems such as foodstuffs where the dielectric data may be influenced by more than one component. In this work, a multivariate analysis approach is proposed to determine the dependence of the dielectric data on the analytical composition of processed meat samples. This project was funded by the Ministry of Agriculture, Fisheries and Food (MAFF).

This chapter starts with an introduction to the subject and overview of the problem. It then explains some statistical tools used throughout the project. The method and materials used in the project are explained and the results are presented afterward.

The results of research explained in this chapter have been presented in the 7th International Conference on Microwave and High Frequency Heating, Sept. 1999,

Valencia, Spain and won the best paper prize of the conference. The work has also been published in the journal of food control, 2001, Vol. 13, pp143-149.

The interest behind the second project presented in chapter 5, comes from the fact that widespread use of mobile phones has caused a substantial public concern about a possible connection between the RF energy emitted by the phone and adverse effects to the human body. There are also concerns that children might be more vulnerable to any adverse effects of RF radiation than adults [13]. This is due to the fact that clear differences between the dielectric parameters of biological tissue in children and adults could lead to significant differences in their absorption of electromagnetic energy. In this chapter the dielectric properties of rat tissues have been measured as a function of age to serve two purposes. First, to provide data for use in the assessment of exposure of animals to electromagnetic radiation at microwave frequencies and second, to quantify the parameters of the γ dispersion and investigate their correlation with the water content of the tissue. Chapter 5 starts with the introduction to the problem and continues with the methods and techniques used throughout the project. The experimental results and observations are explained and a mathematical model is used to fit the measured data and the results are discussed.
This work has been presented at Bioelectromagnetics society (BEMS) 22nd annual meeting, in Munich in June 2000. The more complete results and discussions have been published at Physics in Medicine and Biology, Volume 46, Issue 6, June 2001,pp 1617 - 1629.

Chapter 6 contains the last main project, which looks at the effect of electric pulses on the dielectric properties of cellular membrane. This project unlike the other two deals with the lower frequency side of the dielectric spectrum. The main interest behind this project originates from the need to study the phenomenon of electroporation, which has a great deal of medical and research application such as electrochemotherapy. Electroporation is about applying certain electric pulses to tissues that can increase the permeability of the cellular membrane. However, it is important to study the dielectric

properties of the tissues before and after applying the electric pulses and to monitor the changes that happen in between. Physiological and pathological changes occurring in the tissue as a result of applied electric pulse will change the dielectric behaviour of the tissue at lower frequency region (the site of β dispersion area) of the spectrum. This can be used as an indication of whether the tissue has been damaged or not. This work was part of a multidisciplinary European project, which aimed to build a medical device called Cliniporator in order to deliver anti cancer drugs to tumour cells by increasing the permeability of the cellular membrane. Chapter 6 starts with a brief introduction to the problem and some general definitions of the electroporation phenomenon. The effects of applying electric fields to the dielectric properties of the cellular membrane are discussed next. The material, methods and devices used in the project are explained and finally the experimental results are presented and discussed.

Finally, chapter 7 includes the general conclusion of the thesis. It also contains some suggestions for possible future work in areas studied in this thesis.

References for chapter 1

[1] Mason P A, Hurt W D, Walters T J, Andrea A D, Gajsek P, Ryan K L, Nelson D A, Smith K I and Ziriax J M, 2000, "Effects of frequency, permittivity, and voxel size on predicted specific absorption rate values in biological tissue during electromagnetic – field exposure", *IEEE Trans. Microwave Theory and Techniques,* **48** 2050-2058.

[2] Michaelson S M and Lin J C, 1988, 'Biological effects and health implications of radiofrequency radiation', Plenum Press.

[3] Kuster N, Balzano Q and Lin J C, 1997 'Mobile Communications Safety', Chapman & Hall.

[4] Gandhi O P, 1990 '*Biological effects and medical applications of electromagnetic energy*', Editted by: Gandhi O P, Prentice Hall Publication.

[5] Foster K R and Schwan H P,1996, '*Dielectric properties of tissues*',CRC handbook of biological effects of electromagnetic fields, eddited by: Polk C and Postow E, CRC Press.

[6] Stoy R D, Foster K R and Schwan H P, 1982, Dielectric properties of mamalian tissues from 0.1 to 100 MHz: a summary of recent data, *Phys.Med.Biol.* **27** 501-513.

[7] Stuchly M A and Stuchly S S,1990 'Biological effects and medical applications of electromagnetic energy', Editted by: Gandhi O P, Prentice Hall Publication.

[8] Schwan H P 1957, 'Electrical properties of tissues and cell suspensions', *Adv. Biol. Med.Phys.* **5** 147-209.

[9] Pauly H and Schwan H P, 1966, ' Dielectric properties and ion mobility in erythrocytes', *Biophys. J.* **6** 621-639.

[10] Gabriel C, 2000,"Radio Frequency Radiation Dosimetry and Its Relationship To The Biological Effects of Electromagnetic Fields", Edited by B J Klauenberg and D Miklavcic, Nato Science Series, 73-84 Kluwer Academic Publishers. Printed in the Netherlands.

[11] Kraszewski A, Stuchly S S, Stuchly M A and Smith A M, 1982, In Vivo and In Vitro Dielectric Properties of Animal Tissues at Radio Frequencies *Bioelectromagnetics* **3** 421-32.

[12] Gabriel C, Chan T Y A and Grant E H 1994, "Admittance models for open ended coaxial probes and their place in dielectric spectroscopy", *Phys.Med.Biol.* **39** 2183-2200.

[13] Sir William Stewart (Chairman) Mobile Phones and Health. A report from the Independent Expert Group on Mobile Phones, Chilton, IEGMP Secretariat (May 2000), http://www.iegmp.org.uk/IEGMPtxt.htm

Chapter 2- Dielectric properties of biological tissues

2-1 Introduction

The dielectric properties of biological tissues have been widely studied, reviewed and reported [1-15]. Some studies reviewed the basic concepts of dielectric phenomena in biological material and their interpretation in terms of interaction at the cellular level [1-3]. Others attempted to provide an overview of theoretical explanation of the dielectric properties in terms of underlying molecular processes [4-5]. Also, extensive literature reviews of dielectric properties of biological tissues in different frequency ranges, have been provided, summerised and tabulated [6-8].

This chapter uses the wide range of literature data available, to examine the dielectric properties of biological materials and the extent to which the current knowledge contributes to understanding the mechanisms of interaction. Some of the aspects of the subject will be discussed, including the dielectric relaxation and dispersions and the techniques used in the measurements of dielectric properties of biological materials.

This chapter will start with an overview of dielectric theory, in order to introduce the terminology and to provide a basis for explaining the experimental data. Descriptions of mathematical models and graphical representations are also contained. The techniques that are used for dielectric measurements on biological tissues are also discussed in this chapter, with special reference to those employed here. It is worth to mention that since the biological materials are nearly nonmagnetic, therefore this chapter only deals with the interaction of electric field and the material.

2-2 Dielectric Theory

2-2-1 Definitions

Applying an external electric field to matters can displace charged carriers inside atoms and molecules. This is called **polarisation,** which is the most important effect arising from the interaction of an electric field with a dielectric material, and will be discussed in detail in the next section. Electronic and atomic displacements are the most fundamental effects happening under the influence of the external electric field. Also, dipole molecules exhibit their own specific **polarisation** (i.e. dipole orientation). Another effect of applying an external field to a matter is **charge drift** under the action of the field. This will give rise to charge conduction and the establishment of ionic currents.

Biological materials contain both free and bound charges including ions and polar molecules. Therefore, an external electric field can have two effects on the biological material: to trigger several polarisation mechanisms, each governed by its own time constants and also to cause ionic drift. The overall result is the establishment of both **displacement** and **conduction** currents. This is why biological materials are classified as lossy dielectric materials.

Experimentally, the interaction of the electromagnetic field with the matter is characterised by the dielectric response of the material. An electric field can be presented by the electric field strength (E) and by the electric displacement or electric flux density (D). The magnetic field can also be presented by the magnetic field intensity (H) and the magnetic flux density (B). These field quantities along with the source term of current density (j) are related by Maxwell Equations [10]. Therefore, the dielectric response of a material originates from the classical Maxwell's equations in which the electric and magnetic fields are related to each other as followings:

$$\nabla \times E = -\frac{\partial B}{\partial t} \tag{2.1}$$

and

$$\nabla \times H = j + \frac{\partial D}{\partial t} \tag{2.2}$$

in which :

$$D = \varepsilon E \tag{2.3}$$

$$j = \sigma E \tag{2.4}$$

and

$$B = \mu H \tag{2.5}$$

where ε, σ and μ are the permittivity, conductivity and permeability of the matter respectively. From Equation (2.3), the dielectric response of the matter to the electric field can be obtained by measuring its permittivity, which is the ratio of the electric flux density to the electric field:

$$\varepsilon = \frac{D}{E} \tag{2.6}$$

It is custom to use relative permittivity, which is the permittivity normalised to that of free space (vacuum):

$$\varepsilon_r = \frac{\varepsilon}{\varepsilon_0} \tag{2.7}$$

where ε_0 is the permittivity of the free space, $\varepsilon_0 \approx 8.85 \times 10^{-12}$ F/m.

Depending on the direction of the response and the phase difference between D and E, permittivity can be a real or a complex number. In a static electric field, the permittivity of homogeneous isotropic substance is a real number and is a measure of the response of the material to an electrical stimulation. In time varying fields, there may be a phase lag between the applied field and the resulting effect when the time scale of the mechanism is of the same order of magnitude or longer than the period of the applied field. In such cases, the permittivity is mathematically expressed as a complex number. Assuming a linear, isotropic behaviour, the relative permittivity of biological materials is expressed as:

$$\hat{\varepsilon} = \varepsilon' - j\varepsilon'' \tag{2.8}$$

where $j^2 = -1$. The real part ε' is called the dielectric constant and determines the component of the displacement current. It is a measure of the ability of the material to store electric energy. The imaginary part, is called loss factor and relates to the out of phase or power loss component. Loss factor represents the amount of electric field energy dissipated in the material in the form of heat.

The loss factor is also related to the conductivity of the material σ in the following way:

$$\varepsilon'' = \frac{\sigma}{\varepsilon_0 \omega} \tag{2.9}$$

where $\omega=2\pi f$, f is the frequency and the unit of conductivity is Siemens per meter (S/m).

As mentioned before, two types of current are established as the result of applying an electric field to a biological material: displacement and ionic currents. Therefore, the total conductivity of a biological material is the sum of the displacement and ionic currents.

Throughout this thesis, loss factor and conductivity always refer to the total values since, in practice, these are the parameters that determine the effect of the field on the material and these are the parameters measured.

2-2-2 Polarisation mechanisms

All dielectric phenomena can be attributed directly to the polarisation of a material under the influence of an externally applied electric field [12]. In other words the most important effect arising from the interaction of an electric field with a dielectric material is polarisation. Polarisation happens when charge carriers inside atoms and molecules of a material are displaced in response to an external electric field. There are different

polarisation mechanisms that can be responsible for the dielectric behaviour of a material. Four types of polarisation mechanisms that generally happen inside a material in the presence of an electric field are described here (Figure 2.1).

(a) **Electronic polarisation** is produced if applying an external electric field results in a slight displacement of electrons with respect to the nuclei (Fig 2.1a).

(b) **Atomic polarisation** is produced in a material, if applying an external electric field result in displacement of charged atoms or groups of atoms with respect to one another. This happens because atoms in molecules do not normally share their electrons symmetrically, since the electrons are displaced toward the stronger binding atoms. Therefore atoms acquire charges of opposite polarity and an external field acting on these charges tends to change the equilibrium positions of the atoms (Fig 2.1b).

(c) **Orientation (dipolar) polarisation** is produced when polar molecules tend to orient themselves in the direction of the applied electric field. Polar molecules are of permanent dipole moments that exist also in the absence of the external field. They are produced by the asymmetrical distribution of charges between the unlike components of a molecule. When no field is applied dipoles have no preferred orientation. Under the influence of an external electric field the dipolar molecules tend to orient with the field, and cause the polarisation of the material (Fig 2.1c).

Charges that are locally bound in atoms, molecules or structures of solids and liquids are responsible for the above three polarisation mechanisms. In addition, the matter may contain free-charge carriers (ions) that can migrate in the material.

(d) **Space charge polarisation** is produced because of the non-uniform space charge

distribution in a material. This is due to either the ions become trapped in the material or on interfaces or because they cannot freely discharged or replaced at the electrodes (Fig 2.1d).

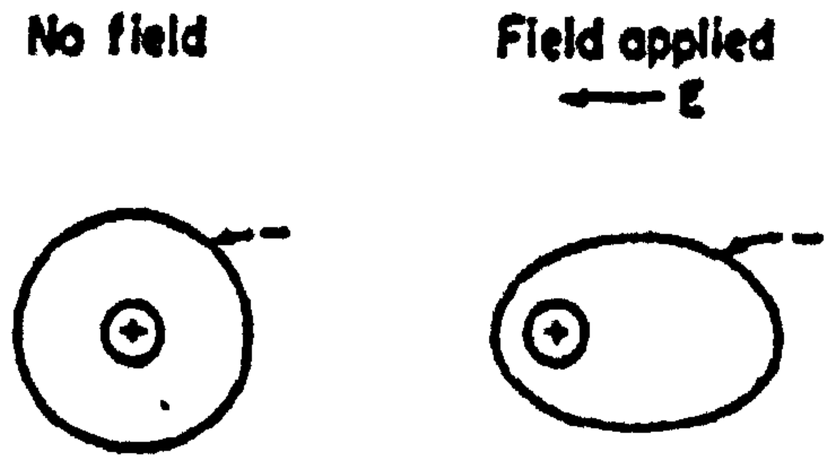

Figure 2.1a: Electronic Polarisation

Figure 2.1b: Atomic Polarisation

Figure 2.1c: Orientation Polarisation

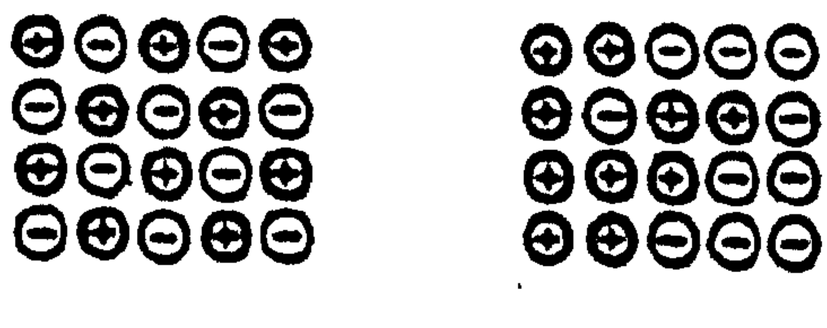

Figure 2.1d: Space-charge Polarisation

Figure 2.1 Polarisation mechanisms (copied from [13])

When a step field is applied to a dielectric material the electronic and atomic polarisations are established almost instantaneously (time scale <picosecond). In the case of polar materials the dipolar orientation (time scale of Pico to nano-seconds depending on the molecular size) follows more gradually until the total polarisation reaches a steady value [12]. When the electric field is removed, the reverse process happens. First the electronic and atomic polarisations subside, and this is followed by a relatively slow decay in dipolar polarisation. The time constant associated with the build up and decay of dipolar orientation is characteristic of the size and shape of dipolar molecules.

It is notable that for biological materials two polarisation mechanisms are of particular importance: the dipolar polarisation from the existence of water molecules and the space charge polarisation from existence of membranes and ions [14].

Any of the polarisation mechanisms explained above result in a relaxation-type behaviour, which leads to changes in the permittivity of the material.

2-2-3 Dielectric relaxation mechanisms

General relaxation theory

The dielectric polarisation arises from physical displacement of charges and requires time to develop. Also the orientation of the polar molecules under the influence of an external electric field does not occur instantaneously. Therefore one can say that the response of a material to an electric field is a more or less relaxation process that depends on the kinetics of the charge displacement.

In the simplest case, the polarisation of a sample will relax towards the steady state as a first order process characterised by a relaxation time τ [15]:

$$D = D_\infty + (D_0 - D_\infty)(1 - e^{-t/\tau}) \qquad (2.10a)$$

In this equation, D_∞ is the instantaneous response that might arise in a real system from electronic polarisation, while D_0 is the response long after the application of the field. The time constant τ, depends on the physical process involved: it can range from picoseconds to microseconds for partial orientation of molecular dipoles, and to seconds for other relaxation processes. Equation (2.10a) can be written as following using Equation (2.3):

$$\frac{D}{E} = \varepsilon_\infty + (\varepsilon_S - \varepsilon_\infty)(1 - e^{-t/\tau}) \qquad (2.10b)$$

One can obtain the dielectric response of this system in the frequency domain to a sinusoidal field ($E = E_0 e^{j\omega t}$) by taking the Laplace transformation of the Equation (2.10a) which yields the Debye equation [15]:

$$\varepsilon = \varepsilon_\infty + \frac{\varepsilon_S - \varepsilon_\infty}{1 + j\omega\tau} \qquad (2.10c)$$

where ε_∞ and ε_S are the permittivities at frequencies much higher ($\omega\tau >> 1$) and much lower ($\omega\tau << 1$) than relaxation frequency ($f_C = \frac{1}{2\pi\tau}$), respectively. ε_∞ arises from the electronic polarisability (would be measured at infinite frequency) and ε_S is also called the static permittivity of the material.

However, Equation (2.10b) does not include the possible existence of currents at infinite time, such as would arise from movement of ions in a constant field. One can expand the model by including a static conductivity σ_S, which will lead to the following:

$$\varepsilon = \varepsilon_\infty + \frac{\varepsilon_S - \varepsilon_\infty}{1 + j\omega\tau} + \frac{\sigma_S}{j\omega\varepsilon_0} \tag{2.10d}$$

Equation (2.10d) can be separated into two terms: real and imaginary terms as follows:

$$\varepsilon^* = \varepsilon' - j\varepsilon'' \tag{2.11a}$$

$$\varepsilon' = \varepsilon_\infty + \frac{\varepsilon_S - \varepsilon_\infty}{1 + (\omega\tau)^2} \tag{2.11b}$$

$$\varepsilon'' = \frac{\sigma_S}{\omega\varepsilon_0} + \frac{(\varepsilon_S - \varepsilon_\infty)\omega\tau}{1 + (\omega\tau)^2} \tag{2.11c}$$

and using Equation 2.9:

$$\sigma = \sigma_S + \frac{(\sigma_\infty - \sigma_S)(\omega\tau)^2}{1 + (\omega\tau)^2} \tag{2.11d}$$

in which the limit values ε_∞, ε_S, σ_∞ and σ_S are interrelated by:

$$\frac{(\varepsilon_S - \varepsilon_\infty)\varepsilon_0}{\tau} = \sigma_\infty - \sigma_S \tag{2.12}$$

σ_∞ and σ_S are conductivity values far above and below the relaxation frequency respectively.

Thus, the permittivity and conductivity can not vary independently, and the frequency dependence of ε' will determine the frequency dependence of σ and conversely.

Similar to the time dependence of electric displacement (electric flux density D), one might as well look at the time dependence of the current density

$$J = J_\infty + (J_S - J_\infty)(1 - e^{-t/\tau}) \tag{2.13a}$$

and using Equation (2.4):

$$\frac{J}{E} = \sigma_\infty + (\sigma_S - \sigma_\infty)(1 - e^{-t/\tau}) \tag{2.13b}$$

This transforms to the admittance equivalent of Equation (2.10c):

$$\sigma^* = \sigma_\infty + \frac{(\sigma_S - \sigma_\infty)}{1 + j\omega\tau} \tag{2.13c}$$

The Debye equation 2.10c describes a single relaxation process in which the relaxation frequency is the frequency at which the permittivity is halfway between its low and high frequency values. Alternatively, the relaxation frequency could be taken as that at which the conductivity is halfway between its two limiting values. For the single time constant relaxation considered here, these two frequencies are the same; they are different if there is a distribution of relaxation times [15].

Figure 2.2 shows the measured variation in the dielectric properties of methanol at 20°C with a single time constant relaxation, which is described by the Debye equation. It can be seen that the permittivity falls from a high value ε_S to ε_∞ as the frequency increases. Meanwhile, the conductivity rises from a small value σ_S to σ_∞. The loss factor peaks at $\omega\tau = 1$ and falls off for both higher and lower frequencies.

Dielectric relaxation behaviour can also be plotted on the complex plane. A plot of ε'' versus ε' will produce a semicircle for single time constant relaxation. The centre of the semicircle is on the real axis at the point $\frac{\varepsilon_S + \varepsilon_\infty}{2}$ and its apex occurs at $\omega = 2\pi f_c$.

Figure 2.3 shows the dielectric properties of Methanol at 20°C in a complex plane.

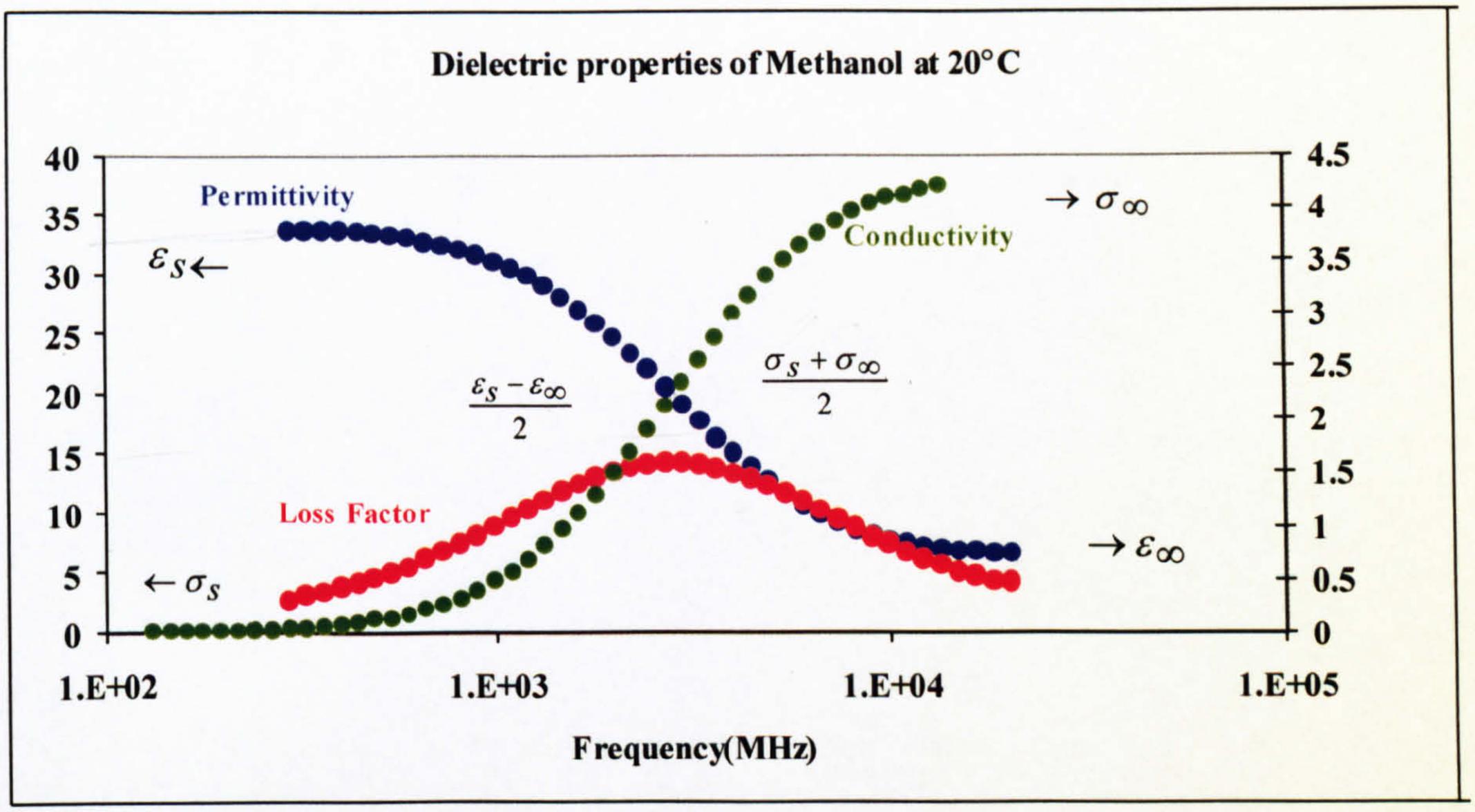

Figure 2.2 The dielectric relaxation behaviour of methanol with a single relaxation
[Data from lab. Measurements by the author.]

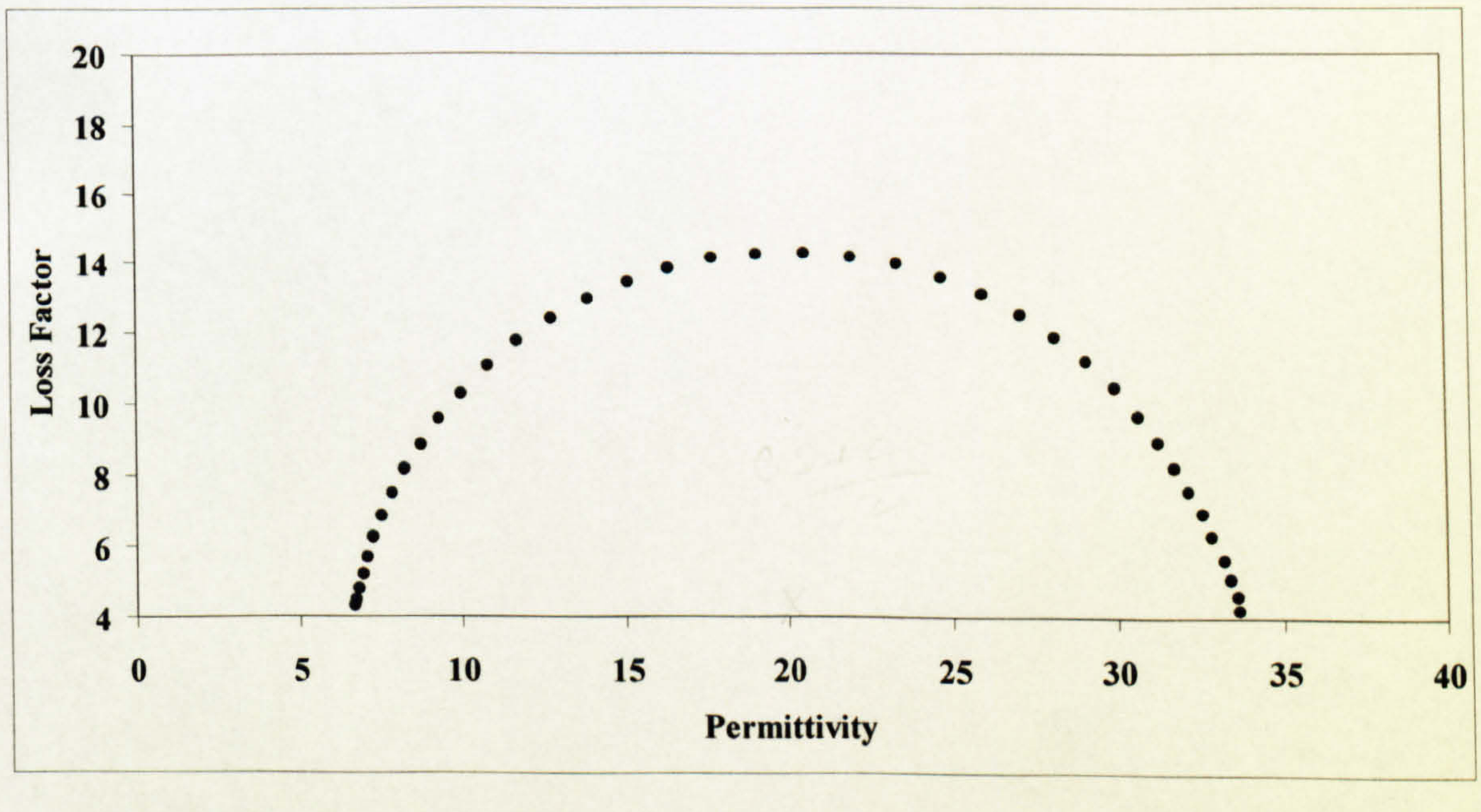

Figure 2.3 Dielectric relaxation behaviour of Methanol at 20°C plotted on the complex plane

Distribution of relaxation times

Not all materials have single relaxation behaviour. Many substances show a broad distribution of relaxation times. For some materials (such as water, methanol...), the dielectric properties are very closely fitted by the simple Debye equation while for others (such as tissues) the departure is very great.

There can be many reasons that the behaviour of a substance may depart from single time constant relaxation. One can be the fact that multiple relaxation processes might occur in parallel, each with a different relaxation time. It is also possible that relaxation processes occur that have kinetics which are not first order. In its simplest case, the dielectric response arises from the presence of independent first order processes. In this case, the dielectric response to a step change electric field can be described as following [15]:

$$D = D_\infty + D_1(1 - e^{-t/\tau_1}) + D_2(1 - e^{-t/\tau_2}) + \ldots \tag{2.14}$$

or

$$\varepsilon^* = \varepsilon_\infty + \frac{\Delta\varepsilon_1}{1 + j\omega\tau_1} + \frac{\Delta\varepsilon_2}{1 + j\omega\tau_2} + \ldots \tag{2.15}$$

where $\Delta\varepsilon = \varepsilon_s - \varepsilon_\infty$.

The broadening of the dispersion could be accounted for by introducing a distribution parameter, thus giving an alternative to the Debye equation known as the Cole-Cole equation [8c]:

$$\hat{\varepsilon} = \varepsilon_\infty + \frac{\Delta\varepsilon}{1 + (j\omega\tau)^{(1-\alpha)}} \tag{2.16}$$

where the distribution parameter, $0 \leq \alpha \leq 1$, is an adjustable parameter, which indicates the relaxation time distribution.

2-2-4 Dielectric dispersions

The electrical properties of biological materials have been shown to display a characteristic dependence on frequency [1-16]. Polarisation is a time dependent phenomenon due to the various physical interactions. The response of the material to these interactions is also time dependent. This is why permittivity exhibits a frequency dependent behaviour.

Typically soft tissues exhibit a continuous decrease in permittivity with frequency increase. This is associated together with an increase in conductivity. Due to different interaction mechanisms, each governed by its own kinetics, a significant change in dielectric properties over a frequency range, can happen which by convention, is called dielectric dispersion [17]. For biological tissues three main spectral regions known as α, β and γ-dispersions are predicted from known interaction mechanisms and have been experimentally identified in the frequency range of hertz to gigahertz [1-17].

The α-dispersion usually occurs below a few kHz, the β-dispersion in the frequency region from tens of kHz to tens of MHz, and the γ-dispersion in the microwave frequency region (Figure 2.4).

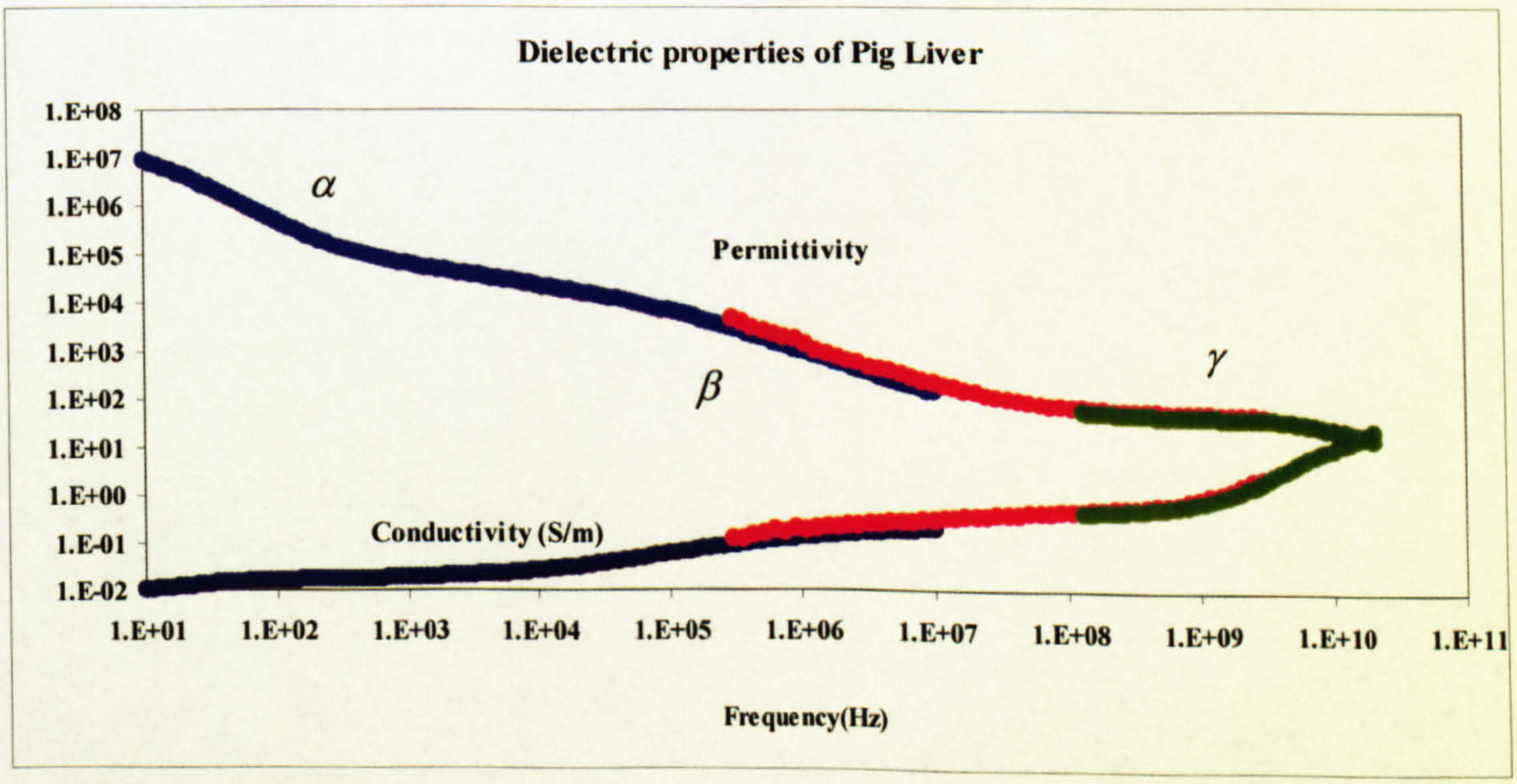

Figure 2.4 Measured dielectric properties of pig liver at 20°C, presenting the different dispersion areas (Data from lab measurements by the author)

The α-dispersion is generally considered to be associated with the properties of the cell membranes and their interactions with the intra and extra cellular media [1-8]
The α-dispersion is characterised by the very large permittivity values that are produced by ionic diffusion processes at the site of the cellular membrane at very low frequencies. In other words, the low-frequency behaviour of the biological tissues can be characterised by their non-homogeneous structure and the ionic activities inside the tissues. The precise mechanism responsible for the α dispersion is the least well understood of the three main dispersions. It is believed that the α-dispersion is due to the relaxation of counterions surrounding the charged cell membrane [2,9].

The β-dispersion occurs at radio frequencies and is mainly due to the polarisation of cellular membranes [2,4,8,9,15]. The membrane structure blocks ion movement under an external electric field, preventing the flow of ions between the intra and extra cellular media. It is also believed that a smaller contribution to the β-dispersion is from the dipolar relaxation of proteins and other organic macromolecules in the tissue [8,15].
β-dispersion can be largely affected by water content [17]. Tissues with less water content have more air gaps or dry components, which will also block ion passage in the same way as the membranes, thus reducing the strength of the β-dispersion significantly.

The γ-dispersion is due to the polarisation and relaxation of the water molecules [2,4,8,9,15]. As the frequency increases to the gigahertz regions, the rotational properties of polar molecules in water become important and cause the γ-dispersion. Since water constitutes 80% of the volume of most soft tissues, the γ-dispersion is of importance in the study of dielectric properties of biological tissues.

In addition to the three major dispersions discussed above, there is a very small dispersion, called δ-dispersion, occurring between the β and γ-dispersion regions. It is believed that δ-dispersion is due to the relaxation of the water molecules bound to the surface of macromolecules, and rotation of amino acids as well as charged side groups of proteins [9,16]. There is no single, dominant relaxation process for this dispersion and

this lack of a single dominant mechanism makes the analysis of this dispersion region in tissues rather difficult.

2-2-5 Dielectric Model for Biological Tissues

As mentioned before, the dielectric spectrum of a biological tissue is characterised by three major relaxation regions of so called α, β and γ-dispersions, at low, medium and high frequencies respectively. Each of these relaxation regions exhibits a polarisation mechanism which is characterised by a single time constant, τ (in a first order approximation). The complex relative permittivity in this situation is given by the Debye equation (2.12) in which the term $\varepsilon_S - \varepsilon_\infty$, describes the magnitude of the dispersion. However, dielectric data from biological systems commonly exhibit relaxation behaviour that is not of the simple Debye type. This may arise from the presence of several relaxation processes due to the complexity of both the structure and composition of biological material [8,15]. This causes a broadening in the dispersion region with a distribution of relaxation time-constants. A common approach to find the distribution of relaxation time-constants is to decompose the relaxation into a sum of single, time constant components (Equation 2.15) which might be identified with different physical processes [15].

This will lead to the Cole-Cole equation (2.16). However, it is suggested [8c] that a multiple Cole-Cole dispersion in addition to a conductivity term may be more appropriate in describing the spectrum of a tissue:

$$\hat{\varepsilon} = \varepsilon_\infty + \sum_n \frac{\Delta\varepsilon_n}{1+(j\omega\tau_n)^{(1-\alpha_n)}} + \frac{\sigma_i}{j\omega\varepsilon_0} \qquad (2.17)$$

where σ_i is the static ionic conductivity.

The above model can be used to describe the frequency dependence of the dielectric properties of biological tissues in the frequency range from Hz to GHz. However,

predictions of this model can be used with confidence for frequencies above 1 MHz, but caution must be taken in using this model for lower frequencies [8c] as there is not sufficient data to support their predictions in the very low frequency region.

2-2-6 Dielectric Properties of Water in Tissues

Since water constitutes a large volume of most biological tissues dielectric properties of tissues in several ways reflect the properties of water. Depending upon whether the water's structural properties are affected by the presence of biological macromolecules or not, its presence in a biological material can be divided into two categories.

Water molecules that are more than a few molecular lengths away from the macromolecule constitute the main bulk of the solution and are referred to as 'bulk' or 'free' water. On the other hand, if the properties of water are affected by the presence of biological molecules, the water is referred to as 'bound' water [9].

It is expected that free water has similar dielectric properties to those of pure water. At 20°C, the permittivity of pure water falls from a static value of about 80 to a little below 20 at 35GHz. The loss factor curve exhibits a peak at around 17 GHz. As the temperature of the water increases, the relaxation time of water decreases almost exponentially. At 37°C the relaxation frequency of normal bulk water is about 25GHz which corresponds to a relaxation time of about 6.36psec.

The bound water molecules are linked to their environment by stronger forces; therefore, relaxation time for bound water is longer compared to that of the pure water. Previous research [18] suggests that about 10% of the water in tissue is strongly bound and rotationally hindered, having relaxation frequencies some 50 to 200 times lower than that of normal bulk water. In the case of biological tissues that consist of both bulk and bound water the relaxation time is higher than that of pure water. For example, in the case of adult rat brain, skull and skin tissues the relaxation times are about 8.23 psec, 9.21psec and 8.22 psec respectively [19]. As the water content of the tissue decreases the

relaxation frequency becomes lower, and therefore higher relaxation times can be observed [19].

Because of the nature of it, bound water can not be subjected to a direct investigation of its dielectric behaviour. The study of the dielectric properties of bound water must be derived from a study of the appropriate biological material in which the water is bound. Furthermore, the quantity of bound water present in most biological tissues is small compared with the amount of 'free' or 'bulk' water. Therefore any changes in the permittivity of the bound water with frequency, temperature or any other physical parameter, takes place against the background of the bulk water [9].

Figure 2.4 shows a typical dielectric behaviour of pure water (de-ionised at 20°) in the frequency range of 0.1-20GHz. The data shown in Figure 2.4 is obtained by dielectric measurements using network analyser HP8720 and 2.98 mm coaxial probe. The network analyser was calibrated prior to the measurement by 0.005Molar NaCl as well as open and short circuits.

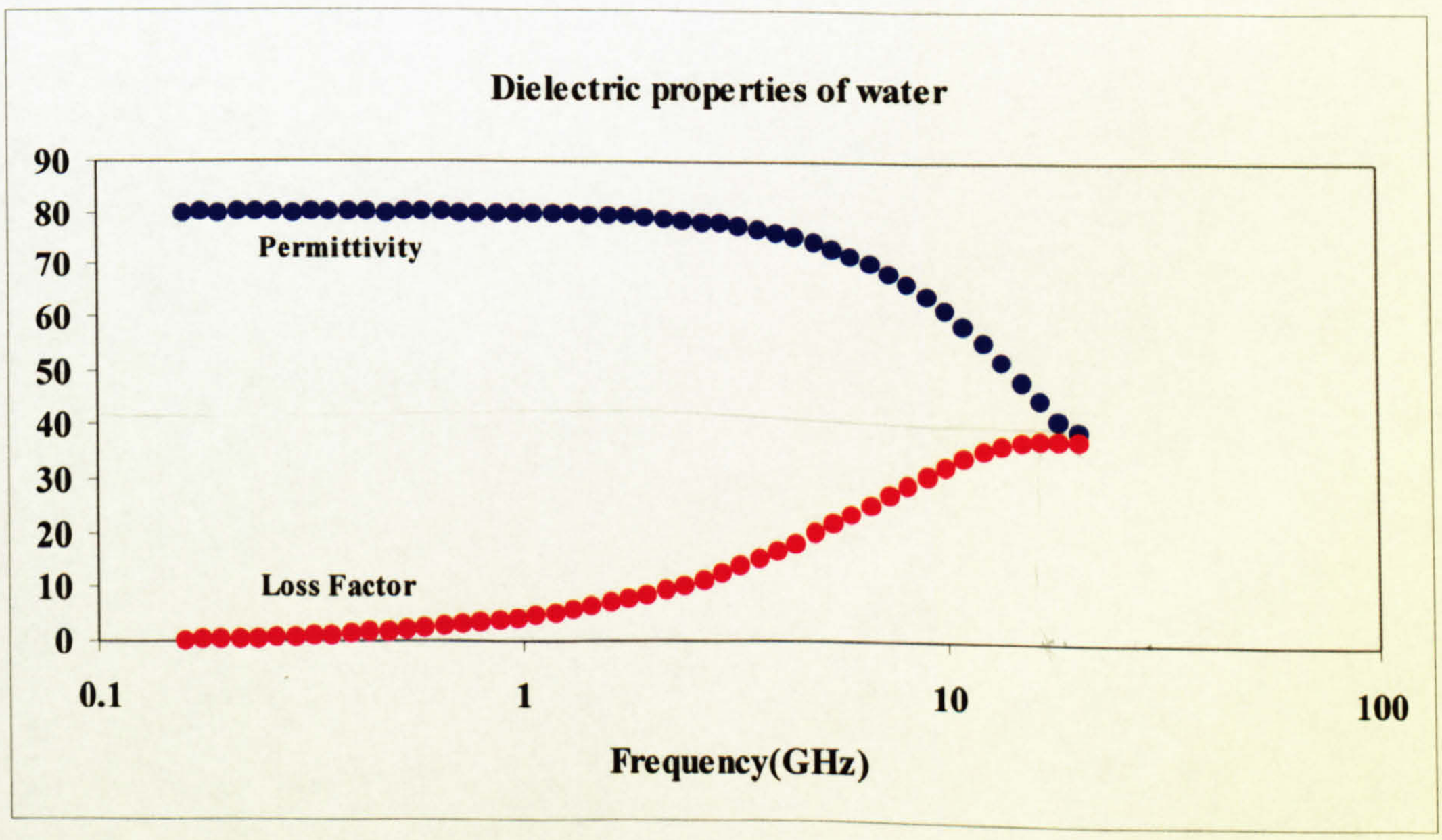

Figure 2.4 Measured dielectric properties of de-ionised water at 20°C
(Data from lab measurements by the author).

2-2-7 Temperature effect

Another factor to consider when one studies the dielectric behaviour of biological tissues, is the effect of temperature. The dielectric properties of tissues vary with temperature. Changes in the temperature of the tissues may cause reversible effects such as changes in the ionic conductivity or irreversible effects such as tissue damage [15]. Increasing the temperature will increase ionic conductivity, and also increase relaxation frequency.

2-2-8 Systematic change in the dielectric properties of biological tissues

It is known that metabolic activity or pathological conditions result in physiological changes in biological tissues. This in turn lead to changes in the dielectric properties of the tissue.

Depending upon the nature of the change, part or sometimes the whole dielectric spectrum may be affected. For example, changes that occur following death affect the ionic environment of cells. This suggests that there should be a difference in the dielectric spectrum below a few kHz between the in-vivo and in-vitro measurements because of the effect on the α dispersion. Such differences have been observed experimentally within hours of death [1 and20]. However similar physiological effects at the ionic level would not affect the dielectric spectrum at frequencies higher than 100MHz [21].

In the β dispersion area, the spectrum is highly affected by the physical and physiological state of cell membrane. It has been reported that the shape, size and capacitive impedance of the cellular membrane are the dominant factors [11]. Destruction of the cellular membrane causes a significant change in the β dispersion. An example of such effect is given in Figures, 2.5a and 2.5b which shows the permittivity and conductivity spectrum of banana before and after the destruction of the cellular

membrane by mashing the banana. From the results it can be seen that the effect of a damaged cellular membrane in the dielectric spectrum is a smaller β dispersion and a higher conductivity.

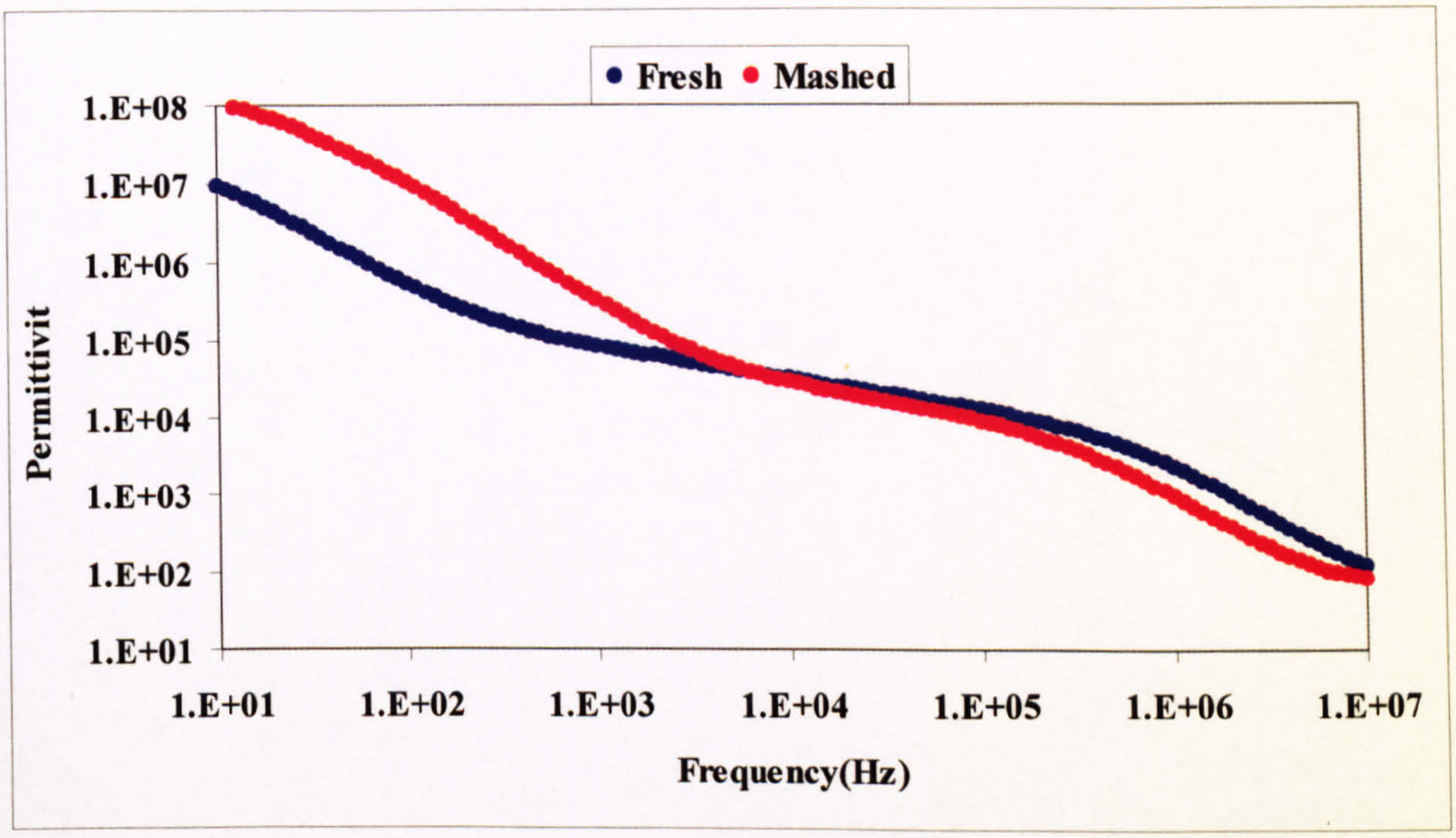

Figure 2.5a

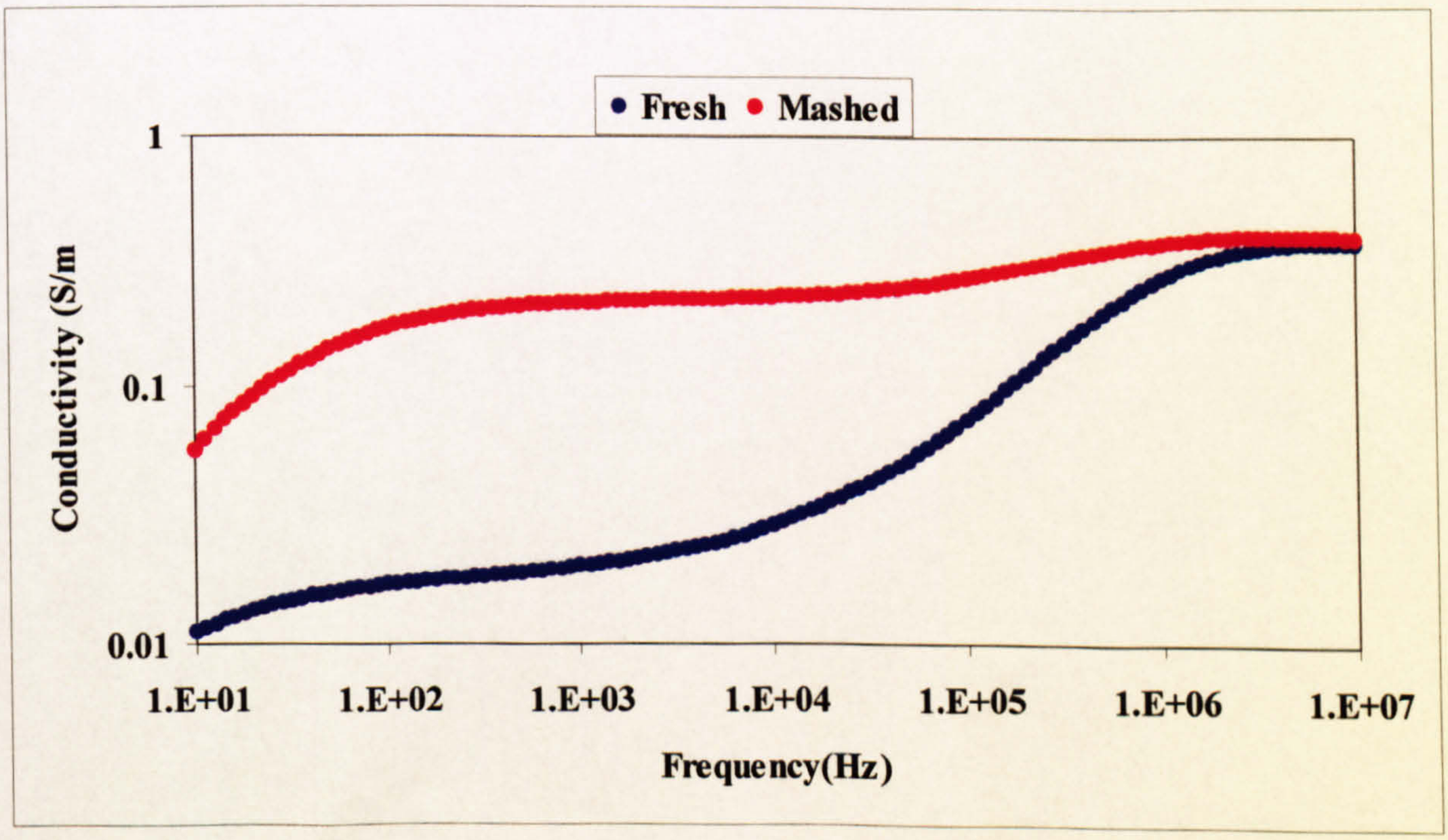

Figure 2.5b

Figure 2.5: Effect of damaging the cellular membrane (mashing) on **a** Permittivity and **b** conductivity of fresh banana. (Data from lab measurements by the author)

Another factor to consider is the anisotropic nature of some of the biological tissues such as muscle on the dielectric spectrum. This depends on the direction of the fibres with respect to the electric field as can be seen in Figures 2.6a and 2.6b in which the permittivity and conductivity of fresh banana have been measured in two different directions, cross and parallel to the electric field. It can be seen that in the case of fibres being parallel to the electric field, the conductivity of banana is higher than that of the fibres being cross to the electric field. This is due to the amount of polarisation occurring in the cellular membrane and the strength of the β dispersion at each case. The more polarisation occurs when the direction of the fibres are cross to that of the electric field, therefore causing stronger β dispersion and lower conductivity compared to the parallel case.

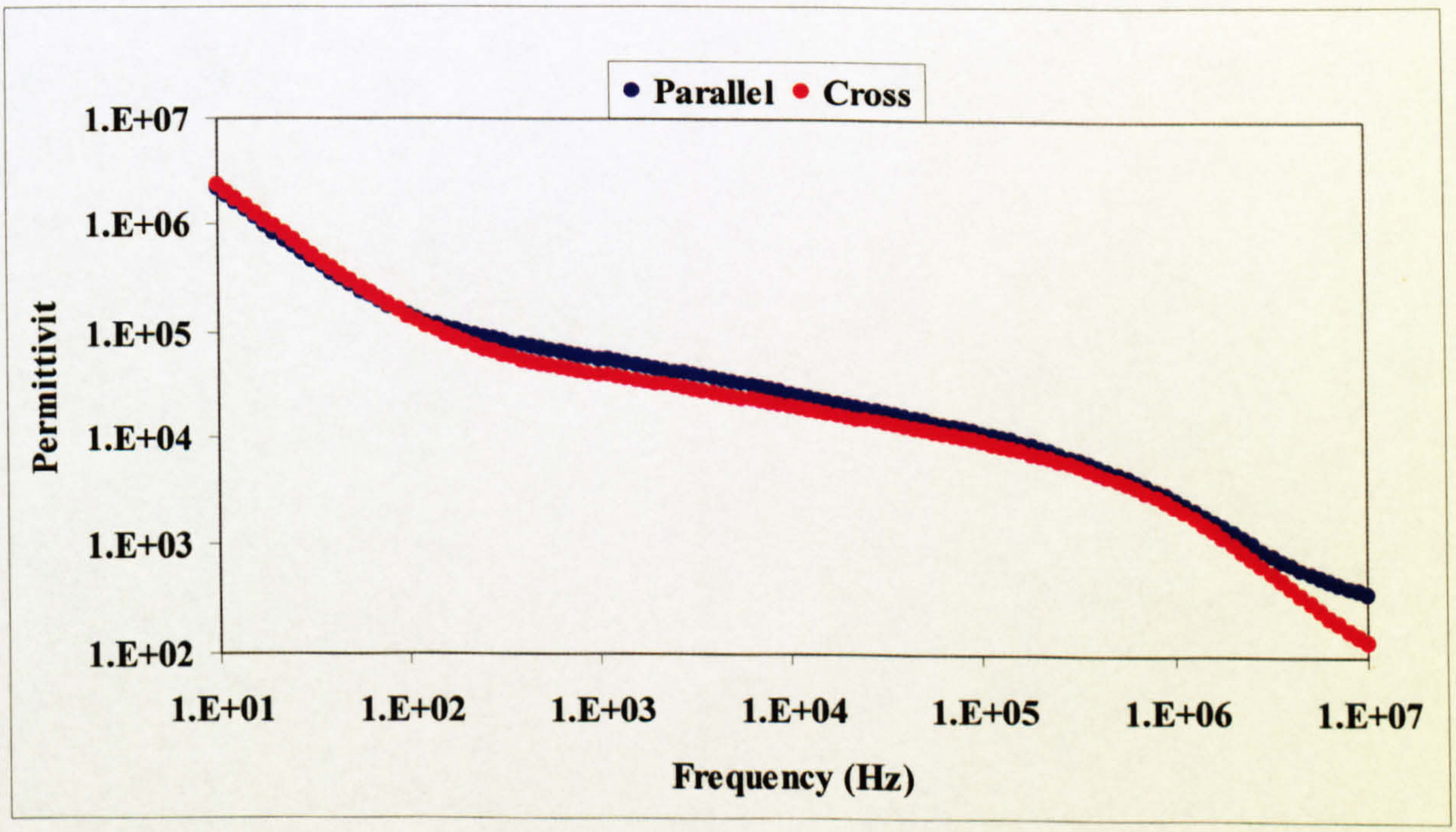

Figure 2.6a

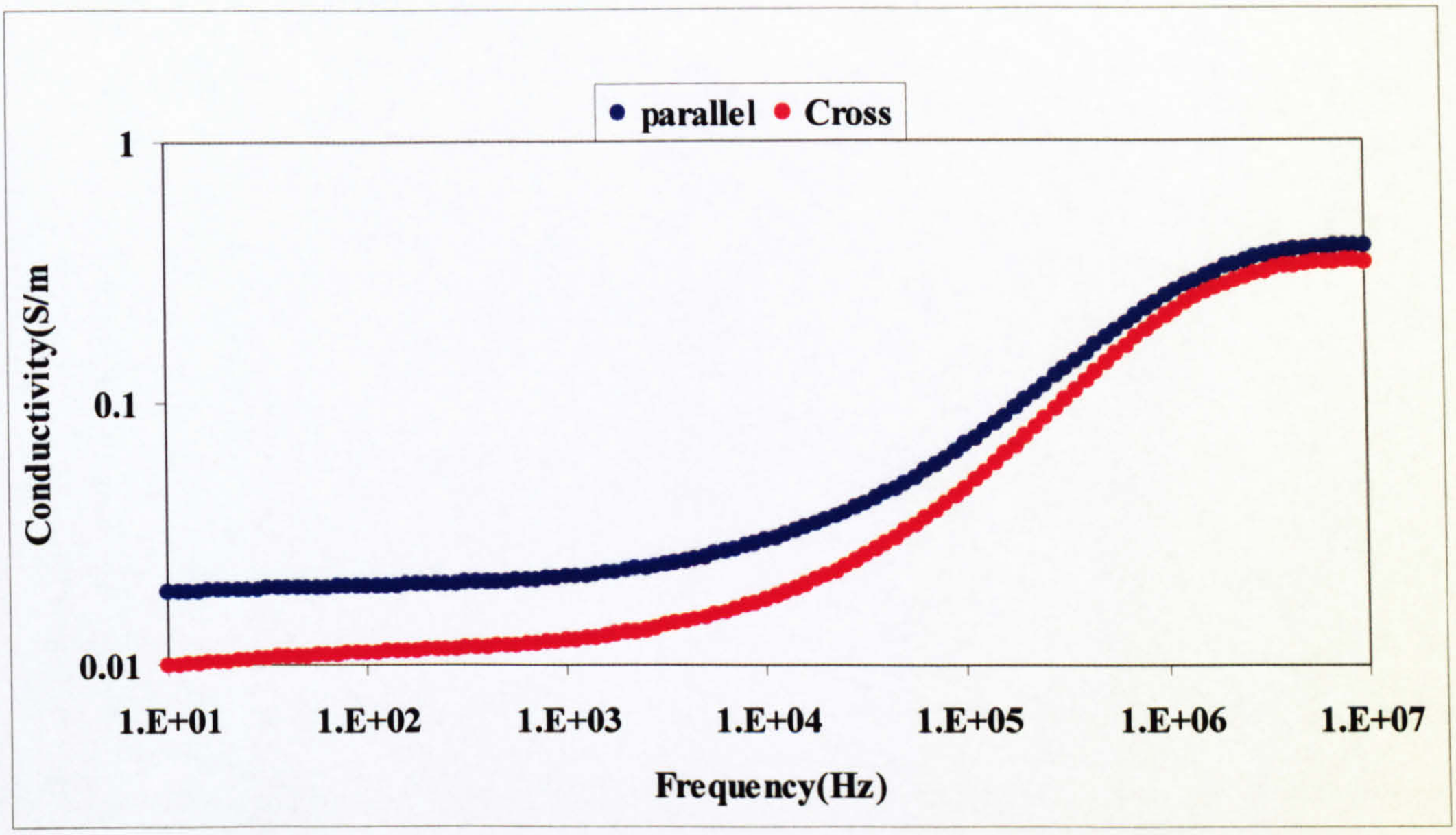

Figure 2.6b

Figure 2.6: Difference in **a** Permittivity **b** conductivity of fresh banana when measured in the directions of parallel and cross to the electric field (data from lab measurements by the author).

Finally, the high frequency end of the dielectric spectrum consists of the γ dispersion, which is due to the polarisation of water molecules. The amplitude of the γ dispersion correlates with the water content of the tissue. The more water the tissue consists of, the larger the amplitude of the γ dispersion will be [19].

2-3 Measurement techniques

2-3-1 Introduction

There are various techniques for measuring the dielectric properties of materials. The difference in techniques arises from the requirement of such measurements over a wide frequency range. In any specific range of frequency a suitable technique for that range

must be used. Generally, dielectric properties are obtained by using electromagnetic transmission theory applied on a circuit in which the sample of interest is a linear and time invariant component.

At low frequency regions (<100MHz), common circuit elements may be used to measure the dielectric constant and conductivity of materials. These kinds of techniques employ a parallel plate capacitor, which serves as a sample holder. The impedance (capacitance and conductance) of the assembly is measured with and without the sample by using sensitive bridges, vector impedance analyser or other similar instrumentation [9,14 and 16]. The change in the impedance introduced by the sample is a measure of its dielectric properties.

Although the parallel plate configuration is very common, coaxial and other capacitor designs can also be used.

At frequencies higher than 100 MHz, Transmission lines are employed [9]. In this case sample is incorporated in a transmission line assembly and the experimental set-up is organised to measure one or more of its scattering parameters. The set-up must contain a source to provide an incident signal, a sample holder, a detection system (such as network analyser) to measure the response of the sample to the signal, and finally transmission line components to guide the electromagnetic signal from one point to another. As mentioned, in these techniques, the reflection and/or transmission coefficients of the sample are determined. These parameters are both functions of the dielectric properties of the sample.

The different measurement techniques are usually distinguished according to the design of the sample holder, which also determines the size, and shape of the sample and the degree of sample handling required. The transmission line techniques are generally subdivided into waveguides and coaxial lines.

In the waveguide technique, a sample of well-defined shape and volume is packed into a waveguide terminated by a short circuit. A slotted line is used to characterise the standing wave formed by superposition of the incident and reflected waves leading to

the calculation of the dielectric properties of the sample. This technique is complex but it self-calibrates and can give accurate results over a narrow range of frequencies determined by the ratio of sample thickness to the propagating wavelength.

Coaxial contact probes are open-ended transmission line sections terminated by an impedance matched lossless window. The sample is placed in contact with the probe and a network analyser or equivalent instrumentation measures its admittance or reflection coefficient. Such techniques are broadband, non-destructive and require minimal sample handling [23]. The success of this technique depends on the theoretical model, which relates the measured quantity to the dielectric properties of the sample, and also on the calibration procedure [24].

Throughout this project, dielectric measurements were performed using automatic swept-frequency network and impedance analysers employing coaxial contact probes. In the following sections, details of these techniques are briefly described.

2-3-2 High frequency technique (contact probe)

The technique used throughout this project was developed by Gabriel et al 1994, and has been used extensively for dielectric measurement of biological tissues since then. In this section, the procedures of how the model has been developed are not explained as details can be found in [24]. However, a quick description of how the technique works and the role of the operator in calibrating and achieving the best performance of the technique is explained briefly.

A measurement system, which is based on the contact probe technique, consists of a computer controlled network/impedance analyser, an open-ended probe, and a mathematical model to convert the measured coefficients to the dielectric properties of the sample. The probe translates changes in the complex permittivity of the sample into corresponding changes in the reflection coefficient of the probe-sample assembly. The vector network analyser measures these reflection coefficients over the specified frequency range. The computer software leads the user through the experimental

procedure and transfers data to the computer for mathematical processing to yield the complex permittivity of the sample.

In the following sections, each element of this technique is explained briefly:

Open-ended coaxial probes

Open-ended co-axial probes are used to interface the measuring equipment with the samples in all cases. A coaxial probe consists of a hollow metal cylinder with a concentric inner conductor. At the end of such a line is a flat metal plate, which acts as a short circuit (Figure 2.7). The most commonly used coaxial probes have PTFE or similar interfaces. The design of the interface is intended to optimise the particular application for which it is devised. They mostly require a sample that extends infinitely in the half space beyond the probe. In practice, the sample volume is finite and proportionate with the dimension of the probe and, to a lesser extent, the sample itself and the frequency [29].

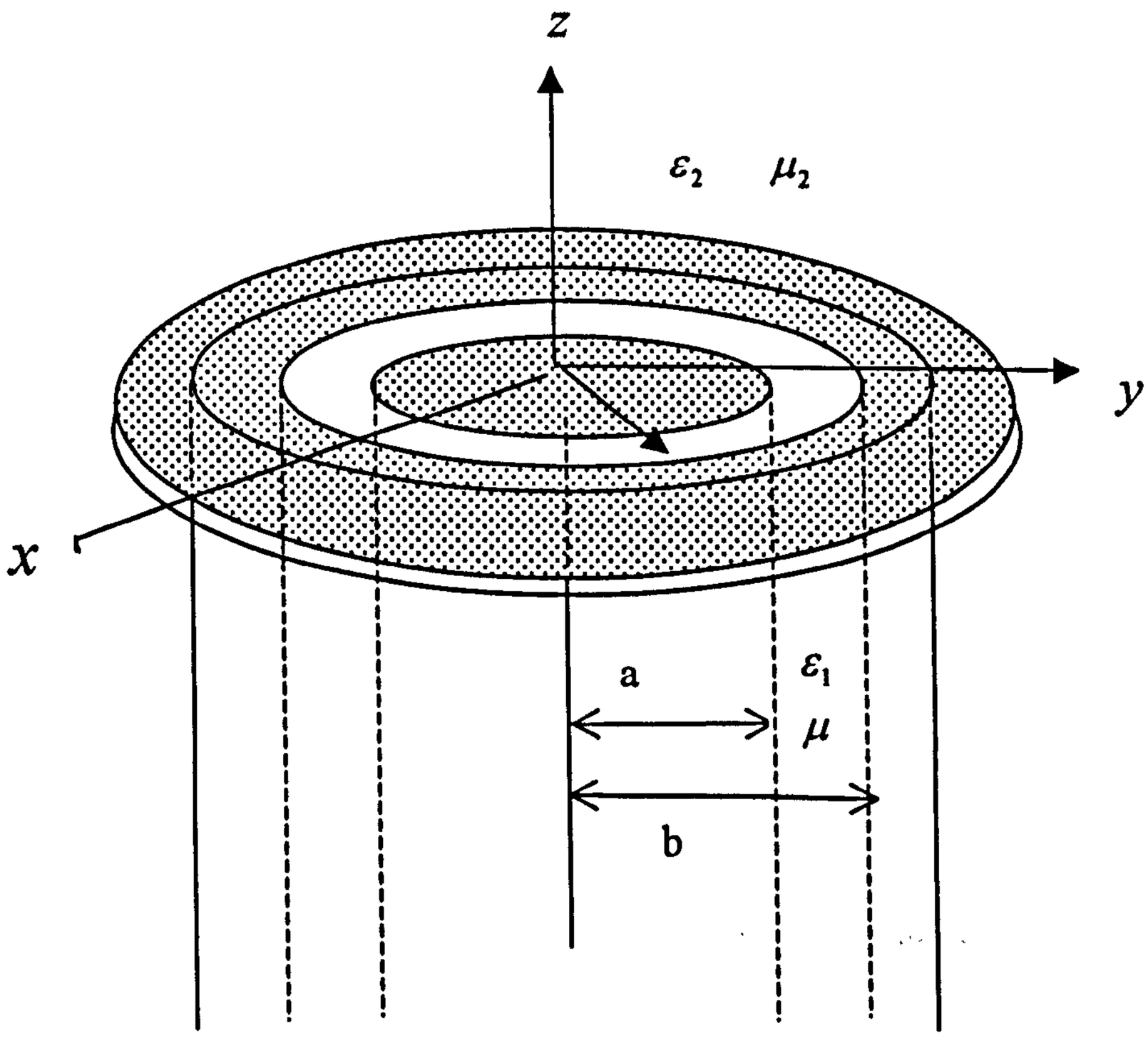

Figure 2.7 A probe of inner and outer radii a and b respectively (copied from [24]).

Figure 2.7 shows an open-ended coaxial line of inner radius of a and outer radius of b. The dielectric medium 1 inside the line is lossless and homogenous with absolute permittivity ε_1 and permeability μ_1. The line radiates into the medium 2 with absolute permittivity ε_2 and permeability μ_2. Medium 2 is linear, isotropic, homogeneous, non-magnetic and semi-infinite [31]. Since both media are non-magnetic, μ_1 and μ_2 are equal to the permeability of free space, μ_0.

The probes used in this project all have a 50Ω impedance, some with flange and some without. The air-lines are fitted with a PTFE bid and connected to the network analyser via SMA connectors. Depending on the frequency range of interest different probe sizes are used in this project. A list of all probes used throughout this project is presented in Table 2.1.

Table 2.1. Different probes used for dielectric measurement and their inner and outer radii

Probe size	Inner radius (a)	Outer radius (b)
10 mm	1.52 mm	5.09 mm
7 mm	1.04 mm	3.5 mm
2.98 mm	0.456 mm	1.49 mm
1.67 mm	0.256 mm	0.838 mm

The characteristic impedance, z_0 of the probes can be calculated from the following:

$$Z_0 = \frac{138}{\sqrt{\varepsilon_r}} \log \frac{b}{a} \tag{2.18}$$

in which ε_r is the relative permittivity of the dielectric medium in the line which is 2.1 in our case.

Using the dimensions of the probes the characteristic impedance of the probes can be calculated which is 50Ω.

Network analysers

In this project two Network Analysers have been used: the HP8753C Network Analyser covering the frequency range from 300 kHz to 3GHz and the HP8720 covering the frequency range of 130 MHz to 20GHz. The role of network analysers is to measure the admittance or reflection coefficient of the probe-sample assembly. The measurement system is controlled by a PC and the measured data are averaged and stored at each frequency. After finishing the sweep of the whole frequency range of interest, the data is recorded for the given number of frequencies (usually 51 frequencies in this project).

As there are a number of inherent errors in any network analyser system, it is common to calibrate the device prior to any measurement. This is to make the network analyser operate on its best performance.

Conventionally network analysers are calibrated for three known terminations i.e. short, open and load. These known terminations must be applied at the probe end. In the method used in this work, a piece of metal foil is used as a short circuit. Leaving the probe open in air is considered as open circuit measurement in the calibration procedure. Finally, a well-known standard liquid is used for load measurements in this technique. Choosing a standard liquid depends on the frequencies in which the network analyser operates and its sensitivity at the frequency range of interest. For most biological tissues, de-ionised water can be used as a reference material. However, water has a low conductivity and its sensitivity is poor at low frequencies. Therefore, different concentrations of salt solutions can be used as a reference material for samples with higher conductivities.

The calibration is a key part of the measurement procedure, and it is therefore important to ensure that it has been performed correctly. It can be checked by re-measuring the short circuit to ensure that the reflection coefficient of $\Gamma = -1.0$ can be obtained consistently.

The mathematical model

As previously mentioned, dielectric measurements are made by placing the open-ended coaxial probes in contact with a sample and then measuring its admittance or reflection coefficient using a network analyser. Gabriel et al, 1994 [24], has developed the admittance model that relates the reflection coefficient to the dielectric parameters of the matter for open-ended coaxial probes and this is a suitable model for the measurements of the dielectric properties of biological materials.

Sources of errors

The uncertainties in the measurements of complex relative permittivity depend on the uncertainty in the measured reflection coefficients from which it is calculated. In other words, it depends on the sensitivity of the admittance model used, which is a function of sample properties, dimensions of sensor and the measurement frequency [31].

This seems to be rather a complex situation, and there are different approaches to evaluate these uncertainties. This project does not intend to perform such error analysis and evaluation of the uncertainties, however, performance of the system can be adequately tested, by doing repeated measurements on selected standard materials. This is reported in chapter 3.

2-3-3 Low frequency technique

In this project an HP4192A impedance analyser has been used to cover the frequency range of 10Hz to 10MHz. The technique developed by Gabriel et al 1996, [8b], employs a 50Ω impedance matched conical co-axial probe [30] to interface the sample to the HP4192A impedance analyser. In this project for practical reasons, parallel plate probes have been used instead of coaxial probes. The probe is characterised by a fringing capacitance C and conductance G, which are functions of its physical dimension and can be measured with the impedance analyser.

The dielectric properties of an unknown sample can be calculated from the measurements of the impedance of the probe against the sample by using the following relationships:

$$\varepsilon' = \frac{C}{K} \text{ and } \sigma = \frac{G\varepsilon_0}{K} \tag{2.23}$$

where, the characteristic parameters of the probe, equivalent to its capacitance in air K, were calculated from the following:

$$K = \frac{C_{reference} - C_{air}}{\varepsilon'_{reference} - \varepsilon'_{air}} \tag{2.24}$$

This is done to normalise the stray capacitive and inductive elements; therefore the impedance components of the probe are measured in air and in a standard sample (water or salt solution).

However these values must be normalised to that of a standard material. For this purpose, a well-known standard liquid with known dielectric properties is measured initially, and the dielectric properties of the unknown sample are normalised to the dielectric properties of this liquid. Choosing the standard liquid depends on the sample of interest and must have the closest dielectric properties to that of the sample.

Sources of errors

According to Gabriel et al 1996,[8b], the low frequency dielectric measurements (10Hz to 10MHz) are affected by two sources of systematic errors: electrode polarisation and lead inductance errors which become apparent in the lower and higher ends of the frequency range.

Electrode polarisation is due to ionic layers occurring at the sample-electrode interface in the presence of water molecules and hydrated ions. The absolute values of both components approximately decrease with increasing frequency.

One factor, which plays an important role in determining the polarisation impedance of the probe, is its material. Gabriel et al, used both gold plated and sputtered platinum electrodes and a choice was made in favour of the latter as the effect of the rough platinum surface was to shift the electrode polarisation effect to lower frequencies.

In this project, considering the material of the probe and the frequency range under study (chapter 6), the contribution of electrode polarisation was reduced and needed no more correction.

The inductance of the probe and the connecting cable, were another sources of error addressed by Gabriel et al. This adds another series component to the measured impedance. This affects the measured capacitance and conductance of lossy media. To take into account for the value of the stray inductance for the experimental set up using the conical coaxial probes, Gabriel et al, performed measurements on standard salt solutions and applied an equivalent circuit analysis. For this set up the stray inductance was $L = 2\times10^{-7}$ Henry and the following equations were used to account for this [8b]:

$$C = \frac{C_m + LG_m\omega^2 + LC_m^2}{(1+\omega^2 LC_m)^2 + (\omega LC_m)^2} \quad \text{and} \quad G = \frac{G_m}{(1+\omega^2 LC_m)^2 + (\omega LC_m)^2} \tag{2.25}$$

where C and G are the corrected capacitance and conductance expressed in terms of measured values C_m and G_m, the lead inductance L and the angular frequency ω. The effect of the stray inductance increases with frequency and with sample conductivity.

However, as mentioned before, for practical reasons, in this project parallel plate electrodes have been used instead of conical coaxial probes. In practice, this in addition to introducing a connection box between the impedance analyser and a pulse generator device caused an increase in the stray inductance effect. In order to reduce this effect,

several measurements were performed with this assembly using different values of lead inductance. The best corrected value for the lead inductance was obtained by narrowing down the values in each measurement. The result of these measurements and the final corrected values for the lead inductance are all reported in chapter 6.

2-4 Summary

Biological tissues are non-homogeneous structures, and composed of cells, macromolecules and other membrane-bound substances. They have a very high permittivity compared with homogenous liquids and solids. The dielectric properties of biological tissue result from the interaction of electromagnetic radiation with its constituents at the cellular and molecular level. The dielectric behaviour of biological tissues is frequency dependent. It also depends on the tissue structure (cells, intra and extra cellular matters...) and composition (water, ions and organic matters). Typically soft tissues exhibit a continuous decrease in permittivity with increasing frequency. This is associated together with an increase in conductivity. Different frequency regions in the dielectric spectrum of a biological tissue are related to different interaction mechanisms in the cellular or molecular level. The dielectric relaxation spectrum of a tissue extends over a wide frequency range extending from hertz to gigahertz and consists of three main regions known as α, β and γ dispersions. The low-frequency α dispersion is associated with ionic diffusion processes at the site of the cellular membrane. The β dispersion extends over 3-4 frequency decades centred in the hundreds of kilohertz region, and is due mainly to the polarisation of cellular membrane and organic macromolecules. Finally, the γ dispersion, in the gigahertz region, is due to the molecular polarisation of tissue water.

One of the most convenient techniques to measure the dielectric properties of biological tissues is to use an open-ended coaxial probe together with a computer controlled network/impedance analyser.

References for chapter 2

[1] Schawn H P, 1957, "Electrical properties of tissues and cell suspensions", *Adv.Biol.Med.Phys.* **5**, 147-209.

[2] Schwan H P and Foster K R, 1980 "RF-Field Interactions with Biological Systems: Electrical Properties and Biophysical Mechanisms", *Proc. of the IEEE* **68** 104-13.

[3] Foster K R and Schwan H P 1989 "Dielectric properties of tissues and biological materials: A critical review" *Crit.Rev. Biomed. Eng.* **17** 25-104.

[4] Pethig R, 1984, "Dielectric Properties of Biological Materials: Biophysical and Medical Applications" *IEEE Trans. Electr. Insul.* **19** 453-73.

[5] Pethig R and KellD B., 1987 "The passive electrical properties of biological systems: their significance in physiology, biophysics and biotechnology" , *Phys.Med.Biol.* **32** 933-70.

[6] Stuchly M A and Stuchly S S 1980 "Dielectric properties of biological substances-tabulated" *J.Microwave Power* **15** 19-26.

[7] Duck F A 1990 "*Physical Properties of Tissue: A Comprehensive Reference Book*" (London: Academic, Harcourt Brace Jovanovich).

[8a] Gabriel C, Gabriel S and Corthout E, 1996a, "The dielectric properties of biological tissues: I. Literature survey" *Phys.Med.Biol.* **41** 2231-2249.

[8b]Gabriel S, Lau R W and Gabriel C, 1996b, "The dielectric properties of biological tissues: II. Measurements in the frequency range of 10Hz to 20GHz" *Phys.Med.Biol.* **41** 2251-2269.

[8c]Gabriel S, Lau R W and Gabriel C, 1996c, The dielectric properties of biological tissues: III. Parametric models for the dielectric spectrum of tissues , *Phys.Med.Biol.* **41** 2271-2293

[9] Grant E H, Sheppard R J and South G P, 1978, "*Dielectric Behaviour of Biological Molecules in Solution*", (Oxford:Clarendon).

[10] Pethig R 1979 "*Dielectric and Electronic Properties of Biological Materials*", (Chichester:Wiley).

[11] Gabriel C, 2000,"*Radio Frequency Radiation Dosimetry and Its Relationship To The Biological Effects of Electromagnetic Fields*" Edited by B.J. Klavenberg and D Miklavcic, Nato Science Series, 73-84 Kluwer Academic Publishers. Printed in the Netherlands.

[12] Hall M, Zhou L and Gabriel C,1994,' *Spectroscopic investigation of the dielectric properties of some foods and food components'*, Microwave Science Series, Report No.8, Ministry of Agriculture , Fisheries and food.

[13] Von Hippel A 1954 "*Dielectric Materials and applications*", The technology press of MIT, John Wiley & Sons, New York.

[14] Stuchly M A and Stuchly S S,1990 '*Biological effects and medical applications of electromagnetic energy'*, edited by: Gandhi O P, Prentice Hall Publication.

[15] Foster K R and Schwan H P,1995, '*Dielectric properties of tissues'*,CRC handbook of biological effects of electromagnetic fields, edited by: Polk C and Postow E, CRC Press.

[16]Michaelson S M and Lin C J, 1988 '*Biological effects and health implications of radiofrequency radiation'*, Plenum Press.

[17] Kuang W and Nelson S O, 1998, "Low-Frequency Dielectric Properties Of Biological Tissues: A review With Some New Insights', *Transactions of American Sosiety of Agricultural Engineers*, **41(1)**, 173-184.

[18] Schwan H P and Foster K R, 1977, "Microwave dielectric properties of tissues:some comments on the rotational mobility of tissue water" *Biophys. J.* **17** 193-197.

[19] Peyman A, Rezazadeh A A and Gabriel C, 2001, "Changes in the dielectric properties of rat tissue as a function of age at microwave frequencies" *Phys. Med. Biol.* **46** No 6 1617-1629.

[20] Surowiec A, Stuchly S S and Swarup A, 1985, "Radiofrequency dielectric properties of animal tissues as a function of time following death", *Phys.Med.Biol* **30** 1131-1141.

[21] Kraszewski A, Stuchly M, Stanlslaw S , Stuchly S and Smith A M, 1982, "In Vivo and In Vitro Dielectric Properties of Animal Tissues at Radio Frequencies", *Bioelectromagnetics,* **3** 421-432.

[22] Stuchly M A, and Stuchly S S , 1980, "Coaxial line reflection methods for measuring dielectric properties of biological substances at radio and microwave frequencies- a review", *IEEE Trans. Instrum. Measure.* **29** 176-183.

[23] Gabriel C, Grant E H and Young I R, 1986, "Use of time domain spectroscopy for dielectric properties with coaxial probe", *J. Phys.E:Sci.Instrum.* **19** 843-849.

[24] Gabriel C, Chan T Y A and Grant E H 1994, "Admittance models for open ended coaxial probes and their place in dielectric spectroscopy", *Phys.Med.Biol.* **39** 2183-2200.

[25] Hall M., Zhou L and Gabriel C,1994,' *Spectroscopic investigation of the dielectric*

properties of some foods and food components', Microwave Science Series, Report No.8, Ministry of Agriculture , Fisheries and food.

[26] Burdette E C, Cain F L and Seals J, 1980, "In vivo probe measurements technique for determining dielectric properties at VHF through microwave frequencies", *IEEE Trans. Microwave Theory Tech.*, **28** 414-427.

[27] Athey T W, Stuchly M A and Stuchly S S, 1982, Measurement of radio frequency permittivity of biological tissues with open-ended coaxial line: part 1.*IEEE Trans. Microwave Theory Tech.* **30** 82-86.

[28] Stuchly M A, Kraszewiski A, Stuchly S S and Smith A M, 1982, "Dielectric properties of animal tissues in vivo at radio and microwave frequencies: comparison between species", *Phys.Med.Biol.* **27** 927-936.

[29] Gabriel C , 1993, "Numerical modelling of fringing fields and their use for complex permittivity measurements at high frequencies", US Air Force, Brooks AFB, AL/OE- TR-1993-0068.

[30] Gabriel C and Grant E H 1989, "Dielectric sensors for industrial microwave measurements and control", *Microwellen HF Mag.* **15** 643-5.

[31] Chan Tsing Yee Amy1993, "Numerical analysis of open-ended coaxial line sensors with application to dielectric measurements up to 20GHz " PhD Thesis.

Chapter 3- Standards

3-1 Introduction

The accuracy of the three experimental techniques based on automatic swept-frequency network and impedance analysers used throughout this project has been tested several times previously [1] *(The techniques used for the dielectric measurements in this study have been described in details in chapter 2)*. The stated accuracy of these techniques is reported to be between 1 and 2% in certain frequency ranges [1]. This is based on the measurement carried on standard liquids of well-known dielectric properties.

It is however essential for the purpose of this project to perform an accuracy test in order to make sure that the uncertainties fall well within the acceptable level.

In this project the following instrumentation have been used: (i) vector network (or impedance) analyser (ii) the open-ended coaxial probe (or parallel plate electrodes) and (iii) methodology and application software to translate measurements to dielectric properties of the samples. The uncertainty in the dielectric measurements can be contributed from all of the above elements as well as the sample size and temperature drift.

In order to obtain accurate results in the dielectric measurements, the errors associated with the equipment and the samples must be reduced as much as possible. The following cares have been taken throughout this project to reduce the experimental errors.

The performance of the network/impedance analysers improved by making sure that the devices are calibrated well and that the calibration is maintained during the long measurement period. The process of calibrating the network analysers requires the measurements of materials with known dielectric properties. As well as short circuit (aluminium foil) and open circuit (air), a third reference material is required. A survey

on some of the dielectric measurements available on polar liquids [12], concluded that deionised water has the lowest uncertainty and is therefore a good standard liquid.

The size of the sample and its proportion to the probe size is also important in the dielectric measurements. Care was always taken to have a sample thickness at least 4-5 times the probe diameter to constitute a semi-infinite lossy sampling volume [13].

Temperature variation can effect both the physical dimensions of the probe and also the dielectric properties of the sample. These undesirable effects can be reduced by a strict temperature control. In this work all efforts have been made in order to maintain a relatively constant temperature by using water bath to keep the samples at certain temperature over a period of time. Also, prior to measurements, the probe itself has been warmed up to the temperature of the interest.

Despite all the efforts to reduce the error in the measurements, the uncertainties can not be removed completely. The evaluation of the uncertainties involves the development of a model, which describes the problem, and formulates different contributions to the uncertainties. The next stage is to apply mathematical calculations to solve the model and derive its parameters. This work does not intend to perform such error analysis and evaluation of the uncertainties, however, performance of the system can be adequately tested, by doing repeated measurements on selected standard materials.
These measurements can be used to demonstrate the extent of random and systematic errors delivered by the system under the given measurement conditions.

In this chapter, some of the standard liquids used in accuracy measurements are introduced and their properties are discussed. The results of dielectric measurements carried out on these liquids using the experimental techniques are also presented. The obtained results are also fitted to well known theoretical models and compared with literature values.

The measurement errors described in this section relate to well-characterised materials of uniform composition; they do not take into consideration uncertainties arising from any variability within a sample and differences between samples.

3-2 Standard liquids

The testing materials must be well defined in terms of purity and preparation and have uniform composition and known dielectric parameters. Choosing a standard liquid for accuracy measurements depends on the frequency range in which the technique can cover and the sensitivity of the technique in that frequency range.

The standard liquids used in this project are Ethanediol, Formamide, Methanol, Dimethyl Sulphoxide and different salt solutions.

Ethanediol $(CH_2OH)_2$ is a colourless liquid used as a solvent, for biological molecules in general and for urea in particular and has a static permittivity of about ½ that of pure water [5]. Ethanediol is an attractive solvent for dielectric investigations in that it has a very low ionic conductivity ($4\times10^{-8} S/m$ at room temperature) [3]. This minimises the problem of electrode polarisation.

Formamide (CH_3NO) is a clear, colourless and slightly viscous liquid that is infinitely soluble and is used as a laboratory reagent. It has physical properties similar to those of water and has a high static permittivity, in the order of 110 at room temperature, which falls to a high-frequency value of around 7 [6].

Methanol (CH_3OH), a colourless liquid, is the simplest alcohol and an important material in chemical synthesis.

Dimethyl Sulphoxide (CH_3SOCH_3) is a colourless organic solvent that has unique biological properties. Dimethyl Sulphoxide and its aqueous solutions have wide use as solvents and reaction media.

The above standard liquids have been selected to cover the range of dielectric properties likely to be encountered when measuring soft and hard tissues.

The result of the dielectric measurements of each standard liquid depends on the frequencies in which the network analyser operates and its sensitivity at the frequency range of interest.

It is well-established [4] that the dielectric behaviour of these materials can be described with the following general relationship:

$$\hat{\varepsilon} = \varepsilon_\infty + \frac{\varepsilon_s - \varepsilon_\infty}{[1+(j\omega\tau)^{1-\alpha}]^\beta} - \frac{j\sigma_i}{\omega\varepsilon_0} \qquad (3.1)$$

where α and β are distribution parameters such that for $\alpha = 0$ and $\beta = 1$, the above relationship becomes the Debye equation; for $\beta = 1$ and $0 < \alpha$ it corresponds to the Cole-Cole equation, and for $\alpha = 0$ and $0 < \beta < 1$, to the Cole-Davidson relationship. The conductivity term (σ_i) is included to characterise the materials that exhibit ionic conductivity.

3-3 Dielectric measurements using network analysers

In this section the results of dielectric measurements using two different network analysers on the standard liquids are presented. The agreement of the two network analysers in the common frequency range is also tested and the results are presented.

3-3-1 Measurements using Network Analyser HP8753C

Dielectric measurements in the frequency range of 10MHz-1GHz were carried out using coaxial probes of 7 and 10-mm diameter, and a computer controlled network analyser HP8753C. Dielectric measurements were performed on all standard liquids in this frequency range at 20°(Dimethyl Sulphoxide measured at 25°C). The experimental data obtained on these measurements are given in Figures 3.1-3.4.

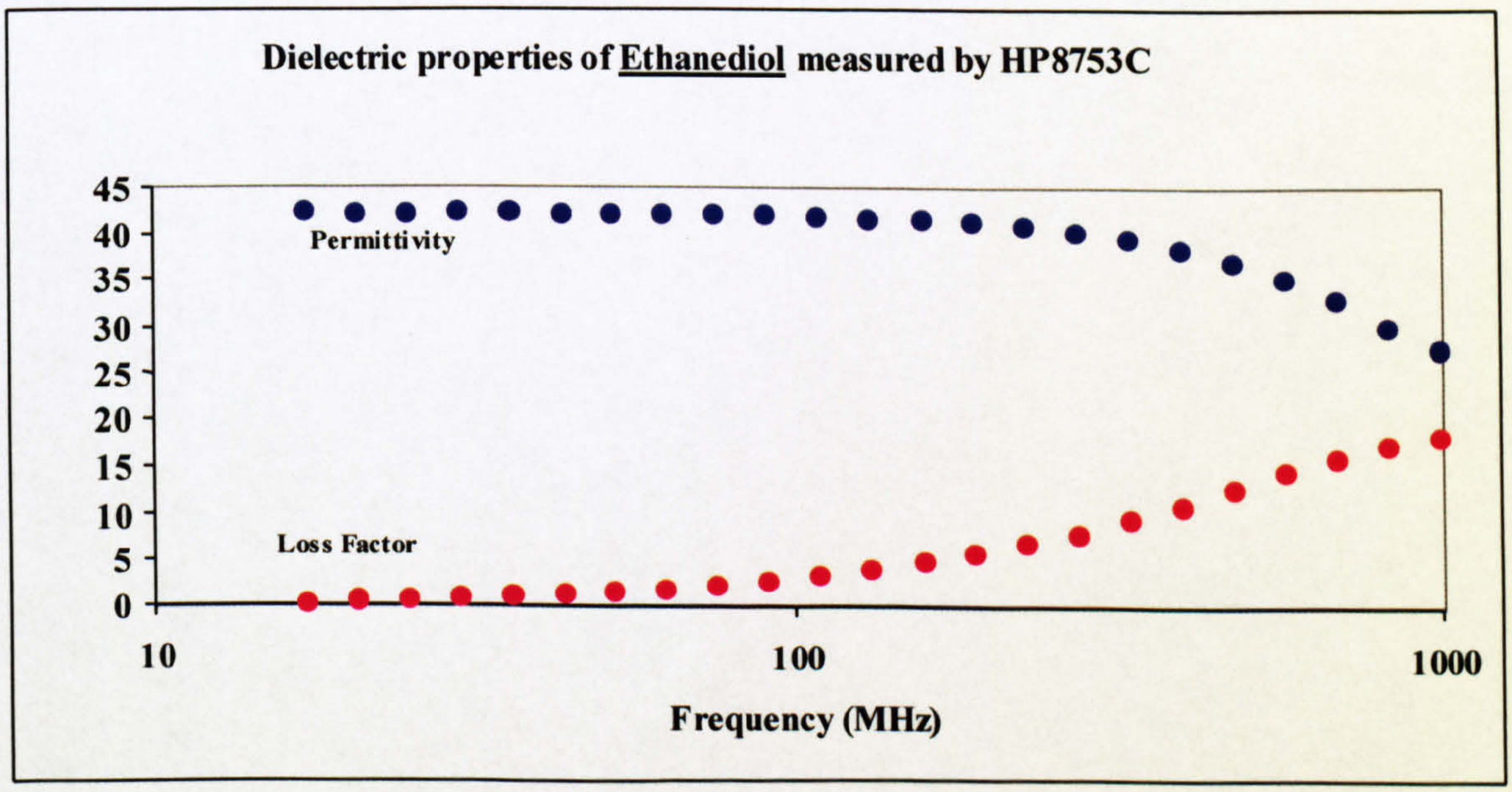

Figure 3.1 Dielectric properties of Ethanediol at 20°C

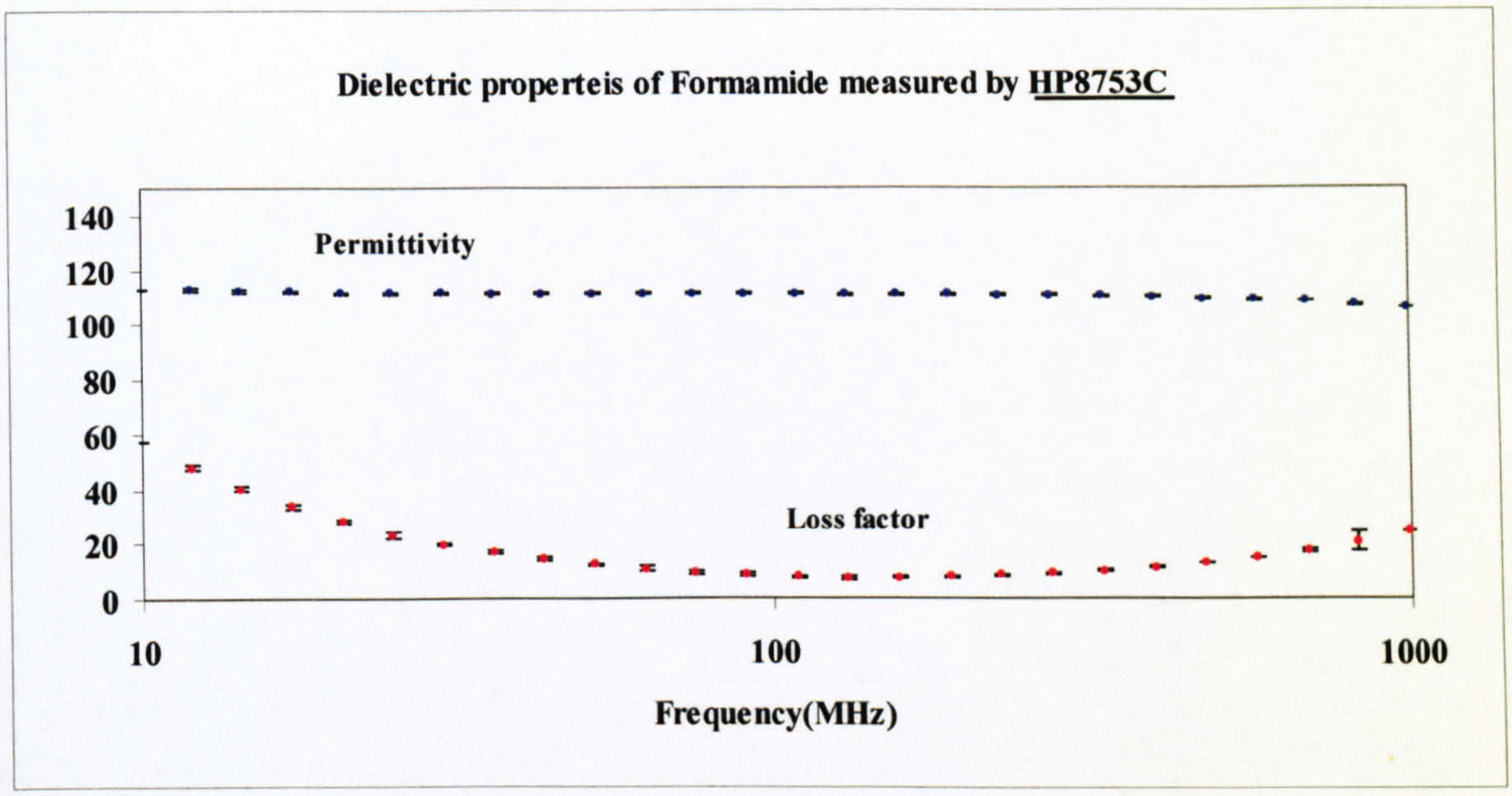

Figure 3.2 Dielectric properties of Formamide at 20°C
(The error bars represent the % standard deviation for 5 measurements and are typically better than 1% at frequencies above 100MHz)

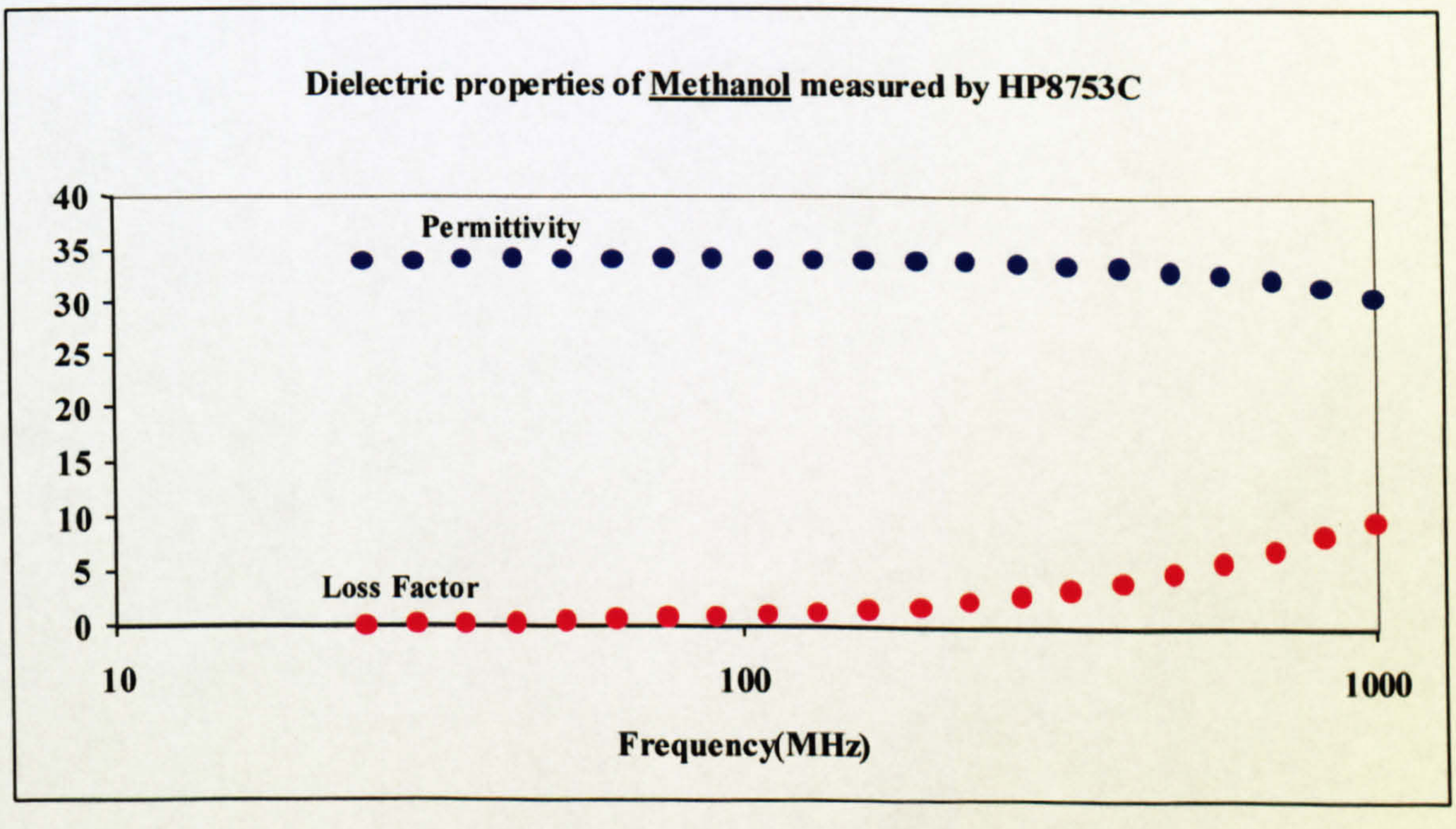

Figure 3.3 Dielectric properties of Methanol at 20°C

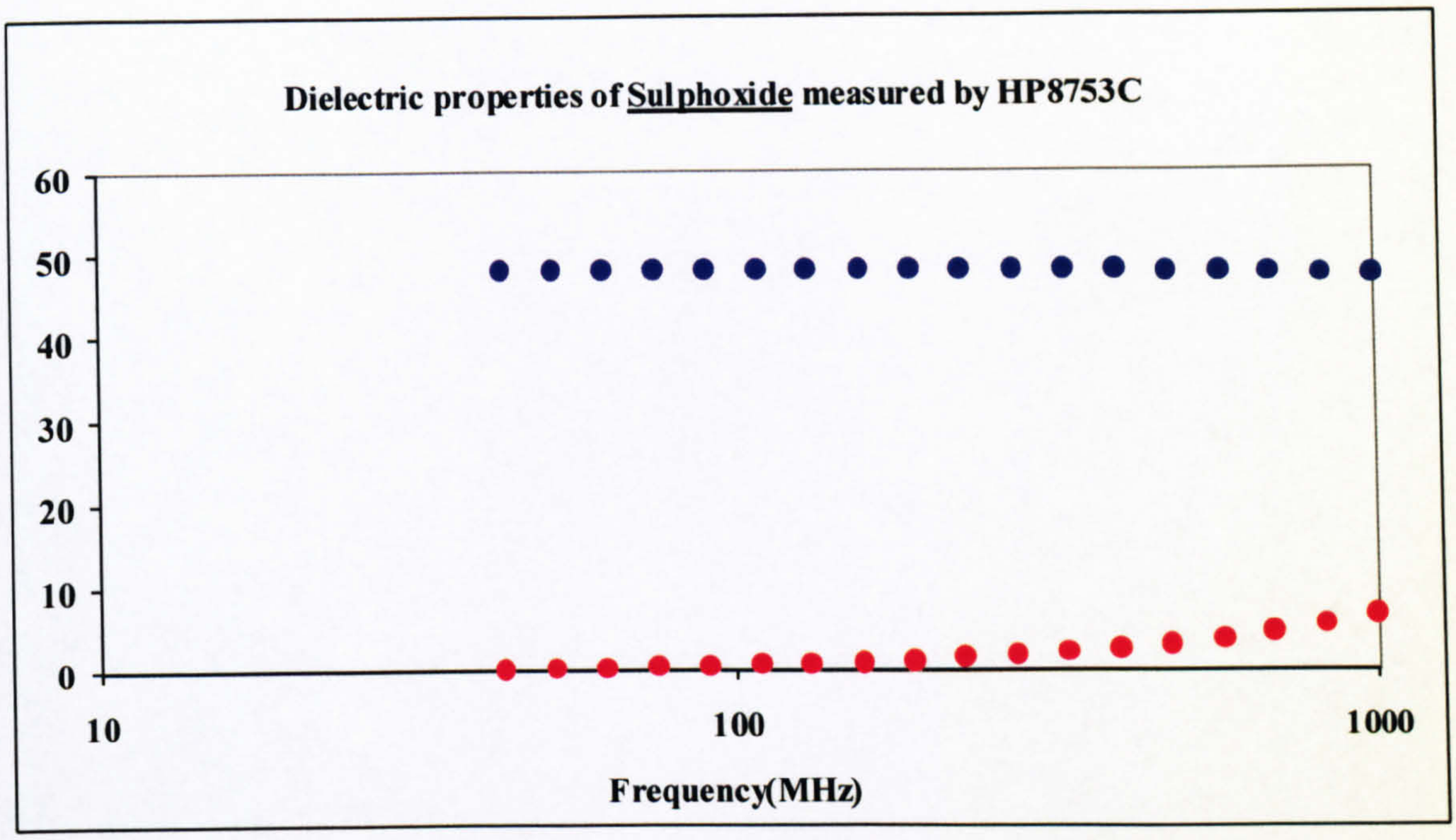

Figure 3.4 Dielectric properties of Dimethyl Sulphoxide at 25°C

The results given in Figures 3.1 to 3.4 show the typical dielectric behaviour of liquids in the frequency range of 10MHz-1GHz. The maximum standard deviation in the frequencies above 100MHz is 1% for all liquids. However standard deviation for Formamide is better than 1% even in frequencies below 100MHz. As mentioned before, the reproducibility of measurements of different liquids depends on the sensitivity of the network analyser in the frequency range of interest.

3-3-2 Measurements using Network Analyser HP8720

The dielectric measurements in the frequency range of 130MHz to 20GHz were carried out using coaxial probes of 2.98mm and 1.67mm diameter, and a computer controlled network analyser HP8720. Dielectric measurements were performed on all standard liquids in this frequency range at 20° (Dimethyl Sulphoxide measured at 25°). The results are given in Figures 3.5-3.8.

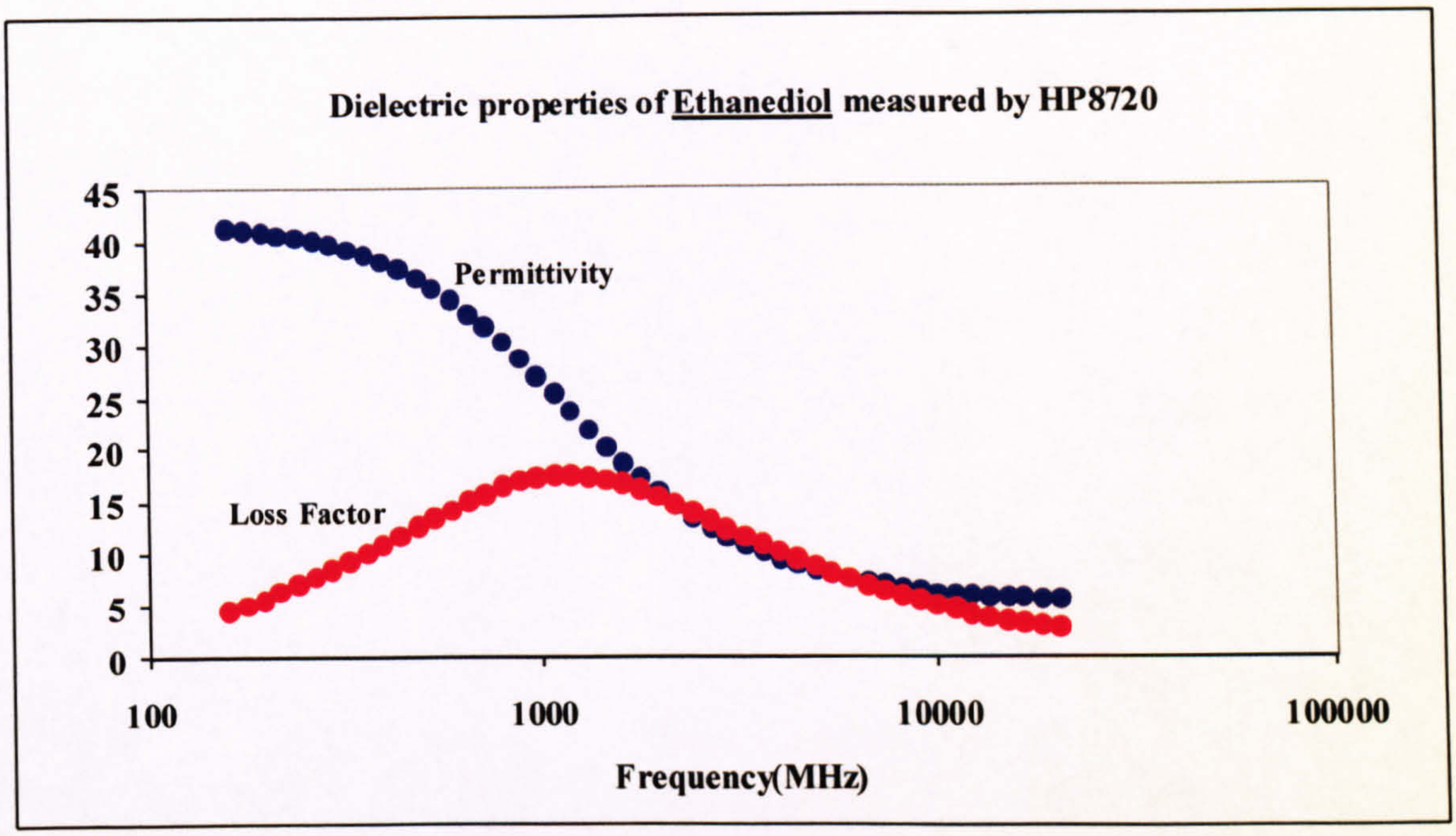

Figure 3.5 Dielectric properties of Ethanediol at 20°C

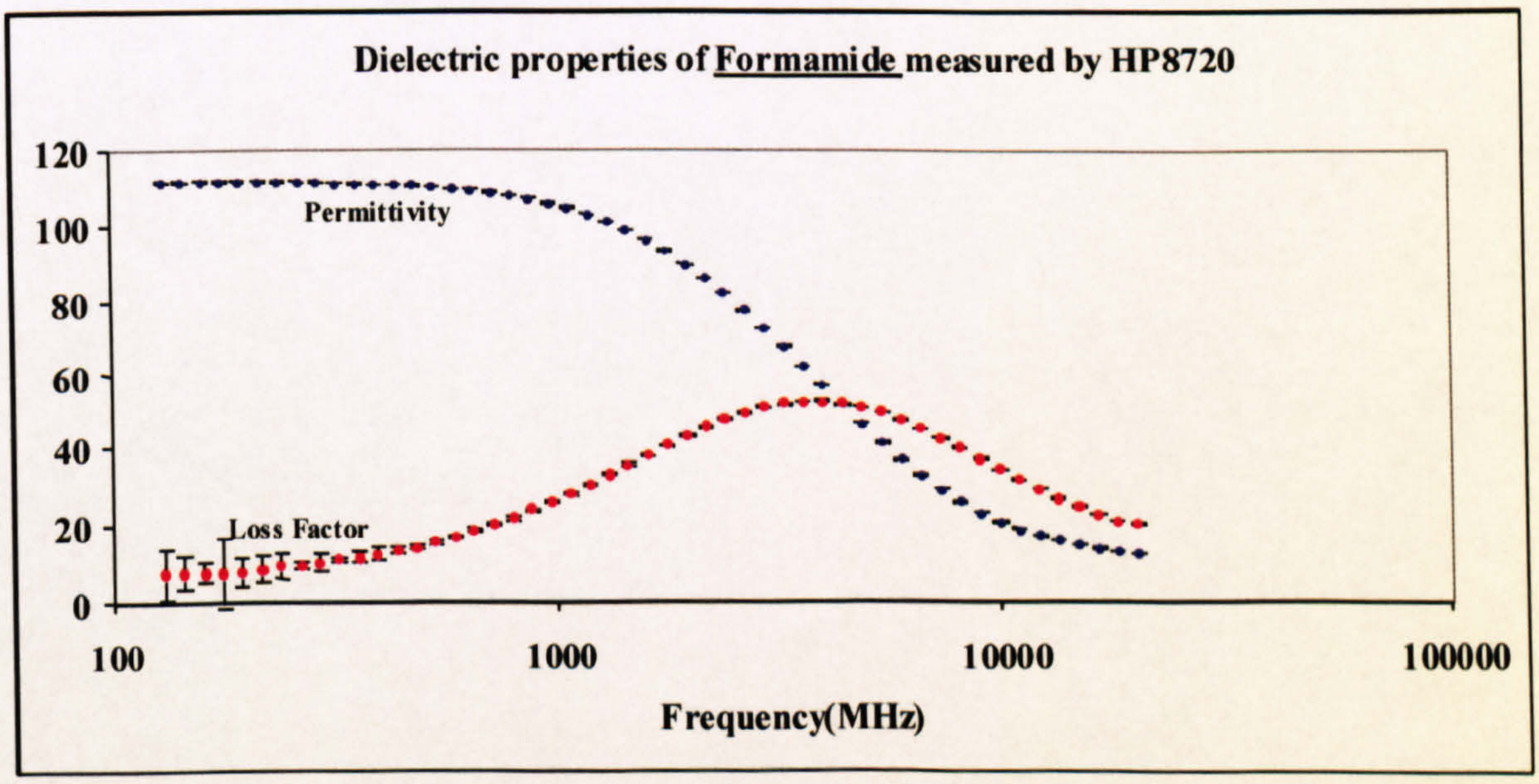

Figure 3.6 Dielectric properties of Formamide at 20°C
(The error bars represent the %standard deviation for 5 measurements and are typically better than 1% at frequencies above 800MHz)

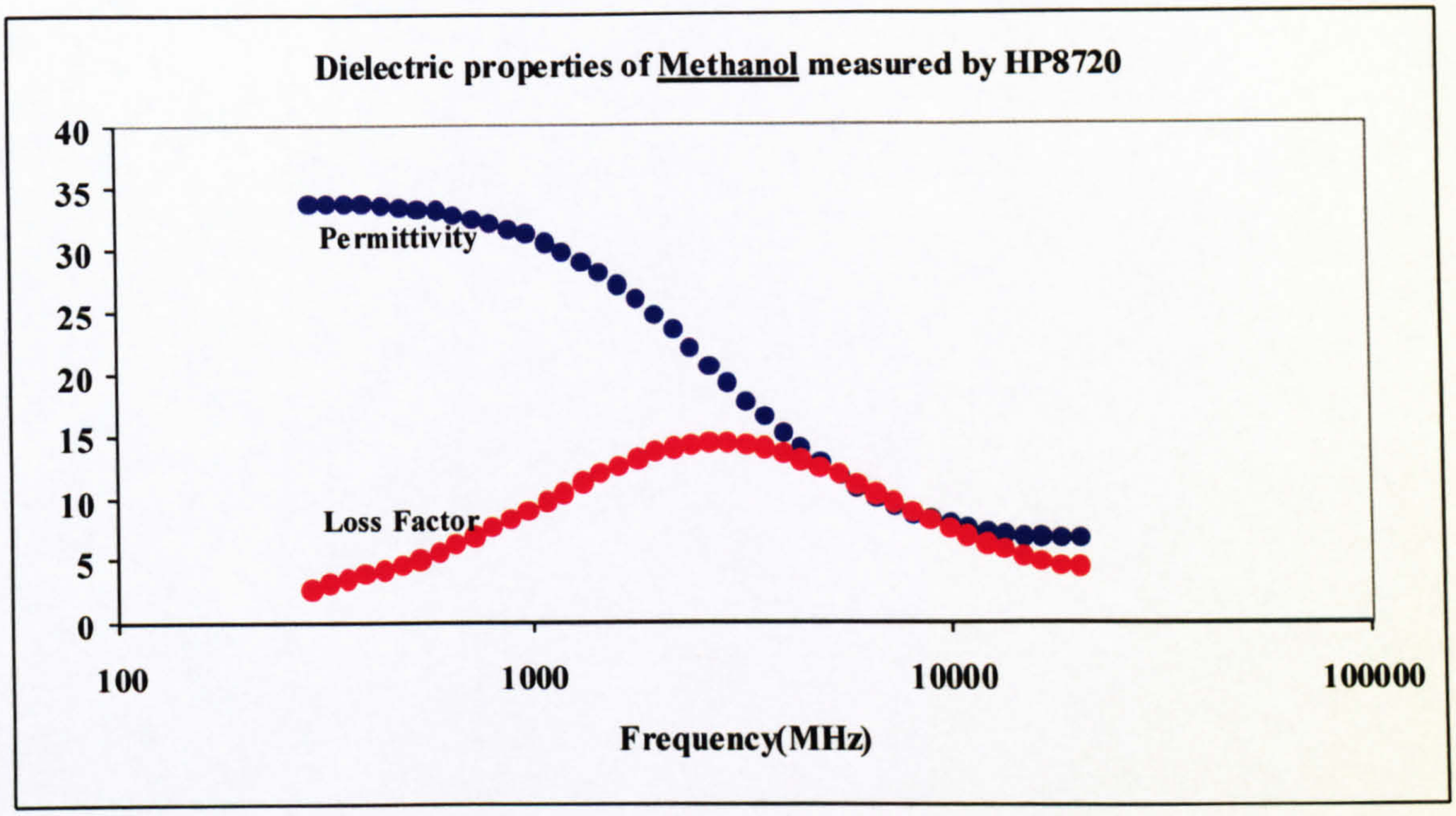

Figure 3.7 Dielectric properties of Methanol at 20°C

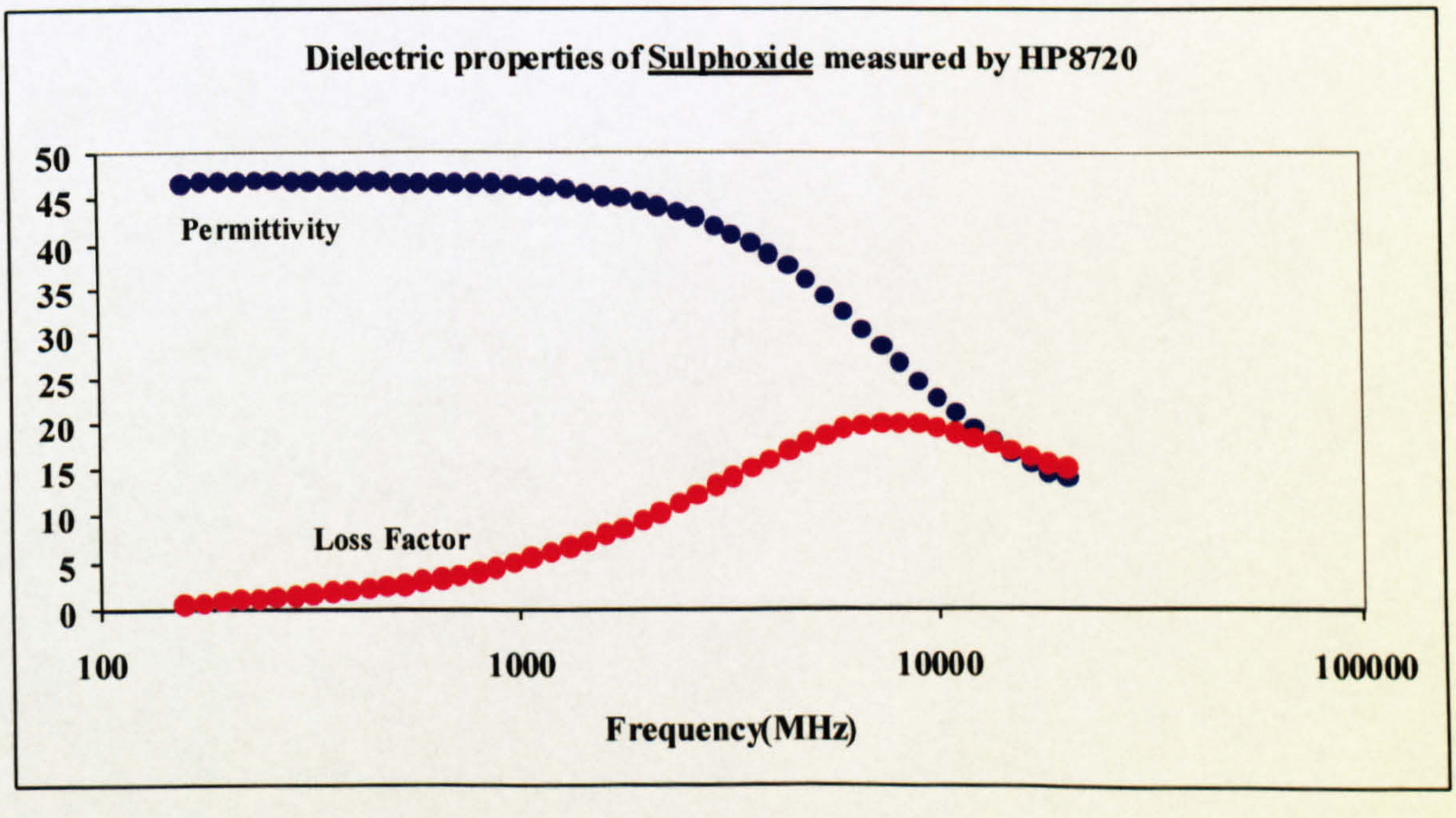

Figure 3.8 Dielectric properties of Dimethyl Sulphoxide at 25°C

The result of dielectric measurements presented in Figures 3.5 to 3.8 show the end tail of β dispersion and a good part of γ dispersion of 4 liquids in the frequency region of

130MHz-20GHz. The repeatability of the measurements is better than 1% at frequencies above 800MHz for all the liquids. However, some showed similar level of repeatability at lower frequencies such as Formamide and Ethanediol.

3-3-3 Agreement between two network analysers

There is a common frequency range which both network analysers can cover. It is important to examine the extent to which the measurements carried out by the two machines agree in that common frequency range. Figure 3.9 shows the dielectric measurements carried out on Ethanediol using both network analysers. The percentage difference in the permittivity and loss factor measured by the two network analysers at some common frequency points has also been calculated (Table 3.1).

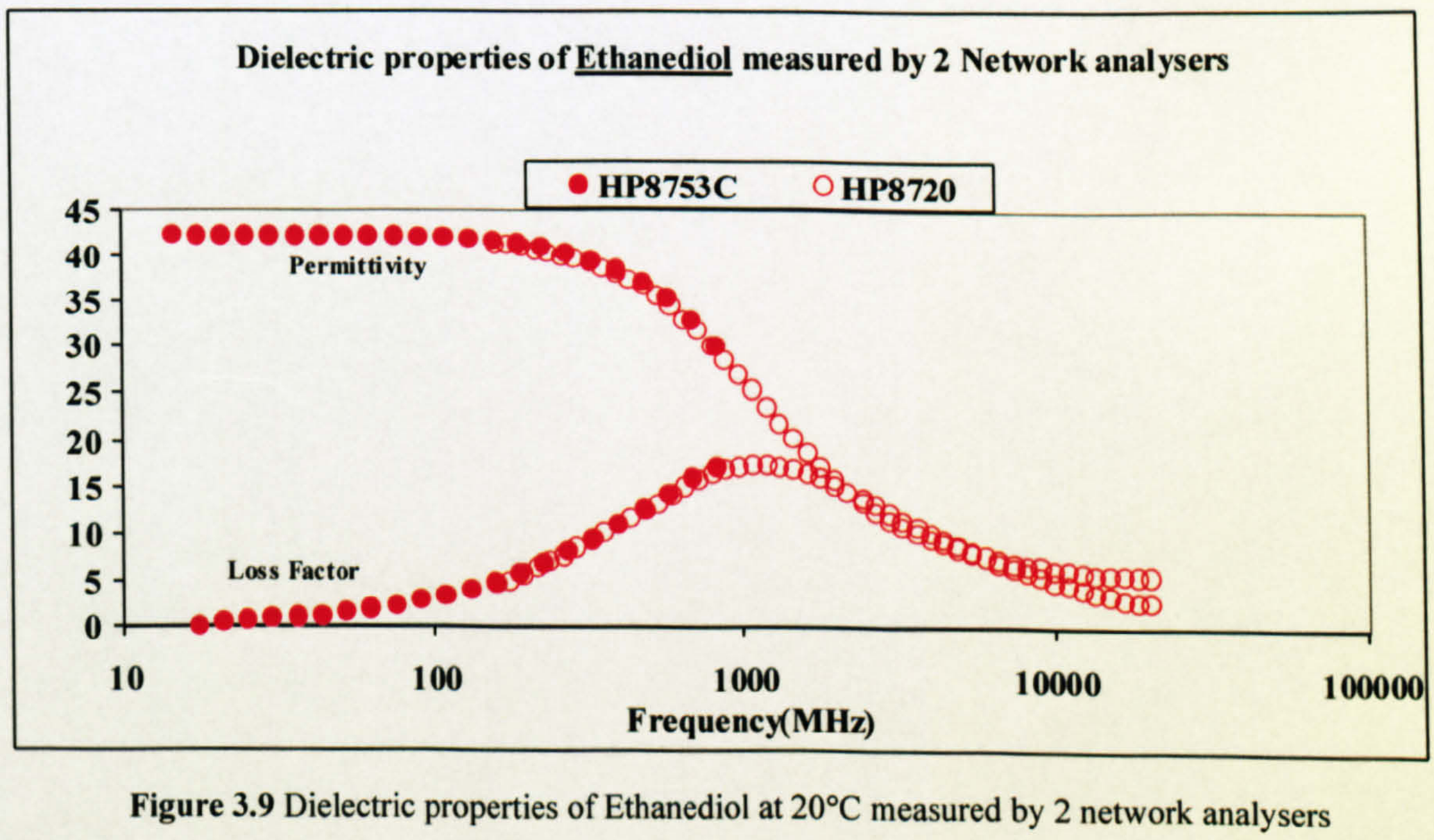

Figure 3.9 Dielectric properties of Ethanediol at 20°C measured by 2 network analysers

Table 3.1 The % difference between the values of dielectric properties of Ethanediol measured by 2 network analysers.

Frequency (MHz)	Permittivity	Loss Factor
	% difference between values from two network analysers	% difference between values from two network analysers
300	1.13	1.15
400	1.48	0.62
600	1.56	2.83
800	1.81	3.06

The results presented in Figure 3.9 and Table 3.1 show the extent to which the dielectric measurements performed by two network analysers agreed with each other. The maximum % difference between obtained values in the common frequency range is about 3%. It is obvious from Table 3.1 that as the frequency increases, larger difference can be observed between the two measured values by two network analysers and this is due to the decrease in the sensitivity of the HP8753C at higher frequencies.

3-3-4 Mathematical analysis

In order to examine the integrity of the above measurements the dielectric data obtained for all standard liquids have been fitted to different versions of Equation 3.1 depending on their characterisation and then the result of the best fit is presented and compared to those reported in the literature.

The analyses were carried out using a complex curve-fitting program. For each liquid the data above 100 MHz were fitted to a suitable model and the fitted parameters and 95% confidence intervals are presented.

Previous dielectric measurements and analysis have been made on Ethanediol, Formamide, Methanol and Dimethyl Sulphoxide by others [1,3,6,7,8 and 9] each suggesting a particular model to be the best representative of the dielectric behaviour of

these liquids. These literature data have been used for comparison with results obtained in this study.

The results of theoretical analyses and their comparison with literature are presented below for each standard liquid separately.

Ethanediol

The experimental data for Ethanediol in the frequency range of 100MHz-20GHz were fitted to the Cole-Davidson equation:

$$\varepsilon(\omega) = \varepsilon_\infty + \frac{\Delta\varepsilon}{(1 + j\omega\tau)^\beta} \tag{3.2}$$

where β is the parameter characterising the distribution of the relaxation time.

The measured data have also been fitted to a Double-Debye equation:

$$\varepsilon(\omega) = \varepsilon_\infty + \left(\frac{\Delta\varepsilon_1}{1 + j\omega\tau_1} + \frac{\Delta\varepsilon_2}{1 + j\omega\tau_2}\right) \tag{3.3}$$

where Δ_1 and Δ_2 are the amplitudes of the dispersions of two processes.

Figure 3.10 shows the experimental data for Ethanediol fitted to Cole-Davidson model, with the solid line representing the theoretical curve corresponding to Equation (3.2). The fitted parameters and their 95% confidence intervals for Cole-Davidson fit are summerised in Table 3.2.

Figure 3.11 shows the experimental data for Ethanediol fitted to Double-Debye model with the solid line representing the theoretical curve corresponding to Equation (3.3). Table 3.3 contains the fitted parameters and their 95% confidence intervals which represents the goodness of the fit.

Table 3.4 contains the dielectric data for Ethanediol at certain frequencies obtained in this study and compared to that of literature [6,7].

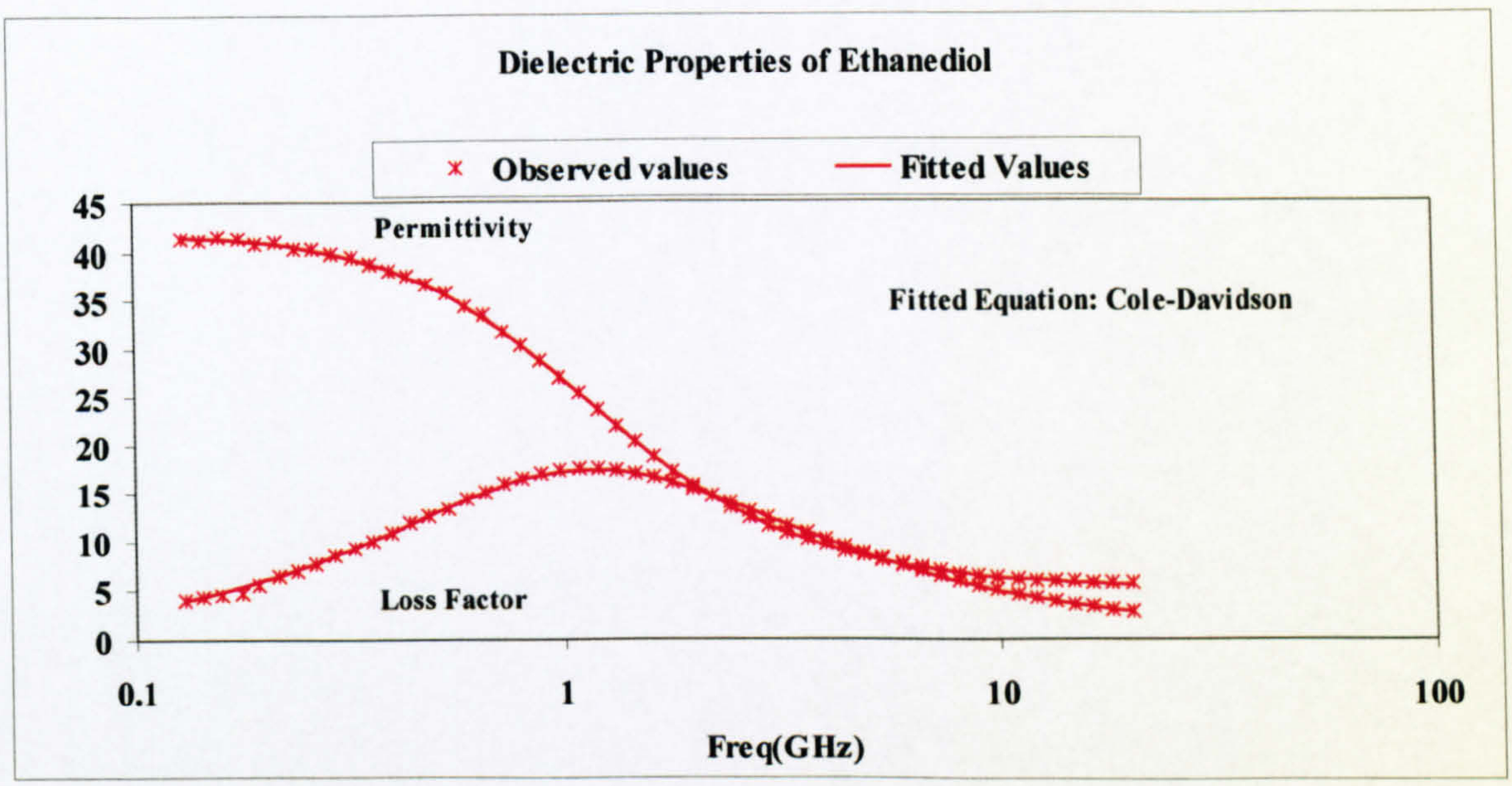

Figure 3.10 Measured and fitted values for dielectric properties of Ethanediol at 20°C

Table 3.2 Dielectric parameters of Ethanediol obtained by fitting the experimental results to Equation (3.2) and comparison to literature. The ± term corresponds to the 95% confidence interval (represents the goodness of the fit)

Ethanediol	Temp	Model Used	ε_s	$\pm\varepsilon_s$	ε_∞	$\pm\varepsilon_\infty$	τ_{relax} (ps)	$\pm\tau_{relax}$ (ps)	β	±β
This study	20°C	Cole - Davidson	41.9	0.07	4.86	0.1	154.44	5.2	0.87	0.008
Levin et al. [7]	20°C	Cole-Davidson	41.4		3.7		164.02		0.8	

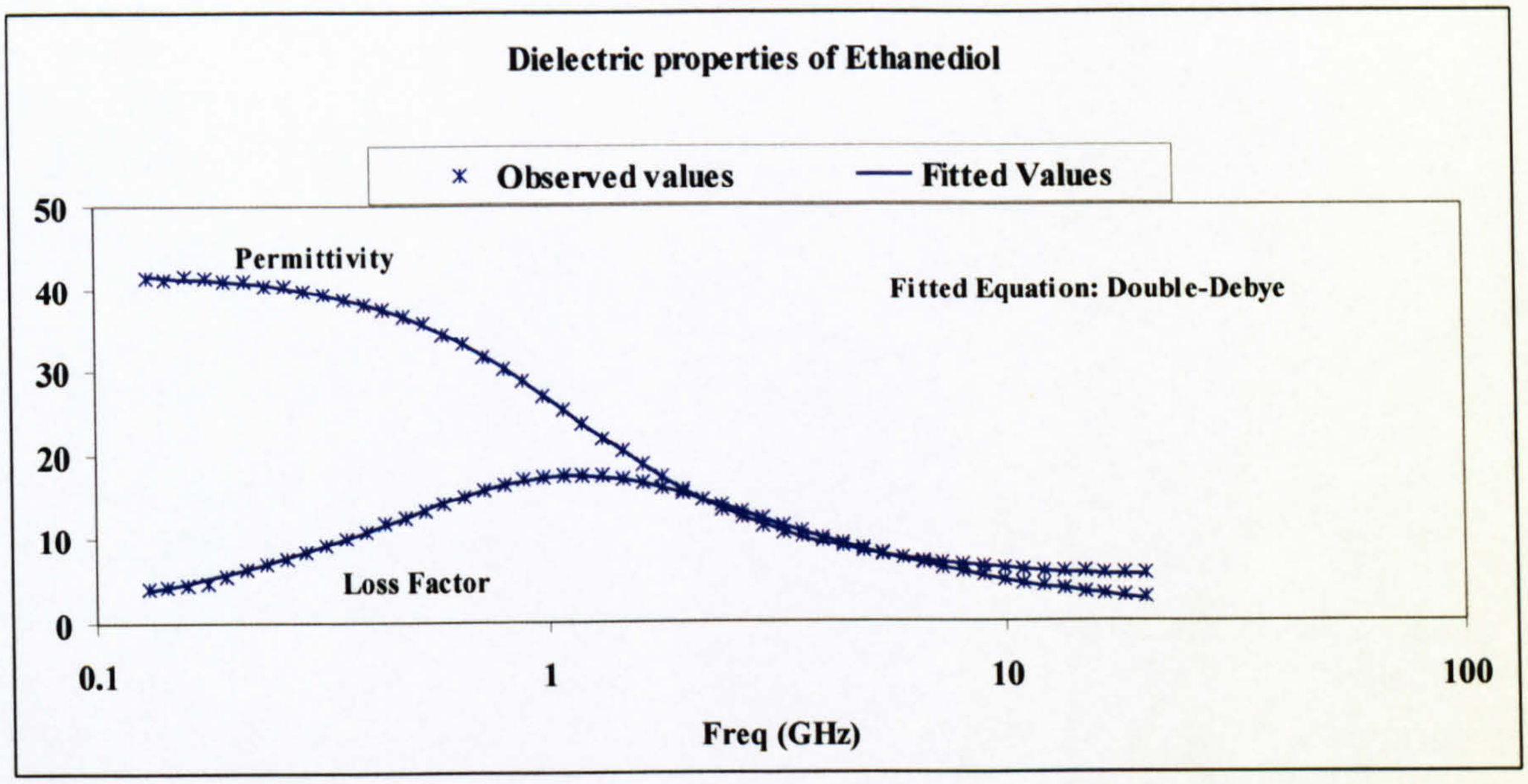

Figure 3.11 Measured and fitted values for dielectric properties of Ethanediol at 20°C

Table 3.3 Dielectric parameters of Ethanediol obtained by fitting the experimental results to Equation (3.3) and comparison to literature. The ± term corresponds to the 95% confidence interval

Ethanediol	Temp	Model Used	Δ_1	$\pm\Delta_1$	Δ_2	$\pm\Delta$	ε_∞	$\pm\varepsilon_\infty$	τ_1 (ps)	$\pm\tau_1$ (ps)	τ_2 (ps)	$\pm\tau_2$ (ps)
This study	20°C	Double-Debye	34	0.25	2.8	0.24	5.16	0.09	142.9	2.41	26.6	6.3
Jordan et al. [6]	20°C	Double-Debye	35.5		3.5		3.8	0.5	145	3	10	4

Table 3.4 The result of fitted dielectric data for Ethanediol at certain frequencies obtained in this study and comparison with literature data.

	This study *Cole-Davidson*		This study *Double-Debye*		Levin et al [7] *Cole-Davidson*		Jordan et al [6] *Double-Debye*		% difference between this study and [7]		% difference between this study and [6]	
Freq. MHz	ε'	ε''	ε'	ε''	ε'	ε''	ε'	ε''	ε'	ε''	ε'	ε''
400	38.00	11.06	38.03	11.00	37.39	10.90	38.34	11.51	1.60	1.47	0.80	4.38
600	34.18	14.48	34.25	14.48	33.62	14.20	34.33	15.07	1.64	1.95	0.23	3.97
800	30.25	16.43	30.30	16.48	29.79	16.06	30.18	17.07	1.51	2.28	-0.42	3.50
900	28.40	16.97	28.43	17.03	28.00	16.56	28.22	17.60	1.39	2.38	-0.76	3.26

It can be seen from the results presented above for Ethanediol, that the Cole-Davidson model gave a better fit to the experimental data obtained in this study, as most of the fitted parameters obtained are closer to that of the Cole-Davidson rather than the Double-Debye (compare to literature values). This is also confirmed from values presented in Table 3.4, which show the % difference between values obtained in this study and those reported in literature. It can be seen that the values obtained in this study are much closer to the Levin et al [7] values. There is about 2% difference in the values obtained in this study and those in the literature data when fitting the experimental data to the Cole-Davidson model.

Formamide

The experimental data for Formamide in the frequency range of 0.1-20GHz were fitted to a single Debye equation plus a conductivity term:

$$\varepsilon(\omega) = \varepsilon_\infty + \frac{\varepsilon_S - \varepsilon_\infty}{(1 + j\omega\tau)} + \frac{\sigma_i}{j\omega\varepsilon_0} \tag{3.4}$$

Figure 3.12 shows the experimental data for Formamide fitted to the Debye model with the solid line representing the theoretical curve corresponding to Equation (3.4). The fitted parameters and their 95% confidence intervals are also summerised in Table 3.5.

Table 3.6 contains the dielectric data for Formamide at certain frequencies obtained in this study and compared to that of literature [6].

It must be noted that the value obtained for the conductivity term (0.027S/m) was omitted when calculating the dielectric values of Formamide, to compare our data with literature data (Jordan et al), which did not include conductivity term in their analysis.

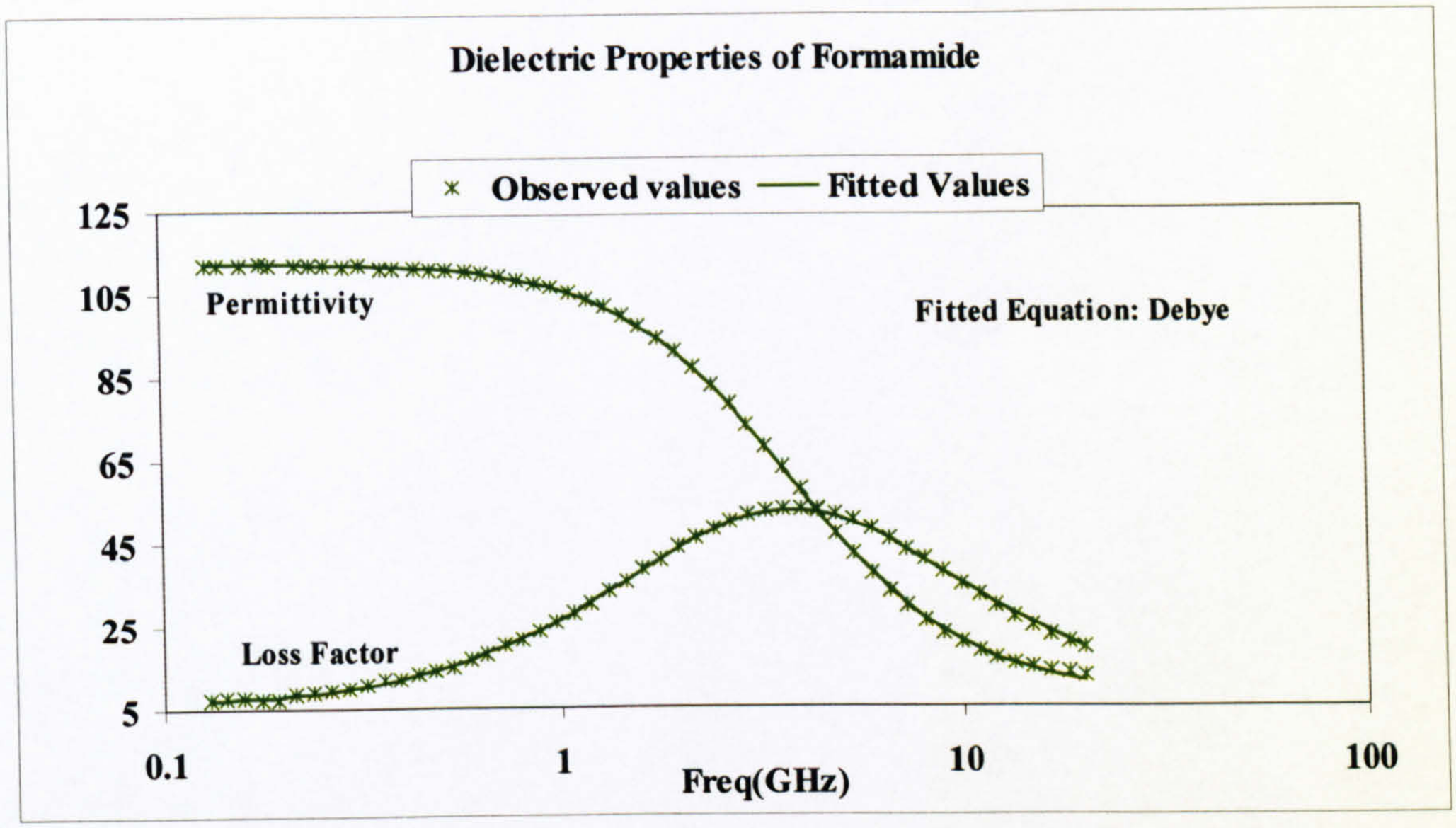

Figure 3.12 Measured and fitted values for dielectric properties of Formamide at 20°C

Table 3.5 Dielectric parameters of Formamide obtained by fitting the experimental results to Equation (3.4) and comparison to literature. The ± term corresponds to the 95% confidence interval

Formamide	Temp	Model used	ε_s	$\pm\varepsilon_s$	ε_∞	$\pm\varepsilon_\infty$	τ (ps)	$\pm\tau$ (ps)	σ S/m	$\pm\sigma$ S/m
This Study	20°C	Debye +Conductivity	112.59	0.16	7.59	0.25	42.12	0.41	0.027	0.003
Jordan et al [6]	20°C	Debye	111.8	0.9	6.9	1	42	1	-	-

Table 3.6 The result of fitted dielectric data for Formamide at certain frequencies obtained in this study and comparison with literature data.

	This study *Debye*		Jordan et al [6] *Debye*		% difference between this study and [6]	
Freq. MHz	ε'	ε''	ε'	ε''	ε'	ε''
400	111.43	10.99	110.64	10.95	-0.707	-0.374
600	110.01	16.26	109.23	16.20	-0.709	-0.370
800	108.09	21.28	107.32	21.20	-0.709	-0.358
900	106.95	23.67	106.20	23.58	-0.710	-0.352

Dielectric properties of Formamide are fitted well to a single Debye model. A conductivity term added to the model improved the fitting results. When the conductivity term is omitted from the calculated values, the result of the dielectric data for Formamide shows a good correlation with literature data [6]. The agreement between the obtained data in this study and those reported in the literature is better than 1% (Table 3.6).

Methanol

The experimental data for Methanol were analysed, first using a single Debye equation, i.e.

$$\varepsilon(\omega) = \varepsilon_\infty + \frac{(\varepsilon_s - \varepsilon_\infty)}{(1 + j\omega\tau)} \tag{3.5}$$

and then employing a Cole-Cole equation:

$$\varepsilon(\omega) = \varepsilon_\infty + \frac{(\varepsilon_s - \varepsilon_\infty)}{(1 + (j\omega\tau)^{1-\alpha})} \tag{3.6}$$

It was found that the program does not fit the values properly when different values of α are introduced. In other words, there was not sufficient evidence to support the model of Equation 3.6. The confidence intervals and correlation coefficients supported the fact that a single Debye dispersion is the best representative of the dielectric data for methanol.

Figure 3.13 shows the experimental data for Methanol fitted to Debye model with the solid line representing the theoretical curve corresponding to Equation 3.5. The parameters obtained from fitting to Equation 3.5 are given in Table 3.7.

Table 3.8 contains the dielectric data for Methanol at certain frequencies obtained in this study and compared to that of literature [9].

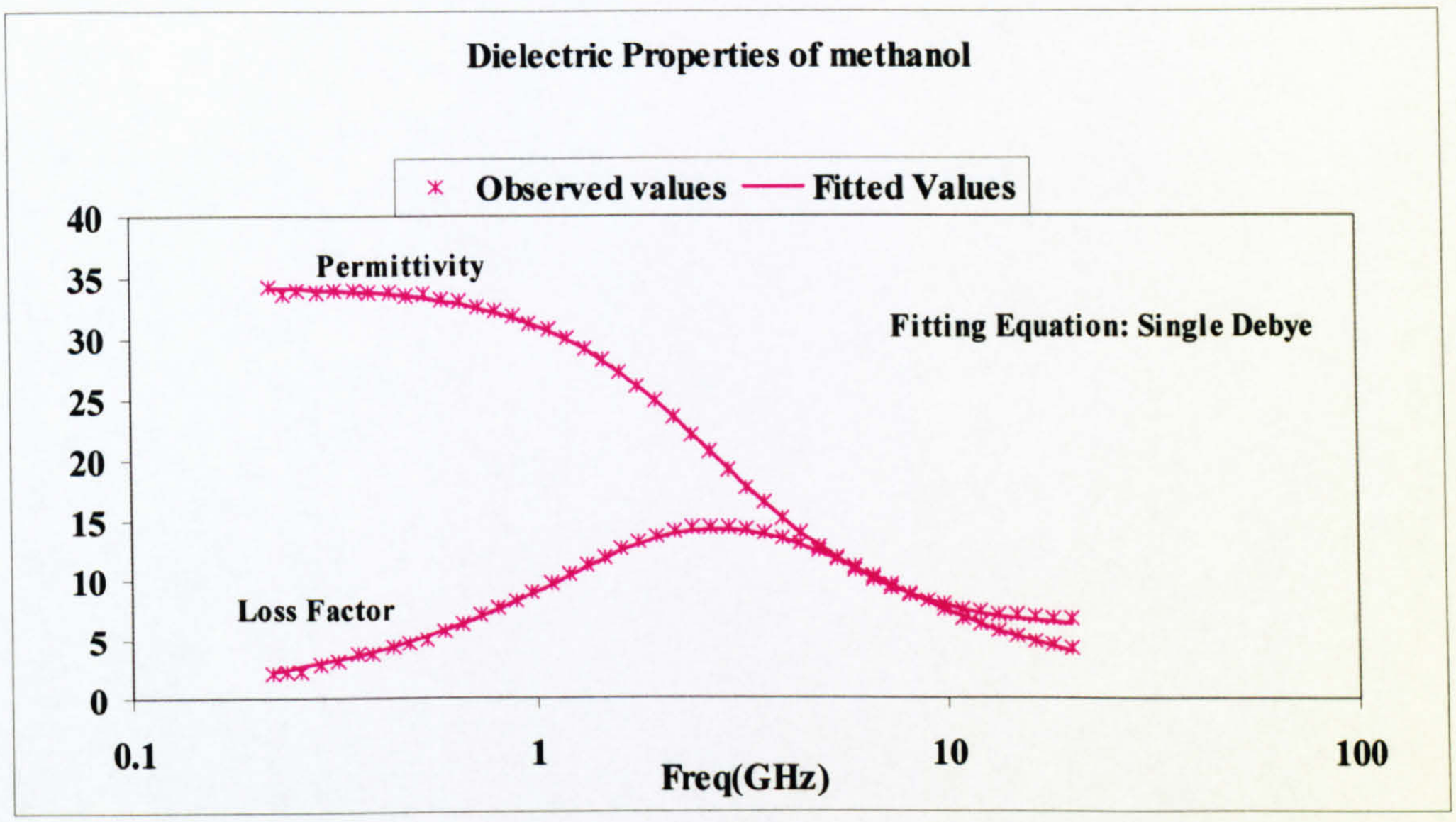

Figure 3.13 Measured and fitted values for dielectric properties of Methanol at 20°C

Table 3.7 Dielectric parameters of Methanol obtained by fitting the experimental results to Equation (3.5) and comparison to the literature. The ± term corresponds to the 95% confidence interval

Methanol	Temp	Model used	ε_s	$\pm\varepsilon_s$	ε_∞	$\pm\varepsilon_\infty$	τ_{relax} (ps)	$\pm\tau_{relax}$ (ps)
This study	20°C	Debye	34.22	0.09	5.72	0.12	56.88	1.04
NPL [9]	20°C	Debye	33.64	0.06	5.68	0.18	56.6	1.05
Jordan et al [6]	20°C	Cole-Cole	34.8	0.5	4.5	0.7	56	2

Table 3.8 The result of fitted dielectric data for Methanol at certain frequencies obtained in this study and comparison with literature data.

	This study *Debye*		NPL [9] *Debye*		% difference between this study and [9]	
Freq. MHz	ε'	ε''	ε'	ε''	ε'	ε''
400	33.65	3.99	33.09	3.90	-1.70	-2.44
600	32.97	5.84	32.42	5.71	-1.68	-2.40
800	32.07	7.53	31.55	7.36	-1.65	-2.36
900	31.55	8.31	31.04	8.12	-1.63	-2.35

The above results show that the dielectric properties of Methanol are better described with a single Debye model. The obtained results didn't support a Cole-Cole model to be a representative of Methanol's dielectric behaviour. Comparing with literature [9], there is about 2% agreement between the values obtained in this study and NPL results.

Dimethyl Sulphoxide

The experimental data for Dimethyl Sulphoxide in the frequency range of 100MHz-20GHz were fitted to the Cole-Davidson. However, the literature data have been fitted to another version of the Cole-Davidson Equation (3.2).

Figure 3.14 shows the experimental data for Dimethyl Sulphoxide fitted to the Cole-Davidson model, with the solid line representing the theoretical curve corresponding to the Equation (3.2). The fitted parameters and their 95% confidence intervals for the Cole-Davidson fit are summerised in Table 3.9.

Table 3.10 contains the dielectric data for Dimethyl Sulphoxide at certain frequencies obtained in this study and compared to that of literature [8].

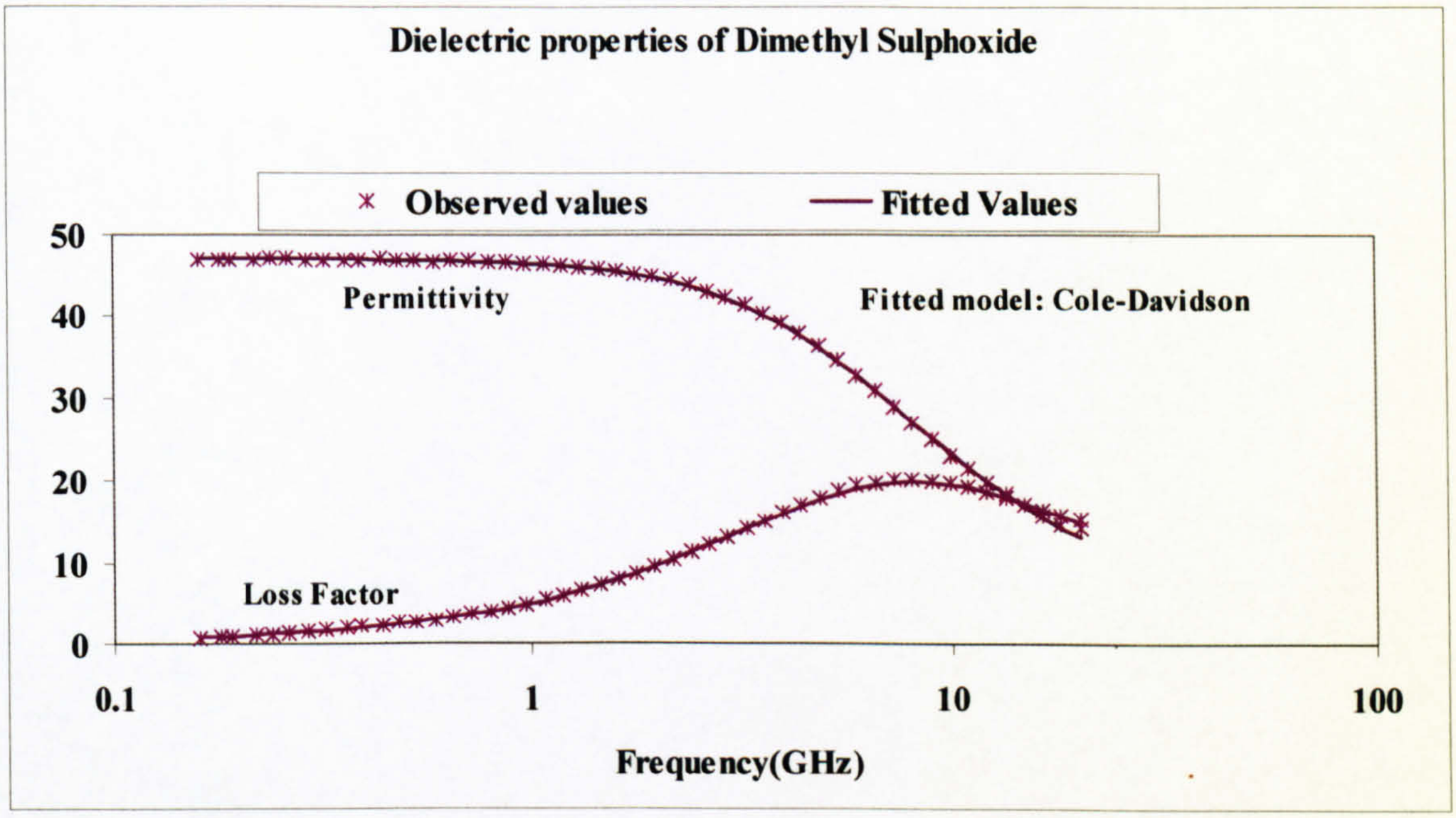

Figure 3.14 Measured and fitted values for dielectric properties of Dimethyl Sulphoxide at 25°C

Table 3.9 Dielectric parameters of Dimethyl Sulphoxide obtained by fitting the experimental results to Equation (3.2) and comparison to literature. The ± term corresponds to the 95% confidence Interval.

Dimethyl-Sulphoxide	Temp	Model Used	ε_s	$\pm\varepsilon_s$	ε_∞	$\pm\varepsilon_\infty$	τ_{relax} (ps)	$\pm\tau_{relax}$ (ps)	β	±β
This study	25°C	Cole - Davidson	47.16	0.07	3.93	0.69	22.8	1.26	0.82	0.03
Kaatze.et al [8]	25°C	Cole-Davidson	47	0.6	3.9	1	21.1	0.2	0.87	0.009

Table 3.10 The result of fitted dielectric data for Dimethyl Sulphoxide at certain frequencies obtained in this study and comparison with literature data

	This study		Kaatze et al [8]		% difference between this study and [8]	
Freq. MHz	ε'	ε''	ε'	ε''	ε'	ε''
400	47.05	2.03	46.90	2.00	0.33	1.23
600	46.92	3.03	46.78	2.99	0.31	1.22
800	46.74	4.02	46.60	3.97	0.29	1.17
900	46.63	4.51	46.50	4.46	0.28	1.15

The results show that when the dielectric properties of Dimethyl Sulphoxide are fitted to a Cole-Davidson model, the results correlate well with literature data [8]. The agreement between the obtained results in this study and the literature values is about 1%.

3-4 Dielectric measurements with impedance analyser

In the last part of this project, an automatic swept-frequency impedance analyser (HP4192A) is used which can cover the frequency range of 10Hz to 10MHz. In this technique, the dielectric parameters are calculated from measurements of the impedance of the probe against an unknown sample. The measured capacitance and conductance are normalised against the parameters of the probe in a reference material *(The detailed description of the technique is presented in chapter 2)*. The accuracy of the technique has been studied when using conical co-axial probes [10,11] and is reported to be about 1% across the frequency range. It is also shown that the electrode polarisation errors affect the results below 1 kHz. This does not affect the data in this study as the frequency range of interest was outside the region in which electrode polarisation occurs.

The sources of errors and the ways to overcome these are mentioned in detail in chapter 6. However, it is necessary to note that for practical reasons, instead of conical probes, specific parallel plate electrodes were used in this project. This limited the process of reducing the measurement errors, as it was not possible to optimise the performance of the probe.

In this section, the experimental result of dielectric measurements on Formamide is presented using parallel plate probes. This is to demonstrate the performance of the impedance analyser HP4192A by itself.

3-4-1 Measurements results

It is important to choose an appropriate reference material for dielectric measurements when using the impedance analyser. The reference material should have well known dielectric parameters similar to the sample to be measured. Here, a series of salt solutions together with the liquids of interest were measured using the network analyser HP8753C. The material, with the closest dielectric properties to the liquid of interest, is chosen to be the reference material in the impedance analyser measurements. Figure 3.15 shows the conductivity of a series of salt solutions and Formamide measured by the network analyser in order to find the best match for Formamide. The 0.007Molar NaCl has been chosen to use as reference material for the dielectric measurements of Formamide.

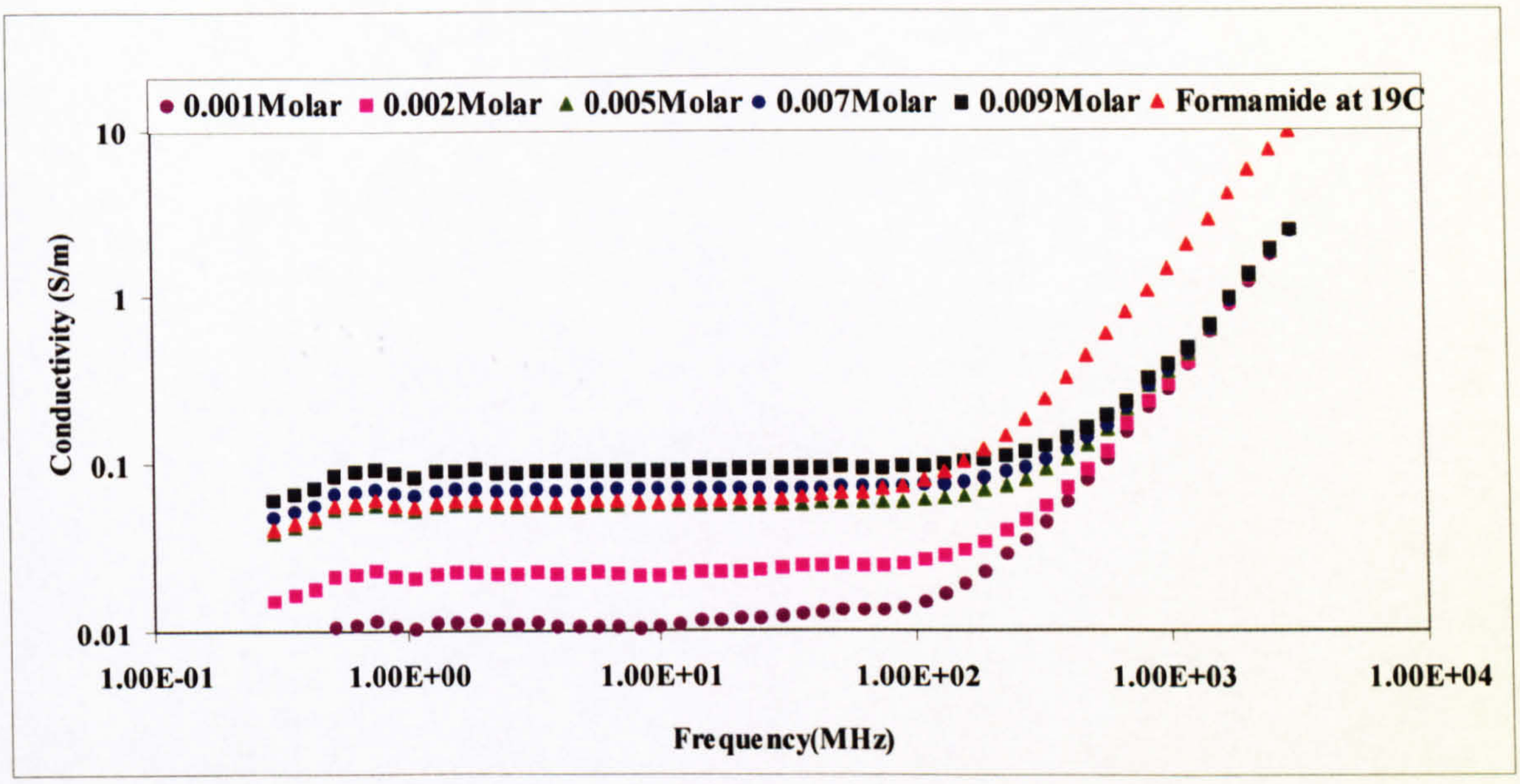

Figure 3.15 Conductivity of a series of salt solutions and Formamide at 19C measured by network analyser HP8753C.

The result of dielectric measurements on Formamide using the impedance analyser is shown in Figure 3.16.

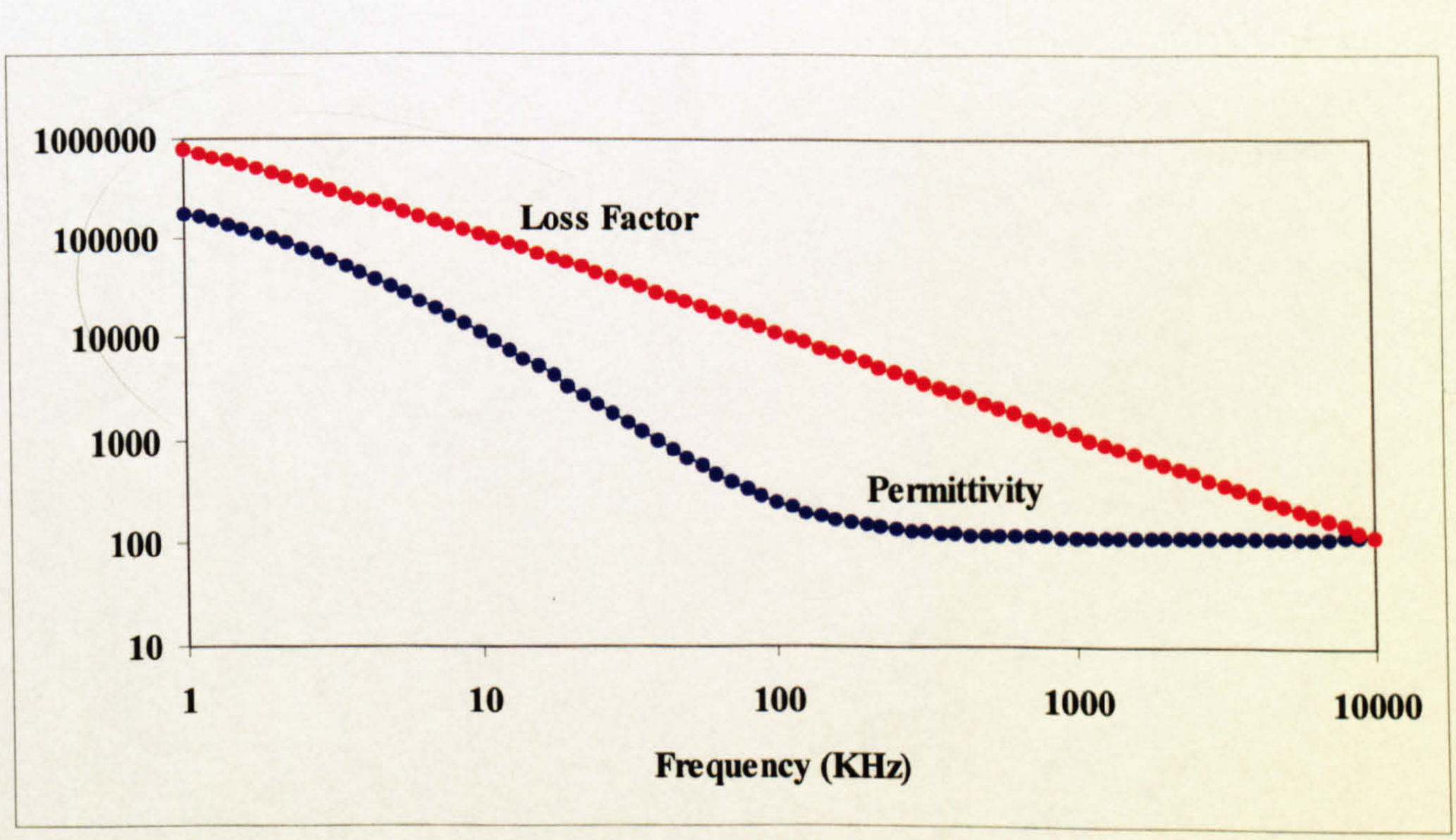

Figure 3.16 Dielectric properties of Formamide measured by impedance analyser HP4192A.

Although one expects to have electrode polarisation effects at frequencies below 1 kHz, there are still evidences of this phenomenon in the dielectric spectrum of Formamide measured by the impedance analyser and parallel plate electrodes shown in Figure 3.16. This may be due to the material that the probe is made of or, the fact that the probe used is not optimised.

3-5 Discussion

Experimental dielectric measurements on four different standard liquids (Ethanediol, Formamide, Methanol and Dimethyl Sulphoxide) showed that the reproducibility of measurements are better that 1% in most of the frequencies in the spectrum covered by two network analysers.

The mathematical analysis of the experimental data showed that the results for all four liquids are in good agreement with literature data (between 1-2%).

A Cole-Davidson model best describes the dielectric spectrum of Ethanediol, while a single Debye model plus conductivity term is the best description of the dielectric behaviour of Formamide.
Dielectric properties of Methanol are fitted well to a single Debye model and a Cole-Davidson model best represents the dielectric behaviour of Dimethyl Sulphoxide.

The outcome of the dielectric measurements of standard liquids in this chapter indicates that the techniques used throughout this project are accurate and are within 1-2% agreement with literature data.
The reproducibility of the measurements is typically better than 1% in most frequencies for all the liquids used (e.g. Figures 3.2and 3.6).

References for chapter 3:

[1] Gabriel C, Chan T Y A and Grant E H 1994, "Admittance models for open ended coaxial probes and their place in dielectric spectroscopy", *Phys.Med.Biol.* **39** 2183-2200.

[2] Chan Tsing Yee Amy1993, "Numerical analysis of open-ended coaxial line sensors with application to dielectric measurements up to 20GHz " PhD Thesis, University of London

[3] Sheppard R J, Jordan B P and Grant E H, 1970, "Least squares analysis of complex data with applications to permittivity measurements"" *J.Phys.D.*, **3** 1759-64.

[4] Hill N E, Vaughan W E, Price A H, and Davies M (1969), *Dielectric Properties and Molecular Behaviour*. London, Van Nostrand.

[5] Grant E H, Keefe S E and Shack R 1972,. *Adv. Mol. Relax. Proc.* **4** 217.

[6] Jordan B P, Sheppard RJ and Szwarnowski S, 1977, "The dielectric properties of Formamide, ethane diol and methanol", *J.Phys.D:Appl.* **11** 695-701.

[7] Levin V V and Podlovchenko T L, 1970, "Dispersion of The Dielectric Permittivity of Ethylene Glycol" *Zhurnal Strukturnoi Khimii* , **11** 766-767.

[8] Kaatzee U, Pottel R and Schafer M, 1989, " Dielectric Spectrum of Dimethyl Sulphoxide/Water Mixtures as a Function of Composition", *J.Phys.Chem.* **93** 5623-5627.

[9] NPL, Report CETM 33, Tables of the complex permittivity of dielectric reference liquids at frequencies up to 5 GHz, Sept. 2001.

[10] Gabriel C and Grant E H 1989, "Dielectric sensors for industrial microwave measurements and control", *Microwellen HF Mag.* **15** 643-5.

[11] Gabriel S, Lau R W and Gabriel C., 1996, "The dielectric properties of biological tissues:II Measurements in the frequency range 10Hz to 20 GHz" , *Phys.Med.Biol.* **41** 2251-2269.

[12] Kraszewski A, Stuchly S S, Stuchly M A and Symons S A, 1983, " On the measurement accuracy of the tissue permittivity *in vivo*", *IEEE Trans.*,**IM-32**, (1), 37-42.

[13] Gabriel C,1993,"Numerical Modelling of Fringing Fields and Their Use For Complex Permittivity Measurements at High Frequencies", Brooks Air Force Base, Technical reportAL/OE-TR-1993-0068.

Chapter 4- Dielectric spectroscopy for compositional analysis of biological material

4-1 Introduction

Knowledge of the amount of added water and other additives to food materials is an important issue in the food industry. Water can be added to food material during the processing. The deliberate addition of water along with other additives to some of the food materials can be justified on some technological grounds such as the reduction of drip-loss from the product or the retention of nutrients and possible antioxidant effects [1]. Using dilute brine solutions for flavouring can also change the amount of water held in the food. However, there are concerns about the misuse of adding water to foodstuff, e.g. increasing the profit margins by selling water instead of the actual product. The chemical and analytical measurements of the additives to food materials are destructive and lengthy, especially for added water. These problems make it necessary to find a relatively easier and less time-consuming technique for compositional studies. It has been shown that the microwave dielectric properties of food materials along with some statistical techniques may provide a solution [2].

The dielectric properties of biological materials, which contain water, are dominated by the polar nature of water itself. This fact has been used to find ways of determining the water content of the biological systems, especially foodstuff [3].

As mentioned in chapter 2, the dielectric response of materials to microwaves is characterised by their complex permittivity, $\hat{\varepsilon}$, which is defined as:

$$\hat{\varepsilon} = \varepsilon' - j\varepsilon'' \tag{4.1}$$

The real part ε' is called permittivity and is a measure of the amount of polarisation produced by an electric field and the imaginary part ε'' is the loss factor associated with

it. The loss factor represents the ability of a material to dissipate electromagnetic fields in the form of heat. The loss factor can be due to both dipolar and ionic conduction losses and may be also expressed as follows:

$$\sigma = \varepsilon'' \varepsilon_0 \omega \qquad (4.2)$$

where σ is the conductivity, ε_0 is the permittivity of free space and ω is the angular frequency of the field. Dielectric properties directly depend on the polarisation of a material under the influence of an applied electric field. The major contribution at microwave frequencies is from molecular orientation polarisation. In a static field this leads to dipolar molecules being orientated in a direction opposite to the applied electric field. When this field is removed, the dipolar polarisation decays slowly. The time for build up and decay of dipolar polarisation (the relaxation time) depends on the size and shape of the dipolar molecules of which the material is made. In the frequency domain this results in a dispersion or relaxation spectrum with maximum loss at the relaxation frequency. The dielectric properties of foods are complex and vary with frequency and temperature. These variations depend, among other things, on the dipolar relaxation frequencies of the polar molecules involved. Therefore, the shape of the dielectric spectrum over a range of frequencies can give us information about the material composition [2,4].

Water added to foodstuffs can have quite different effects on the shape of the dielectric spectrum. In the native state the water has a particular range of relaxation frequencies dictated by its interactions at the molecular level with other constituents in the tissue. As water is added other constituents, notably ionic salts, become diluted and these can also diffuse into the exterior water. This causes a fall in loss factor, ε'', at low frequencies because the dielectric losses depend on both polar and ionic conduction effects. The latter increases with decreasing frequency. On the other hand polyphosphate or NaCl solutions add conducting ions as well as water and the resultant spectrum is quite different showing a markedly increased loss factor at low frequencies (Figure 4.1b). A typical dielectric

spectrum of some pork products with different amount of added water (0-20 % of total weight) is shown in Figures 4.1a and 4.1b.

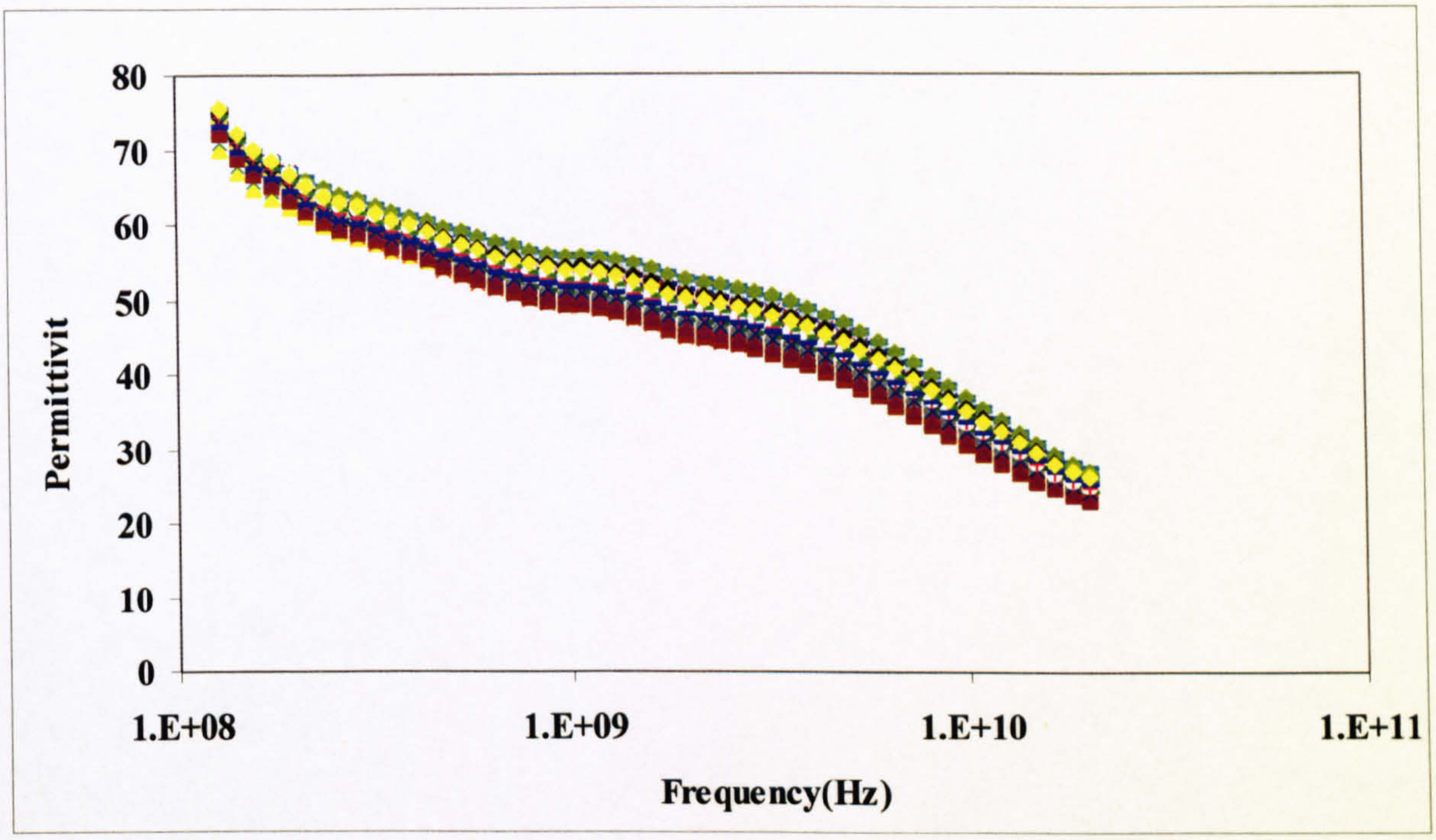

Figure 4. 1a

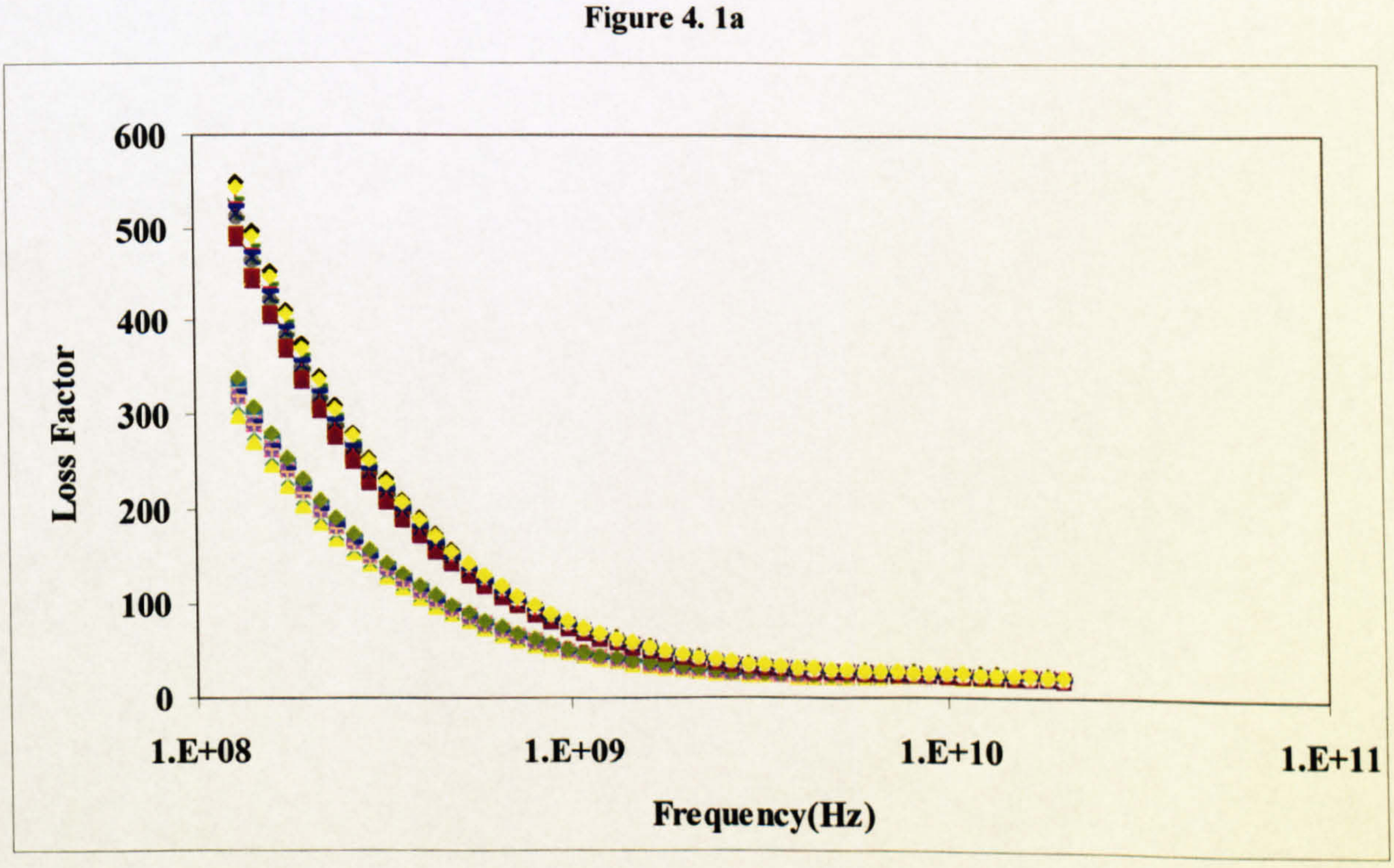

Figure 4.1b

Figure 4.1: a Permittivity and **b** loss factor of 35 pork samples with different amounts of added water

The main dispersion above 1 GHz in the dielectric spectrum is attributed to the polarisation of the aqueous component of biological material and is known as the γ dispersion. Its spectral parameters correlate with the water content and can provide a means to determine this component. However, the range of relaxation frequencies for water is affected by interactions at the molecular level with other constituents in the material.

The main aim here was to investigate the extent to which dielectric spectroscopy can be used in the determination of added water and other composition variables in pork products.

One way of achieving this goal is to develop a model to describe the spectrum in terms of the components contributing to different elements of the spectrum. Then the parameters that describe the spectrum can be extracted and correlated with the compositional variable of interest.

However, the dielectric data of complex biological systems such as foodstuffs may be influenced by more than one component and such a model would require too many assumptions about the underlying causes of the spectral shape. This can lead to missing some important variation in the spectrum.

The other method is to directly regress the variables of interest against values of the dielectric spectrum at specific frequencies. Because of the high degree of co-linearity between adjacent parts of the spectrum it is often impossible to perform a multilinear regression and choice of frequencies at which to make the measurements becomes constrained. Such an approach has been taken in the determination of moisture content of wheat using well-separated frequencies in the spectrum [5].

Because of the above problem, in this work, a multivariate analysis approach is proposed to determine the dependence of the dielectric data on the analytical composition of processed meat samples. The dielectric spectrum is transformed by using a multivariate analysis technique called Principal Component Analysis (PCA). This will produce sets

of uncorrelated orthogonal variables that can be used in regression equations independently. In the last few years the PCA technique has been applied to dielectrics with some success [2, 6, and 7].

4-2 Statistical tool

4-2-1 Principal Component Analysis (PCA)

The multivariate approach of the Principal Component Analysis (PCA) reveals the relationships among a set of correlated variables. In other words, PCA decomposes the data to detect 'hidden phenomena'. One of the objectives of using principal component analysis (PCA) is to reduce a large number of variables to a smaller number with almost the same amount of information. In PCA a linear transformation is applied to a set of correlated variables to produce a new set of uncorrelated variables called 'Principal Components', (PCs) [8]. These components are a linear combination of the original variables; in this case the complex spectral values. This is expressed as follows,

$$Y_j = a_{1j}X_1 + a_{2j}X_2 + \ldots a_{pj}X_p \qquad (4.3)$$

where Y_j is the j th PC, the Xj s are the mean centred and standardised original variables (in this study: ε' and ε'') and the coefficients in the eigenvector a_{ij} are constants referred to as 'loadings'.

The PCs are orthogonal and the loadings are calculated in sequence by maximising the variance of each PC. Often the first few PCs account for a large proportion of the total variance of the original set of variables. If this is the case, they may be used to summarise the original data and as an input to further analyses. The concept of variance is very important in PCA. The main assumption in this analysis is that there is a more or less direct relationship between maximum variance and the 'hidden phenomena'. PCs are

derived in decreasing order of importance. In other words, the first PC contains as much as possible of the variation in the original data and is in the direction of the largest variance. The second PC lies along a direction that is orthogonal to the first PC and in the direction of the second largest variance and so on. The aim of PCA is to see if the first few PCs account for most of the variation in the original data. The information on the proportion of the variance associated with each PC is given by eigenvalues associated with the eigenvectors.

4-2-2 Principal Component Regression (PCR)

An important result of PCA is that the transformed variables are orthogonal and uncorrelated and can thus be used in regression equations independently. After PCA, principal component regression is carried out. The variables of interest (compositional variables in this study) can be regressed against those PCs that are associated with the most of the variance.

Each time a PCR is performed a calibration equation (regression equation) is obtained for each variable of interest. This equation consists of regression coefficients resulting from regressing the variable of interest against those PCs selected before. The equation can then be tested for a different set of unknown data (validation).

There is no specific rule on how many PCs should be chosen for the regression and it is always up to the analyst to decide how many PCs to use in the model. Some statistical texts recommend choosing the PCs with associated eigenvalues greater than or equal to one [8]. However, here the number of PCs used has to remain within MAFF guideline [9] of being a number less than one third of the number of samples used in the calibration.

When the calibration equation is obtained, the PCs for the unknown spectra in the validation set can be obtained by multiplying the validation data by the PC loadings calculated from the calibration set. The validation data must be standardised and mean centred using the calibration data. The new PCs are then used together with the

calibration equation to predict the values of the variables of interest. The difference between the predicted values and the actual values are used to obtain the amount of error in the prediction.

The result of any PCR can be summarised by the following parameters:

1- Adjusted Coefficient of determination (R^2):

A statistic that is widely used to determine how well a regression fits is the coefficient of determination. It can be expressed as:

$$R^2 = 1 - \frac{Variance(residuals)}{Variance(total)} \tag{4.4}$$

where residuals are the difference between the predicted and actual values. Mathematically, R^2 is expressed as:

$$R^2 = 1 - \frac{\sum_{i=1}^{n}(y_i - y_{predicted})^2}{\sum_{i=1}^{n}(y_i - y_{mean})^2} \tag{4.5}$$

where n is the number of observations, y_i is the ith observation of y (actual value), $y_{predicted}$ is its prediction and y_{mean} is its mean.

R^2 is the most common form of expressing the correlation between two variables and represents the proportion of total variation that is explained by the linear regression model. The coefficient of determination can have only positive values ranging from $R^2 = +1$ for a perfect correlation (positive or negative) down to $R^2 = 0$ for a complete absence of correlation. The advantage of the coefficient of determination, R^2, is that it provides a measure of the strength of the correlation. It is also true to say that the coefficient of determination gives the percentage of the explained variation (by the linear regression) compared to the total variation of the model. Thus R^2 is a relative measure of the "goodness" of fit of the observed data points to the regression line. For example, $R^2 = 0.7$, means that 70% of the total variation in the observed values is

explained by the linear regression. If the regression line perfectly fits all the observed data points, then all residuals will be zero, which means that $R^2 = 1$. In other words, a perfect straight-line fit will always yield $R^2 = 1$. The lowest value of R^2 is 0, which means that none of the variation in observed values is explained by the linear regression. The R^2 can be inflated by the addition of independent variables to the model. Therefore often instead of R^2 an adjusted value is used because the latter is adjusted for the degree of freedom of the model and represents the variation in a more realistic way. The reason for this adjusting is to avoid the danger of overfitting (will be explained in detail later) and to give a realistic impression of the prediction error.

$$R^2(adj) = 1 - (1 - R^2)(\frac{n-1}{n-p-1}) \tag{4.6}$$

Where n is the number of observations (samples) and p is the number of regression coefficients. In this report all the calculated R^2s are the adjusted values and are expressed as %.

2- Standard error of calibration (SEC):

The standard error of calibration SEC is a direct measure of the modelling error (sources of errors could be sampling, measurements and analysis). SEC is calculated from the calibration residuals (the difference between predicted and actual values). It is expressed as:

$$SEC = \sqrt{\frac{\sum_i (y_i - y_{predicted})^2}{n-p-1}} \tag{4.7}$$

Where n is the number of samples (observations) and p is the number of coefficients in the regression equation. Clearly it is a measure of the spread of the results around the calibration line.

3- Standard error of prediction (SEP):

The standard error of prediction is a comparable variable to the SEC but is calculated from the validation data set. It is a direct measure of the prediction error. SEP expresses the error we can expect in future predictions.

$$SEP = \sqrt{\frac{\sum_i (y_i - y_{predicted})^2}{n-1}} \qquad (4.8)$$

High SEP means either a poor model or a non-representative validation set. The smaller the SEP the better the results.

Since in this project all the compositional variables are expressed as %, therefore the SEC and SEP values are also expressed as %. For example SEP =5 means that the variable of interest can be determined within approximately ±5%.

4-2-3 Internal Cross Validation (ICV)

Sometimes even when the measured data do not contain the information that conforms to the proposed group structure, it is still possible to obtain good classification results for the samples used in the modelling procedure. However in such instances the success rate of classification is unlikely to hold for new samples. This phenomenon is referred to as overfitting. Any situation where the data analysis produces over-optimistic results (results that will not be satisfactory for unknown data) due to inappropriate use of the method is regarded as over-fitting [9].

The best way of avoiding overfitting is to carry out a validation step. This can be achieved either with using a completely independent test set or the method of internal cross validation (ICV). In ICV, a part of the data is used to make a calibration model while the rest is used to test the model. This is repeated until all the samples have been used in calibration and validation. For a small number of samples it is recommended by

statistical texts to make as many models as there are samples but each time leave one of the samples out and only use it for testing. Cross validation is the best alternative we have when there are not enough samples for a separate test set.

4-3 Calculation of added water

In order to produce a model (calibration equation), information are needed about the added water and other compositions of different samples. It is also important to notice that the method can only be as good as, no better than, the method used to calibrate it. Therefore, the more accurate the calculation of added water and other compositions, the better the expected results should be.

The standard way in which added water is calculated [11] is to measure all the compositional variables by various means, then to calculate the added water using what is assumed to be the known characteristics of an unadulterated sample. The method to calculate the added water in meat products is described in Appendix 1.

In calculating the added water, the proportions of meat (including fat), additives, and salt (NaCl) values are needed. Additives can be carbohydrates, polyphosphate, and nitrate / nitrites etc. The meat content is calculated from the total nitrogen content, which is assumed to be partly due to protein and partly to added carbohydrate. The proportion of nitrogen in the carbohydrate is assumed to be 2% of the carbohydrate mass. Also the proportion (percentage) of nitrogen in meat is needed in estimating the meat content of pork products. This so-called nitrogen factor (NF) can vary with age and weight of the animal and also with the particular joint or cut taken from the carcass. It will also depend on whether fat and skin are included in a particular joint. There will be considerable doubt about NF for products made of several components. It can vary from 3.4 for neck or collar joints up to 3.9 for loin or back containing rind. A figure of 3.5 has been recommended for general use in the analysis of pork products [12] which is also very

close to that measured for the defined national (UK) average processing carcass (70 kg weight with 12.3 mm back fat). It is important therefore to understand that both the errors of measurement of composition and the error in the assumed NF contribute to uncertainty in the added water determination.

4-4 Materials and methods

4-4-1 Sample preparation

Throughout this work four series of samples have been measured and analysed. The samples were categorised into canned pork, supermarket samples, and prepared meat. At the end a series of samples have been prepared especially according to factory procedures.

The result of chemical analysis on all samples for total moisture content, Fat, Ash (liquid, semi solid and solid products), Protein, and salt (NaCl) were available. The added water content then was calculated from these values (Appendix 1).
For some samples, the actual added water values were available.

In this report the added water values are referred to as **actual values** or **calculated values**. The actual values are the amount of water nominally added to the pork samples and the calculated values are the result of calculation of added water using the other compositions obtained from the chemical analysis. Also, in the case of canned pork, the actual values for added salt were available.

For the last two sets of samples, several were designated as 'blind' and initially no compositional values were determined until after the experiments.
The detail of preparing each category of samples are described in the following:

Canned pork:

35 samples were prepared by blending known amounts of water, salt and phosphate to lean pork meat. The range of added water was 0-20%, added salt 0-4%, and added phosphate 0-0.2% of the total weight. All samples had 150 ppm of nitrite. The mixtures were canned before analytical and dielectric measurements. It was found that some of the water had been separated from the meat on the opening of the cans. Therefore, samples were blended again with their excess water to make a homogenous paste and the mixtures were used for dielectric measurements.

Both actual and calculated values for added water and salt were available for canned pork samples. For the rest of the compositions, only the calculated values were available.

Supermarket samples:

Although the canned pork results demonstrated the potential of the used method to predict the added water content, it was essential to have a set of samples with variation in all composition variables. The samples collected from supermarkets fulfilled this requirement.

The supermarket samples contained 30 samples of pork products both cooked and raw with different descriptions of cut such as leg meat, ham and streaky bacon. Also different processing types of samples were included, such as smoked, honey roasted, cured and dry-cured.

Prepared Meat:

In order to investigate the variability caused by differences between one product and another, various samples were prepared with no added water and then known amounts of water were added to them. Samples were well mixed and homogenised. The added water contents ranged from 0 to 25% of the untreated sample weight.

These samples were categorised as leg meat, streaky bacon and ham with 30 samples in each category. Although each category consisted of 30 samples, the chemical analysis

data were not provided for all those samples. The number therefore ranged from 27 to 30.

Within each category 4 samples were labelled as unknown (compositional values not provided in the first instance). Dielectric measurements were also carried out on the unknown samples for validation of the method.

Factory samples

The last set of samples (26) were prepared from pork leg meat according to factory procedures, to represent commercial samples prepared under controlled conditions. The added water and salt content varied in different samples.

4-4-2 Dielectric measurements

The dielectric measurements were carried out over 51 frequencies, in the frequency range of 130MHz to 20 GHz, using an open-ended coaxial probe and a computer controlled network analyser following a previously reported procedure [10]. At least three measurements were carried out at room temperature, for each sample and average values were calculated to produce the raw data. On some occasions spoiled data were rejected due to air bubbles or a liquid filled depression being close to the dielectric probe.

For the first set of samples (canned pork), the temperature of the samples were recorded at the time of the measurements. For this set of samples, temperature was included in the calibration data. The variation in temperature was small (20.5° ± 0.6), therefore, for the rest of the samples, temperature was not included in the calibration data.

The 51 measured frequencies were reduced to an approximately harmonic set of 9 frequencies. This gives 18 dielectric variables (ε' and ε'') which were used as a calibration set of data.

4-4-3 Statistical analysis

Generally, all samples have been subjected to the following statistical analysis:

- In order to reduce the errors in computation due to the large differences in magnitude of different variables, the reduced dielectric data were standardised using the mean and standard deviations of the calibration.

- The standardised complex spectra were then subjected to PCA and PCR. In the case of canned pork the temperature data was also included in the calibration.
- The number of PCs was kept at 7 or less for individual sample sets. In the case of pooled data when the number of samples were very large, 10 PCs were used without risk of overfitting.
- Internal cross validation (ICV) was used for each data set by removing one sample at a time and using it as a validation data set and the calibration obtained without it. When the data were pooled (all types of pork meat) and the number of data were large, a random set of samples was removed from the complete set and used to validate the calibration obtained without them.

All the calculations were done by using the Excel spread sheet and a statistical package called 'Minitab'.

Any further action and analysis performed on different samples are explained in details in the followings:

Supermarket samples

In the case of supermarket samples, initially, analysis was made on the complete set of 30 samples, including cooked and raw products and different cuts e.g. ham and bacon. In

the next stage, the samples were separated into two groups of ham and bacon. This helped investigating the effect of sample types. Since the number of samples was reduced to 15 in each group by this separation, the maximum number of variables permitted in the PCA was restricted to 14. This was because the number of samples must be greater than the number of variables used.

Also when performing the internal cross validation procedure, here only 14 of the 15 available samples would be used at any time and this is another constraint on the number of frequencies. Considering all these facts, for more accurate results, 6 frequencies were chosen for the analysis.

In addition the number of PCs used in the regression was reduced to 5.

Prepared meat

For these samples PCA and PCR were carried out for each sample category separately (leg meat, streaky bacon and ham). Then all data were pooled together and the statistical analysis carried out for the pooled data.

In predicting the composition of unknown samples, two approaches were used. First separate calibrations were used, each relevant to the type of each sample, and second, all data were pooled and one single calibration was used for all the samples.

Pooled calibration

Experience with the prepared samples showed that combining all the samples into one calibration eliminated the effects of correlation between the compositions of the samples. Similar practice can be done with all the measured data. Therefore, the dielectric data of canned pork, supermarket samples and prepared samples were all pooled together (149 samples). In this case the number of samples was very large, instead of doing ICV, a random selection of 120 samples was removed and used as a calibration set. The remaining 29 were then used to validate the model. Because of the large number of data 10 PCs were used.

Factory samples

As mentioned before, the factory samples were of pork leg meat and prepared according to factory procedures to represent commercial samples prepare under controlled conditions.

The aim was to use all available data from previous measurements (canned pork, leg meat, bacon, ham and supermarket samples) as a pooled calibration and use it to predict the composition of these latest samples. The pooled calibration consists of 120 randomly selected samples from canned pork, homogenised leg meat, streaky bacon, ham and supermarket samples. Because the number of calibration data is quite large, it is safe to use 10 PCs instead of 7 and avoiding the problem of overfitting.

Grand pooled calibration

A good practice of examining the potential of data obtained in this project is to pool all data to one grand calibration. This calibration is then used to predict the composition of all unknown samples (blind), supplied throughout the project. Because the actual added water was not known for the supermarket samples, when all the data were pooled into one 'Grand' calibration, only the calculated added water could be considered. Again because the number of calibration data was large, 10 PCs were used and this was permissible under the MAFF guideline. To validate this grand calibration, different blind samples supplied throughout the project were used.

4-5 Results and observations

The maximum percentage of standard deviation in the dielectric measurements was up to 5% for ham samples and 7% for bacon samples. In the case of prepared meat at a couple of occasions where the samples were not blended very well the maximum variation of 15% was observed, but for most of the samples variation lied between 0.1-5%.

The result of PCA and PCR for each sample category is summerised below:

Canned pork

The results of the prediction of different compositional variables for canned pork samples are shown in Figures 4.2a-e. Also the results of PCA and PCR carried out on the canned pork samples are summerised in Table 4.1.

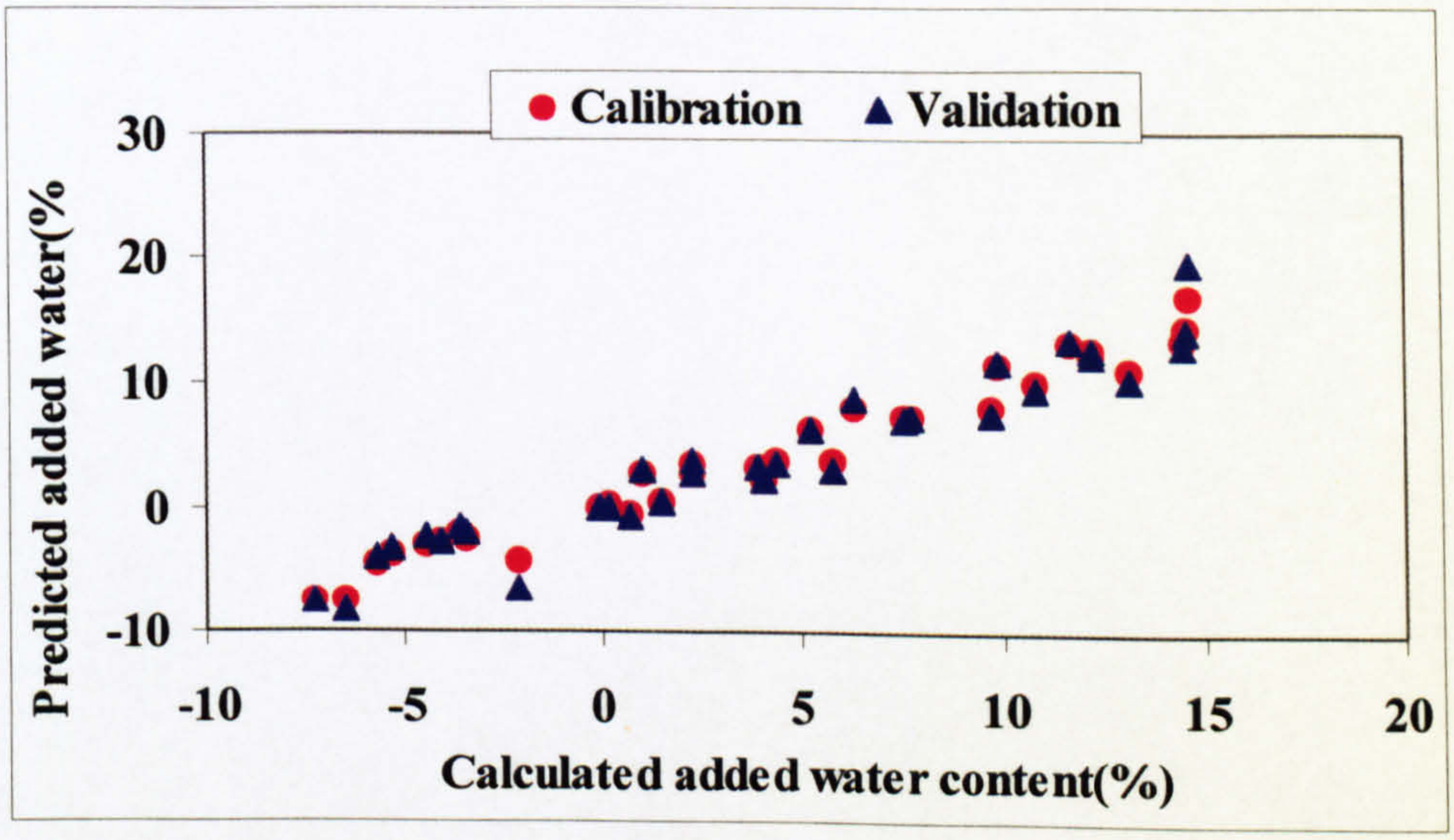

Figure 4.2a

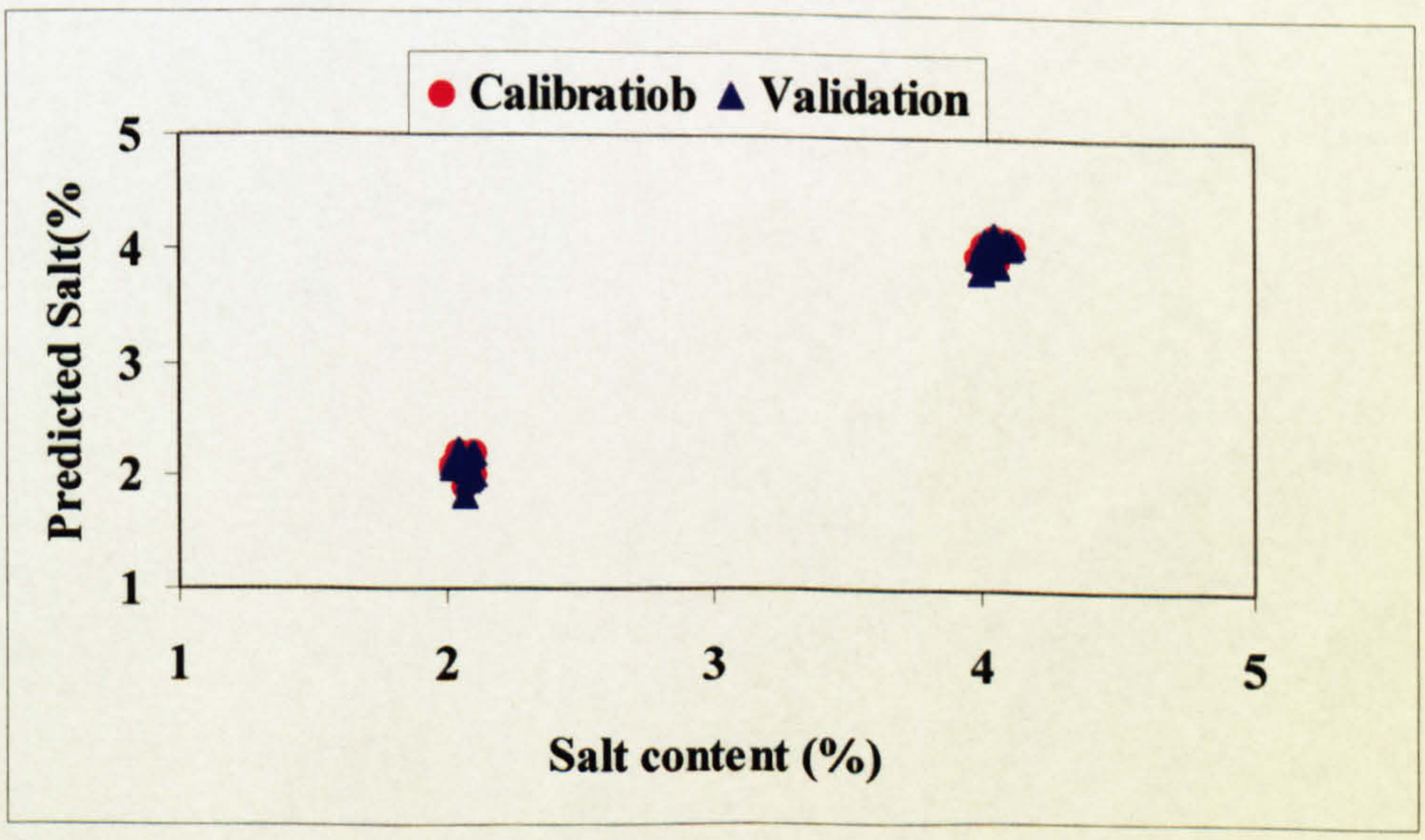

Figure 4.2b

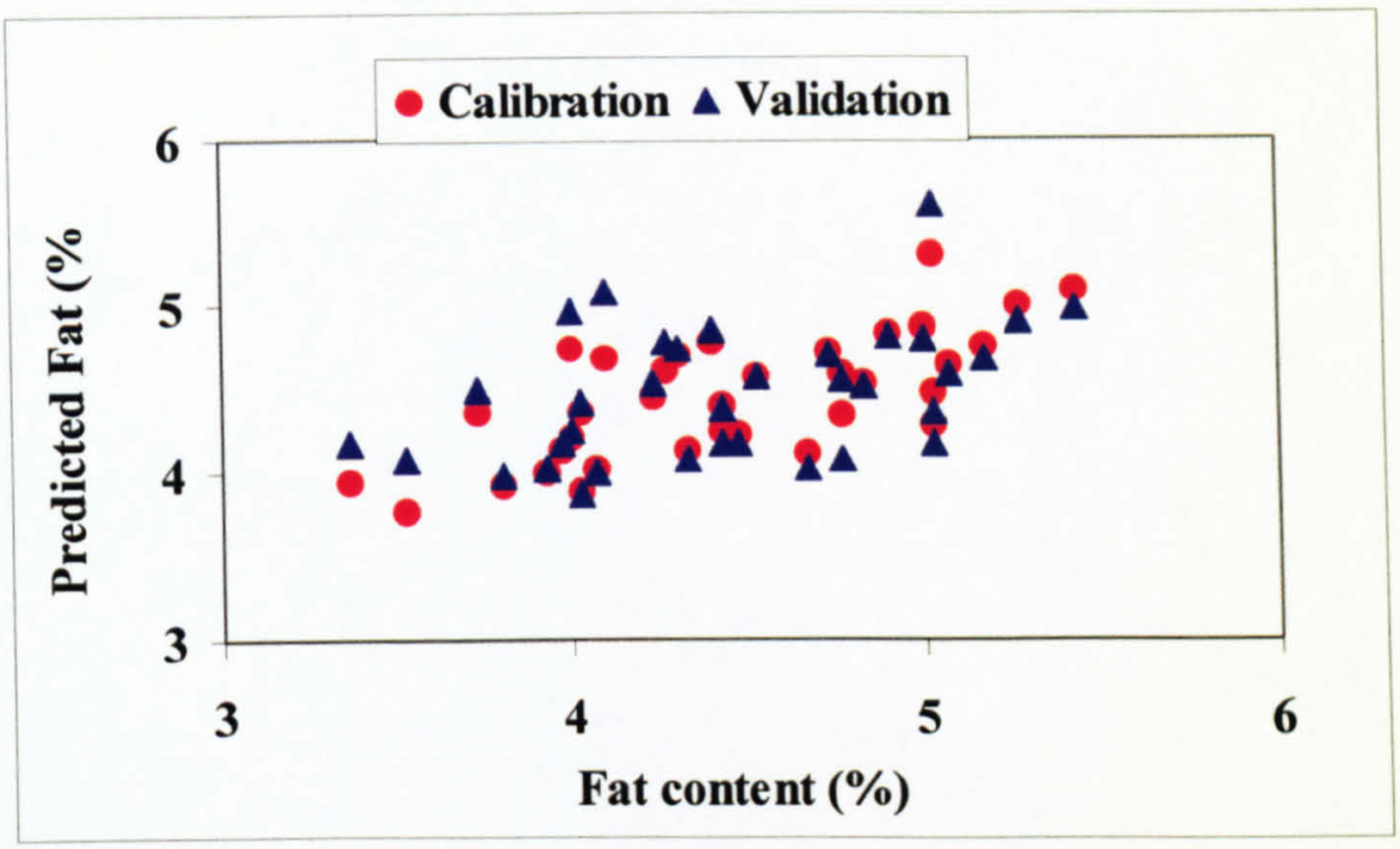

Figure 4.2c

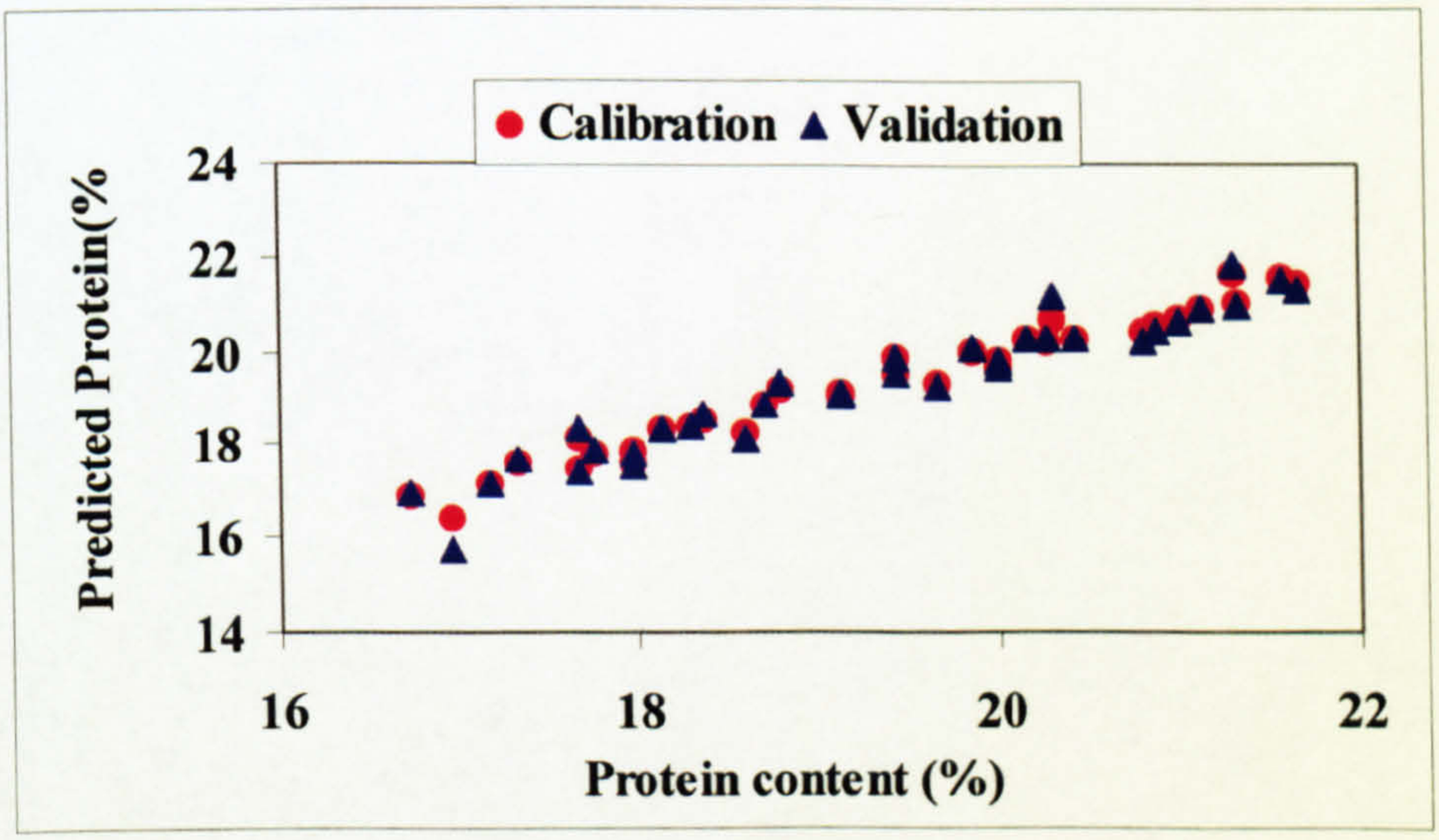

Figure 4.2d

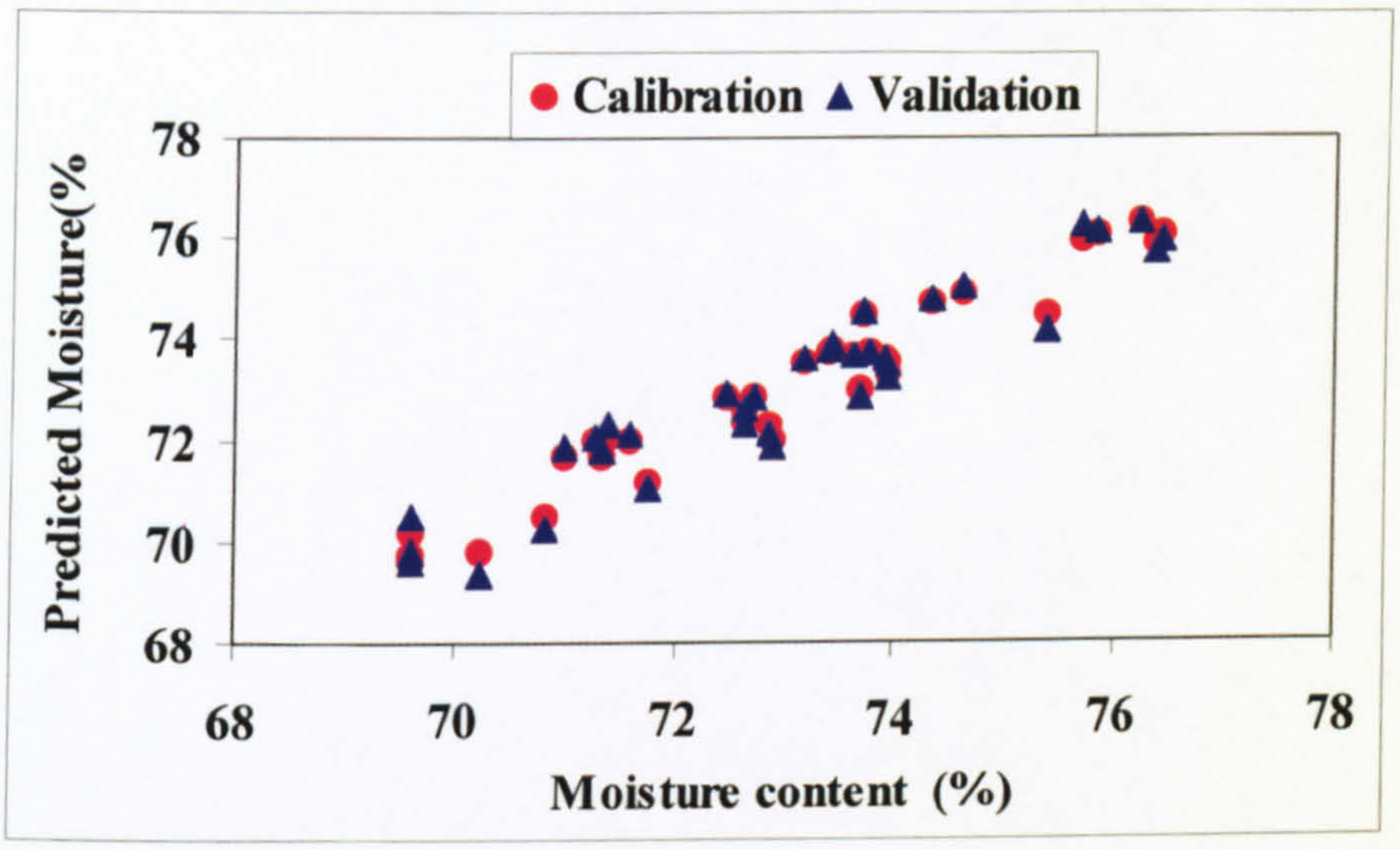

Figure 4.2e

Figure 4.2: Prediction of **a** added water **b** salt **c** fat **d** protein and **e** moisture content of canned pork samples

Table 4.1. Results of PCA and PCR for canned pork samples (7 PCs used)

	R^2_{adj}	SEC	SEP
Moisture (%)	92.6	0.5	0.6
Fat (%)	36.3	0.4	0.5
Protein (%)	95.7	0.3	0.4
Salt (actual) (%)	99.5	0.07	0.09
Salt (calculated) (%)	99.4	0.1	0.1
Added water (actual) (%)	90.3	2.07	2.5
Added Water (calculated) (%)	95.5	1.4	1.89

When using the actual values, the added water content can be determined to within approximately ±2.5% (Table 4.1). When using the calculated values of added water, the SEP drops to ±1.89%.

Added salt can be predicted to within ±0.09% and ±1% when using actual and calculated values respectively. In the case of salt there are only two groups of data with a wide spacing, which will automatically give a high R^2. However the fact that only two levels of salt content (2 and 4%) were considered makes the fitting of the model mathematically unsound.

It can be seen from Table 4.1 that protein and moisture can be predicted to within ±0.4% and ±0.6% respectively. An R^2 < 50% for fat content, only means that the overall variation in the fat content (the range) is too small to give a good linear model.

In all cases, it is necessary to judge the results on a combination of R^2, SEC and SEP. Having high R^2 might only signify a broad range of data if at the same time the standard error is large also.

However in these samples the only two variables changed were water and NaCl contents so the results merely demonstrate the potential of the method. What is needed is a set of samples with variation in all composition variables.

Supermarket samples

The results of predicting different compositional variables for supermarket samples are summerised in Tables 4.2 and 4.3.

Table 4.2. Results of PCA and PCR for all supermarket samples (7PCs used)

	R^2_{adj}	SEC	SEP
Moisture (%)	92.5	1.7	2.1
Fat (%)	95.4	1.5	1.8
Ash (%)	89.1	0.20	0.24
Protein (%)	18.7	1.7	2.0
Salt (%)	80.3	0.29	0.37
Added Water (%)	35.7	6.3	8.0

Table 4.3 Results of PCA and PCR for all supermarket samples and dividing them in two groups (5PCs used)

	R^2_{adj}	SEC	SEP
Mixed samples			
Moisture (%)	93.2	1.6	1.9
Fat (%)	95.5	1.5	1.7
Ash (%)	88.4	0.20	0.24
Protein (%)	24.8	1.7	1.9
Salt (%)	80.8	0.29	0.37
Added Water (%)	36.2	6.0	6.7
Bacon samples			
Moisture (%)	71.5	2.3	2.8
Fat (%)	88.0	1.6	2.0
Ash (%)	96.4	0.15	0.19
Protein (%)	49.6	1.3	1.6
Salt (%)	69.5	0.4	0.5
Added Water (%)	24.4	5.9	7.2
Ham samples			
Moisture (%)	78.9	0.9	1.2
Fat (%)	66.1	0.8	1.1
Ash (%)	77.0	0.18	0.25
Protein (%)	73.4	1.0	1.5
Salt (%)	93.6	0.09	1.3
Added Water (%)	74.7	4.4	6.6

The obtained results for the predicted added water when all samples were used (Table 4.2) were poor compared to the canned pork results (SEP=8%). This value should be seen in the context of legislation, which requires that products be labelled to indicate the added water content to the nearest 5%.

This may be partly due to the difficulty in obtaining homogenous samples as even after blending there were often some large pieces of fat or connective tissue which probably had significantly affected the dielectric measurements.

When separating samples, the results of predicted added water slightly improved. The fact that some of the samples contained components such as fat and some were reformed

and contained fractions of different leg meat may effect the calculation of added water if the nitrogen factor is just assumed to be 3.5 (value for pork products). This is especially true in bacon samples where a variety of cuts were used. Because ham and bacon products had only 15 samples each, it was not possible to use more PCs in the regression in an attempt to take this additional variation into account.

The ham results were better compared to the bacon and pooled data in terms of SEP for the moisture and fat content but there was no significant improvement in the prediction of added water. Having a wide range of water content in the pooled data was the reason behind differences in the R^2_{adj} values.

Prepared meat

The results of PCA and PCR are summerised in Table 4.4. The results of the prediction of added water and other compositions for the pooled data set are shown in Figures 4.3 to 4.6d.

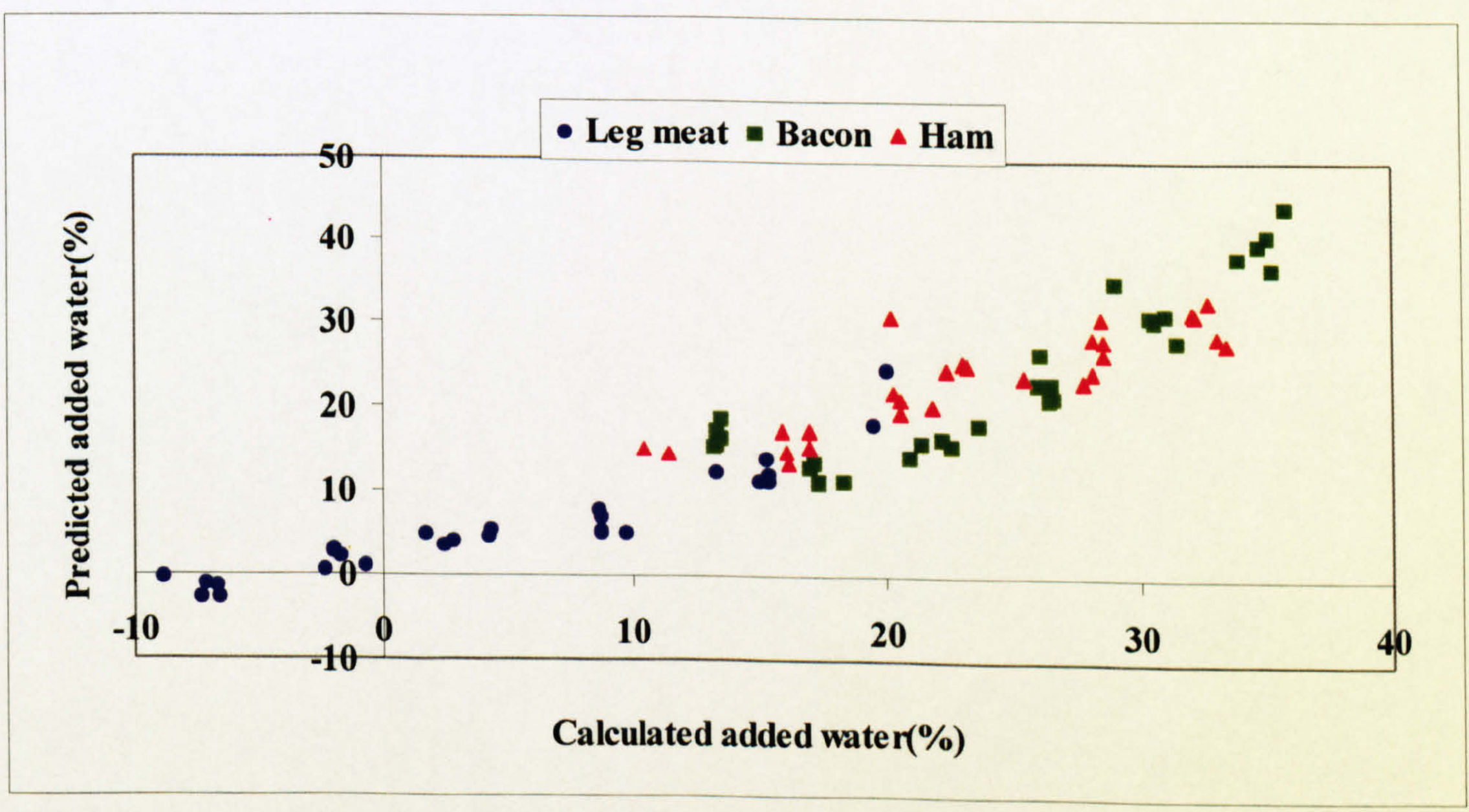

Figure 4.3 Prediction of calculated added water content of prepared meat samples using the pooled calibration.

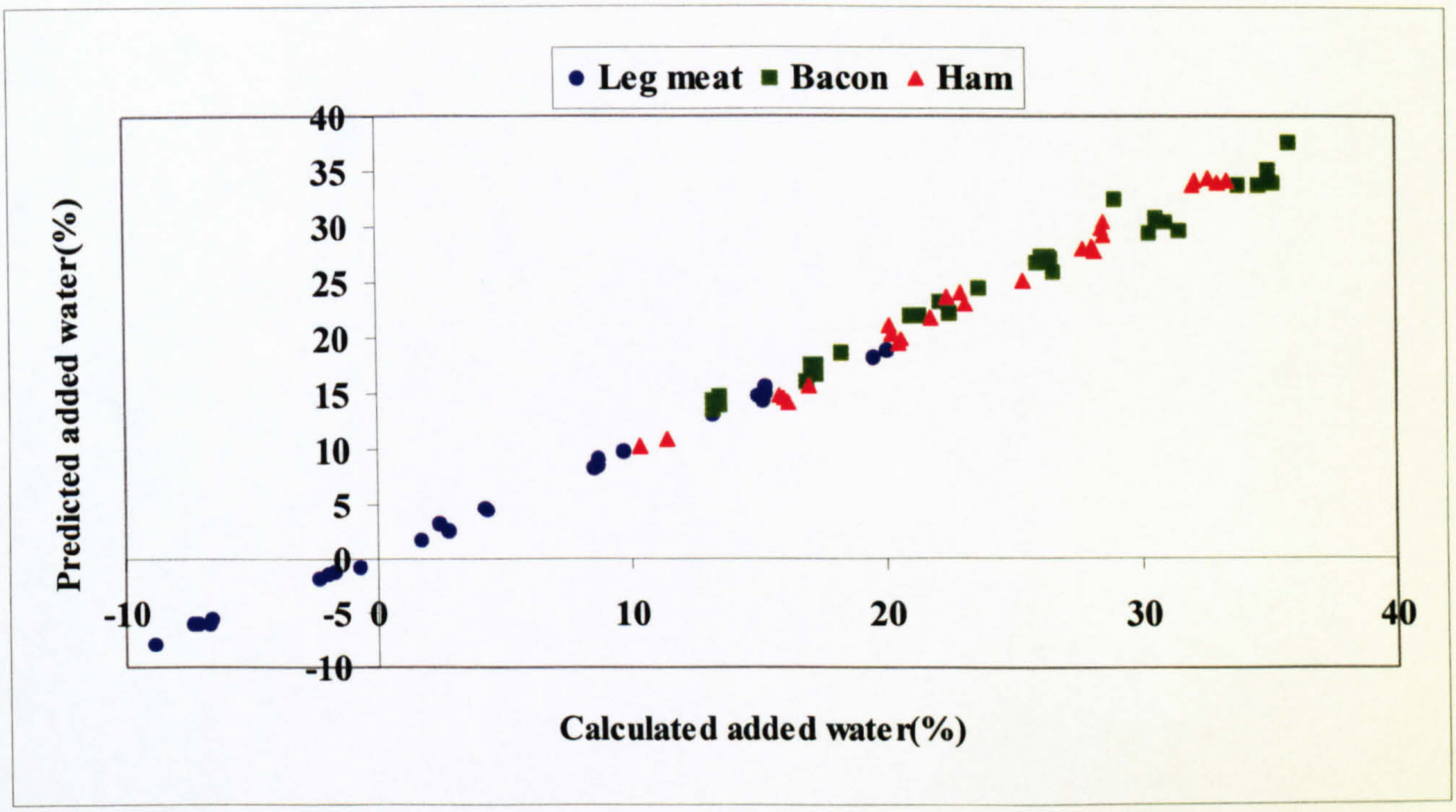

Figure 4.4 Prediction of calculated added water content of prepared meat samples using the pooled calibration (protein content included in the calibration)

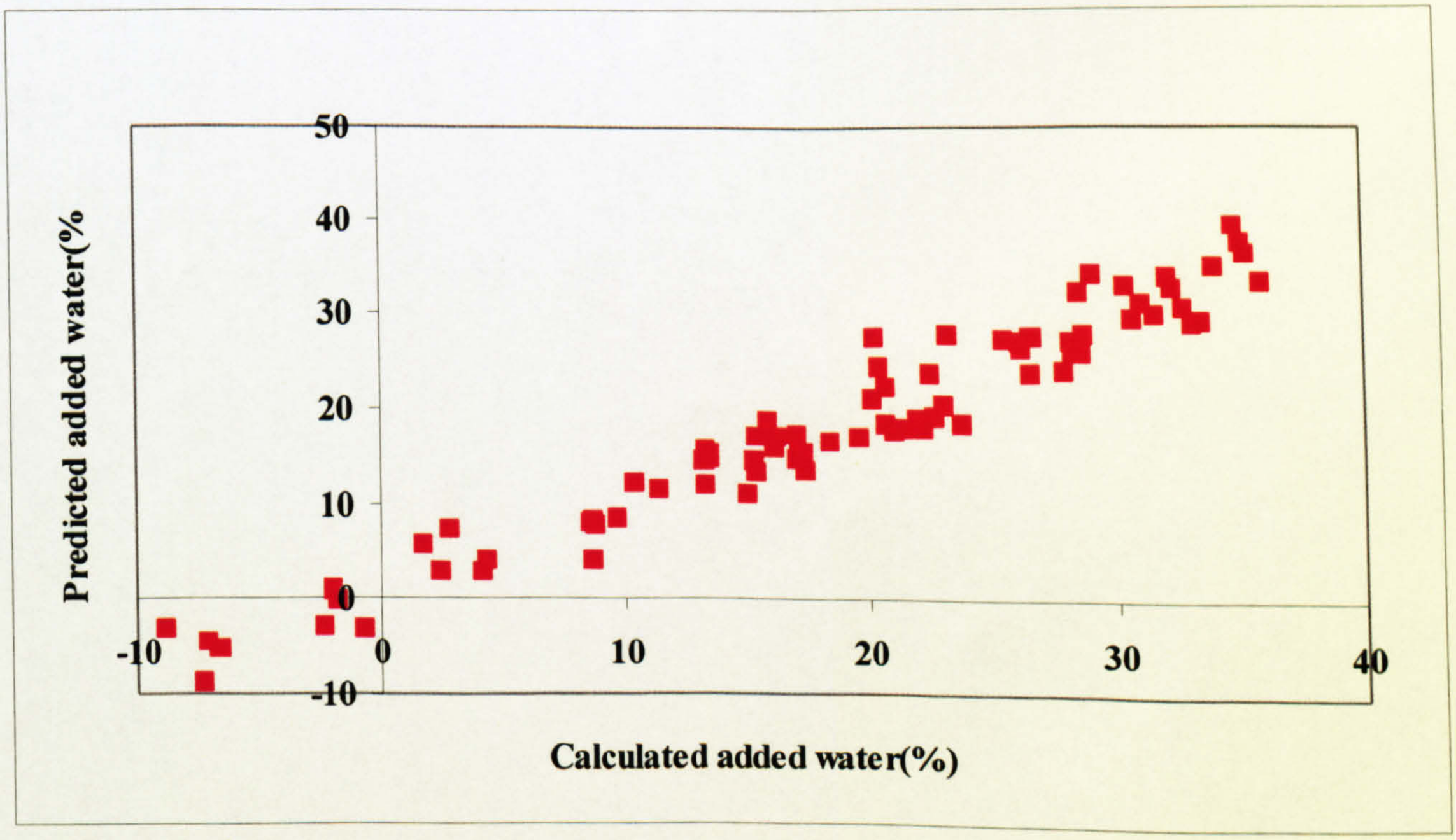

Fig 4.5 Prediction of calculated added water for the pooled data set using 10 PCs

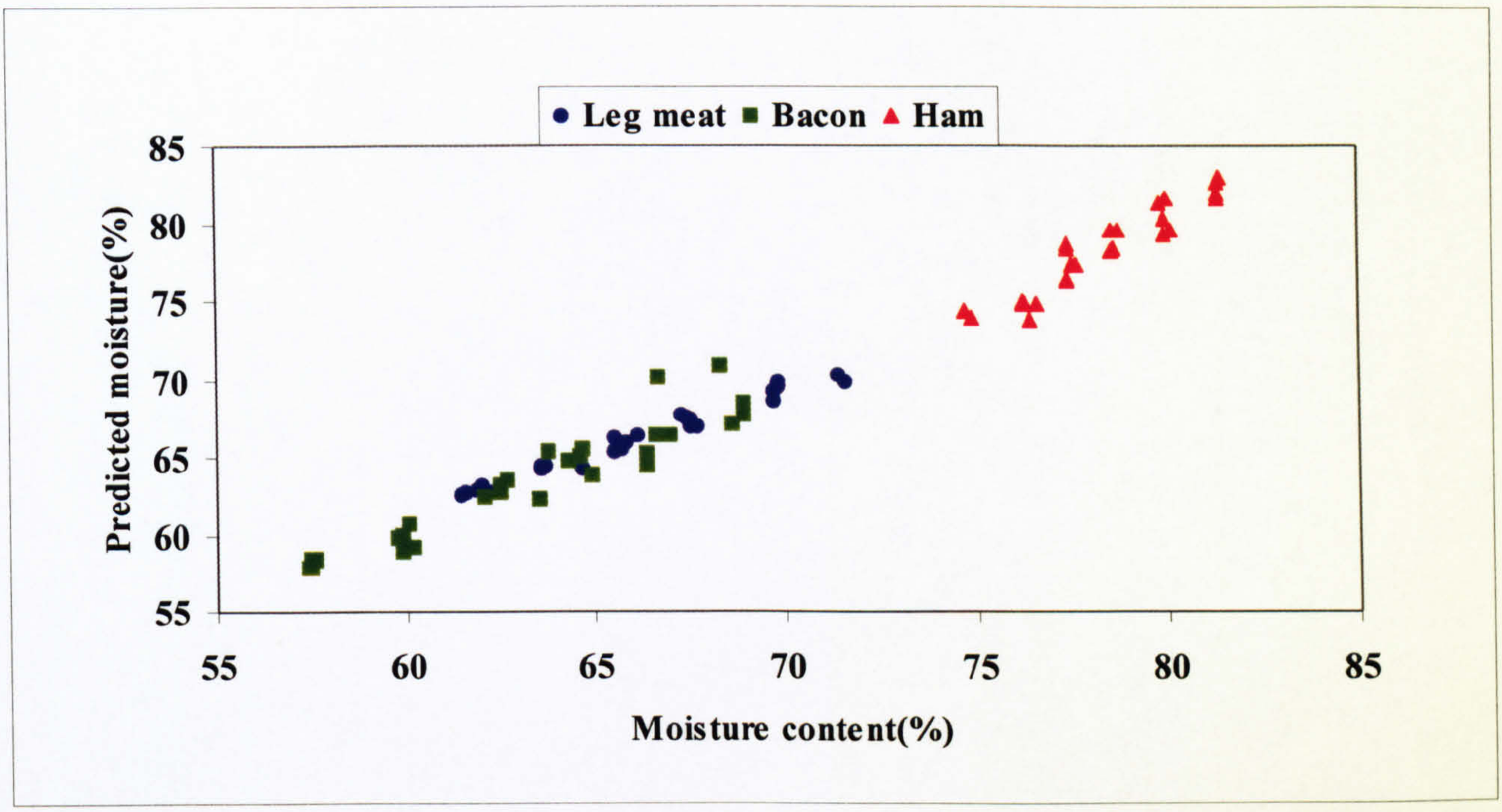

Figure 4.6a

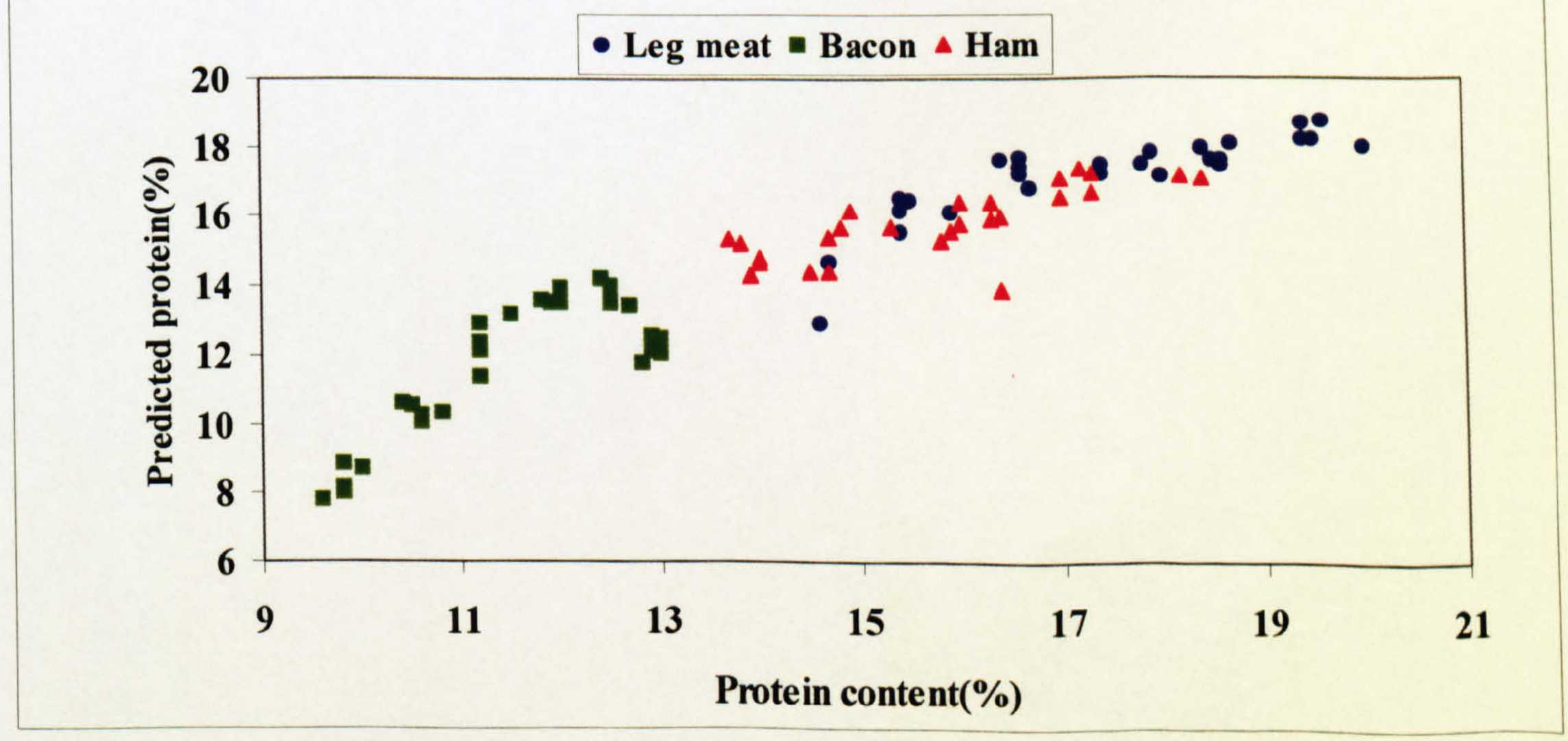

Figure 4.6b

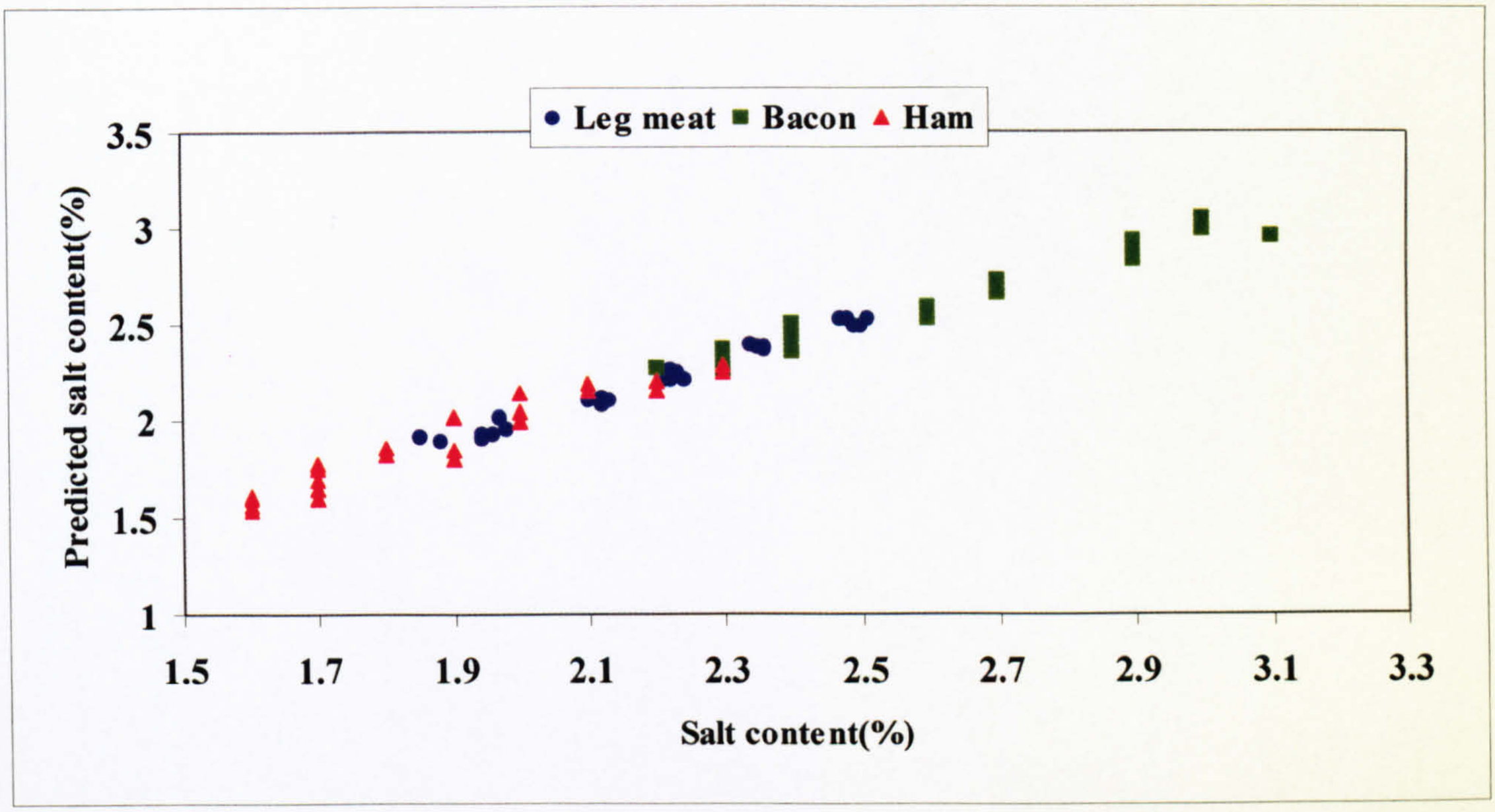

Figure 4.6c

Figure 4.6d

Figure 4.6 Prediction of **a** moisture **b** protein **c** salt and **d** fat content of different prepared pork samples using pooled calibration data.

Table 4.4. Results of PCA and PCR for prepared samples using 7 PCs unless otherwise stated.

	Actual added water			Calculated added water		
Sample	**R^2_{adj}**	**SEC**	**SEP**	**R^2_{adj}**	**SEC**	**SEP**
Leg meat	99.1	0.8	0.95	98.3	1.1	1.4
Streaky bacon	98.6	1.0	1.2	98.0	1.1	1.3
ham	98.6	0.9	1.2	95.5	1.4	1.7
Pooled results	94.1	2	2.1	89.9	3.7	4.0
Pooled results with inclusion of protein content	98.5	1	1.1	99.2	1.1	1.1
Pooled results using 10 PCs	97.4	1.4	1.5	95.9	2.4	2.7

When separate sample categories (leg meat, streaky bacon and ham) were used in the analysis, the result of the prediction of the calculated added water was not as good as the actual added water (Table 4.4).

When all data were pooled together to form one calibration, still the calculated added water was not well predicted compared to the actual values. In fact an apparent non-linearity was observed for the calculated added water data, which increased both the SEC and the SEP for the linear regression model (Figure 4.3). It was realised that if the protein content was included in the calibration the non-linearity would have disappeared (Figure 4.4). However, the principal source of the random error is not clear.

The reason that the inclusion of protein improved the calibration can be due to the fact that the major factor in the calculation of the added water is the nitrogen content, which gives a high degree of correlation in the regression analysis.

There was also some improvement in the non-linearity of the calculated added water results when the number of PC's increased from 7 to 10 as it can be seen in Figure 4.5 and Table 4.4.

Unknown samples of prepared meat

The results of predicting the composition of unknown prepared meat samples are summerised in Figure 4.7 and Table 4.5.

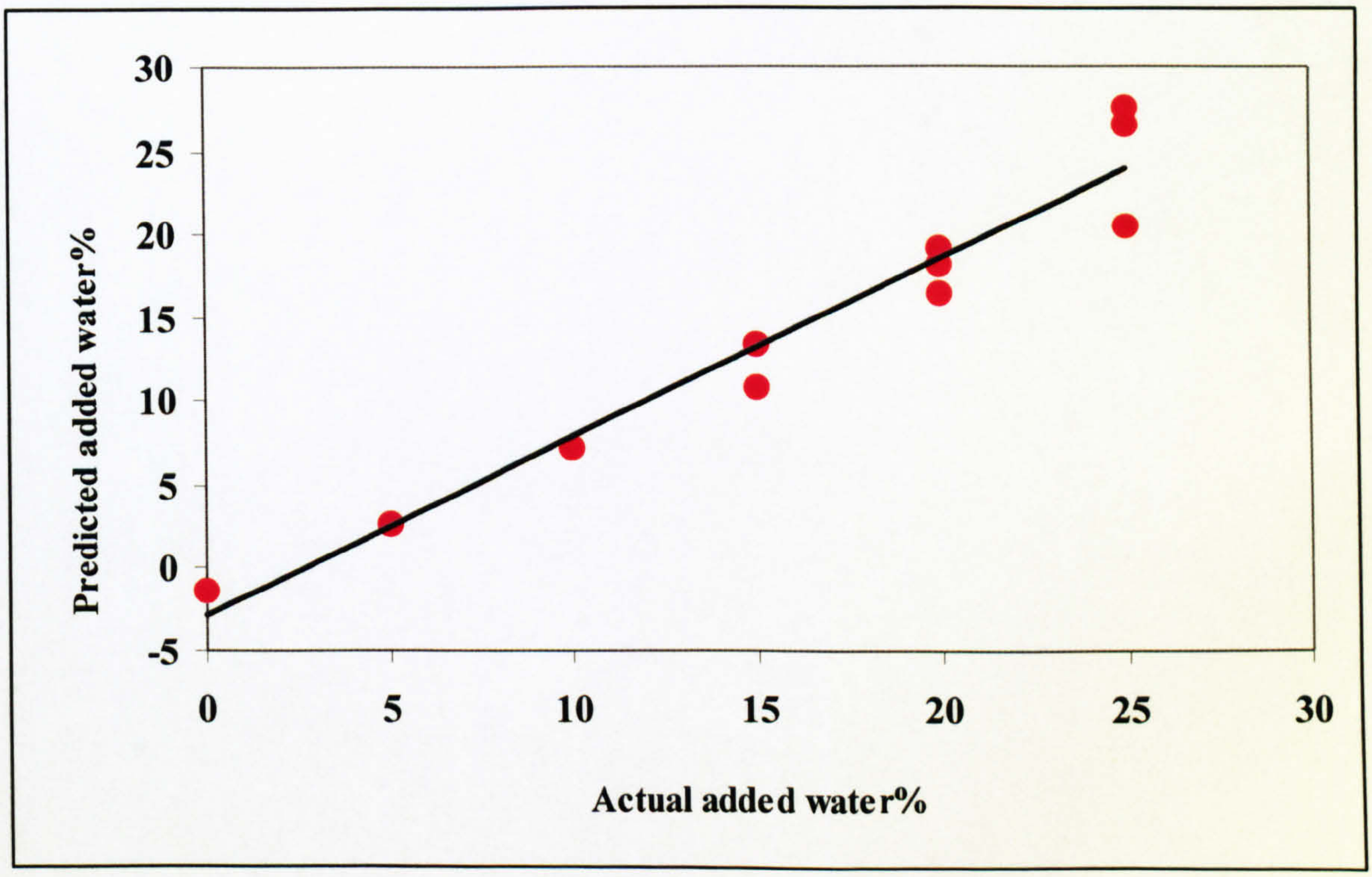

Figure 4.7 Prediction of actual added water content of unknown samples using the pooled calibration

Table 4.5 Predicted values of actual added water for the unknown samples

	Sample	Actual added water (%)	Predicted added water (%)
Leg meat	A	0	0.7
	B	15	14.4
	C	20	19.5
	D	25	25.8
SEP =0.8			
Ham	E	5	6.6
	F	15	13.8
	G	20	20.4
	H	25	25.0
SEP =1.2			
Streaky bacon	I	10	7.6
	J	15	14.2
	K	20	17.3
	L	25	24.3
SEP=2.2			

It can be seen that actual added water can be predicted to within ±0.8, ±1.2 and ±2.2 for leg meat, ham and streaky bacon respectively.

Pooled calibration

The prediction of added water using pooled calibration is shown in Figure 4.8 and the results for compositional variables are presented in Table 4.6. Figure 4.9 shows the relationship between added water and protein content for the 29 validation samples. The effect of inclusion of protein content in the calibration data is shown in Figure 4.10.

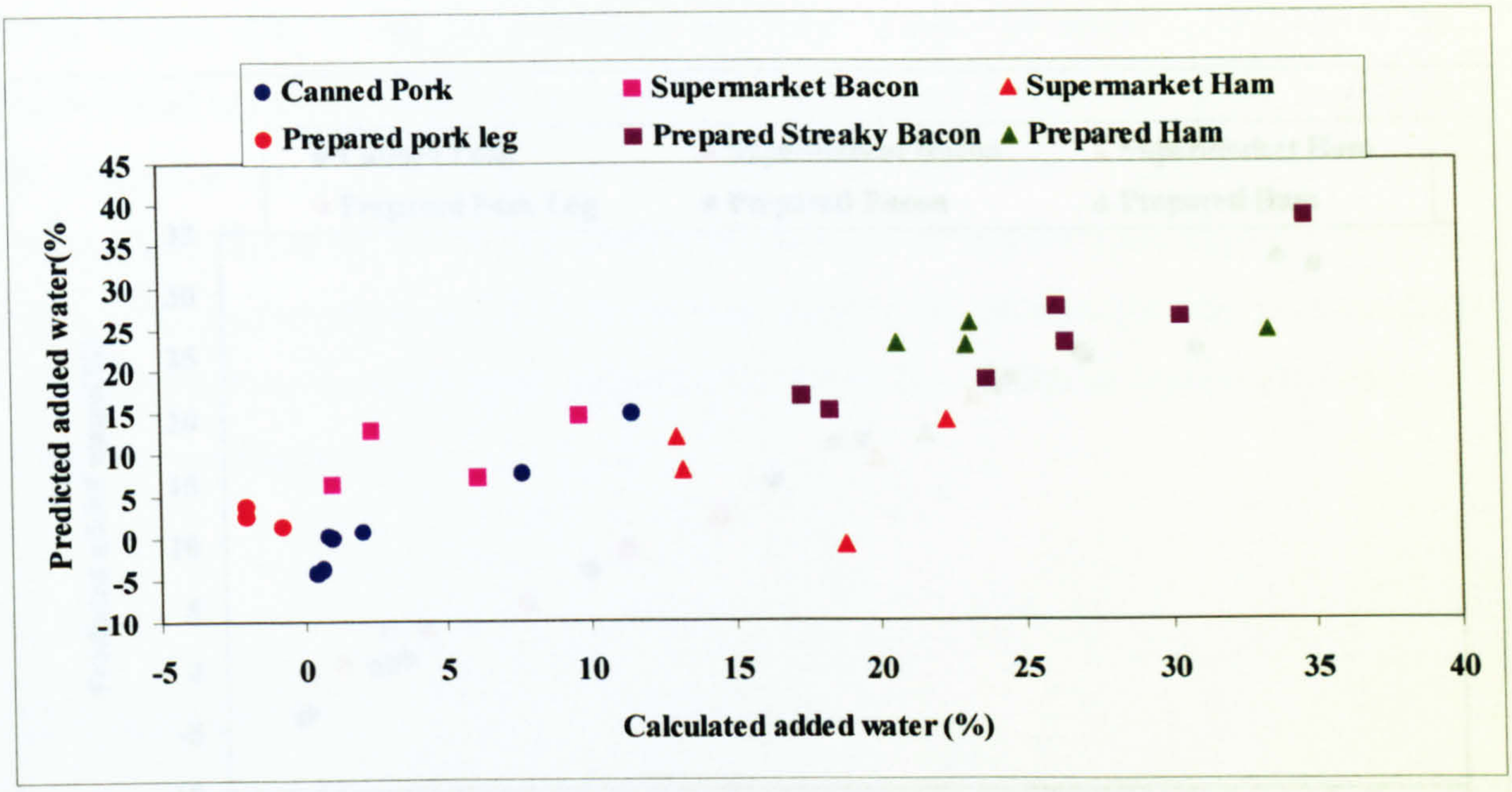

Figure 4.8 Prediction of added water using pooled calibration.

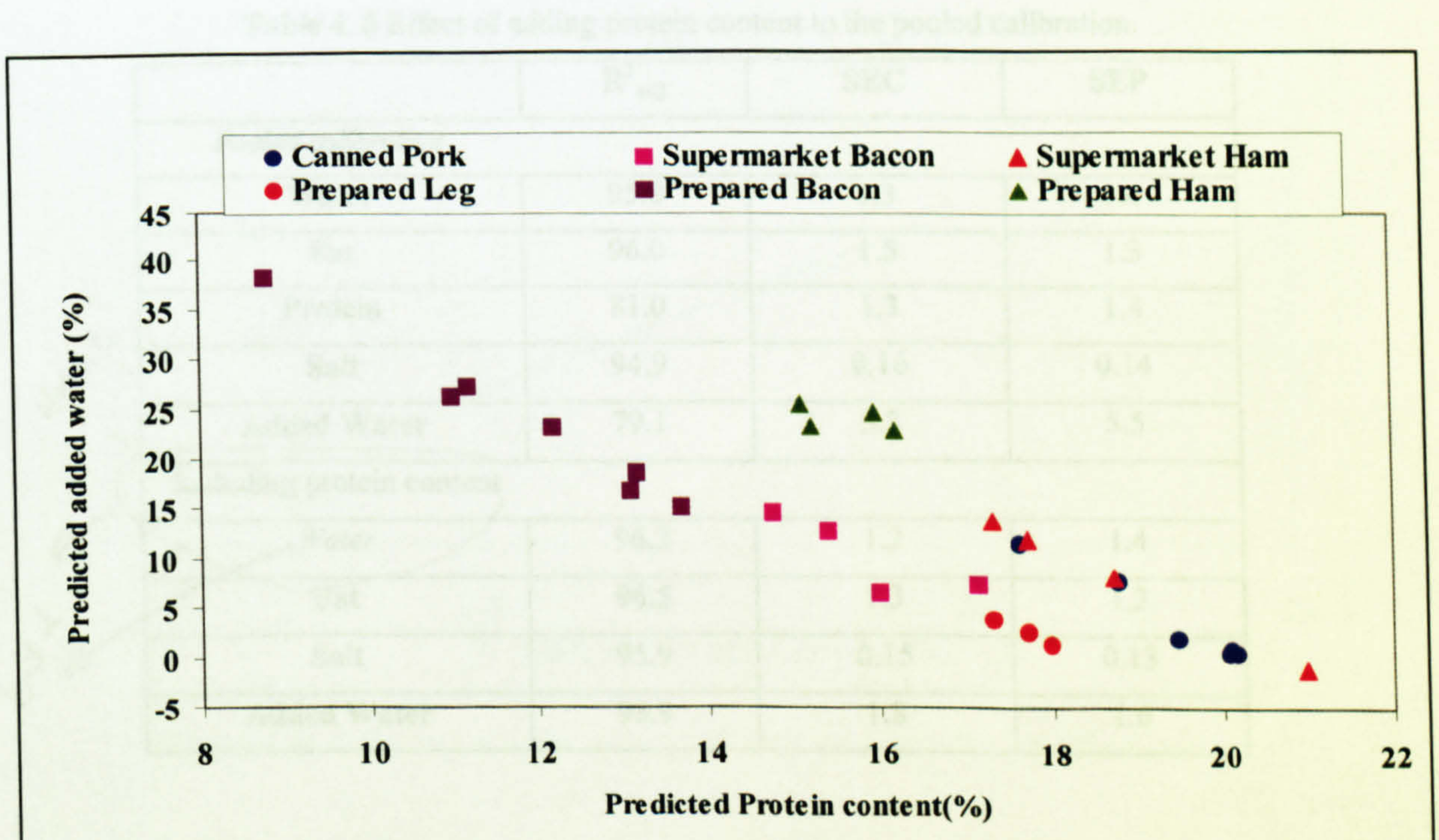

Figure 4.9 Relationship between added water and protein content for the 29 validation samples.

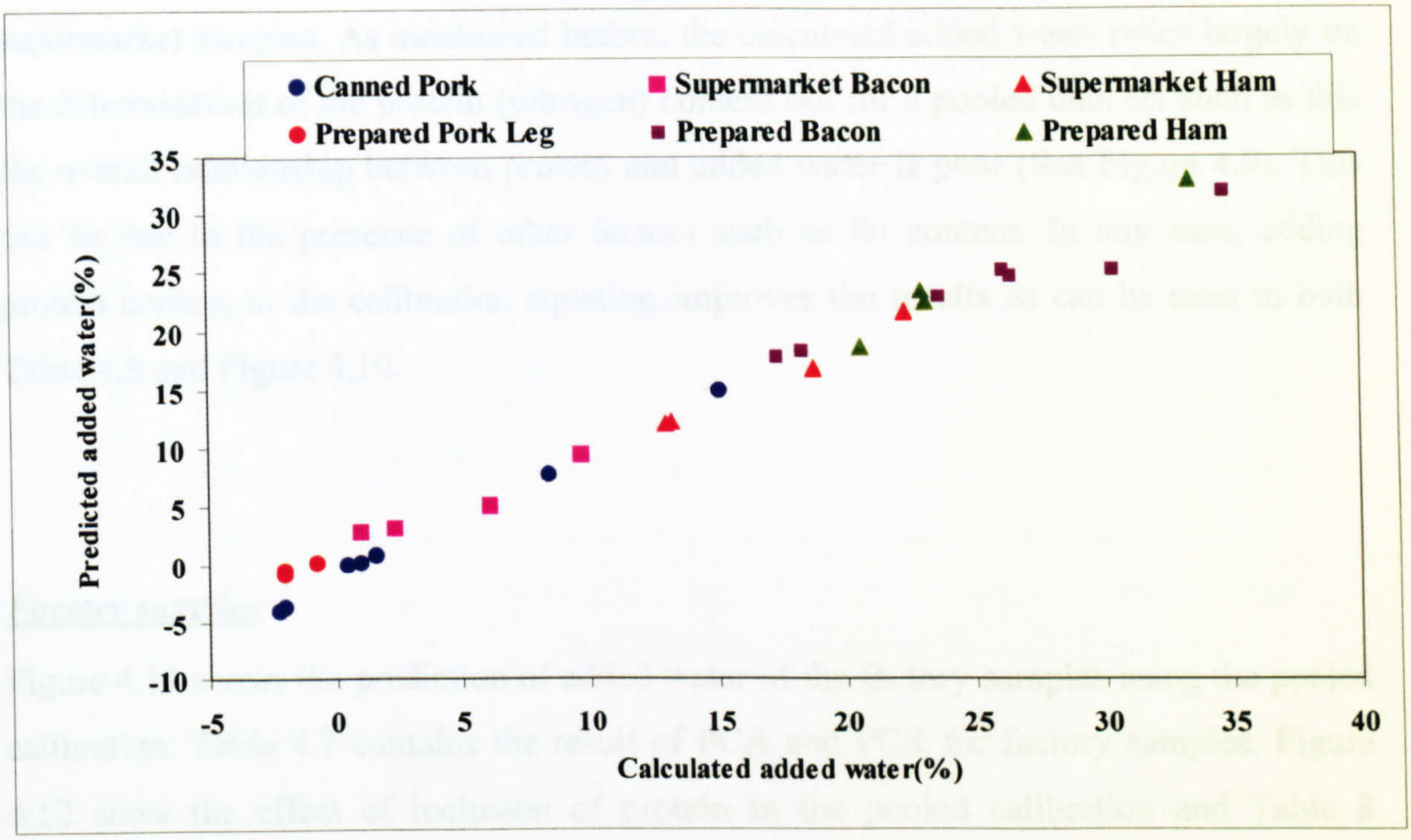

Figure 4.10 Prediction of added water using pooled calibration, including protein in the calibration

Table 4. 6 Effect of adding protein content to the pooled calibration.

	R^2_{adj}	SEC	SEP
Pooled calibration			
Water	95.8	1.3	1.4
Fat	96.0	1.5	1.3
Protein	81.0	1.3	1.4
Salt	94.9	0.16	0.14
Added Water	79.1	5.3	5.5
Including protein content			
Water	96.2	1.2	1.4
Fat	96.5	1.3	1.3
Salt	95.9	0.15	0.13
Added Water	98.9	1.8	1.6

From Figure 4.8, It can be seen that the main source of errors comes from the supermarket samples. As mentioned before, the calculated added water relies largely on the determination of the protein (nitrogen) content but for a pooled data set such as this the overall relationship between protein and added water is poor (See Figure 4.9). This can be due to the presence of other factors such as fat content. In any case, adding protein content to the calibration equation improves the results as can be seen in both Table 4.6 and Figure 4.10.

Factory samples

Figure 4.11 shows the prediction of added water of the factory samples using the pooled calibration. Table 4.7 contains the result of PCA and PCR for factory samples. Figure 4.12 show the effect of inclusion of protein in the pooled calibration and Table 8 contains the PCA and PCR results for this practice.

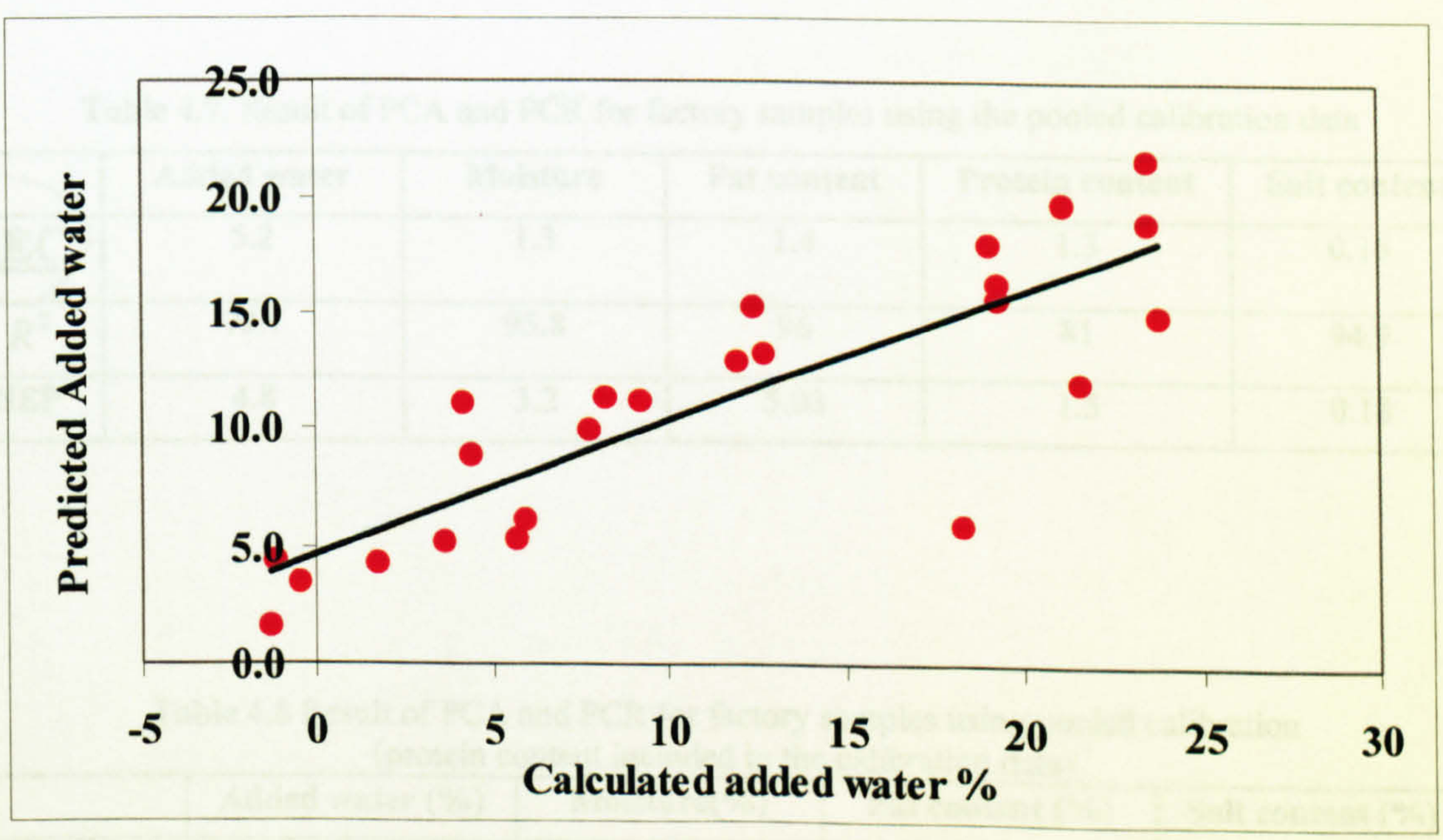

Figure 4.11 Prediction of added water of factory samples using pooled calibration.

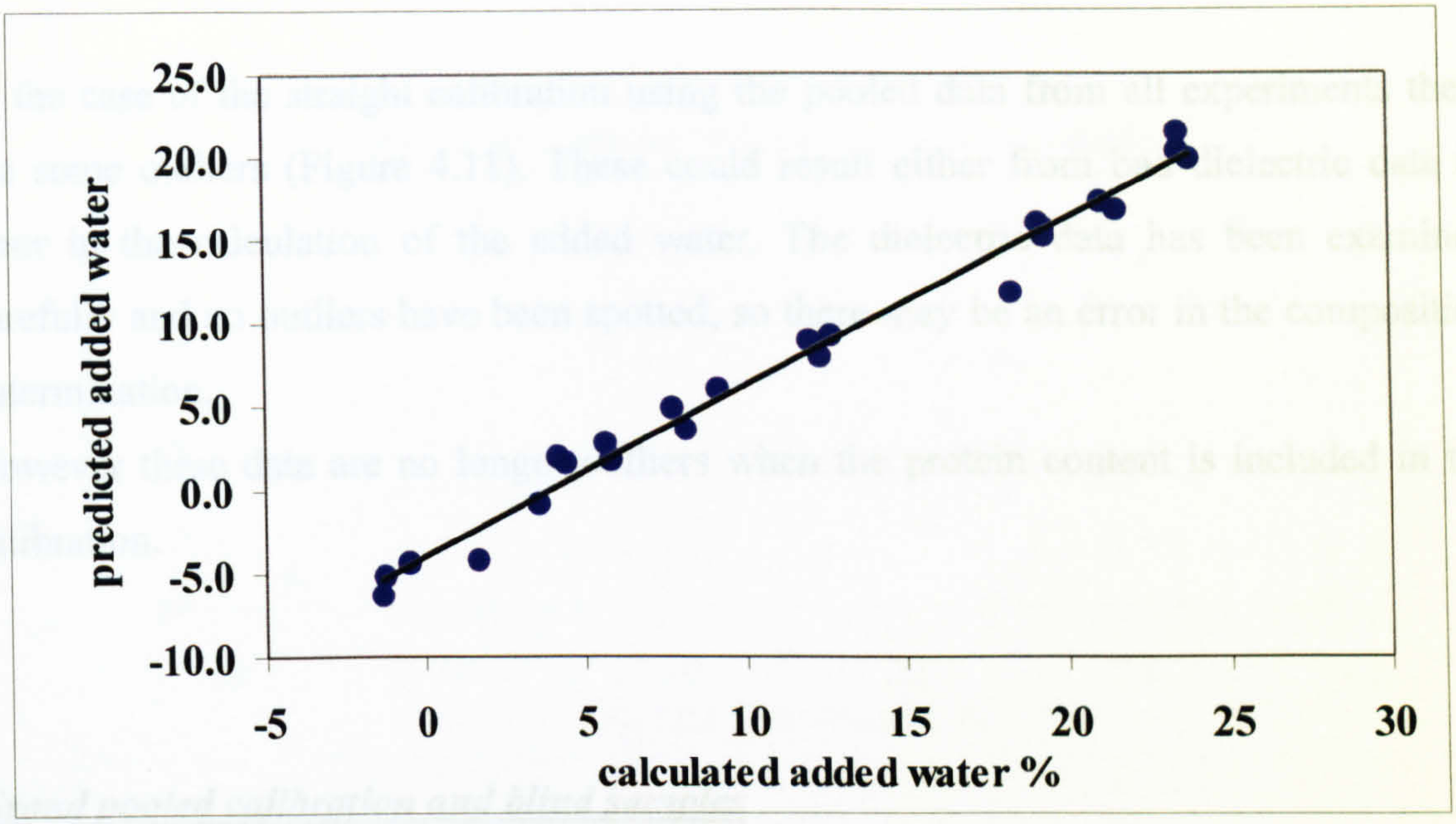

Figure 4.12 Prediction of added water for factory samples using pooled calibration (Protein content included in the calibration).

Table 4.7. Result of PCA and PCR for factory samples using the pooled calibration data

	Added water	Moisture	Fat content	Protein content	Salt content
SEC	5.2	1.3	1.4	1.3	0.16
R^2	79.1	95.8	96	81	94.9
SEP	4.8	3.2	5.03	1.5	0.18

Table 4.8 Result of PCA and PCR for factory samples using pooled calibration (protein content included in the calibration data)

	Added water (%)	Moisture(%)	Fat content (%)	Salt content (%)
SEC	1.2	1.3	1.4	0.15
R^2	98.9	96	96.3	95.6
SEP	4.06	3.4	4.4	0.24

In the case of the straight calibration using the pooled data from all experiments there are some outliers (Figure 4.11). These could result either from bad dielectric data or error in the calculation of the added water. The dielectric data has been examined carefully and no outliers have been spotted, so there may be an error in the composition determination.

However these data are no longer outliers when the protein content is included in the calibration.

Grand pooled calibration and blind samples

The predictions of different compositions for unknown samples using the grand pooled calibration are shown in Figures 4.13a-f. Also the results of PCA and PCR on unknown samples using grand pooled calibration is presented in Table 4.9.

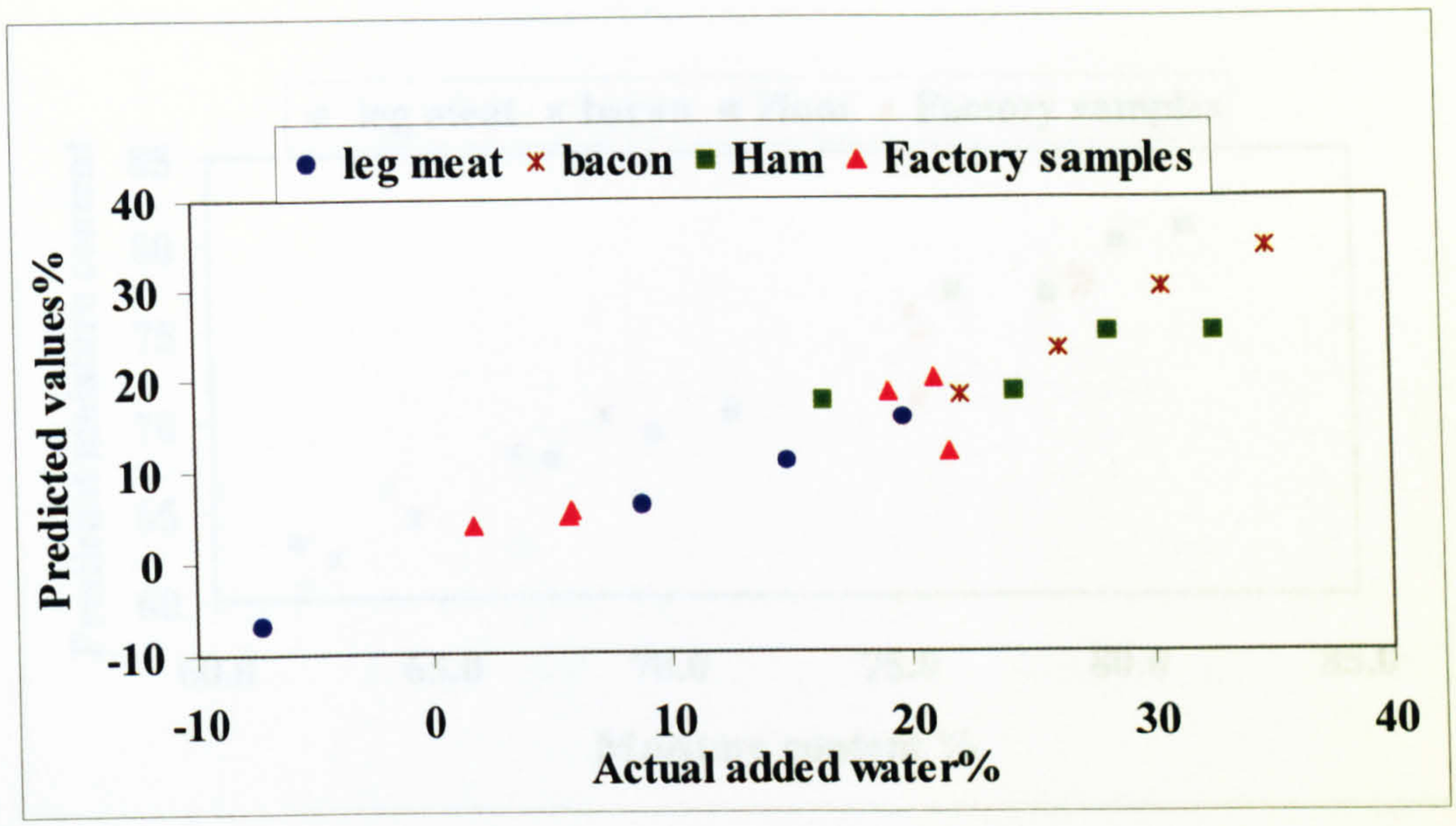

Figure 4.13a

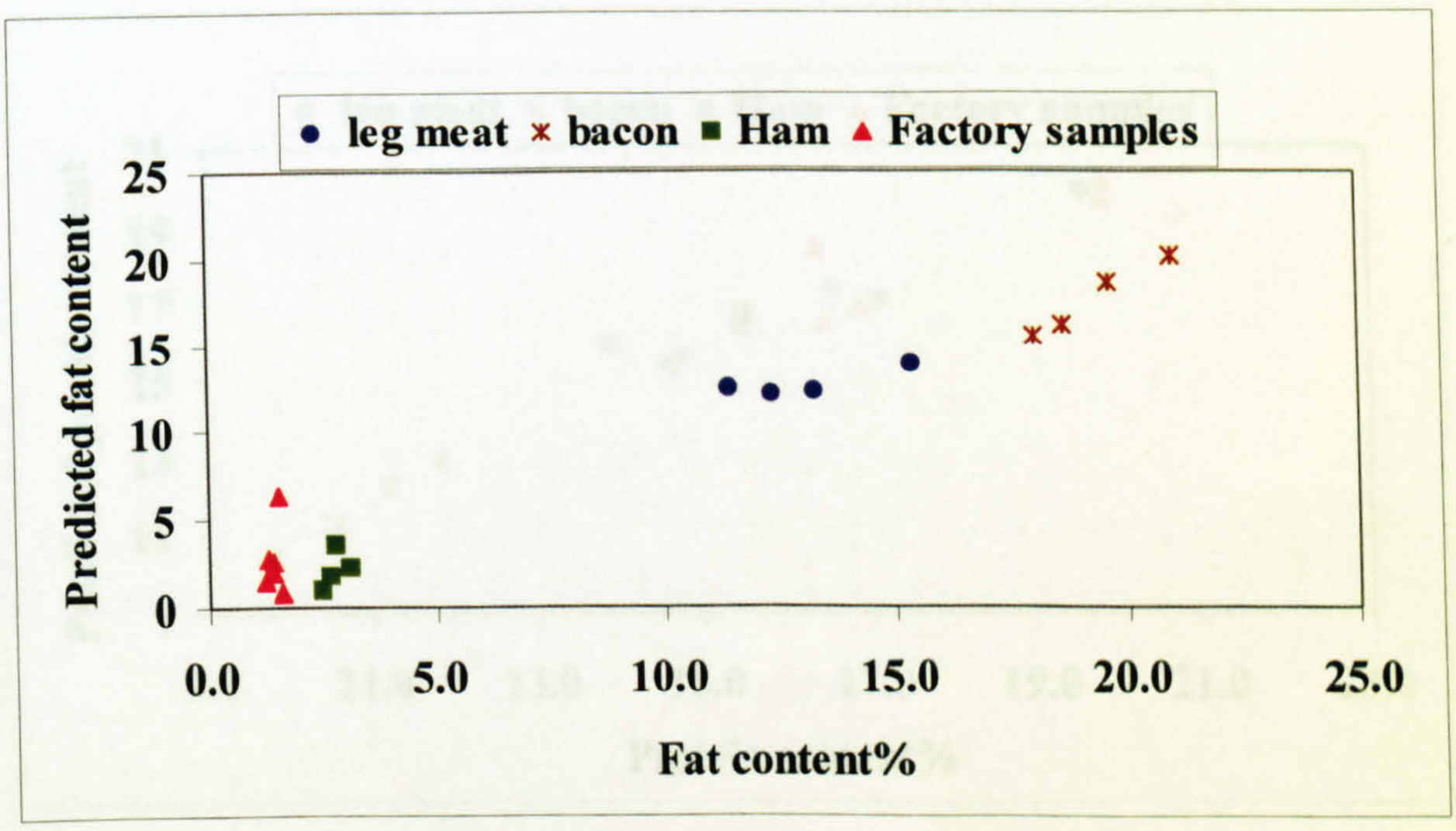

Figure 4.13b

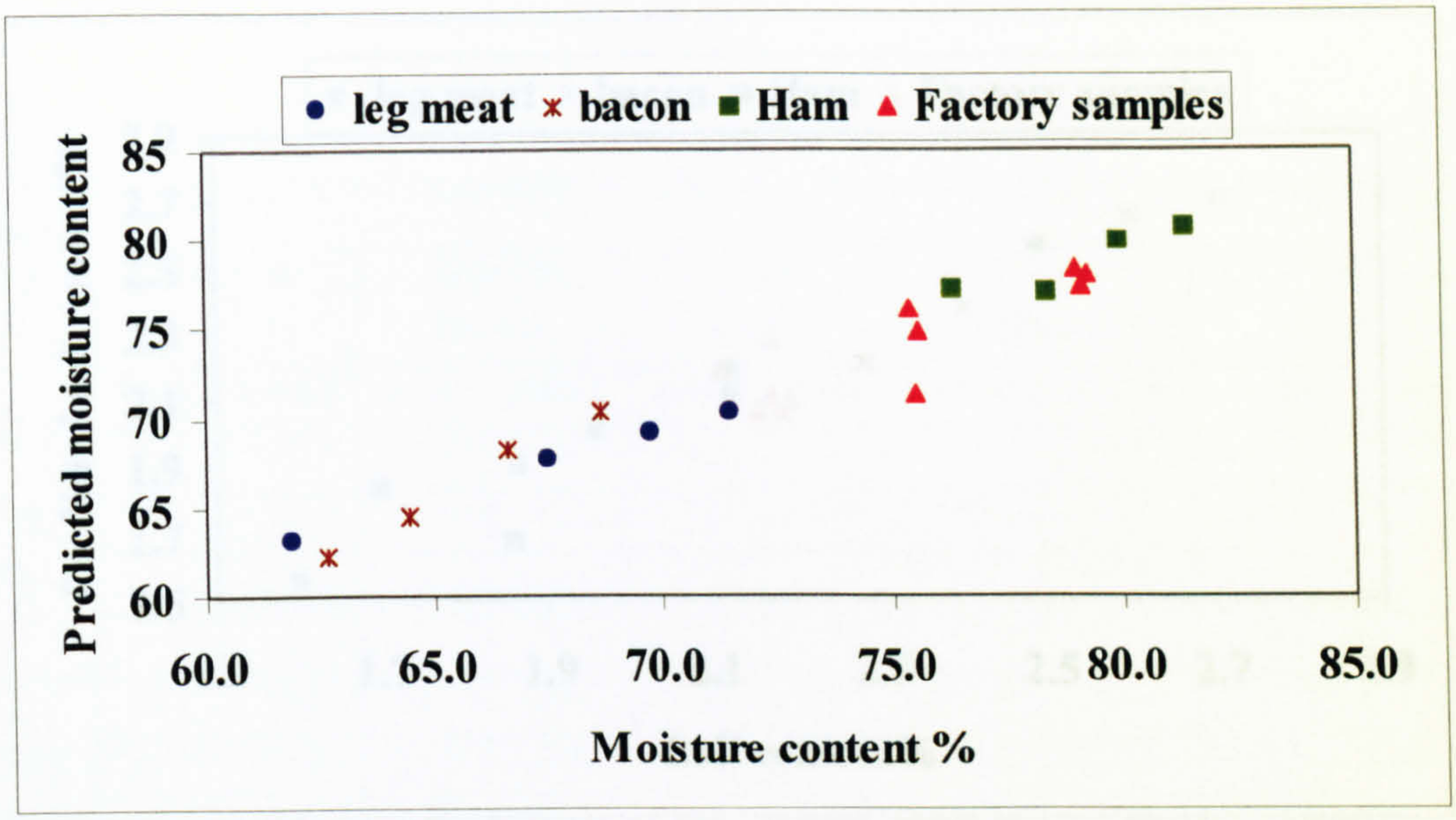

Figure 4.13c

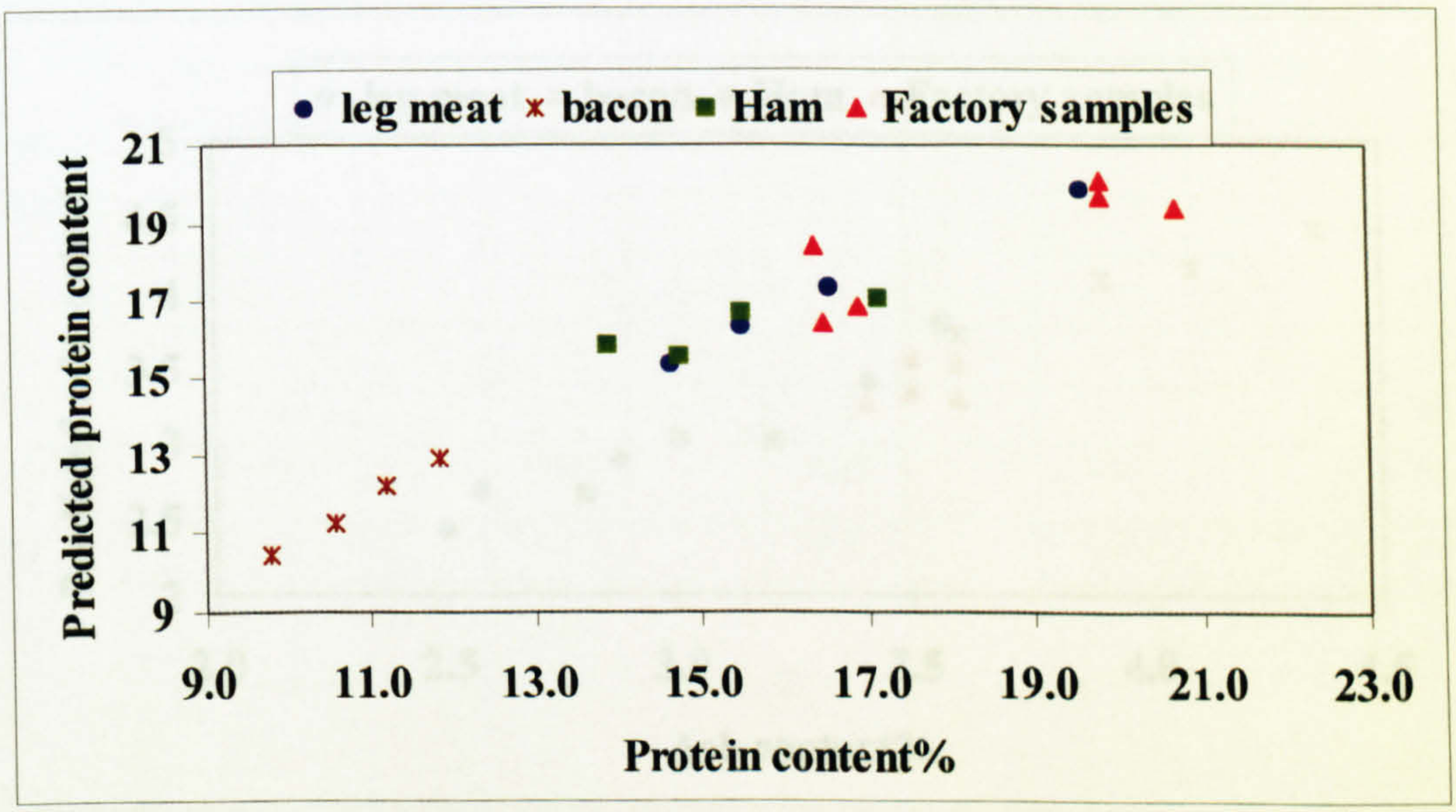

Figure 4.13d

Figure 4.13 Prediction of added water and other composition of blind samples using the saved pooled calibration data set versus the values obtained from proximate analysis.

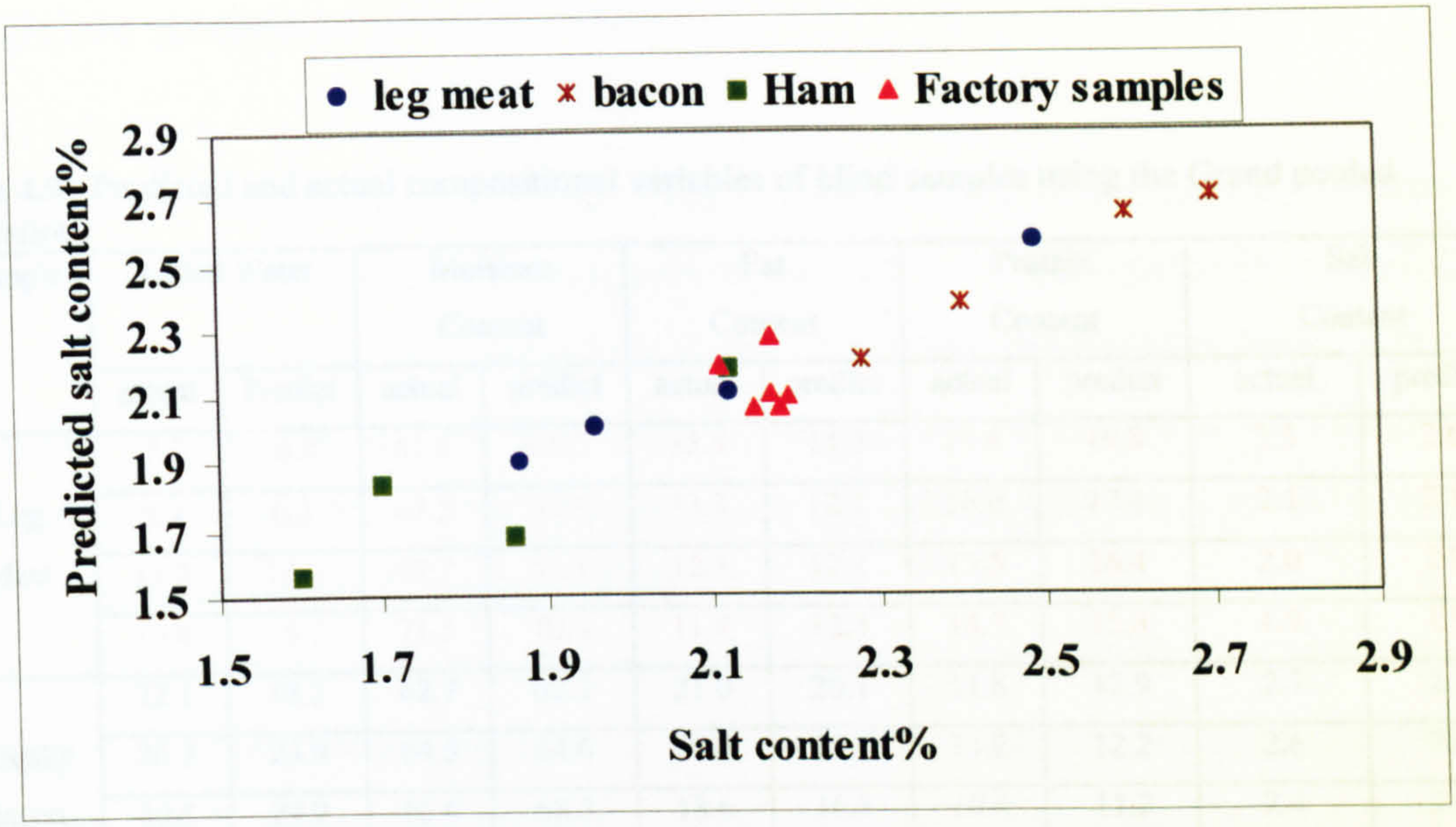

Figure 4.13e

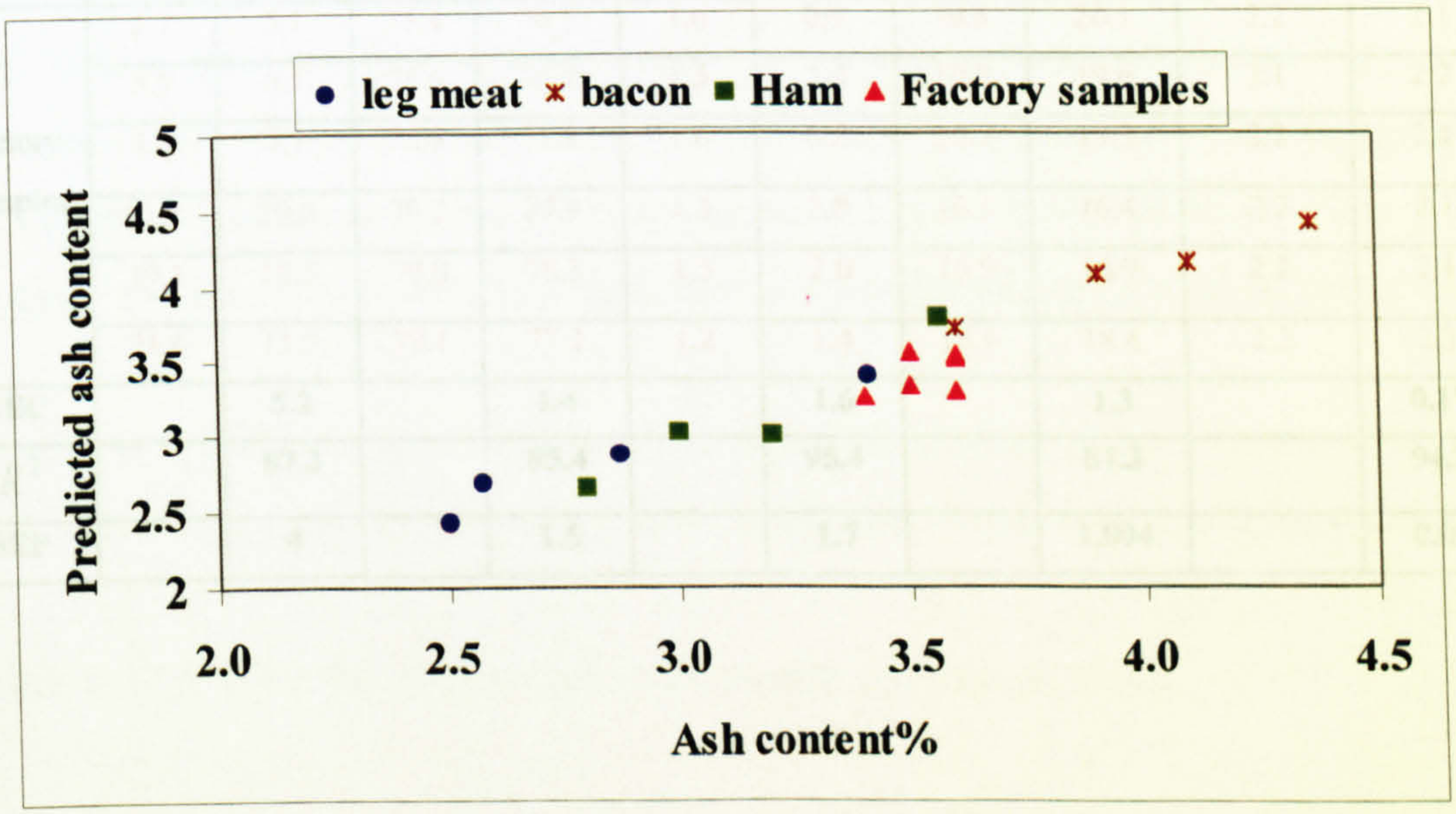

Figure 4.13f

Figure 4.13 Prediction of added water and other composition of blind samples using the grand pooled calibration data set versus the values obtained from proximate analysis.

Table 4.9. Predicted and actual compositional variables of blind samples using the Grand pooled calibration.

Sample	Added Water		Moisture Content		Fat Content		Protein Content		Salt Content	
	actual	Predict	actual	predict	actual	predict	actual	predict	actual	predict
Leg Meat	-7.3	-6.8	61.9	63.2	15.4	14.0	19.6	19.8	2.5	2.6
	8.9	6.3	67.5	67.8	13.3	12.4	16.6	17.4	2.1	2.1
	14.8	11.0	69.7	69.1	12.3	12.2	15.5	16.4	2.0	2.0
	19.8	15.7	71.5	70.3	11.4	12.5	14.7	15.3	1.9	1.9
Streaky Bacon	22.1	18.3	62.7	62.2	21.0	20.1	11.8	12.9	2.7	2.7
	26.3	23.0	64.5	64.6	19.6	18.6	11.2	12.2	2.6	2.6
	30.5	29.9	66.6	68.2	18.6	16.3	10.6	11.2	2.4	2.4
	34.9	34.5	68.7	70.3	18.0	15.6	9.8	10.4	2.3	2.2
Ham	16.4	17.4	76.3	77.1	3.1	2.2	17.2	17.1	2.1	2.2
	24.4	18.5	78.3	77.0	2.8	3.5	15.5	16.7	1.9	1.7
	28.3	25.1	79.9	79.8	2.7	1.7	14.8	15.6	1.7	1.8
	32.7	25.0	81.3	80.7	2.5	1.0	13.9	15.9	1.6	1.6
Factory Samples	5.7	5.1	75.4	76.0	1.6	0.9	19.8	20.1	2.2	2.1
	5.9	5.7	75.6	74.7	1.5	2.5	19.8	19.6	2.1	2.2
	1.7	3.9	75.5	71.2	1.6	6.2	20.7	19.3	2.2	2.1
	21.1	20.0	79.2	77.9	1.3	2.8	16.5	16.4	2.2	2.1
	19.1	18.5	79.0	78.3	1.5	2.0	16.9	16.9	2.2	2.1
	21.6	11.9	79.1	77.2	1.2	1.4	16.4	18.4	2.2	2.3
SEC		**5.2**		**1.4**		**1.6**		**1.3**		**0.17**
R^2		**87.3**		**95.4**		**95.4**		**81.3**		**94.2**
SEP		**4**		**1.5**		**1.7**		**1.004**		**0.09**

4-6 Other statistical procedures

The multivariate approach of PCA and PCR in combination with dielectric spectroscopy showed the ability to predict the composition of pork products, especially added water. However, in using PCR, the assumption is that the model produced is linear. This may not truly describes the system, which can be non-linear. As a solution to this problem other analytical approaches may be used which can make a non-linear model if required such as Artificial Neural Network (ANN).

Artificial Neural Network is a system loosely modelled on the human brain. It is an attempt to simulate within specialised hardware or sophisticated software, the multiple layers of simple processing elements called neurones. The neurones in a layer may communicate with each other, or they may not have any connections. The neurones of one layer are always connected to the neurones of at least another layer. In this system a set of interconnected signal processors can be 'trained' to map a set of inputs to a set of outputs. Apart from input and output layers of connections, such a system contains so-called 'hidden layers' of neurones for which a non-linear activation function is defined.

The most common use for neural networks is to project what will most likely to happen (prediction). For example in this study the inputs are the complex dielectric data at each frequency and the outputs are the compositional variables which have to be predicted.

This approach has been applied [13] to the dielectric studies of the moisture content of wheat. It is effective but requires very many calibration samples to avoid over-fitting.

For this project using the pooled data in future can test this approach.

4-7 Discussion

The results presented in this work showed that actual added water can be determined to within approximately ±2.5% for canned pork. A prediction of up to ±1.89 can be obtained when calculated added water values are used in the calibration. Therefore, in the case of canned pork, the calculated added water values gave better prediction than the actual values.

Although the results obtained on supermarket samples showed that added water could be determined with the dielectric spectroscopy method, the results were poor compare to the canned pork results. One reason for this could be the errors in the calculation of added water. In doing so, some of the assumptions made were about the proportion of nitrogen associated with carbohydrate and the level of protein in the standard pig carcass. It has been assumed in these calculations that the protein content of the meat is constant over all types of joint and all ages and sizes of pig which in fact is not the case.

In the case of prepared samples, combining all the samples into one calibration eliminated the effects of correlation between the compositions of the samples. Including the protein content in the pooled data for prepared samples improved the SEP from ±4 to ±1.1for calculated added water. The reason why including protein improves the calibration is that the major factor in the calculation of the added water is the nitrogen content. The nitrogen factor gives a high degree of correlation in the regression analysis. It is also notable that for prepared meat samples the actual added water was predicted with SEP of only ±1.5% compared to ±2.7% when using calculated values. This may again be due to the derivation of added water, which is based on an assumption about the nitrogen content of the native meat that may not be truly general.

The method of pooling all data in one calibration set has been shown to work better in the prediction of added water when protein content is included in the calibration equation. The standard error of prediction was in this case ±1.6% compared to ±5.5% when only the principal components were used in the calibration.

References for chapter 4

[1] Aitken A, 1976 'Changes in water content of fish during processing' *Chemistry and Industry*, 1048-1051.

[2] Kent, M and Anderson D, 1996, 'Dielectric studies of added water in poultry meat and Scallops', *Journal of Food Engineering*, **28**, 239-259.

[3] Kraszewski A (2000), *'Recent bibliography on moisture sensing: 1990-1998 (sensors,methods,applications)*, in 'Sensors Update' eds H Baltes, W Göpel and J Hesse, 393-414, Wiley-VCH, Weinheim, Germany.

[4] Hall M, Zhuo L and Gabriel C, 1994,'Spectroscopic investigation of the dielectric properties of some foods and food components', *Microwave Science Series*, Vol.8, Ministry of Agriculture Fisheries and Food London, UK.

[5] Archibald DD, Trabelsi S, Kraszewski AW and Nelson SO (1998) '*Regression analysis of microwave spectra for temperature-compensated and density independent determination of wheat moisture content'* Applied Spectroscopy, **52**, 1435-1445.

[6] Kent, M, Knöchel, R, Daschner, F, and Berger, U-K., (2000a), *'Composition of foods using microwave dielectric spectra.'* Eur Food Res Technol. **210** 5, 359-366.

[7] Lawrence KC, Windham WR and Nelson SO (1998) '*Wheat moisture determination by 1 to 110 MHz swept frequency admittance measurements'* Transactions of the ASAE , 4, 135-142.

[8] Chatfield C. and Collins A.J., *'An Introduction to Multivariate Analysis'*, 1980, Chapman & Hall, London.

[9] MAFF (1998) 'Establishment of guidelines for the application of chemometric methods to food authenticity problems', Project n. AN0663, Ministry of Agriculture Fisheries and Food, London, UK.

[10] Gabriel C, Chan T Y A and Grant E H 1994, "Admittance models for open ended coaxial probes and their place in dielectric spectroscopy", *Phys.Med.Biol.* **39** 2183-2200.

[11] British Meat Manufacturer Association, 1998, Analytical Schedule (P014)

[12] Analytical Methods Committee, Royal Society of Chemistry, UK (1991) '*Nitrogen factors for pork: a reassessment*', Analyst, **116** 761-766.

[13] Bartley, P.G., McLendon, R.W., and Nelson, S.O. (1997) *'Moisture determination with an artificial neural network from microwave measurements on wheat'*, IEEE Instrumentation and Measurement Technology Conference,**2**, 1238-1243.

Chapter 5- Changes in the dielectric properties of rat tissue as a function of age at microwave frequencies

5-1 Introduction

The dielectric properties of tissues have been widely studied, reviewed and reported [1-4]. As mentioned in chapter 2, it is well established that the dielectric relaxation spectrum of a tissue extends over a wide frequency range extending from hertz to gigahertz and that it consists of three main regions known as α, β and γ dispersions. The low-frequency α dispersion is associated with ionic diffusion processes at the site of the cellular membrane. The β dispersion extends over 3-4 frequency decades centred in the hundreds of kilohertz region, and is due mainly to the polarisation of cellular membrane and organic macromolecules. Finally, the γ dispersion, in the gigahertz region, is due to the molecular polarisation of tissue water [6]. The study of α dispersion is outside the scope of this project. The β dispersion area of dielectric spectrum is investigated in chapter 6. The frequency range investigated in this chapter (and chapter 4) extends from 130 MHz to 10 GHz, revealing the tail end of the β dispersion and a good part of the γ dispersion.

As mentioned in chapter 2 the γ-dispersion is due to the polarisation and relaxation of the water molecules. As the frequency increases to the gigahertz regions, the relaxation of polar molecules in water become important and cause the γ-dispersion. There is a single relaxation frequency for γ-dispersion, which is slightly lower than that of pure water. The centre frequency in which the γ-dispersion occurs is near 25 GHz at body temperature. Since water constitutes 80% of the volume of most soft tissues, the γ-dispersion is of importance in the study of dielectric properties of biological tissues.

Also metabolic activity or pathological condition results in physiological changes in the biological tissues which in turn lead to changes in the dielectric properties of the tissue.

Depending on the nature of the change, part or sometimes the whole dielectric spectrum may be affected. The amplitude of the γ dispersion correlates with the water content of the tissue. The more water the tissue consists of, the larger the amplitude of the γ dispersion will be.

The water content of tissues varies throughout the lifetime of animals. For example, in mice the water content of the brain decreases from 85% for a newly born to 77% for an adult [7]. The human brain also loses water, as the person grows older. For a 13-14 week old foetus there is 914gr of water per each kilogram of fresh whole brain, while this figure is 897gr for a new born and 774gr for an adult [8]. Also in the case of human skin, a 13-14 week old foetus has 917gr of water per each kilogram of fresh fat free skin. This amount will fall to 828gr for a new-born baby and 694gr for an adult [8].

The changes in the amount of water content of tissue are such that one can anticipate corresponding variations in the dielectric properties at microwave frequencies. This can be investigated by measuring the dielectric properties of different tissues at different stages of growth of an animal. The extent of the variation of dielectric properties with age is particularly relevant to the rigorous assessment of the exposure of experimental animals throughout their lifetime. It gives an indication of the extent to which variation in the dielectric properties needs to be taken into consideration in the assessment of exposure of children and adults as recently highlighted by the Independent Expert Group on Mobile Phones [9].

While a strong variation of the dielectric properties of mouse and rabbit brain tissue has been observed with age [10,11], there are no equivalent data for other tissues. The data obtained in this study will add to those in the literature and provide data for rigorous dosimetry at microwave frequencies in lifetime animal studies and show that there are parallels between changes in the composition of tissues and the parameters of the γ dispersion.

The purpose of this work is twofold. First, to provide data for use in the assessment of exposure of animals to electromagnetic radiation at microwave frequencies and second, to quantify the parameters of the γ dispersion and investigate their correlation with the water content of the tissue.

5-2 Material and method

Dielectric measurements have been carried out on brain, skin, skull, masseter muscle, salivary glands (submaxillary glands), liver, kidney, spleen, tongue and tail of wistar strain rats, in the frequency range of 130MHz-10GHz. The measurements were made using an open-ended coaxial probe and a computer controlled network analyser, following a previously reported procedure [12].

The probes used were 50-Ohm PTFE filled coaxial probes. Depending on the size of the tissue, one of the following small probes was used. The dimensions of the probes were as follows:

2.98 mm Probe: inner radius of 0.456mm and outer radius of 1.49mm.
1.67 mm Probe: inner radius of 0.256mm and outer radius of 0.838mm.

This procedure is suitable for dielectric measurement of biological tissue, its stated accuracy is between 1 and 2%, assessed by measurement on standard liquids of well-known dielectric properties, and the reproducibility of a measurement is about 1% (*See chapter 3*)

The following age groups have been considered in this experiment: new-born (less than 24 hours old), 10, 20, 30, 50, and 70 days old. The 70 day old rat is considered a mature animal. All measurements were performed within 2-4 hours of the sacrifice of the animal. Care was taken to avoid loss of moisture from the tissue and to reduce to a

minimum the handling of the samples. Physiological changes that are known to occur as a function of time after death affect mostly the dielectric data at low frequencies, the site of the α dispersion [13].

why?

At microwave frequencies the data are sensitive to the moisture content and are much less affected by the physiological processes that take place within hours of death. No preservative material was used. Tissues were kept in small containers and placed in a water bath to maintain a 37 °C temperature. The sample thickness was at least 4-5 times the probe diameter to constitute a semi-infinite lossy sampling volume [14]. Elaborate

At least 5 sets of measurements were made on each tissue and averages and standard deviations were calculated. Skin was measured from the inside rather than the outside in order to avoid the contact to the covering fur. Tissues from new-born rat are in some cases too thin to provide sufficient sample volume, in such cases several tissue layers were used and care was taken to have a good contact with the probe prior to measurement. Measurements were repeated for three different rats at each age for brain, muscle, skull, skin, salivary glands and tongue. For the rest of the tissues two rats were measured at each age.

To quantify the γ dispersion, the data were fitted to the well-known Cole-Cole expression plus a conductivity term:

mathematical expression of measured data not physical

Semi empirical because we can mathematically describe the relaxation time distribution of τ.

$$\hat{\varepsilon}(\omega) = \varepsilon_\infty + \frac{\Delta\varepsilon}{1+(j\omega\tau)^{(1-\alpha)}} + \frac{\sigma_i}{j\omega\varepsilon_0} \qquad (5.1)$$

where $\hat{\varepsilon}$ is the complex relative permittivity and ω the angular frequency. $\Delta\varepsilon$, the amplitude of the dispersion, is defined as $\Delta\varepsilon = \varepsilon_s - \varepsilon_\infty$ where ε_∞ is the permittivity at high frequencies where $\omega\tau >> 1$ and ε_s is the permittivity at low frequencies where $\omega\tau << 1$.

τ is the relaxation time constant, and α is a parameter that allows for the broadening of the dispersion. Finally, σ_i is an ionic conductivity term and ε_0 is the permittivity of free space. This is essentially an empirical formulation, not recommended for detailed mechanistic investigations. It is, however, quite suitable for comparative studies where there is a known, dominant interaction mechanism such as the molecular rotation of tissue water as in this case [5].

The fitted parameters also allow some parallels to be drawn with the changes in tissue composition and in particular the water content. The analysis was carried out using a complex curve-fitting program. The data of each tissue at each age were fitted separately and the value for ε_∞ was fixed at 3. The choice of parameter value for ε_∞ is based on the knowledge that the corresponding value for water is about 5 and that the water content of tissue is of the order of 60%. Moreover, a variation of about 20% on the value of ε_∞ has very little effect on the other fitted parameters.

5-3 Results and observations

The measured permittivity and conductivity data for different tissues of rats of different ages are given in figures 5.1 and 5.2.

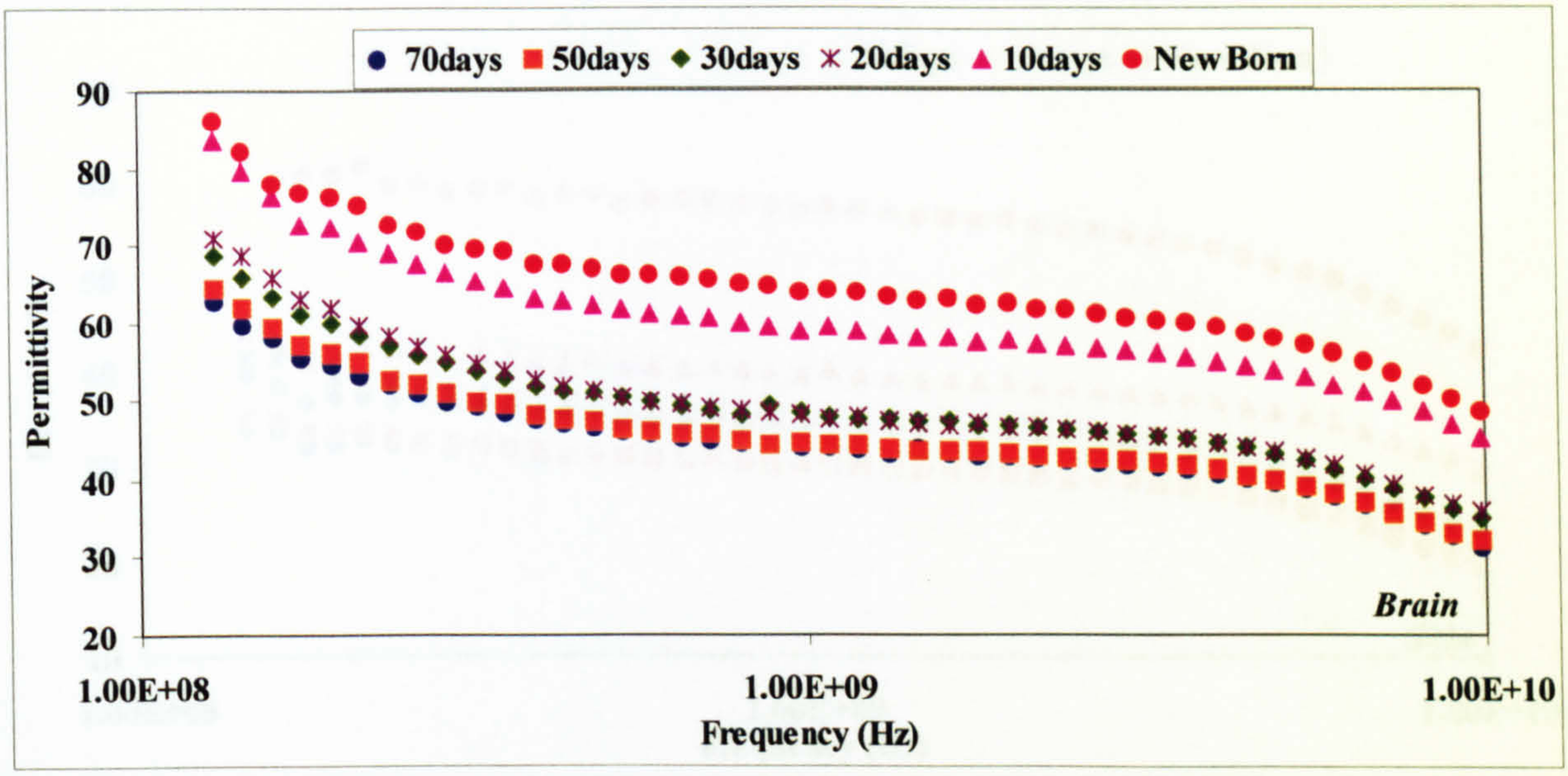

Figure 5.1a

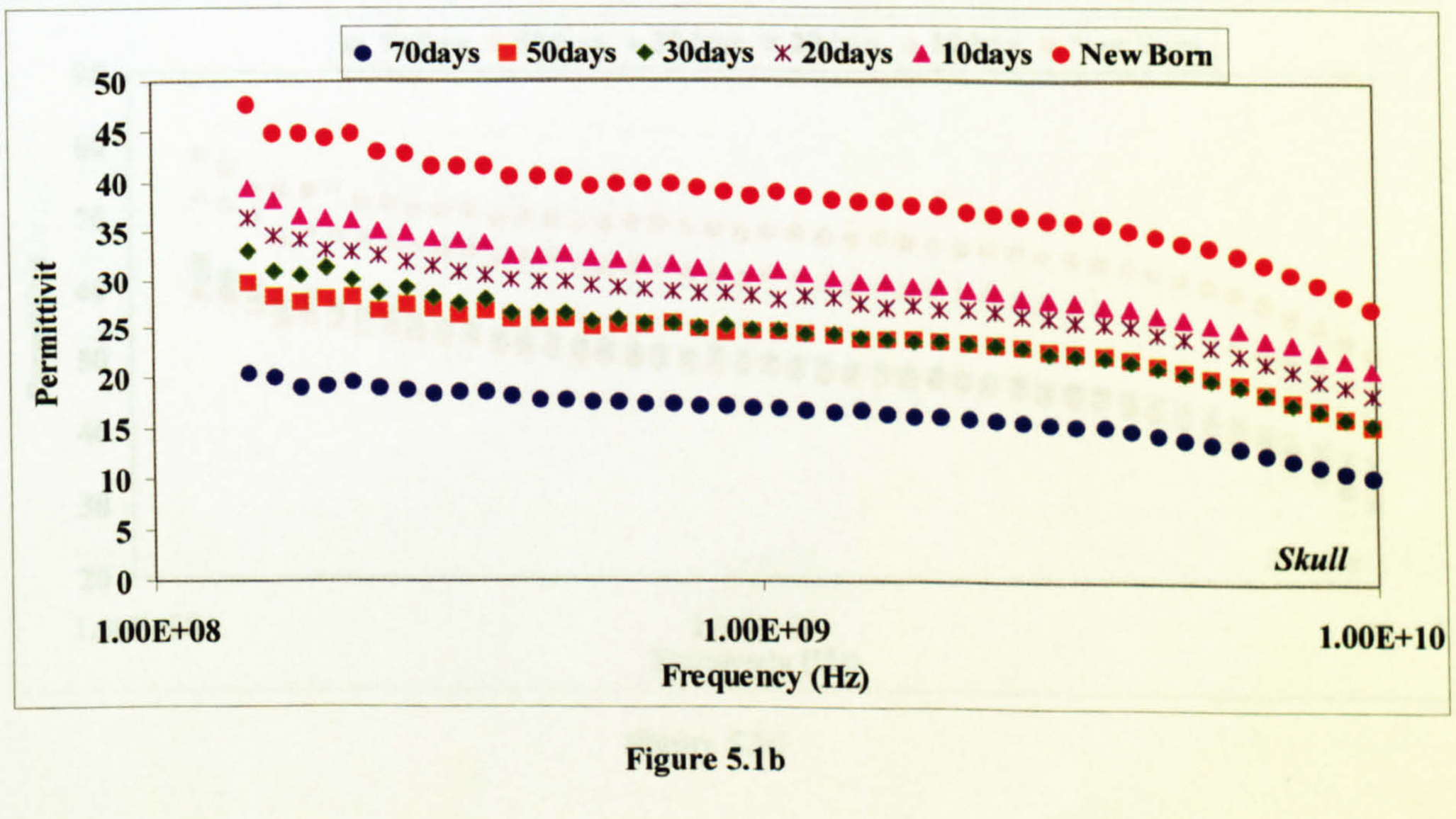

Figure 5.1b

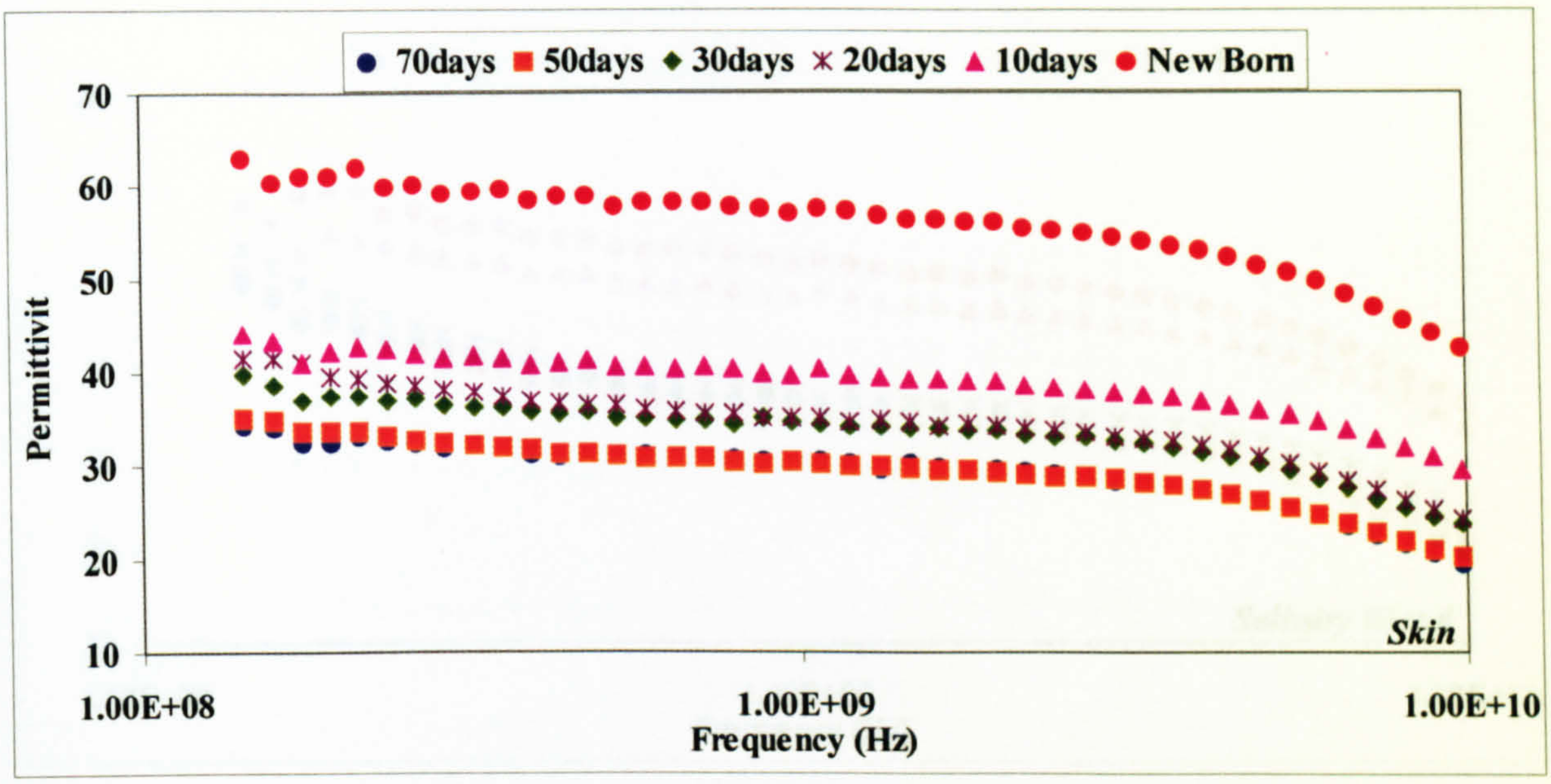

Figure 5.1c

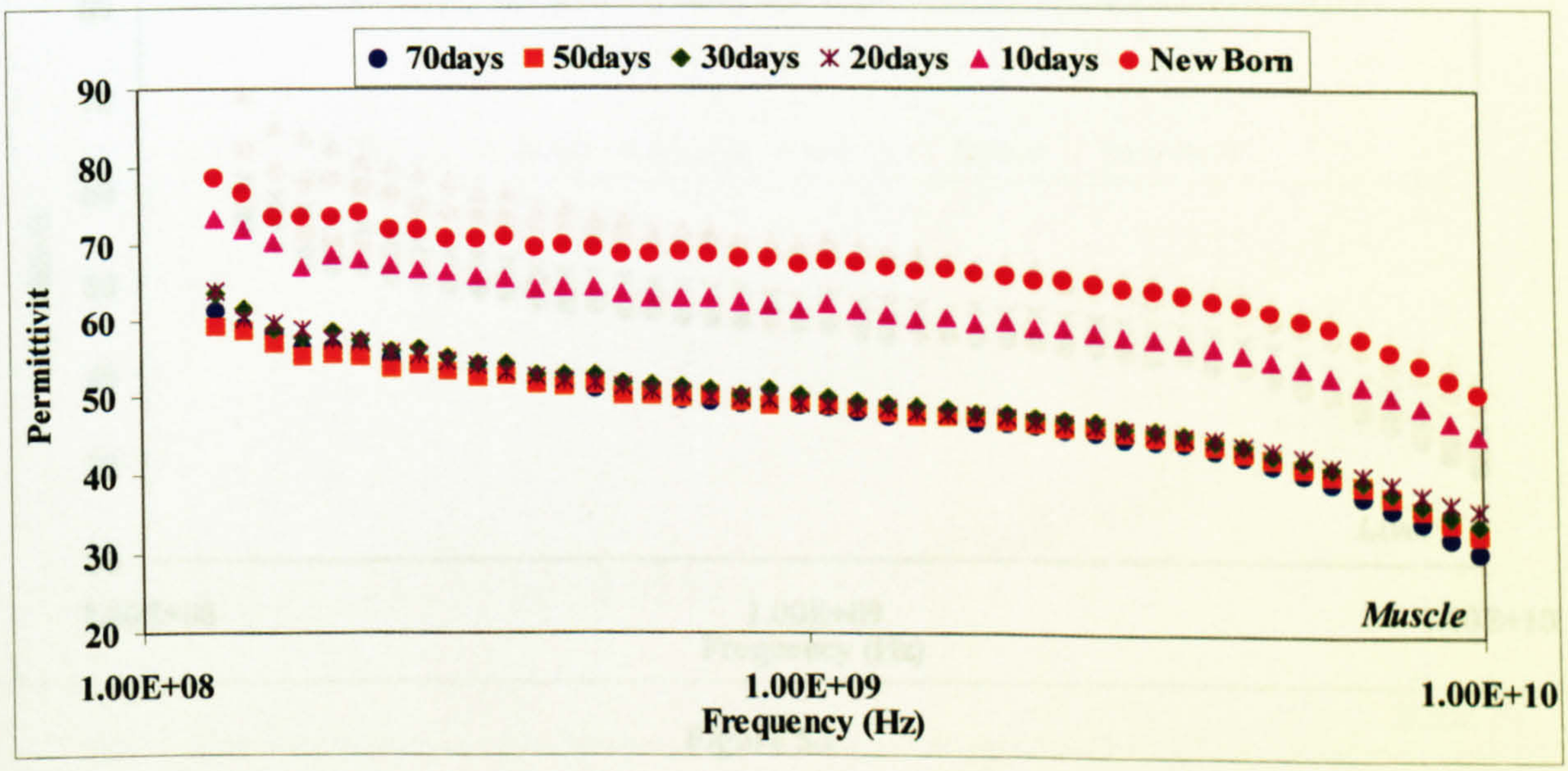

Figure 5.1d

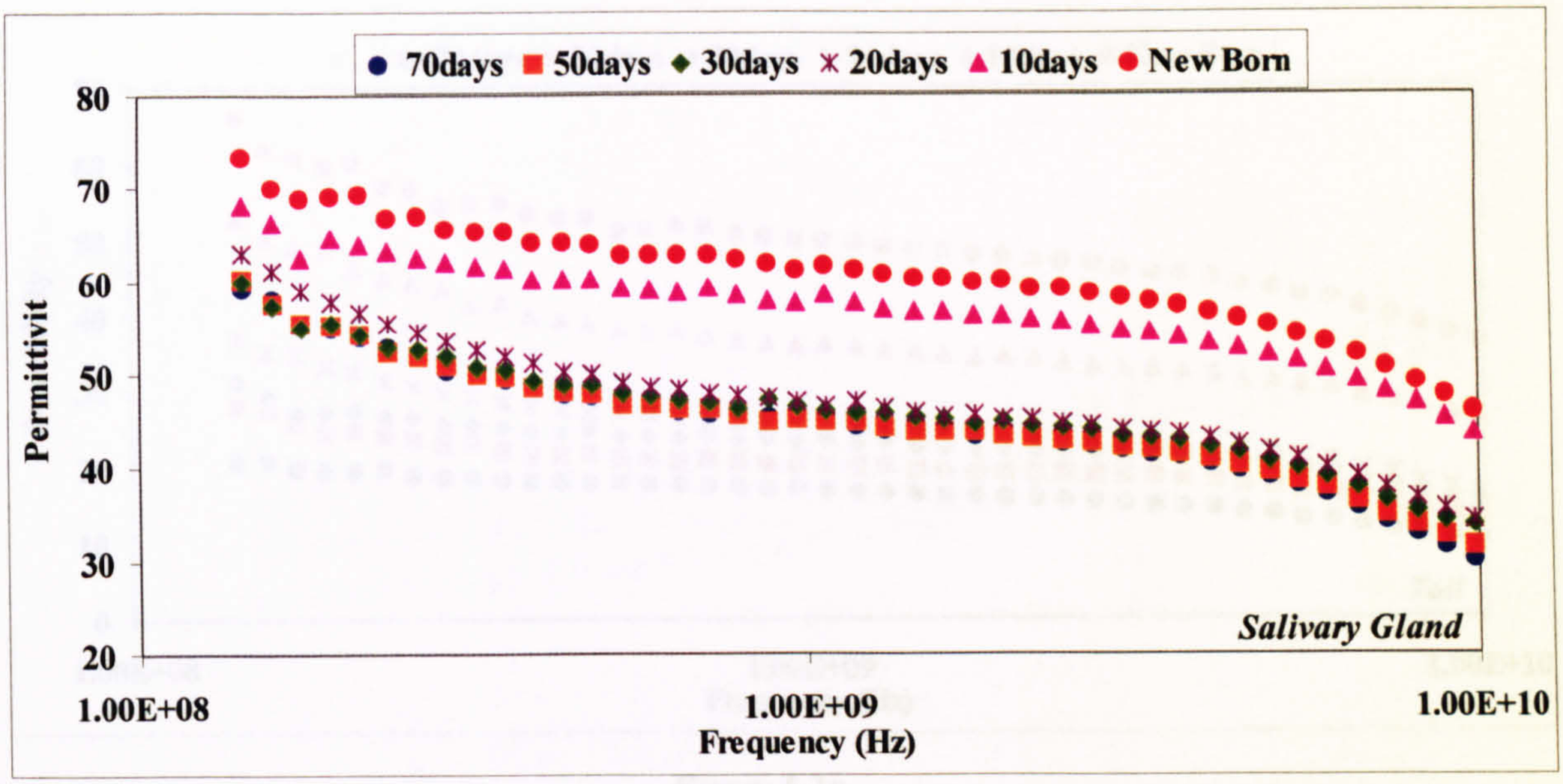

Figure 5.1e

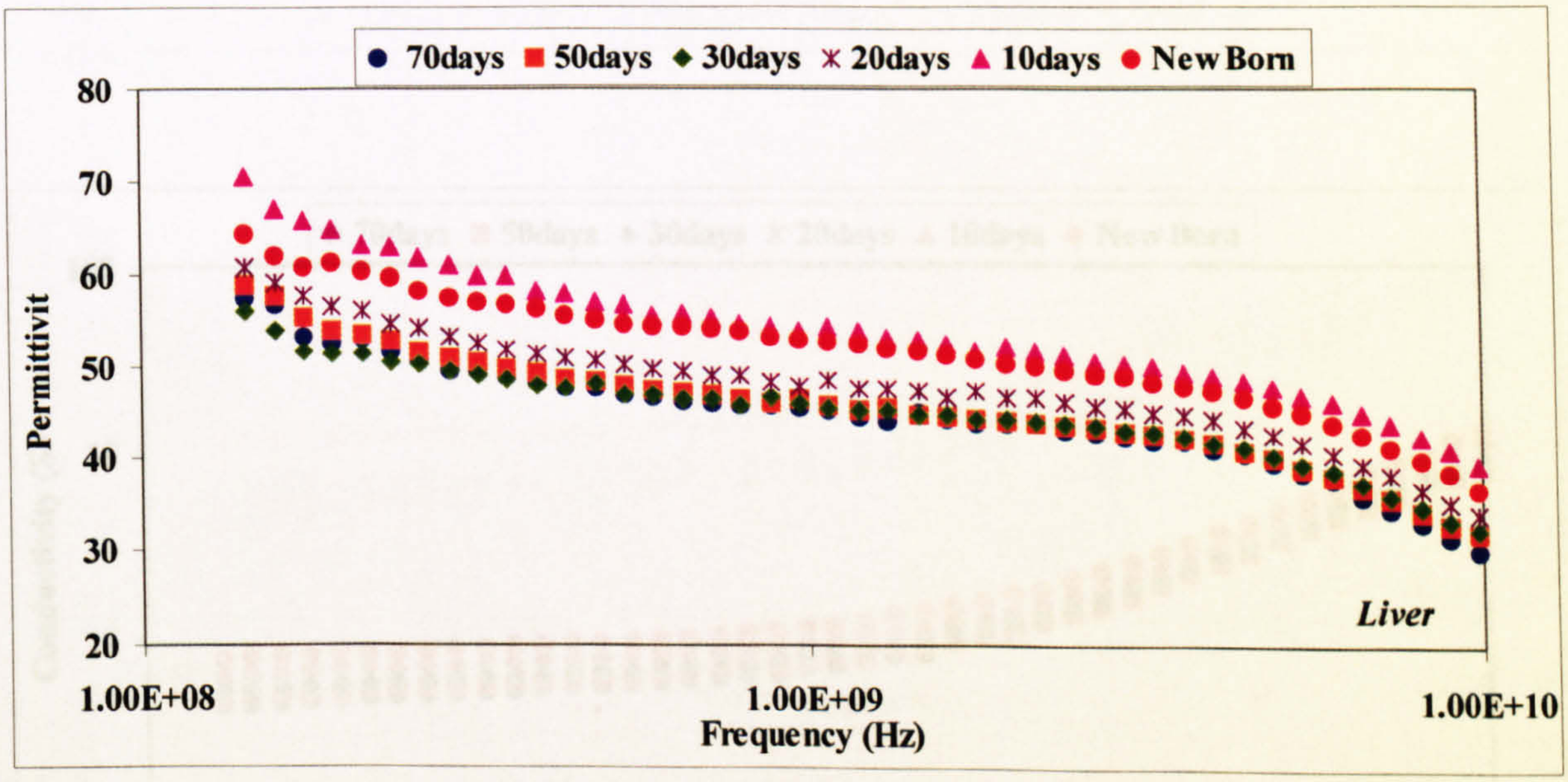

Figure 5.1

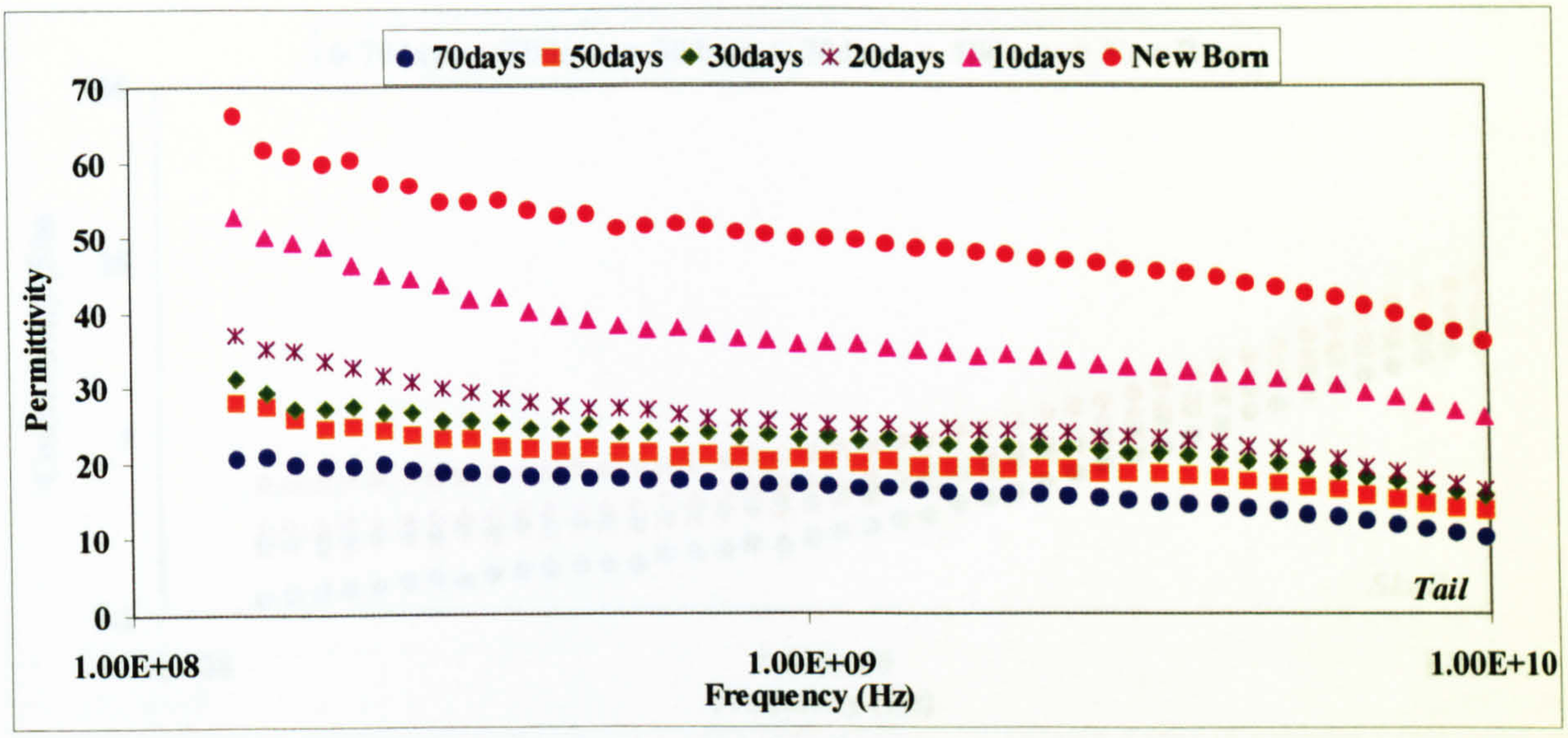

Figure 5.1g

Figure 5.1 Relative permittivity of **a** brain **b** skull **c** skin **d** muscle **e** salivary gland **f** liver and **g** tail tissue from rats of different ages in the frequency range of 130MHz to 10GHz.

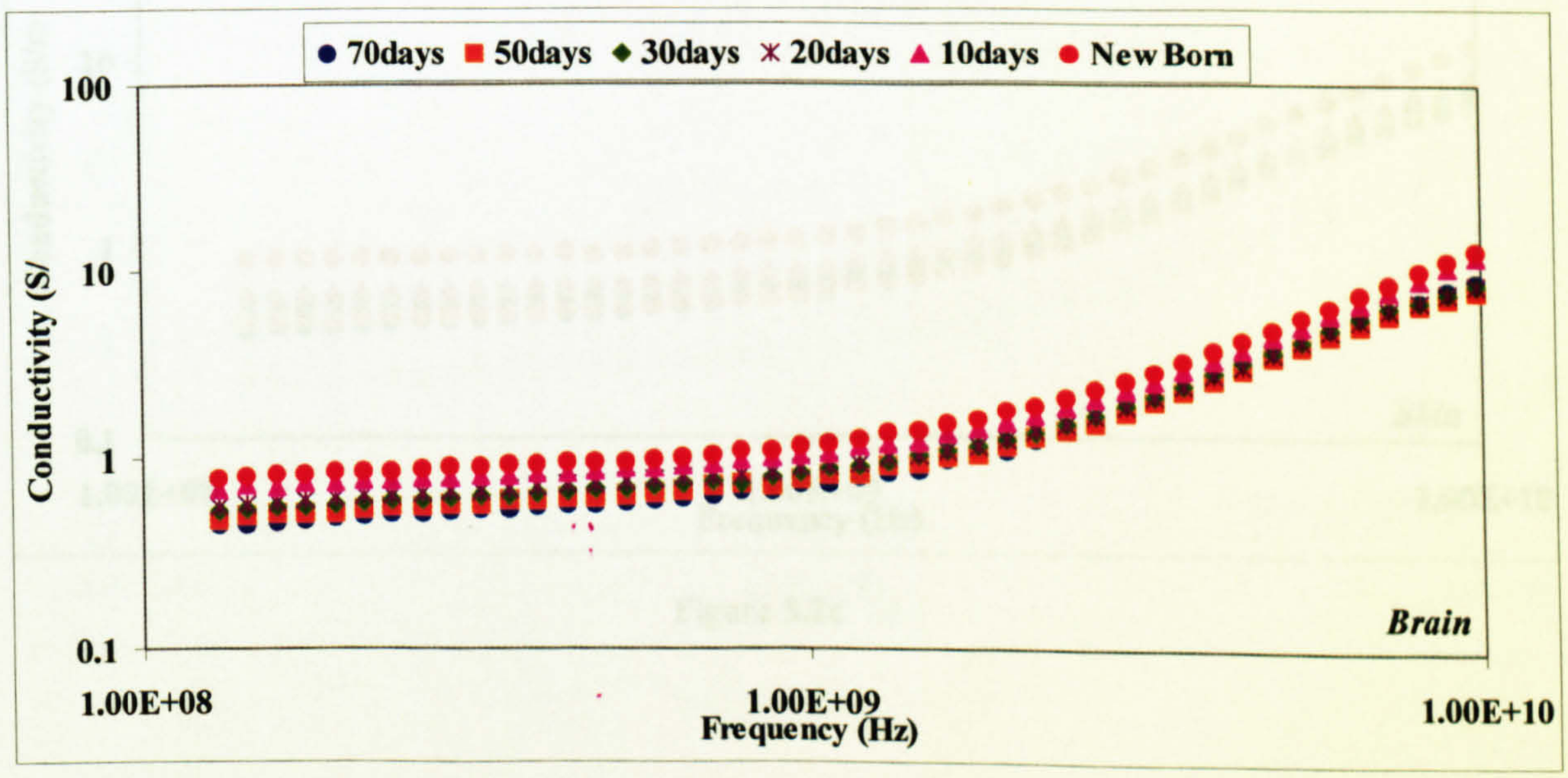

Figure 5.2a

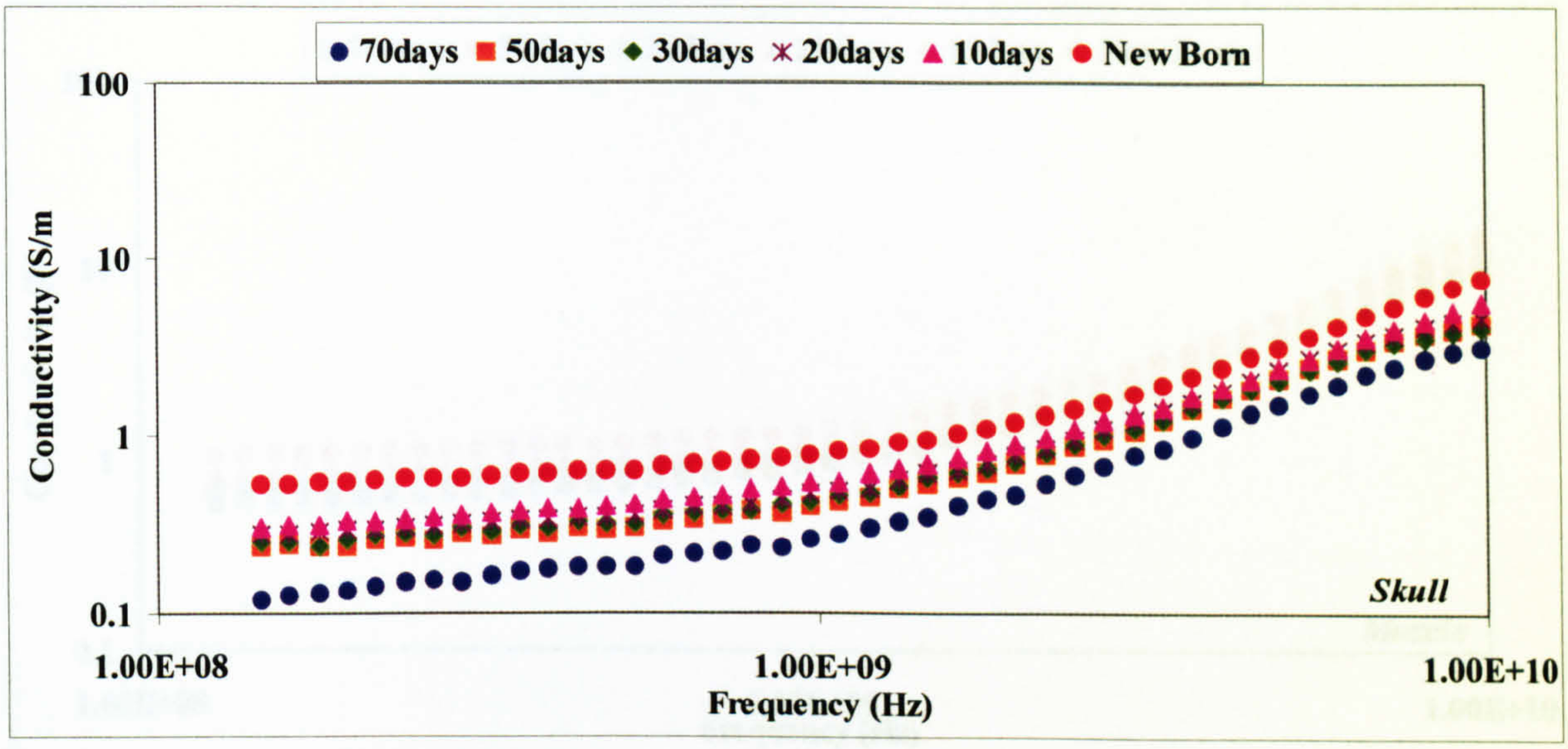

Figure 5.2b

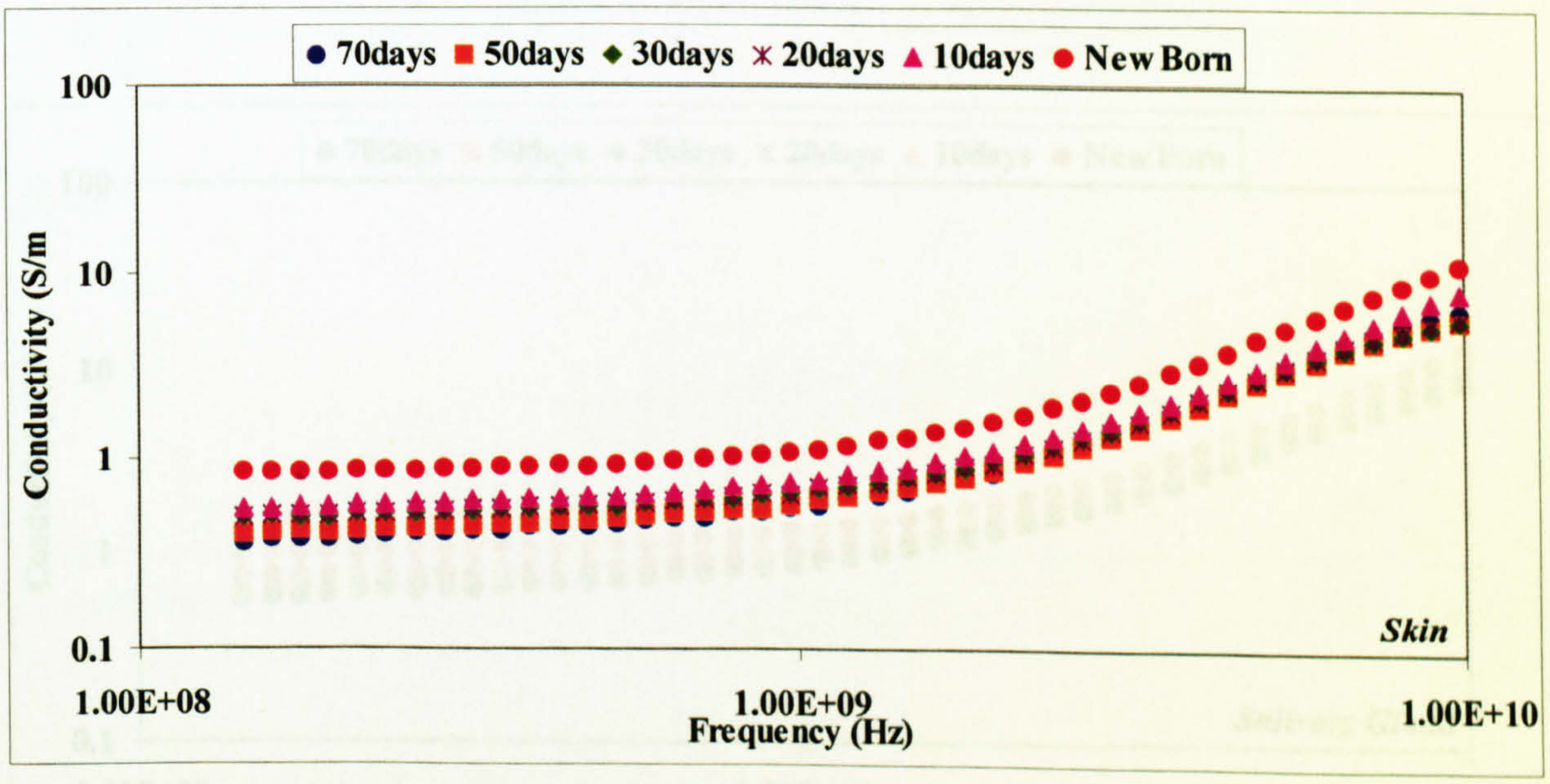

Figure 5.2c

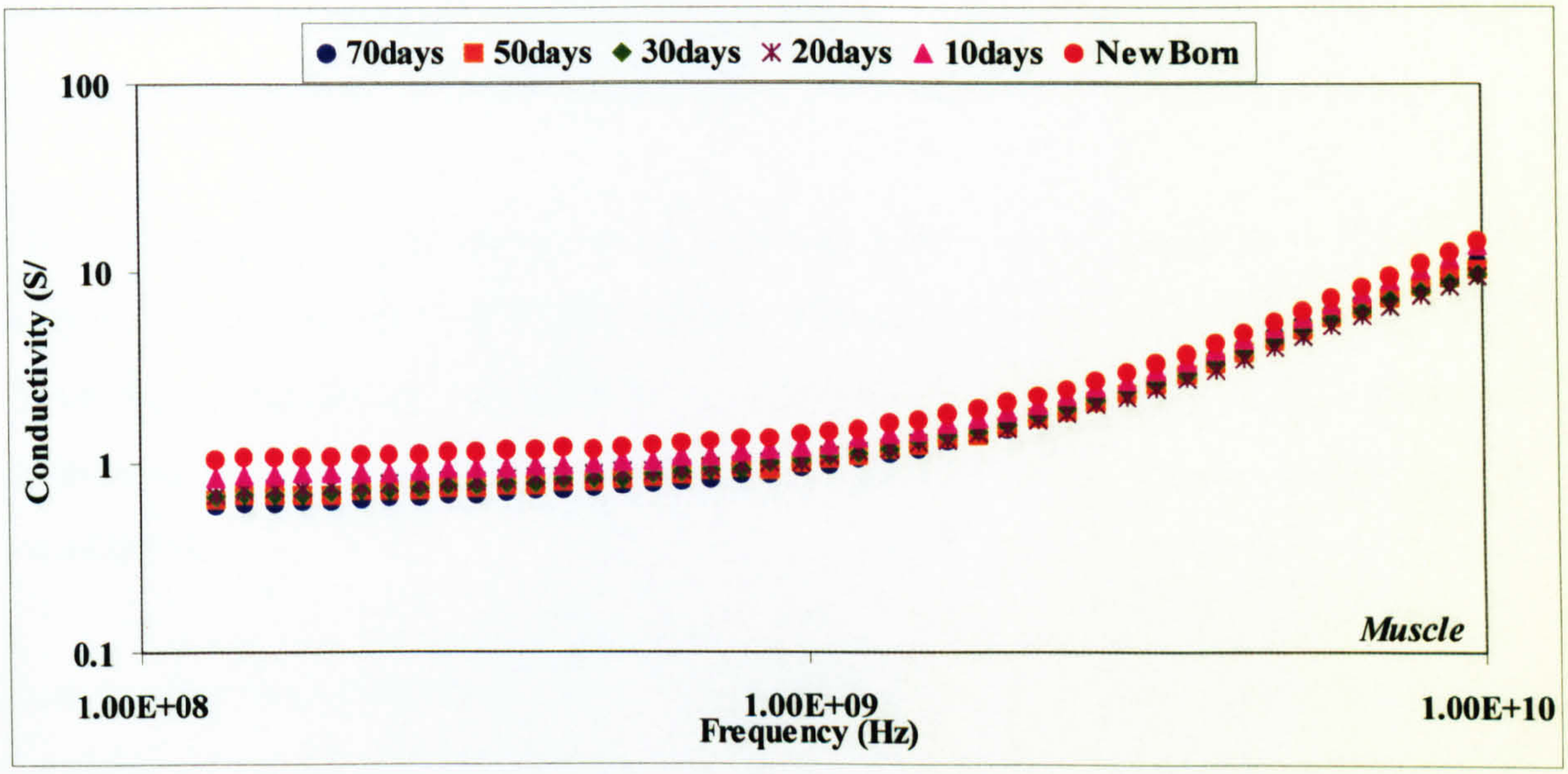

Figure 5.2d

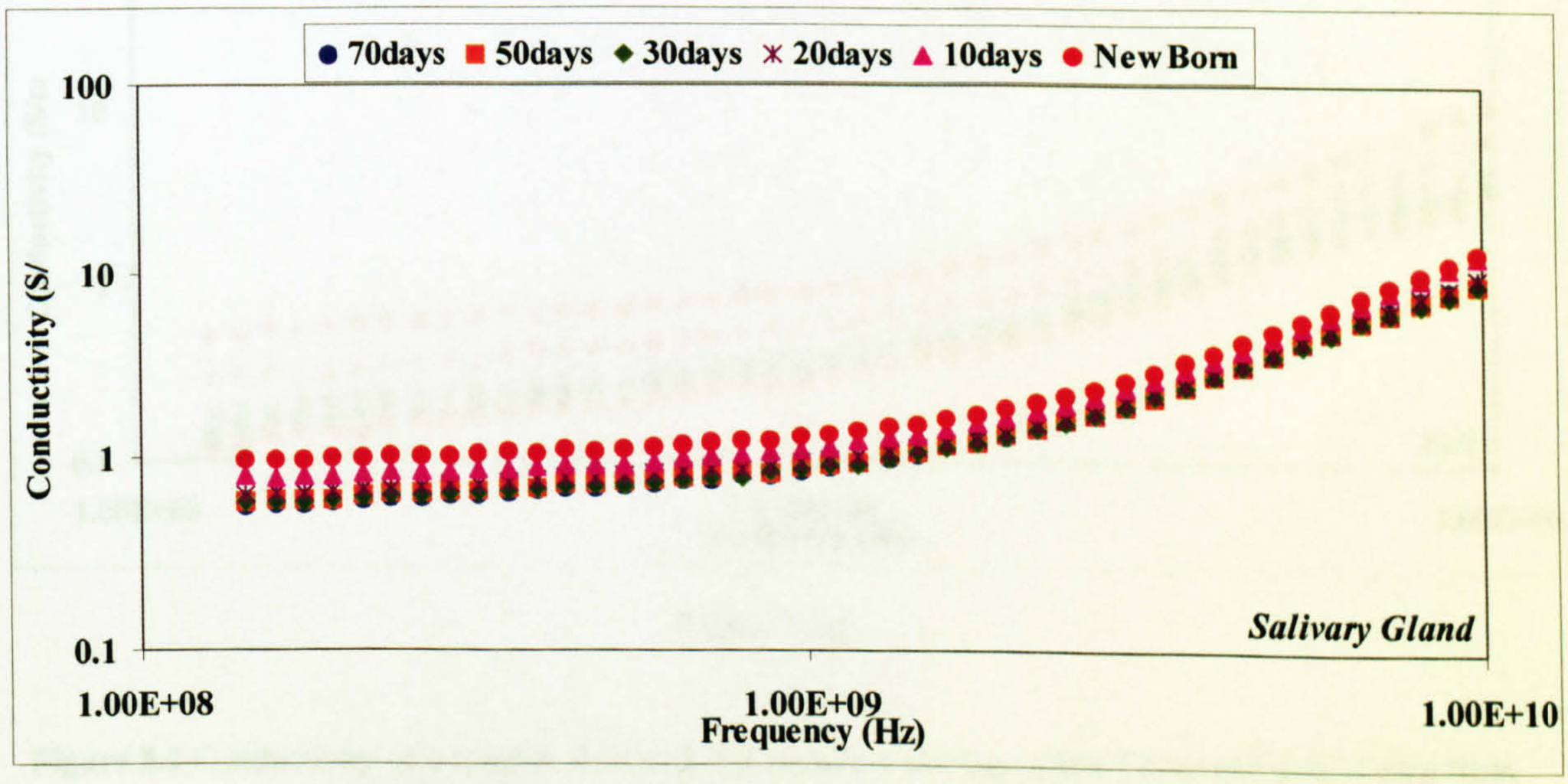

Figure 5.2e

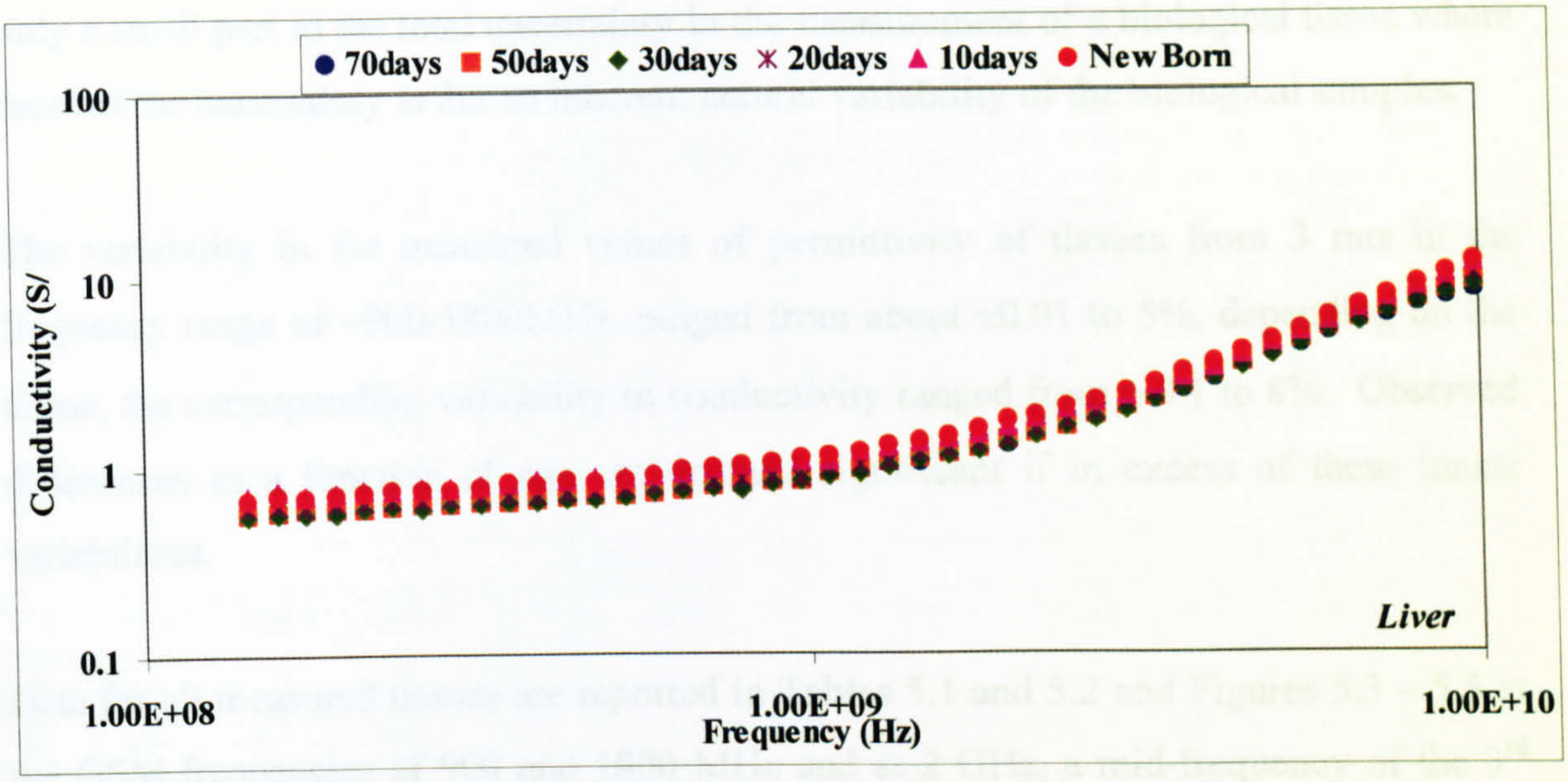

Figure 5.2f

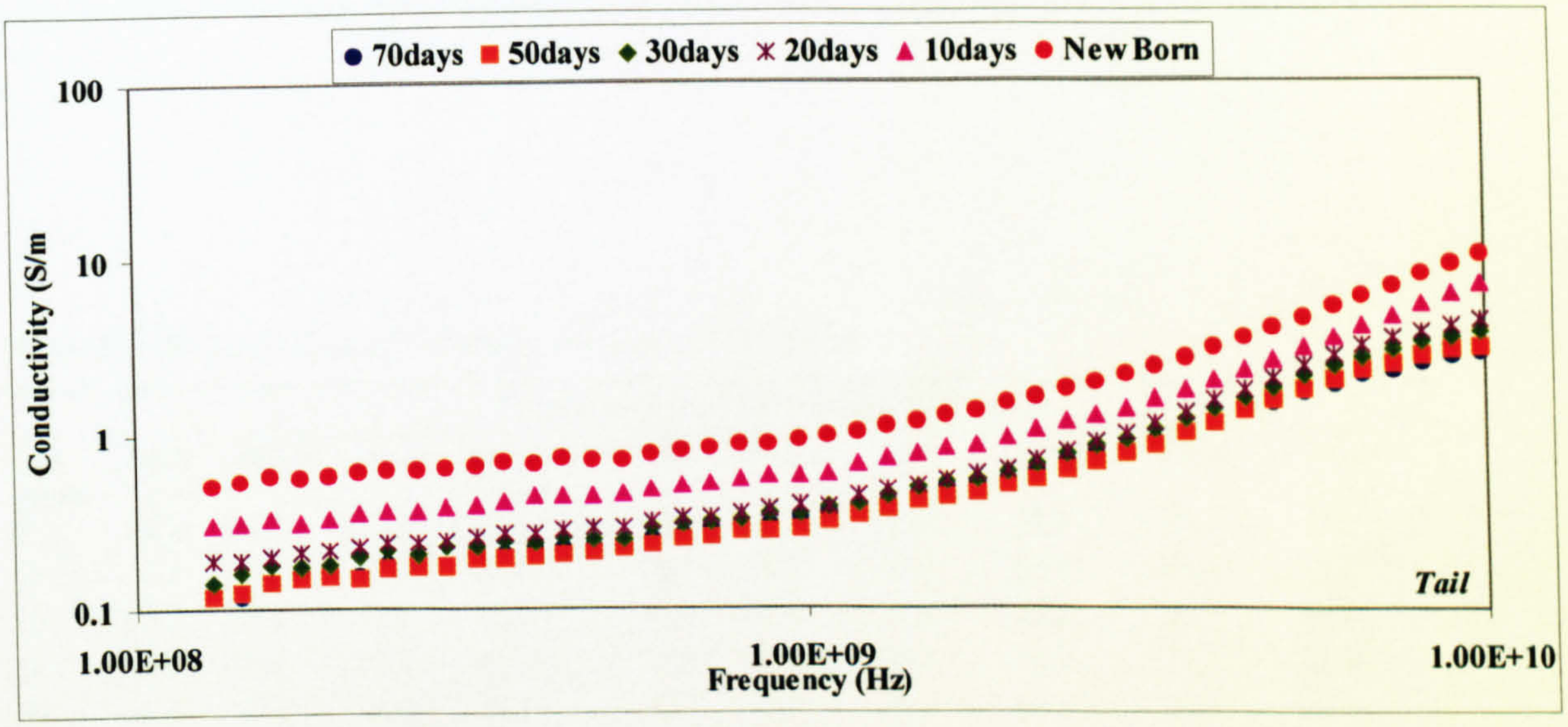

Figure 5.2g

Figure 5.2 Conductivity of **a** brain **b** skull **c** skin **d** muscle **e** salivary gland **f** liver and **g** tail tissue from rats of different ages in the frequency range of 130MHz to 10GHz.

Each data point is the average of multiple measurements on tissues from two or three rats. The standard deviations were calculated but omitted from the graphs for the purpose of clarity. The measurement errors discussed in the previous section contribute

only a small part to the total uncertainty in the measurement of a biological tissue where most of the uncertainty is due to inherent natural variability of the biological samples.

The variability in the measured values of permittivity of tissues from 3 rats in the frequency range of ~900-1800MHz, ranged from about ±0.01 to 5%, depending on the tissue, the corresponding variability in conductivity ranged from ± 0.1 to 8%. Observed differences as a function of age are deemed significant if in excess of these innate variabilities.

Data for all measured tissues are reported in Tables 5.1 and 5.2 and Figures 5.3 – 5.5 at the GSM frequencies of 900 and 1800 MHz and at 2 GHz, a mid-frequency of the 3rd generation universal mobile telecommunication system (UMTS).

Table 5.1 Dielectric data of different rat tissue at 900 MHz

Permittivity at ~900 MHz(8.81E+08Hz)										
Age (days)	Brain	Muscle	Skull	Salivary Gland	Skin	Spleen	Liver	Kidney	Tail	Tongue
0	64.6	68.2	39.0	61.8	57.6	56.0	53.4	59.9	50.1	59.5
10	59.5	62.0	31.0	57.9	39.8	55.1	54.4	60.0	36.1	60.2
20	48.5	49.6	28.7	47.4	35.1	53.9	48.3	46.9	25.4	50.6
30	49.2	51.2	25.6	47.1	35.0	52.6	46.6	48.3	23.6	47.0
50	44.3	48.8	24.7	44.9	30.0	50.2	45.9	45.9	20.2	50.5
70	44.3	49.1	17.3	45.3	30.4	48.5	45.8	43.8	17.1	53.0
Conductivity at ~900MHz										
Age (days)	Brain	Muscle	Skull	Salivary Gland	Skin	Spleen	Liver	Kidney	Tail	Tongue
0	1.1	1.3	0.8	1.3	1.1	1.2	1.0	1.2	0.9	1.2
10	1.0	1.2	0.5	1.1	0.8	1.2	1.0	1.2	0.6	1.1
20	0.8	1.0	0.4	0.9	0.7	1.1	0.9	1.0	0.4	0.9
30	0.8	1.0	0.4	0.9	0.7	1.1	0.8	0.9	0.3	0.9
50	0.7	0.9	0.4	0.8	0.6	1.0	0.8	0.9	0.3	0.9
70	0.7	0.9	0.2	0.8	0.5	0.9	0.8	0.9	0.3	1.0

Table 5.2 Dielectric data of different rat tissue at 1800 MHz

Permittivity at ~1800 MHz(1.78E+09Hz)										
Age (days)	Brain	Muscle	Skull	Salivary Gland	Skin	Spleen	Liver	Kidney	Tails	Tongue
0	62.3	66.3	37.5	59.7	56.0	53.7	50.9	57.4	47.7	57.3
10	57.3	59.8	29.5	56.1	38.7	53.0	51.9	57.4	33.8	57.8
20	46.9	47.6	27.5	45.6	34.3	52.4	47.4	45.5	24.1	49.8
30	46.7	48.1	23.8	44.7	33.5	49.7	44.5	45.8	22.1	44.8
50	43.2	47.4	24.0	43.5	29.3	48.2	44.4	44.3	19.2	49.4
70	42.6	46.7	16.2	43.2	29.4	46.0	43.9	41.7	15.8	51.2
Conductivity at ~1800MHz										
Age (days)	Brain	Muscle	Skull	Salivary Gland	Skin	Spleen	Liver	Kidney	Tails	Tongue
0	1.60	1.89	1.09	1.76	1.55	1.67	1.53	1.74	1.36	1.80
10	1.44	1.70	0.82	1.58	1.08	1.68	1.47	1.69	0.87	1.67
20	1.16	1.41	0.70	1.28	0.95	1.57	1.27	1.37	0.60	1.33
30	1.15	1.43	0.65	1.22	0.94	1.46	1.17	1.28	0.55	1.29
50	1.04	1.38	0.61	1.22	0.82	1.43	1.22	1.26	0.46	1.35
70	1.04	1.39	0.43	1.25	0.84	1.39	1.24	1.27	0.52	1.46

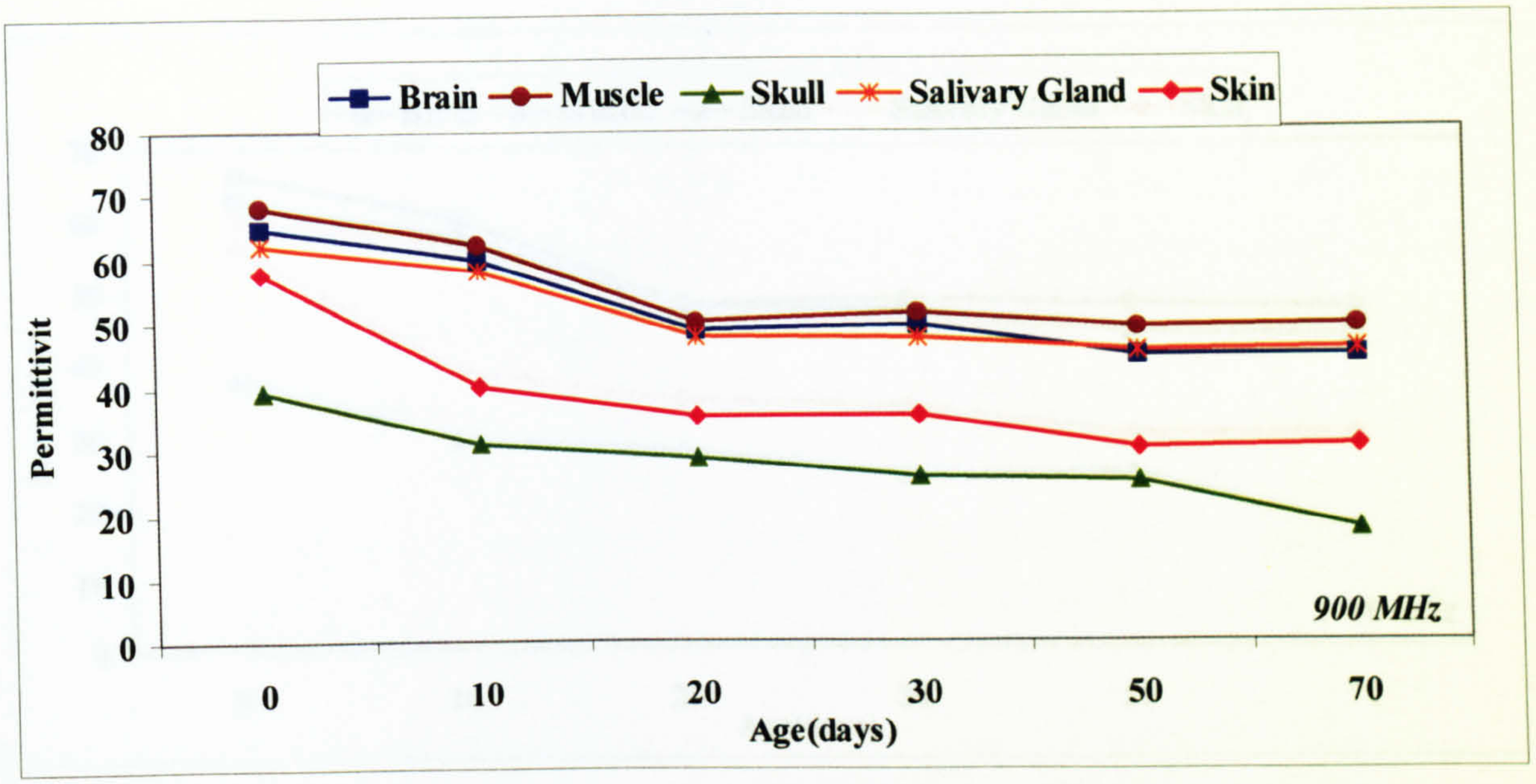

Figure 5.3a

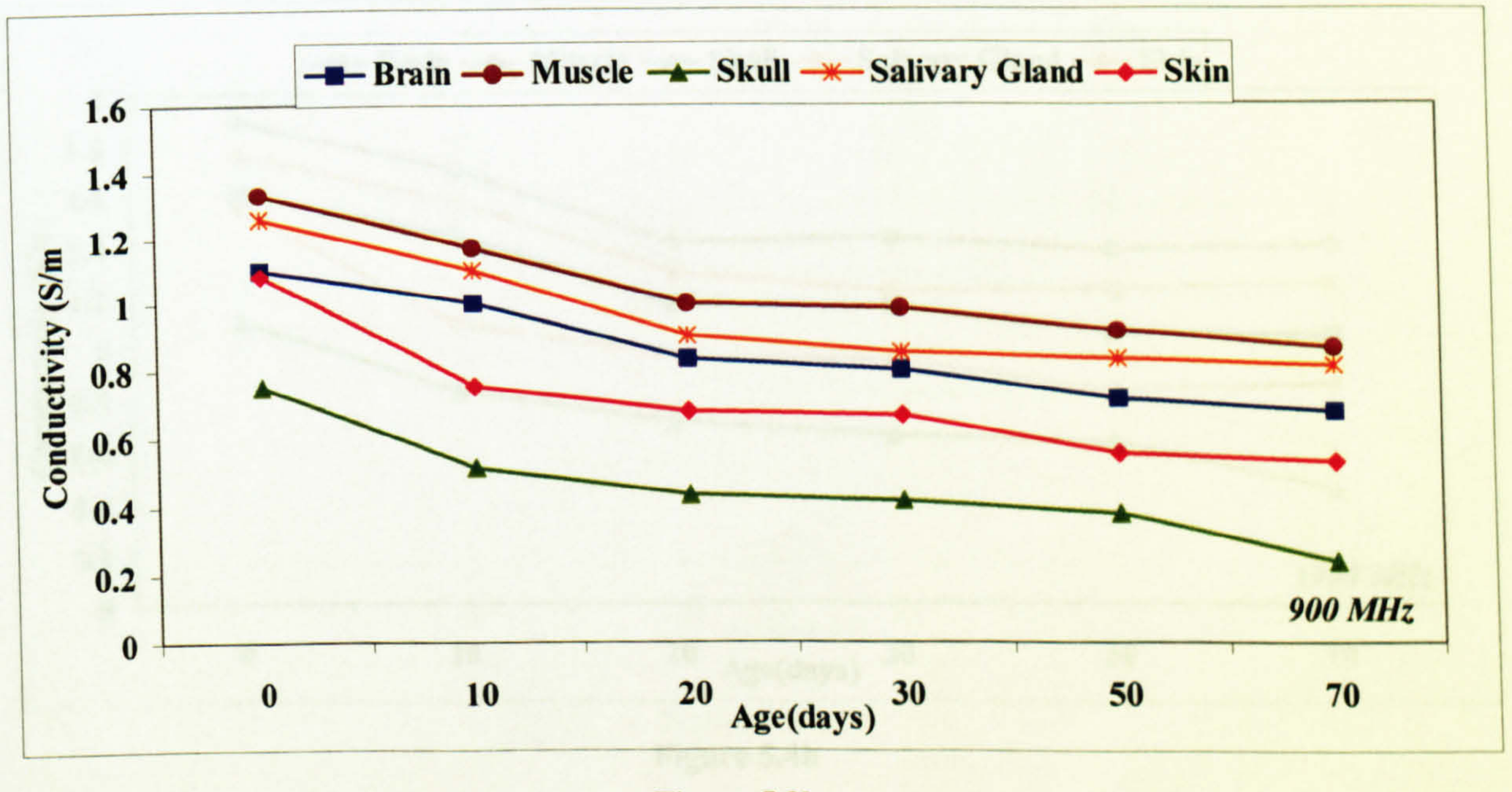

Figure 5.3b

Figure 5.3 a Permittivity and **b** conductivity of rat tissue as a function of age at 900 MHz

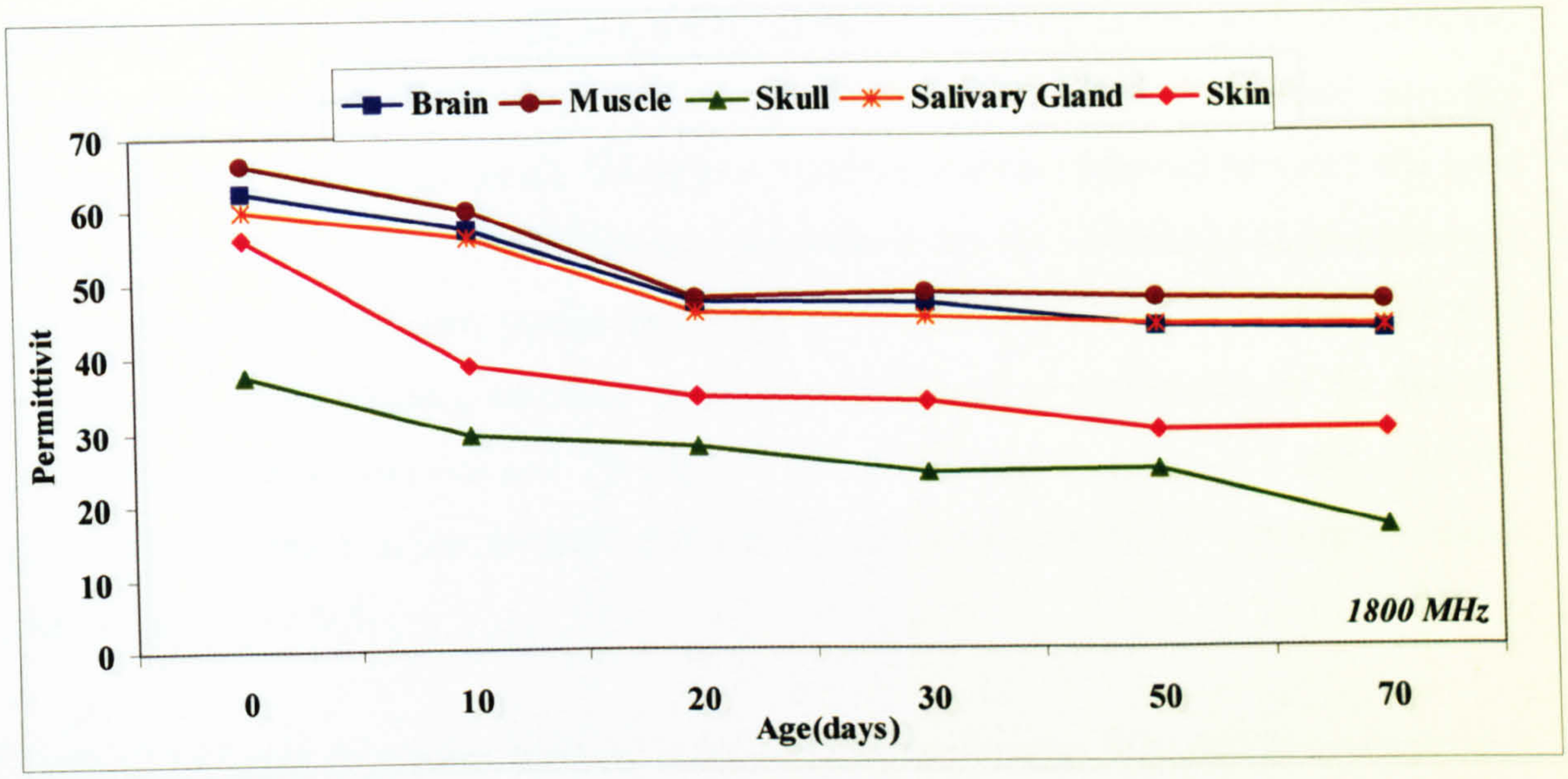

Figure 5.4a

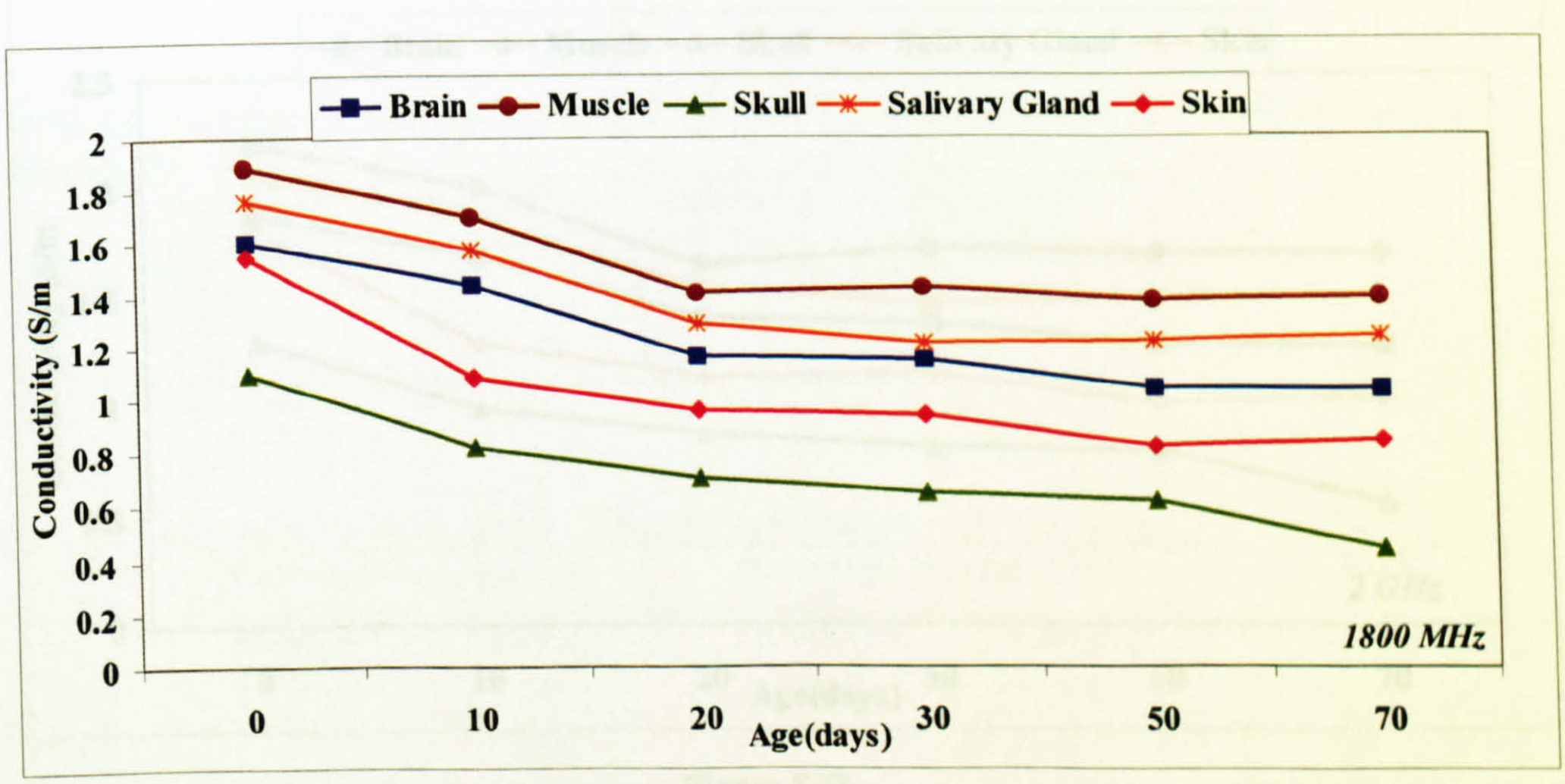

Figure 5.4b

Figure 5.4 a Permittivity and **b** conductivity of rat tissue as a function of age at 1800 MHz

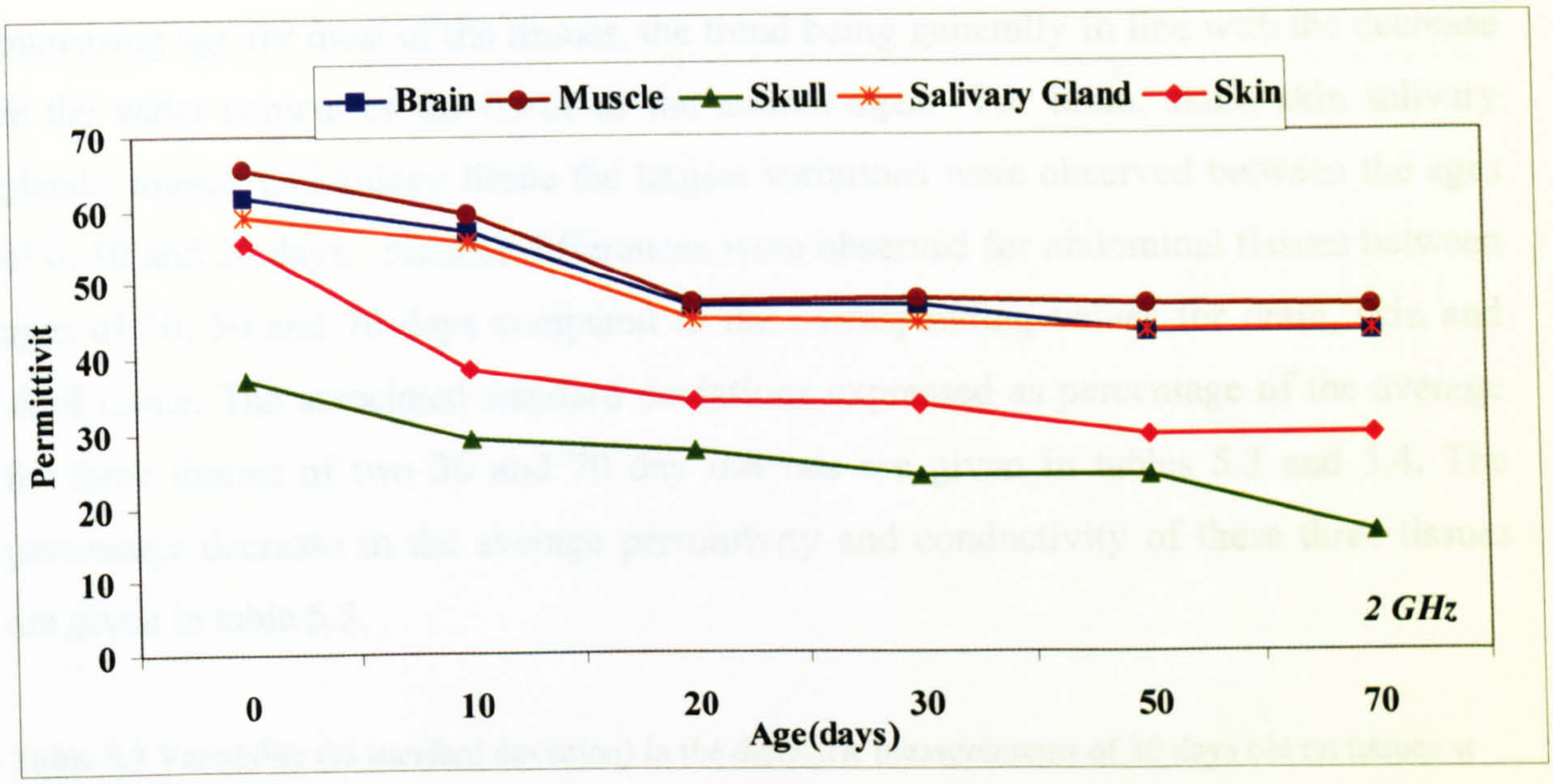

Figure 5.5a

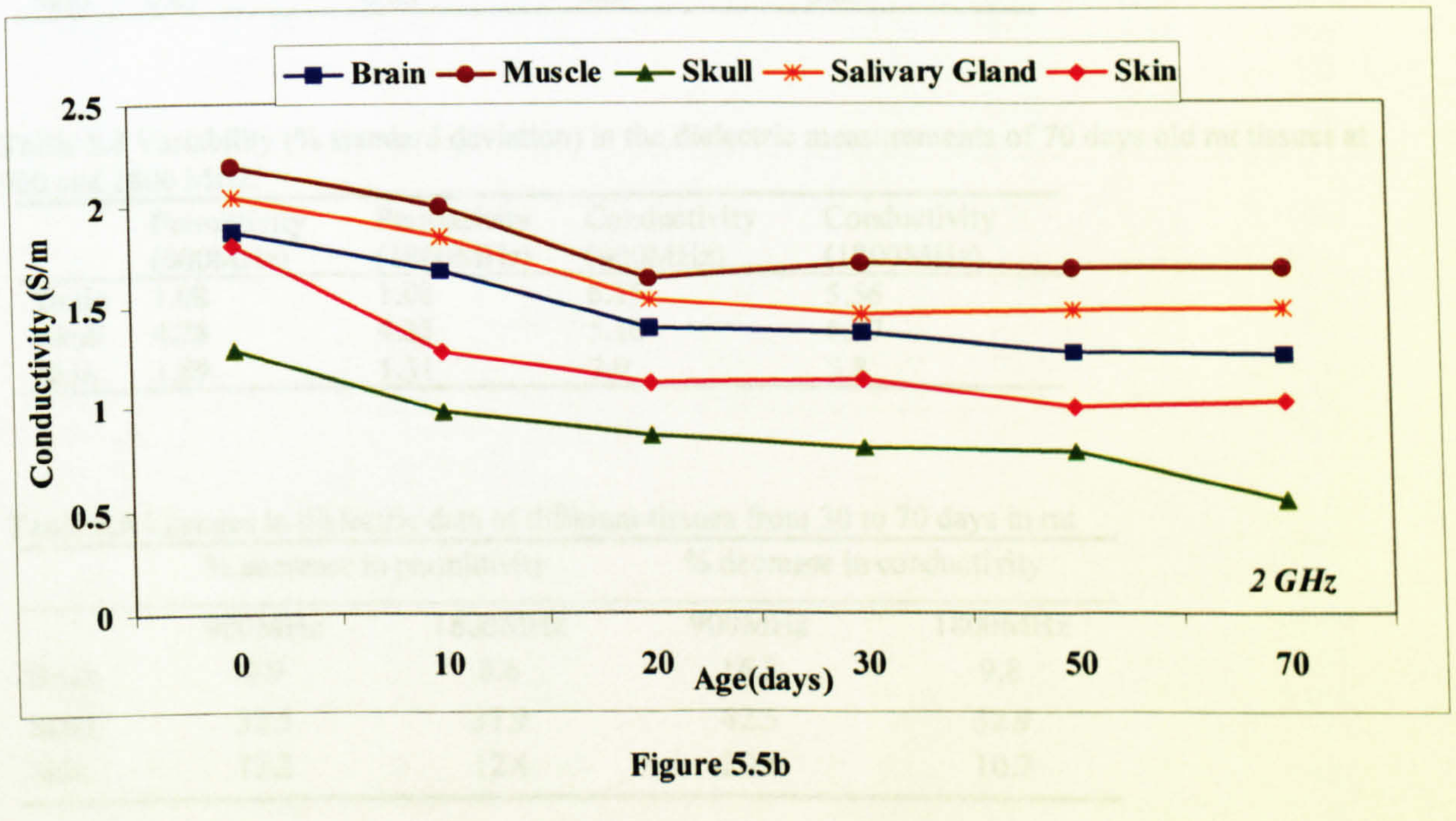

Figure 5.5b

Figure 5.5 a Permittivity and **b** conductivity of rat tissue as a function of age at 2 GHz.

The data show a general trend of decreasing permittivity and conductivity with increasing age for most of the tissues, the trend being generally in line with the decrease in the water content of the tissue as the animal ages. For brain, skull, skin salivary glands, muscle and kidney tissue the largest variations were observed between the ages of 0, 10 and 20 days. Smaller differences were observed for abdominal tissues between ages of 30, 50 and 70 days compared to the corresponding values for brain, skin and skull tissue. The associated standard deviations expressed as percentage of the average for three tissues of two 30 and 70 day old rats are given in tables 5.3 and 5.4. The percentage decrease in the average permittivity and conductivity of these three tissues are given in table 5.5.

Table 5.3 Variability (% standard deviation) in the dielectric measurements of 30 days old rat tissues at 900 and 1800 MHz.

	Permittivity (900MHz)	Permittivity (1800MHz)	Conductivity (900MHz)	Conductivity (1800MHz)
Brain	0.17	0.02	4.80	2.67
Skull	1.60	1.33	7.67	4.47
Skin	0.67	0.63	0.85	0.66

Table 5.4 Variability (% standard deviation) in the dielectric measurements of 70 days old rat tissues at 900 and 1800 MHz.

	Permittivity (900MHz)	Permittivity (1800MHz)	Conductivity (900MHz)	Conductivity (1800MHz)
Brain	1.08	1.08	6.15	5.56
Skull	4.28	4.33	5.16	6.87
Skin	1.89	1.31	7.9	5.8

Table 5.5 Changes in dielectric data of different tissues from 30 to 70 days in rat

	% decrease in permittivity		% decrease in conductivity	
	900MHz	1800MHz	900MHz	1800MHz
Brain	9.9	8.6	16.3	9.8
Skull	32.5	31.9	42.5	32.9
Skin	13.2	12.4	20.5	10.7

For each tissue the data above 600 MHz were fitted to the Cole-Cole expression, the fitted parameters and 95% confidence intervals for ten rat tissues at different ages are shown in table 5.6.

Table 5.6 Dielectric parameters of water dispersion in tissues obtained by fitting the experimental results at 37°C. The ± term corresponds to the 95% confidence interval.

Tissue/Age	ε_s	$\pm\varepsilon_s$	τ_{relax} (ps)	$\pm\tau_{relax}$ (ps)	α	$\pm\alpha$	σ (Sm^{-1})	$\pm\sigma$ (Sm^{-1})
Brain								
New Born	65.0	0.3	8.23	0.30	0.11	0.01	0.91	0.016
10days	60.0	0.3	8.06	0.29	0.10	0.01	0.82	0.015
20days	49.4	0.4	7.83	0.46	0.18	0.02	0.67	0.017
30days	49.7	0.4	8.31	0.47	0.18	0.02	0.62	0.018
50days	45.8	0.5	8.38	0.56	0.19	0.02	0.57	0.019
70days	44.8	0.3	9.40	0.38	0.12	0.01	0.54	0.013
Skull								
New Born	39.9	0.2	9.21	0.31	0.17	0.01	0.61	0.009
10days	32.5	0.3	10.05	0.43	0.24	0.01	0.37	0.008
20days	30.2	0.5	11.04	1.03	0.25	0.03	0.3	0.017
30days	27.1	0.6	12.72	1.49	0.28	0.03	0.27	0.01
50days	27.8	1.0	13.55	2.96	0.32	0.04	0.23	0.03
70days	18.3	0.3	15.60	1.44	0.22	0.02	0.15	0.01
Skin								
New Born	58.68	0.23	8.22	0.22	0.15	0.009	0.89	0.002
10days	40.48	0.17	8.81	0.24	0.12	0.01	0.62	0.001
20days	36.58	0.46	9.32	0.71	0.21	0.03	0.54	0.003
30days	36.35	0.59	9.44	0.89	0.24	0.03	0.49	0.003
50days	31.12	0.3	11.08	0.60	0.15	0.02	0.43	0.002
70days	31.06	0.19	12.27	0.42	0.11	0.01	0.41	0.001
Muscle								
New Born	68.81	0.24	8.41	0.20	0.10	0.009	1.14	0.01
10days	62.63	0.33	9.00	0.31	0.10	0.01	0.96	0.01
20days	50.70	0.27	8.64	0.28	0.18	0.01	0.85	0.01
30days	52.33	0.39	10.00	0.41	0.21	0.01	0.75	0.01
50days	50.24	0.35	10.51	0.42	0.14	0.01	0.76	0.01
70days	49.64	0.33	12.21	0.41	0.10	0.01	0.67	0.01
Salivary Glands								
New Born	62.71	0.25	8.29	0.22	0.14	0.01	1.07	0.011
10days	58.56	0.30	8.65	0.30	0.10	0.01	0.91	0.014
20days	47.92	0.28	8.85	0.32	0.15	0.01	0.75	0.012
30days	47.79	0.27	8.78	0.30	0.19	0.01	0.66	0.011
50days	46.43	0.38	9.37	0.46	0.18	0.02	0.68	0.015
70days	46.33	0.37	10.51	0.47	0.16	0.02	0.64	0.016
Liver								
New Born	53.42	0.33	9.87	0.32	0.12	0.01	0.85	0.02
10days	54.51	0.38	8.74	0.35	0.12	0.02	0.85	0.02
20days	49.05	0.34	9.69	0.35	0.12	0.02	0.69	0.02
30days	47.10	0.41	9.14	0.42	0.17	0.02	0.62	0.02
50days	47.09	0.43	9.93	0.46	0.15	0.02	0.64	0.02
70days	47.11	0.87	9.64	0.88	0.19	0.04	0.64	0.04

Table 5.6 (Continued)

Tissue/Age	ε_s	$\pm\varepsilon_s$	τ_{relax} (ps)	$\pm\tau_{relax}$ (ps)	α	$\pm\alpha$	σ (Sm^{-1})	$\pm\sigma$ (Sm^{-1})
Spleen								
New Born	56.93	0.33	9.00	0.33	0.15	0.01	0.99	0.01
10days	55.67	0.39	8.81	0.41	0.11	0.02	1.04	0.02
20days	54.63	0.34	9.09	0.36	0.13	0.01	0.94	0.01
30days	53.65	0.29	8.05	0.28	0.23	0.01	0.84	0.01
50days	51.71	0.38	9.40	0.41	0.17	0.02	0.8	0.02
70days	50.25	0.57	9.54	0.62	0.23	0.02	0.74	0.02
Tongue								
New Born	60.32	0.34	9.57	0.33	0.12	0.01	1.05	0.01
10days	61.14	0.38	9.68	0.35	0.12	0.01	0.94	0.02
20days	51.37	0.27	9.66	0.30	0.01	0.01	0.78	0.01
30days	47.37	0.24	9.00	0.29	0.15	0.01	0.76	0.01
50days	51.59	0.26	9.41	0.30	0.19	0.01	0.78	0.01
70days	53.94	0.38	10.09	0.41	0.13	0.02	0.79	0.02
Kidney								
New Born	60.09	0.30	8.98	0.24	0.13	0.01	1.02	0.02
10days	60.05	0.45	8.35	0.38	0.11	0.02	1.03	0.03
20days	47.37	0.39	9.80	0.41	0.12	0.02	0.8	0.02
30days	48.60	0.42	8.52	0.41	0.18	0.02	0.73	0.02
50days	46.76	0.43	9.61	0.46	0.14	0.02	0.71	0.02
70days	44.80	0.74	10.28	0.81	0.18	0.03	0.67	0.04
Tail								
New Born	50.99	0.41	9.16	0.45	0.17	0.02	0.72	0.02
10days	36.90	0.45	8.95	0.68	0.20	0.03	0.43	0.02
20days	26.52	0.43	11.49	1.01	0.22	0.03	0.25	0.01
30days	24.60	0.36	11.08	0.93	0.26	0.03	0.23	0.01
50days	21.50	0.39	11.29	1.17	0.28	0.03	0.18	0.01
70days	18.32	0.27	16.99	1.38	0.25	0.02	0.21	0.008

5-4 Discussion

The physiological development of an organism or tissue involves structural and biochemical changes, the rate at which the changes occur depends on the species and the type of tissue such that some tissues mature faster than others do [8]. For example, foetal liver and kidney are much nearer to the biochemical composition of the adult organs than are skeletal muscle or skin. As an animal matures, it goes through various stages of growth, which include changes in cells size, structure and the ratio of free to bound water. The data in Table 5.6 show that for all tissues there is a decrease in the values of ε_s (and consequently the amplitude of the γ dispersion), as animal grows older which correlates with the reduction of the water content. For most tissues, there is a tendency of an increase in the value of τ and α with age that can be attributed to the changes in the proportion of free and bound water content of the tissues. The relaxation times are higher than 6.36 ps, the corresponding value for water.

The study of skin growth in human and pig by Widdowson E and Dickerson J, 1960, reports changes in the ratio of free to bound water due to an increase in bound and a decrease in free water as the species grow from foetus to adult. This correlates with the systematic lengthening of the relaxation time (Table 5.6).

In the case of brain, the brain tissue of the new-born, which consists predominantly of grey matter, undergoes numerous branching of dendrites during growth to form a more complex and highly structured tissue with a gradual change in the ratio of the grey and white matters. Grey matter is known to contain a higher proportion of water than white matter [15]. The variation in the dielectric properties of brain tissue is consistent with the previous research [10 & 11]. It is also in line with the studies on the water content of rat brain, which is reported to fall rapidly with age from 9 to 45 days after birth [16]. Figure 5.6 shows the comparison between the permittivity of mouse brain at different ages reported by [10] and that of the rat observed in this study.

The skull hardens as it develops and increases its calcium content, it contains red bone marrow in young animals. The cellular composition of bone marrow varies in different regions of the skeleton. It also varies with the age of the individual. Nearly all the bones of the foetus contain red marrow; the colour indicates that the marrow is capable of producing blood cells. Following birth, the number of active hemocytoblasts (primitive stem cells that blood cells are derived from) decreases in most areas of bone marrow, and they are replaced with fat cells [17]. The abundance of fat cells causes the colour of the marrow to change from red to yellow. In the adult most bones contain yellow marrow, with red marrow present only in the ends of certain long bones, the ribs, sternum, vertebrae, and pelvis. The red marrow has higher water content as compared to yellow bone marrow that is mostly found in adult long bones. These developmental changes have implications on the dielectric properties. The largest variations in dielectric parameters are those observed for skull and for the bony tail (Table 5.6). For both tissues the decrease in permittivity and conductivity and the increase in relaxation time are the highest observed.

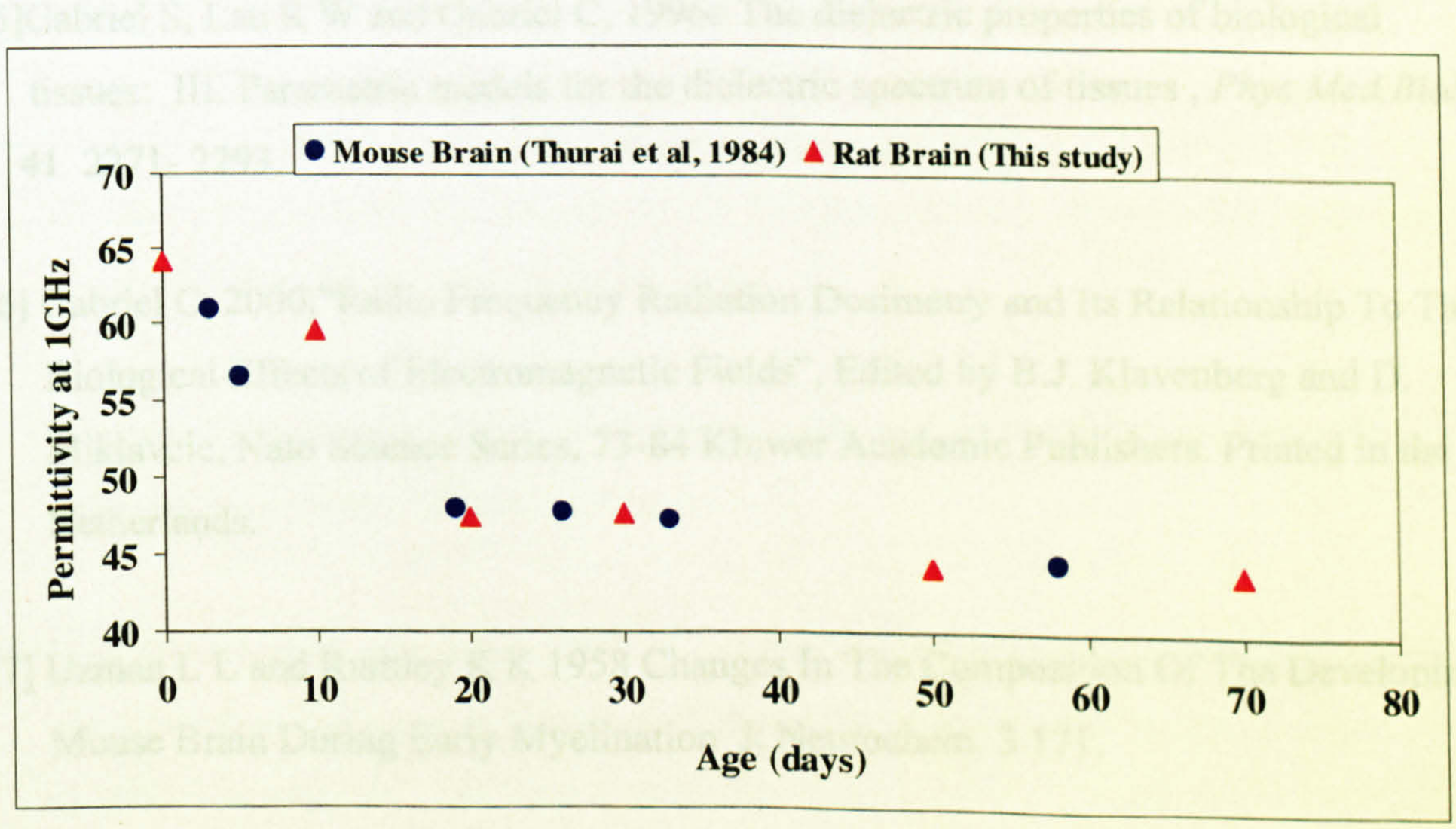

Figure 5.6 The permittivity of mouse brain at 1GHz for different ages (Thurai et al. 1984) compared with the permittivity of rat brain at different ages (this study)

References for chapter 5

[1] Schwan H P and Foster K R, 1980 RF-Field Interacions with Biological Systems: Electrical Properties and Biophysical Mechanisms, *Proc. of the IEEE* **68** 104-13.

[2]Pethig R and KellD B, 1987 The passive electrical properties of biological systems: their significance in physiology, biophysics and biotechnology , *Phys.Med.Biol.* **32** 933-70.

[3]Gabriel C, Gabriel S and Corthout E, 1996a, The dielectric properties of biological tissues: I. Literature survey *Phys.Med.Biol.* **41** 2231-2249.

[4]Gabriel S, Lau R W and Gabriel C, 1996b, The dielectric properties of biological tissues: II. Measurements in the frequency range of 10Hz to 20GHz *Phys.Med.Biol.* **41** 2251-2269.

[5]Gabriel S, Lau R W and Gabriel C, 1996c The dielectric properties of biological tissues: III. Parametric models for the dielectric spectrum of tissues , *Phys.Med.Biol.* **41** 2271- 2293.

[6] Gabriel C, 2000,"Radio Frequency Radiation Dosimetry and Its Relationship To The Biological Effects of Electromagnetic Fields", Edited by B.J. Klavenberg and D. Miklavcic, Nato Science Series, 73-84 Kluwer Academic Publishers. Printed in the Netherlands.

[7] Uzman L L and Rumley K K 1958 Changes In The Composition Of The Developing Mouse Brain During Early Myelination J. Neurochem. **3** 171.

[8] Widdowson E M, and Dickerson J W T 1960 The Effect of Growth and Function on the Chemical Composition of Soft Tissues *Biochem. J.* **77** 30-43.

[9] IEGMP 2000, Mobile Phones and Health 2000,Independent Expert Group on Mobile Phones" ISBN 0-85951-450-1.National Radiological Protection Board, Chilton, Didcot, UK.

[10] Thurai M., Goodridge VD, Sheppard RJ and Grant EH, 1984 Variation with age of the dielectric properties of mouse brain cerebrum *Phys.Med.Biol.* **29** 1133-1136.

[11] Thurai M., Steel M.C, Sheppard R.J and Grant E.H, 1985 Dielectric Properties of Developing Rabbit Brain at 37°C Bioelectromagnetics **6** 235-242.

[12] Gabriel C, Chan T Y A and Grant E H 1994, Admittance models for open-ended coaxial probes and their place in dielectric spectroscopy *Phys.Med.Biol.* **39** 2183-2200.

[13] Kraszewski A, Stuchly S S, Stuchly M A and Smith A M, 1982, In Vivo and In Vitro Dielectric Properties of Animal Tissues at Radio Frequencies *Bioelectromagnetics* **3** 421-32.

[14] Gabriel C,1993,"Numerical Modelling of Fringing Fields and Their Use For Complex Permittivity Measurements at High Frequencies", Brooks Air Force Base, Technical Report AL/OE-TR-1993-0068.

[15] Stewart-Wallace A M, 1939, "Biochemical study of cerebral tissues, and of the changes in cerebral cedema", *Brain*, **62** 426.

[16] Donaldson H H, and Hatai S 1931, "On the weight of the parts of the brain and on the percentage of water in them according to brain weight and to age, in albino and in wild Norway rats". *J.Comp Neurol.* **53** 263.

[17] Spence A.P, 1990, "Basic Human Anatomy", 3rd edition, The Benjamin/Cummings Company Inc.

Chapter 6- Changes in the dielectric properties of cellular membrane following applying electric pulses (electroporation)

6-1 Introduction

The effect of "strong" electromagnetic fields on cells and tissues can be dramatic but not necessarily harmful. External electric fields have been traditionally applied to probe ionic and dielectric properties of molecules and membranes and to manipulate biological cells and tissues. Ordinarily the cell membrane is a formidable barrier to the transport of ions and charged molecules. However, applying electric field pulses can results in a large increase in transmembrane conductance. This results in a large increase in molecular transport and allows polar molecules to be introduced into the cell [1,2]. The method of increasing the permeabilisation of cellular membrane by applying external electric pulses is called electroporation, which is a membrane phenomenon, and involves the fundamental behaviour of cell and bilayer membrane.

In particular, the membrane electroporation techniques have gained increased importance for clinical medicine. Short and intense electric pulses can be used to transiently and reversibly permeabilise cells, in order to introduce various molecules such as DNA, proteins and drugs into cells. The clinical applications of this technology have been developed as the cytotoxicity of anti cancer drugs can be dramatically enhanced by membrane permeabilisation of tumour cells using local delivery of short and intense electric pulses to the tumour mass (electrochemotherapy) [1-3].

Some aspects of electroporation have been studied, however, there is still a need to advance the knowledge of the effects of the electric pulses, in particular the way in which the electropermeabilisation progress in the tissue as a function of time during the electric pulse application. The distribution of the electric field and the prevention of cell damage are of utmost importance.

It is true that the electric properties of the tissue vary with the progressive electropermeabilisation of the cells of the tissue exposed to the electric pulse. Therefore it is possible to monitor the cell electropermeabilisation through the measurements of the electric and dielectric properties of the tissues submitted to the electric pulse.

In summary, the application of an electrical pulse to a biological tissue may, if sufficiently intense, alter the characteristics of cell membranes. This in turn will alter the dielectric properties (permittivity and conductivity) at RF frequencies. The aim of this project is to study the dielectric properties of the cellular membrane before and after applying certain electric pulses, which in turn will help to achieve better understanding of the electroporation phenomenon.

The aim of this work is to obtain some knowledge on the dynamics of tissue electropermeabilisation by measuring tissue conductivity and permittivity *ex vivo* before and after applying electric pulses to the tissue.

6-2 Electroporation and Electropermeabilisation

6-2-1 Definitions

Electropermeabilisation is a phenomenon in which a transient increase in the permeability of plasma membrane is observed. This phenomenon is based on membrane electroporation after exposing the cells to short and intense electrical pulses as opposed to irreversible electric breakdown leading to cell damage or vesiculation [4]. Electroporation results in a large increase in transmembrane conductance, which is believed to be caused by ion transport through temporary membrane openings ("pores"). A large increase in molecular transport generally occurs for the same conditions and allows polar molecules to be introduced into cells. The transient membrane electroporation may be also viewed as a cycle of electropore formation and resealing, resembling a relaxation hysteresis [5,6]. In other words, as it is shown in Figure 6.1a, in

the presence of an electric pulse with limited duration, the cell membrane (initial state C) becomes porous (state A). The state transition in the electric field $E \geq E_c$, above a critical value E_c, is unidirectional [6,7].

If the electric pulse is switched off before the cells become ruptured or damaged, the electropores slowly anneal at $E = 0$ (Figure 6.1b). At $E = 0$, the membrane resealing is also unidirectional.

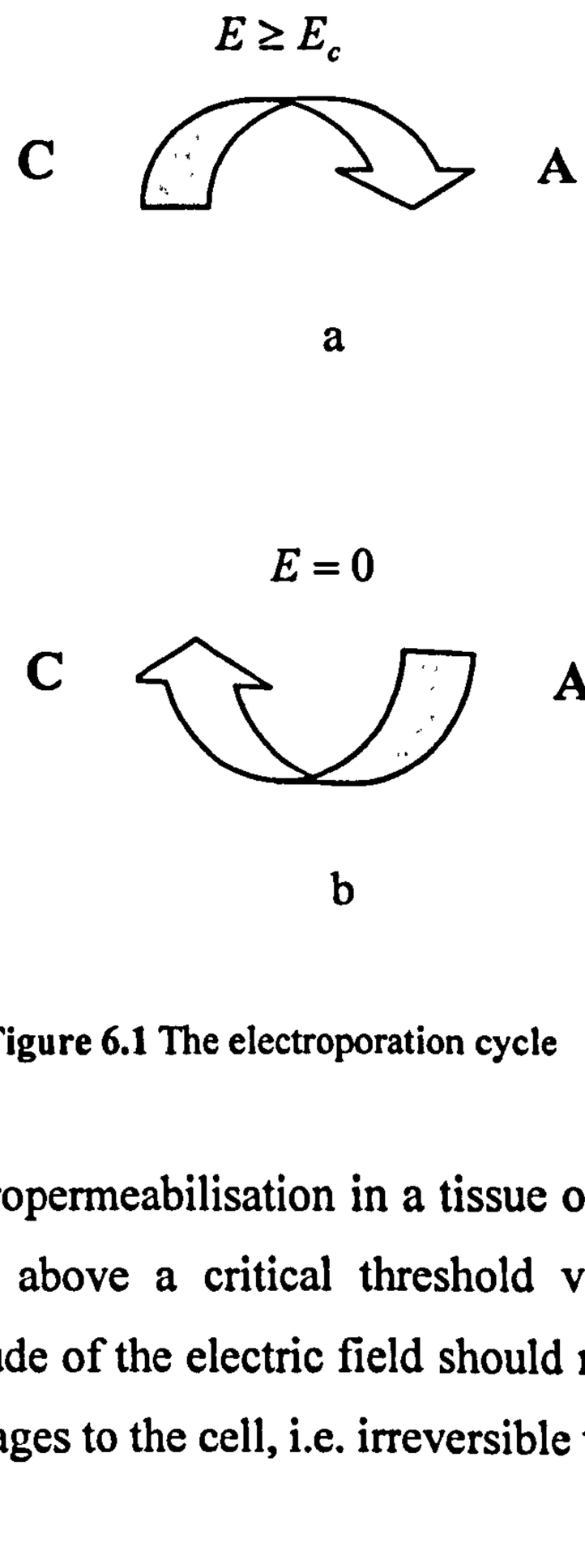

Figure 6.1 The electroporation cycle

In order to achieve electropermeabilisation in a tissue of interest, the magnitude of the electric field has to be above a critical threshold value, i.e. reversible threshold. Furthermore, the magnitude of the electric field should not exceed the value that would produce irreversible damages to the cell, i.e. irreversible threshold.

Finally, the fundamental processes of the electroporation of membranes can be summerised in table 6.1.

Table 6.1 Fundamental processes of electroporation of membrane (Adopted from [5])

Physical –chemical processes	**Electric terms**
I-Reversible Primary Processes:	
1. Primary electric events 1.1 Electric dipole induction and dipole orientation 1.2 Redistribution of mobile ions at phase boundaries membrane	Dielectric polarisation Ionic-dielectric interfacial polarisation (β-dispersion)
2. Structural rearrangements 2.1 Conformational changes in protein and lipid molecules 2.2 Phase transition in lipid domains, resulting in pores 2.3 Annealing and resealing processes	Electro-restructuring Electroporation, Electropores
II- Irreversible secondary processes:	
1. Transient material exchange 1.1 Release of internal compounds, e.g. hemolysis 1.2 Uptake of external material, e.g. drug, antibodies 1.3 Transfer of genetic material, e.g. DNA with stable cell transformation	Electropermeabilisation Electrorelease Electroincorporation Electrotransfection Electrotransformation
2. Membrane reorganisation 2.1 Cell fusion (if membrane contact) 2.2 Vesicle formation (budding) 2.3 Electromechanical rupture	 Electrofusion Electrovesiculation Dielectric breakdown
3. Tertiary effects 3.1 Temperature increase due to dissipative processes 3.2 Metal ion release from metal electrodes 3.3 Electrode surface	 Joule heating, dielectric losses Electroinjection Electrolysis

6-2-2 Electric field distribution

The progression of electropermeabilisation of cells in tissues during the electric pulse application is not yet known well. Electropermeabilisation should result in changes in the dielectric properties of the tissue that will result in a progressively quite different electric field distribution.

The strength of the electric field around the electrodes is always the highest. Therefore, tissue electropermeabilisation, which is a threshold phenomenon and is associated with the induction of transmembrane electric voltage across the cell plasma membrane, will first occur in the area around the electrode. After that area becomes permeabilised a redistribution of the electric field in the tissue occurs. If the voltage is kept constant (or a new pulse of the same amplitude is delivered) further permeabilisation will be achieved as a result of this new electric field distribution in the tissue.

The importance of electrode configurations for electric field distribution has previously been examined [8]. It has been found that electrode configuration significantly affected the electric field distribution. For example in the case of needle electrodes, the electric field distribution is not as homogeneous as for the plate electrode [9]. It is therefore, important to choose the appropriate electrode type for the task required.

6-3 Effects of the applied field on the dielectric properties of membrane

Applying an external electric field should result in changes in the dielectric properties of the tissue. This is due to the fact that changes in the dielectric properties of biological material occur in response to changes in physiological conditions of the tissue.

The β dispersion area of the dielectric spectrum of biological tissues which extends over 3-4 frequency decades centred in the hundreds of kilohertz region, is highly affected by the physical and physiological state of cell membrane. Destruction of the cellular membrane can cause a significant change in the β dispersion. An example of such effect is given in Figures, 2.5a and 2.5b of chapter 2 which show the permittivity and

conductivity spectrum of banana before and after the destruction of the cellular membrane by mashing the banana. Another practical example of the effect of applying an external electric field on the β dispersion can be observed in Figures 6.2a and 6.2b where the permittivity and conductivity of potato at room temperature have been measured before and after applying 8 pulses of 2.5ms and amplitude of 100V.

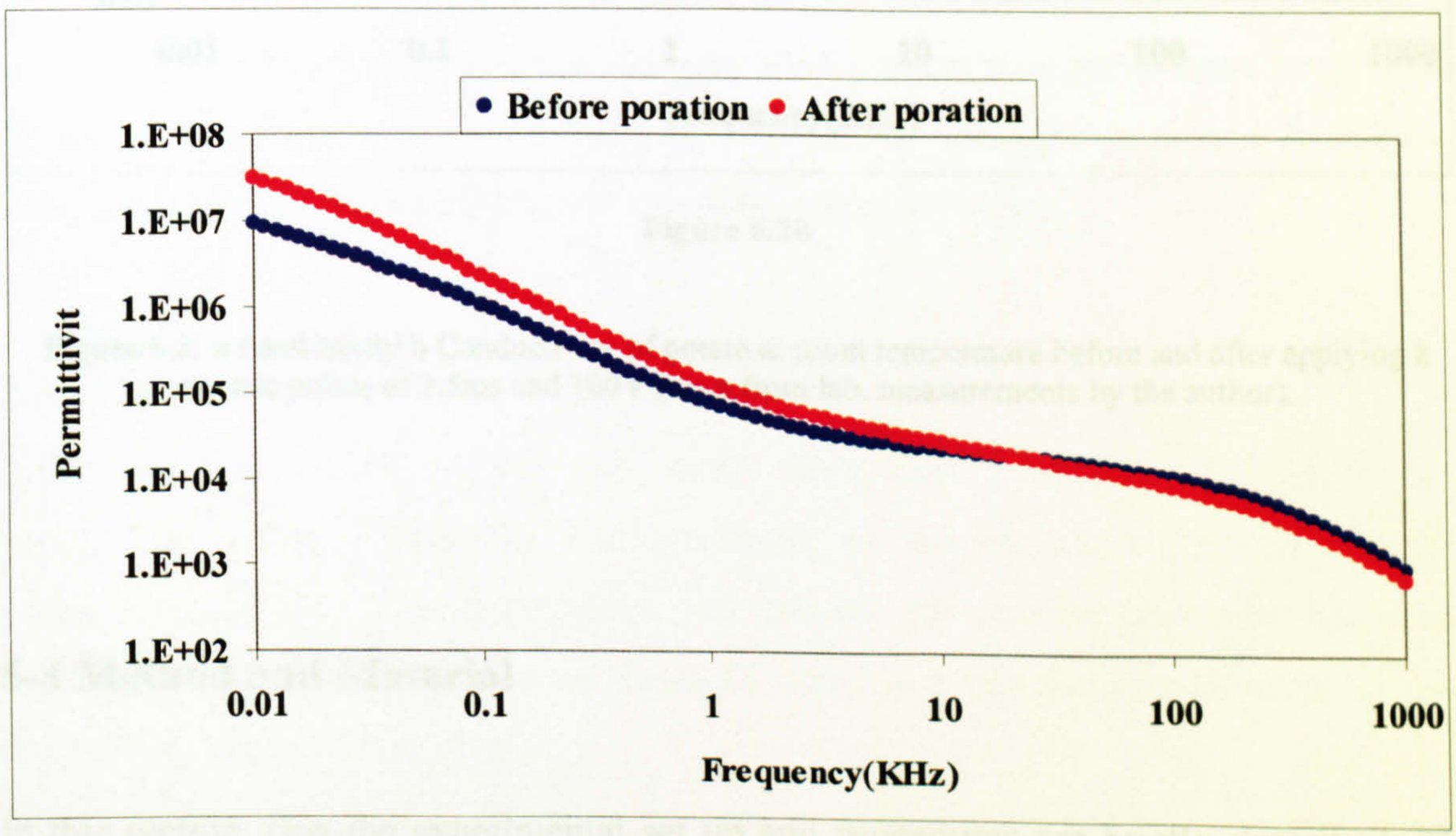

Figure 6.2a

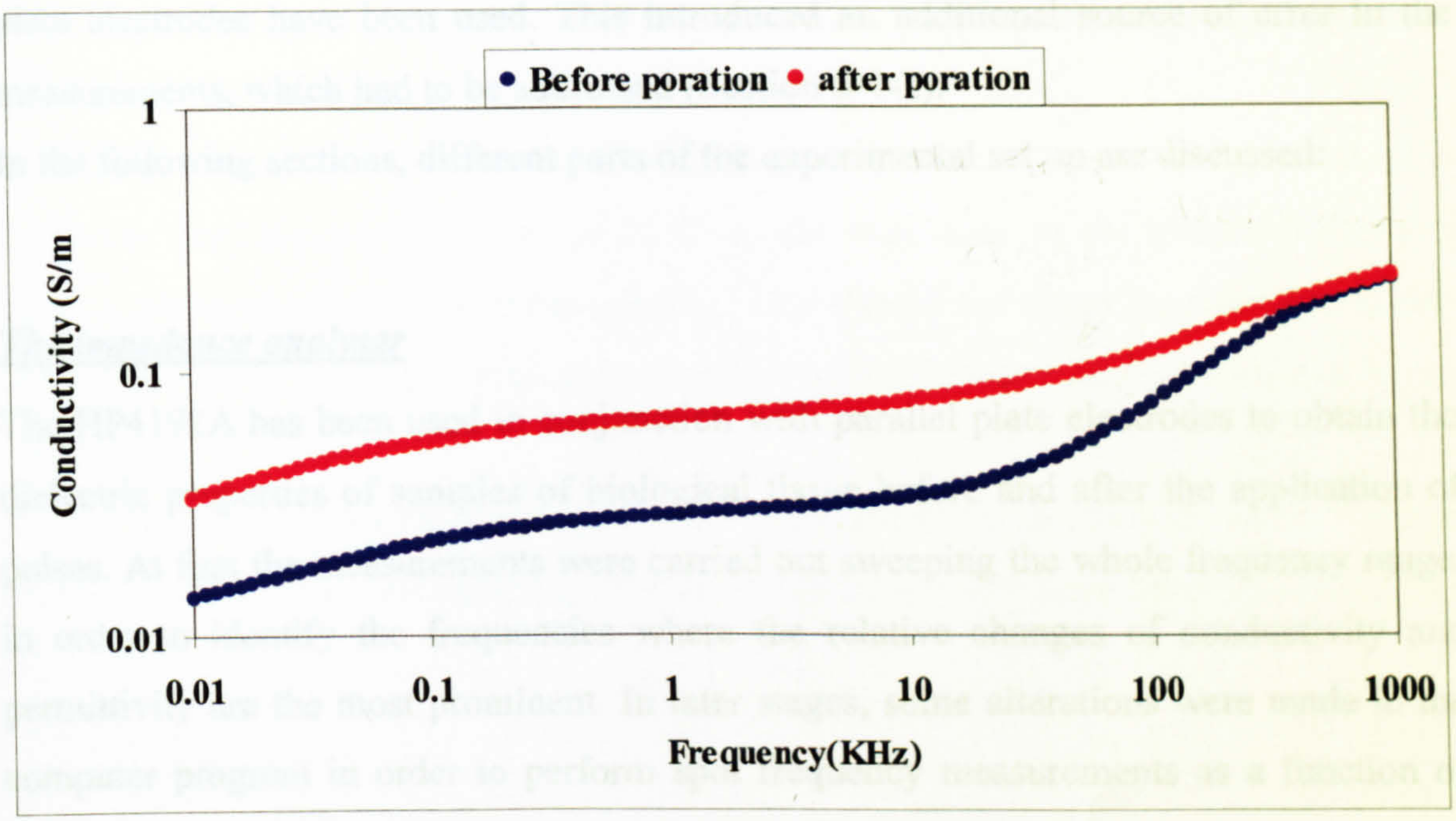

Figure 6.2b

Figure 6.2: a Permittivity **b** Conductivity of potato at room temperature before and after applying 8 electric pulses of 2.5ms and 100V (Data from lab. measurements by the author).

6-4 Method and Material

In this section, first the experimental set up and procedures are briefly described. The accuracy of measurements is also addressed.

6-4-1 Experimental set up

Tissue conductivity and permittivity changes due to electropermeabilisation have been measured in the whole frequency range of 1 kHz-1MHz using a swept frequency impedance analyser HP4192A. The measurement technique has been described in detail in chapter 2. However, in this project instead of coaxial conical probes, specific parallel

plate electrodes have been used. This introduced an additional source of error in the measurements, which had to be addressed (Section 6-4-2).
In the following sections, different parts of the experimental set up are discussed:

The impedance analyser

The HP4192A has been used in conjunction with parallel plate electrodes to obtain the dielectric properties of samples of biological tissue before and after the application of pulses. At first the measurements were carried out sweeping the whole frequency range, in order to identify the frequencies where the relative changes of conductivity and permittivity are the most prominent. In later stages, some alterations were made to the computer program in order to perform spot frequency measurements as a function of time. This would help identifying any resealing effect with time.

Electrodes

Electrodes used in this project were made from Inox Steel AISI 321 10/10 with appropriate surface roughness. The roughness of the surface shifts the electrode polarisation effect to lower frequencies. The distance between the electrodes was either 2 or 4 mm. The plate electrodes are mounted solely in a 50-Ohm coaxial cable in order to ensure a minimum distortion.
The impedance components of the probe were measured in air and in a standard sample (water). Then the characteristic parameters of the probe, equivalent to its capacitance in air K, were calculated from the Equation 2.23 (chapter 2). The result was as follows:
For 2mm electrode: $K = 1.45 \times 10^{-12}$ and for 4mm electrode: $K = 7.6 \times 10^{-13}$

The samples

Samples were obtained from freshly sacrificed animals (sheep and/or pig). The tissues of interest were liver, kidney, muscle, skin, bone and tumours. Unfortunately because of the occurring of foot and mouth disease in the UK while this project was running, it was

extremely difficult to obtain all the tissues of interest and all efforts to obtain tumour tissues were unsuccessful.

The tissues were kept at room temperature. However, because they were obtained quite fresh, the tissues were warm (about 30°C) at the beginning of the measurements and there was a temperature drift as time passed. This should not affect the results as in this project the study is comparative and the effect of temperature is cancelled out in the comparison.

It must however be mentioned that in some cases due to the application of very strong electric pulses, there were temperature rises in the tissues that have been recorded at the time.

The pulse generator

A prototype of a specially designed pulse generator "Electroporator 1", was supplied by other partners in this project. Electroporator is an electronic device that generates trains of high voltage pulses. The device is capable of generating pulse width (Ti) of 5μsec to 5ms and pulse amplitude (A) of 25V to 500V. The number of pulses (Ni) can vary from 1 to 128 and the pulse sequences (Ns) can be from 1 to 255. The current of the produced pulses is 40A.

A digital oscilloscope was used to monitor the produced pulses randomly throughout the measurements.

The pulse protocol in this project was to apply pulses of 5 to 2500 μsec, in increments to be determined experimentally with number of pulses of 1 to 10 at 1Hz repetition frequency of 50 to 500V, in increments to be determined experimentally.

Switch box

In order to be able to frequently switch from the impedance analyser to the pulse generator and vice versa, a switch box was designed by colleagues of the author. This enabled the operator to apply the electric pulses by the pulse generator and then

switching to the impedance analyser immediately and measuring the dielectric properties of the affected area without changing the position of the probe. Figure 6.4 shows a schematic picture of the measurement devices arrangement.

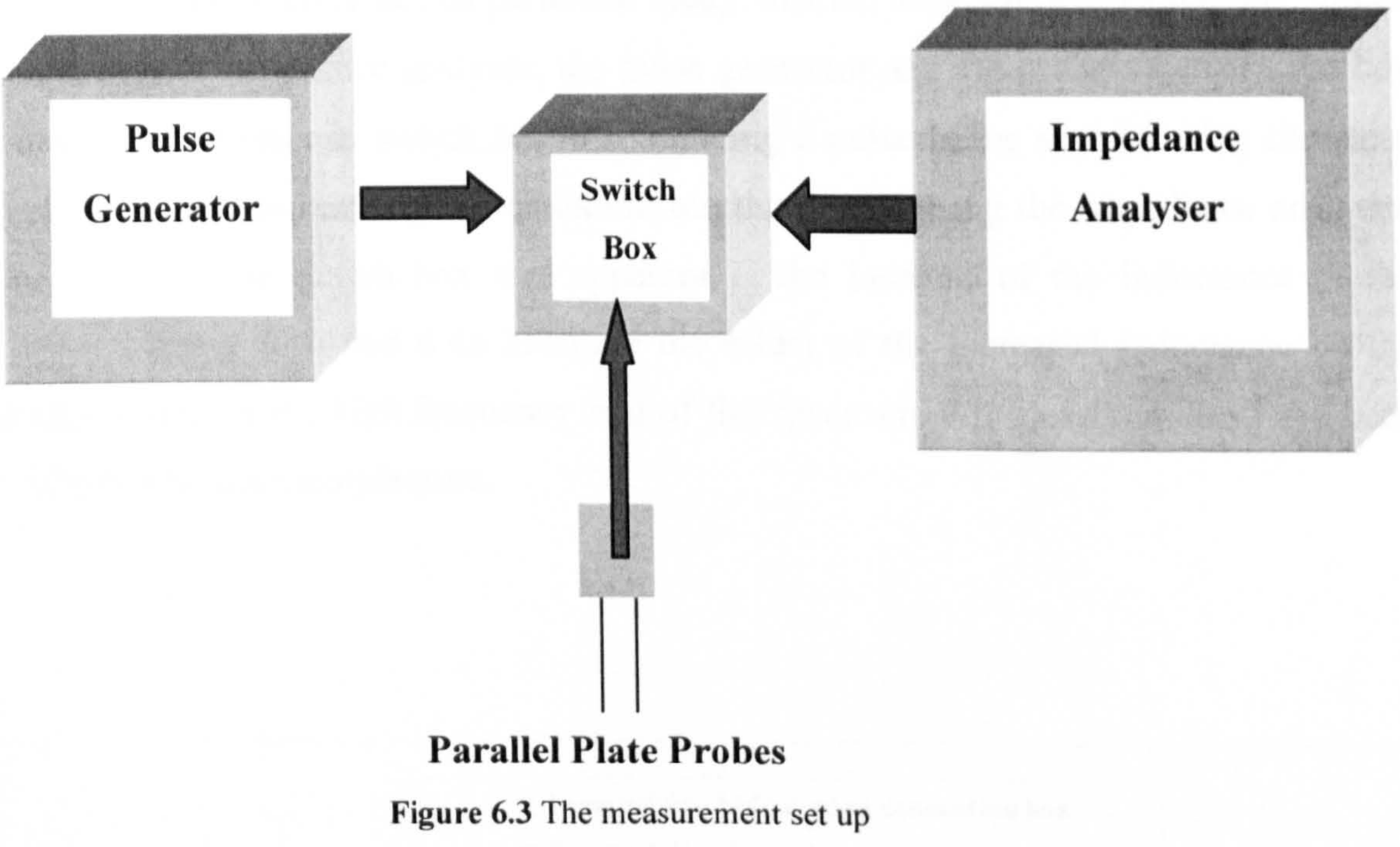

Figure 6.3 The measurement set up

6-4-2 Accuracy of measurements

The accuracy of the technique was studied when using conical co-axial probe (Chapters 2 and 3). Two sources of errors were recognised in these studies: the electrode polarisation and the lead inductance errors, which become apparent at the lower and higher ends of the frequency range that the device can cover. However, as mentioned before, for practical reasons, instead of conical probes, specific parallel plate electrodes were used in this project. This limited the process of reducing the measurement errors, as it was not possible to optimise the performance of the probe.

In this particular study the electrode polarisation was not a problem for two reasons. First: the frequency range of interest was outside the region in which electrode polarisation occurs (<1 kHz), and second: the study is a comparative kind in which the dielectric values are compared before and after certain electric pulses are applied to the tissue. Hence the effect of electrode polarisation is cancelled out in the comparison.

Another source of error in this particular study was the addition of a switch box, which connected the impedance analyser, the pulse generator and the probe together. The box allowed the operator to switch between applying a pulse to the sample using the pulse generator and then perform the dielectric measurements using the impedance analyser. The effect of the switch box was apparent in the increase of the inductance of the system. Figures 6.4a and 6.4b illustrate the effect of the increased inductance on the measurements at the high frequency end of the spectrum. All measurements have been performed at room temperature.

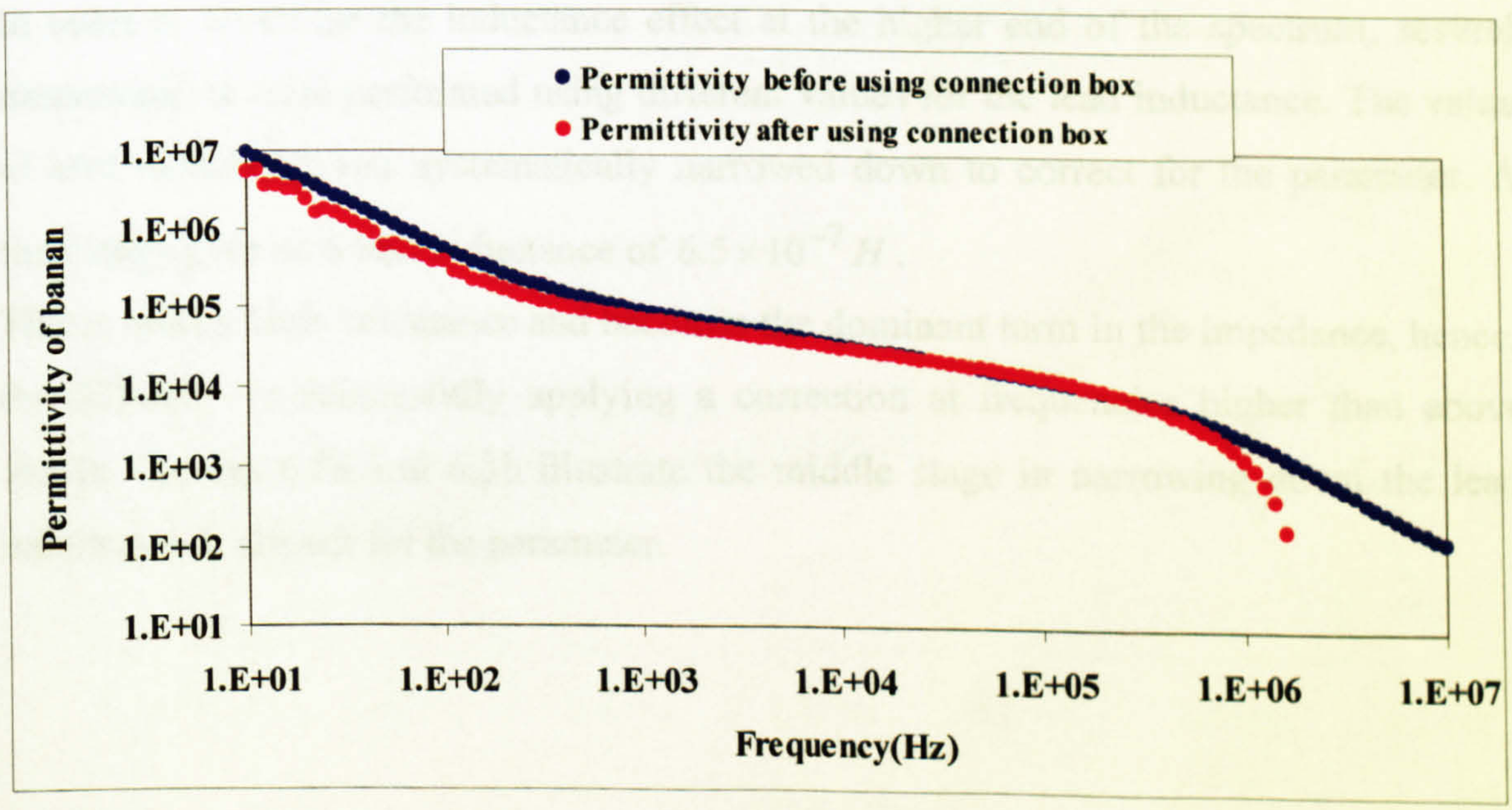

Figure 6.4a

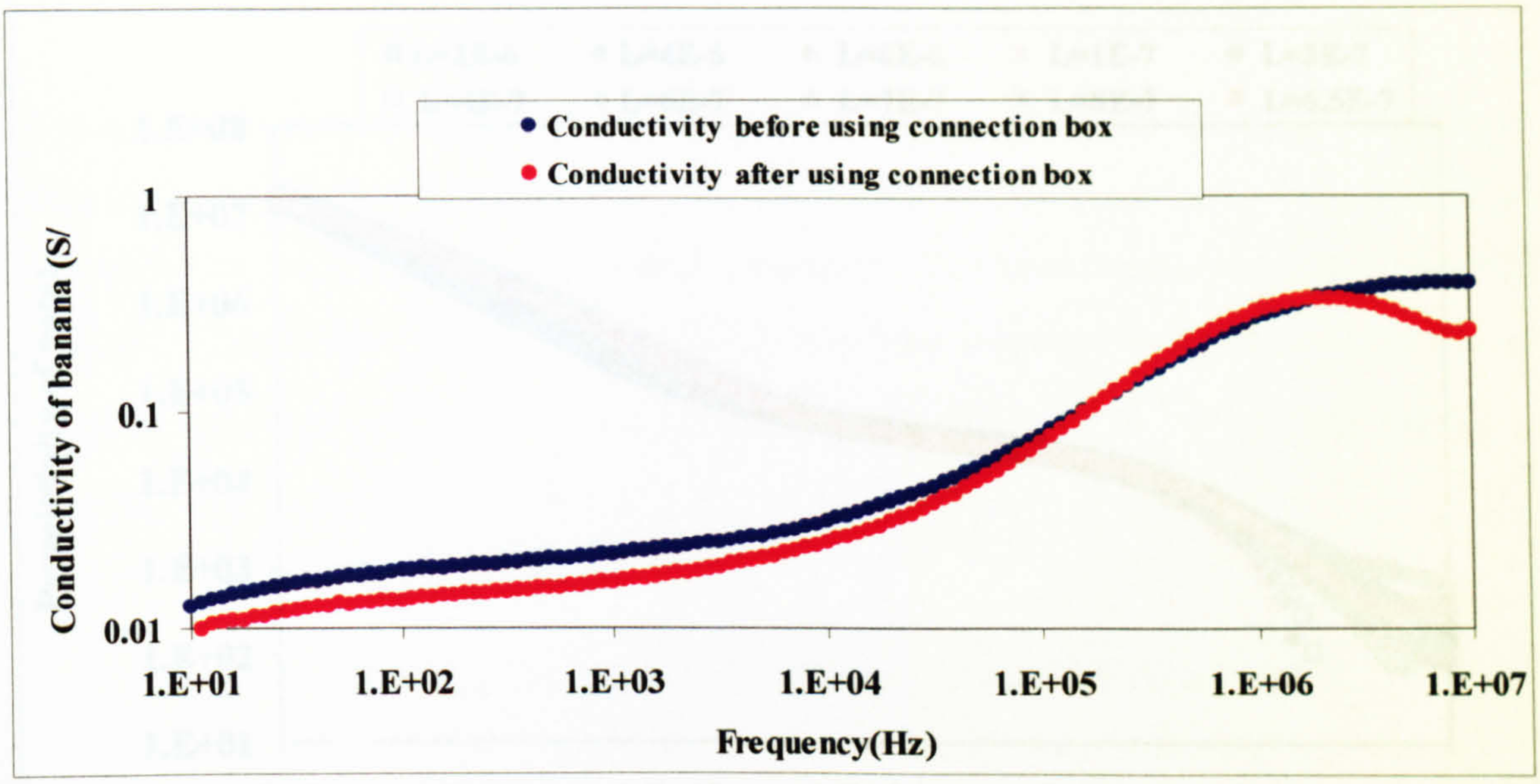

Figure 6.4b

Figure 6.4: **a** Permittivity **b** Conductivity of banana measured with 2mm probe, with and without the connection box

In order to minimise the inductance effect at the higher end of the spectrum, several measurements were performed using different values for the lead inductance. The value of lead inductance was systematically narrowed down to correct for the parameter. A final stage gave us a lead inductance of $6.5 \times 10^{-7} H$.

This is quite a high inductance and becomes the dominant term in the impedance, hence, the difficulty in successfully applying a correction at frequencies higher than above 5MHz. Figures 6.5a and 6.5b illustrate the middle stage in narrowing down the lead inductance to correct for the parameter.

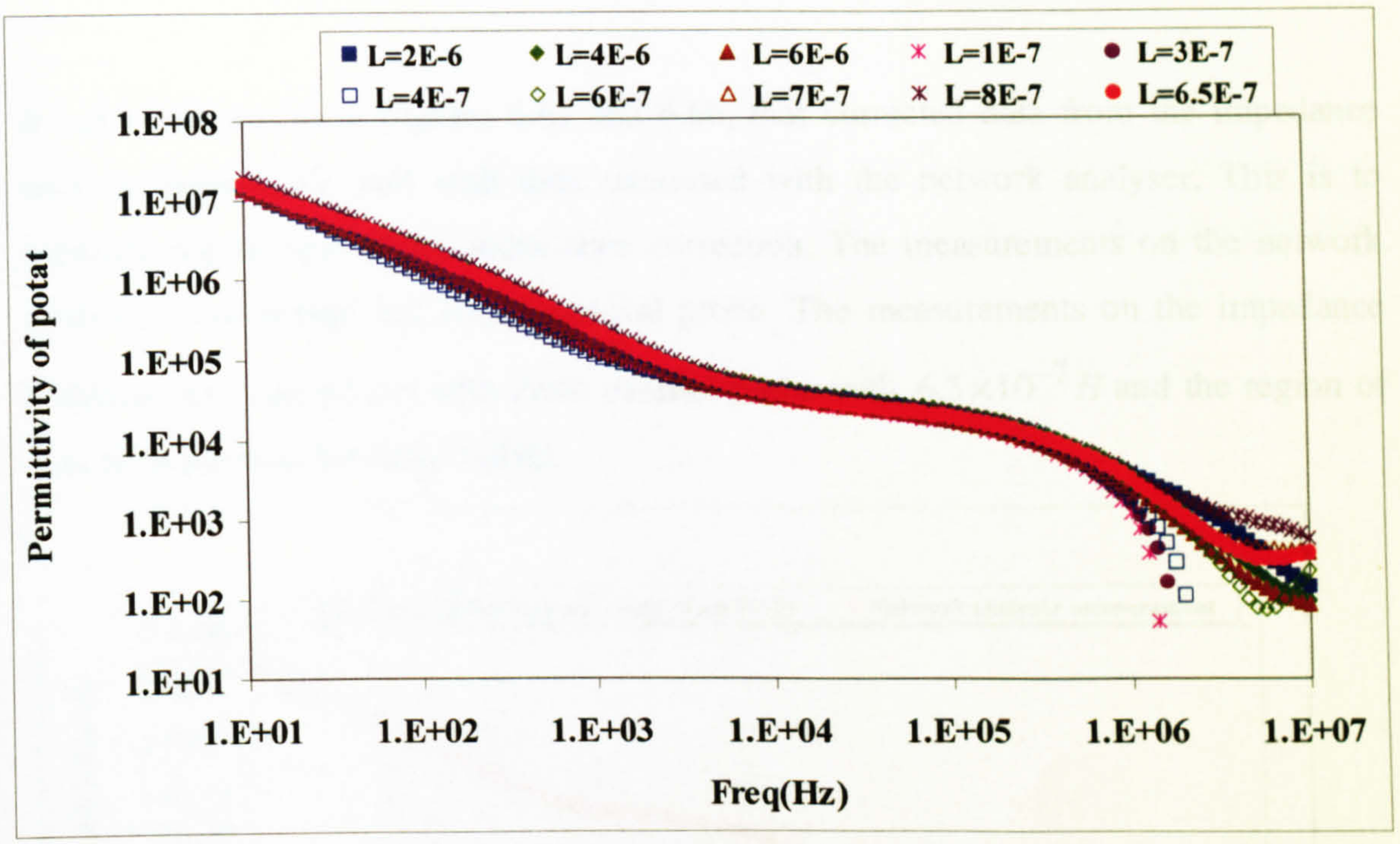

Figure 6.5a

Figure 6.5b

Figure 6.5: a Permittivity b Conductivity of potato using different values of Lead inductance

It can be shown as in Figures 6.6a and 6.6b, that corrected data from the impedance analyser agree very well with data measured with the network analyser. This is to illustrate the success of the inductance correction. The measurements on the network analyser were carried out with a coaxial probe. The measurements on the impedance analyser were carried out with 2mm parallel probe with $6.5\times10^{-7}\,H$ and the region of overlap were from 500 kHz-5MHz.

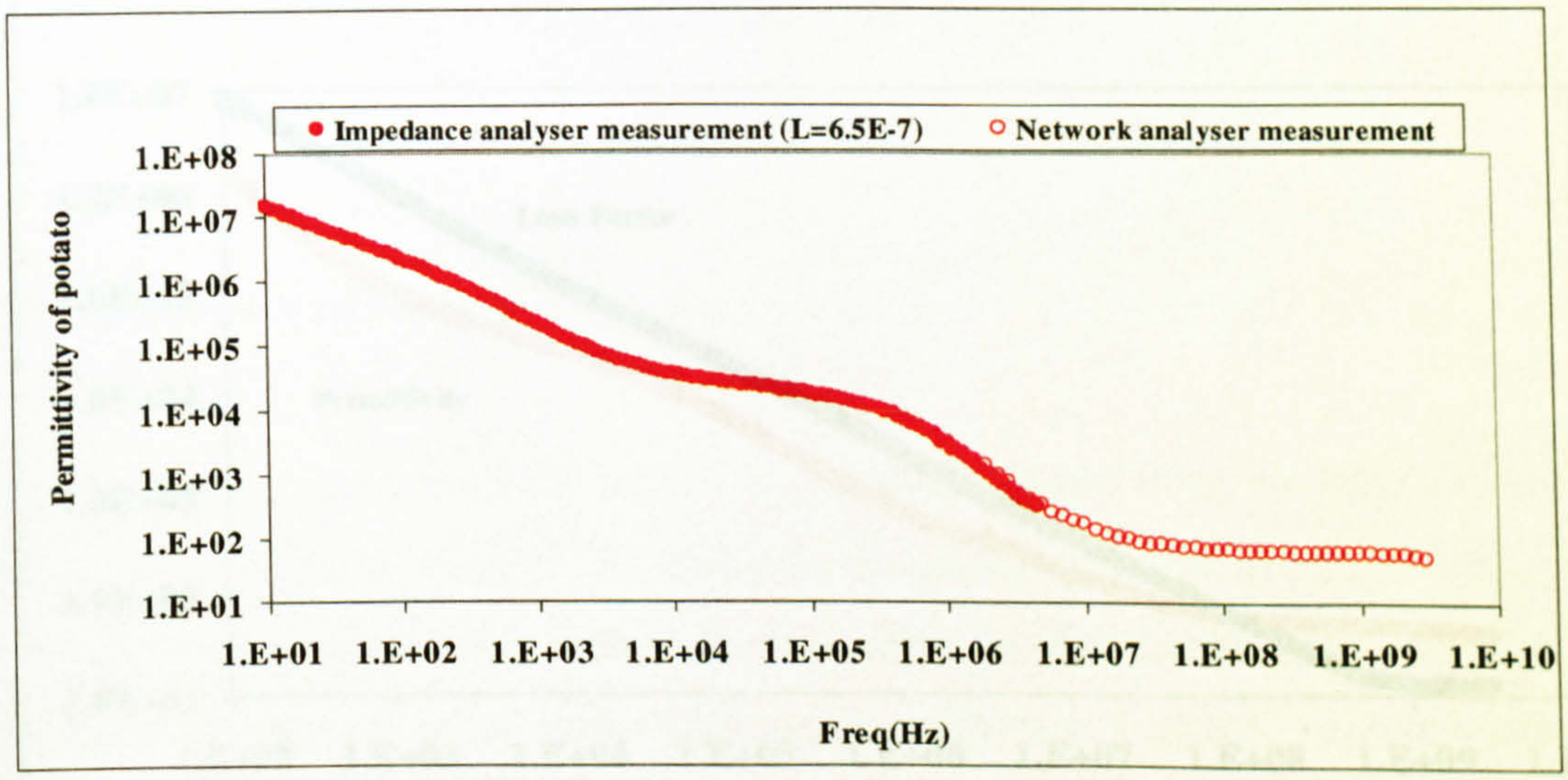

Figure 6.6a

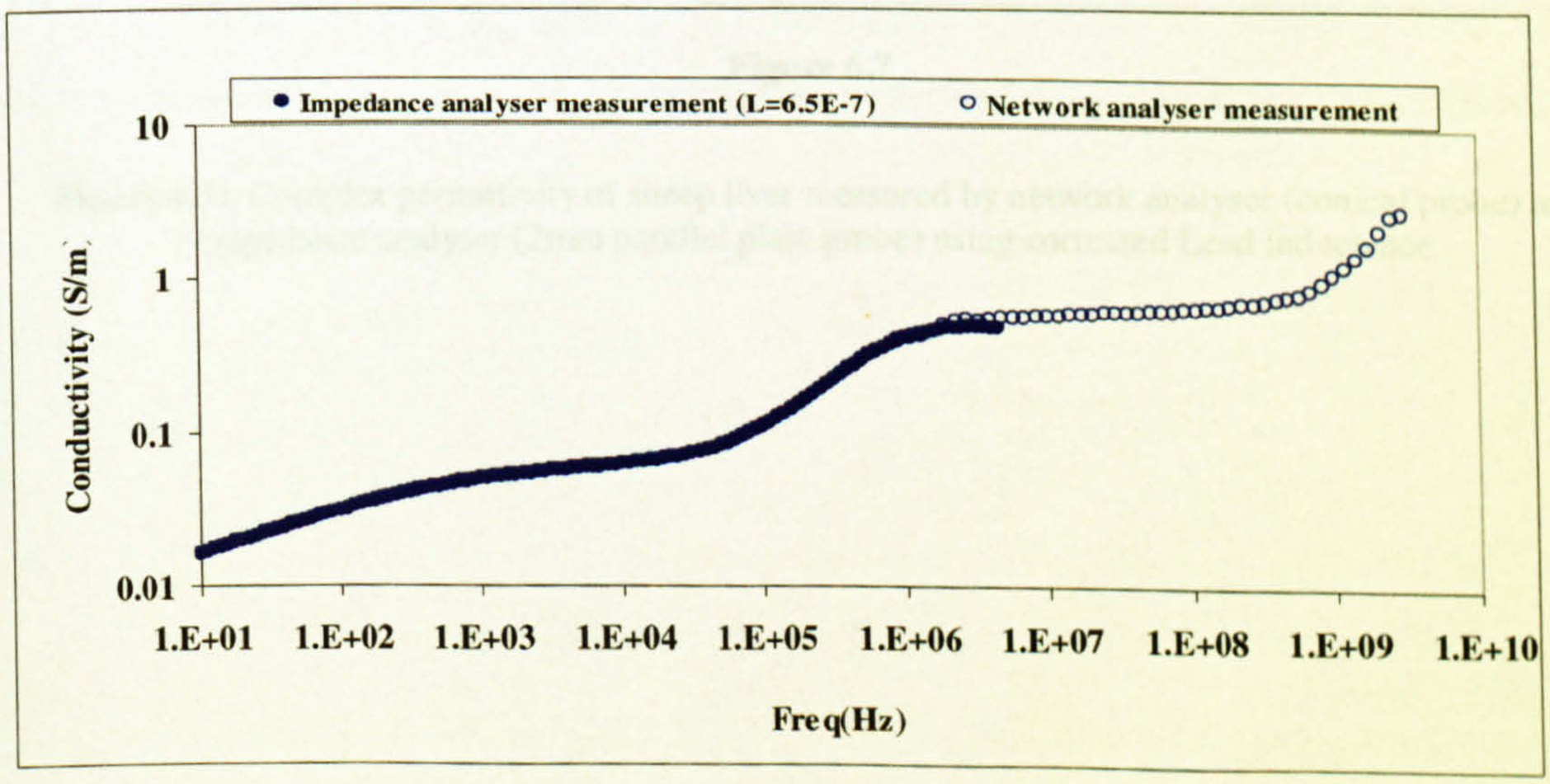

Figure 6.6b

Figure 6.6: a Permittivity **b** Conductivity of potato measured by network analyser (conical probe) and impedance analyser (2mm parallel plate probe) using corrected Lead inductance

As this project deals with animal tissues, it is a good practice to illustrate the success of the induction correction on the measurements on freshly sacrificed sheep liver with both the impedance and network analysers (Figures 6.7)

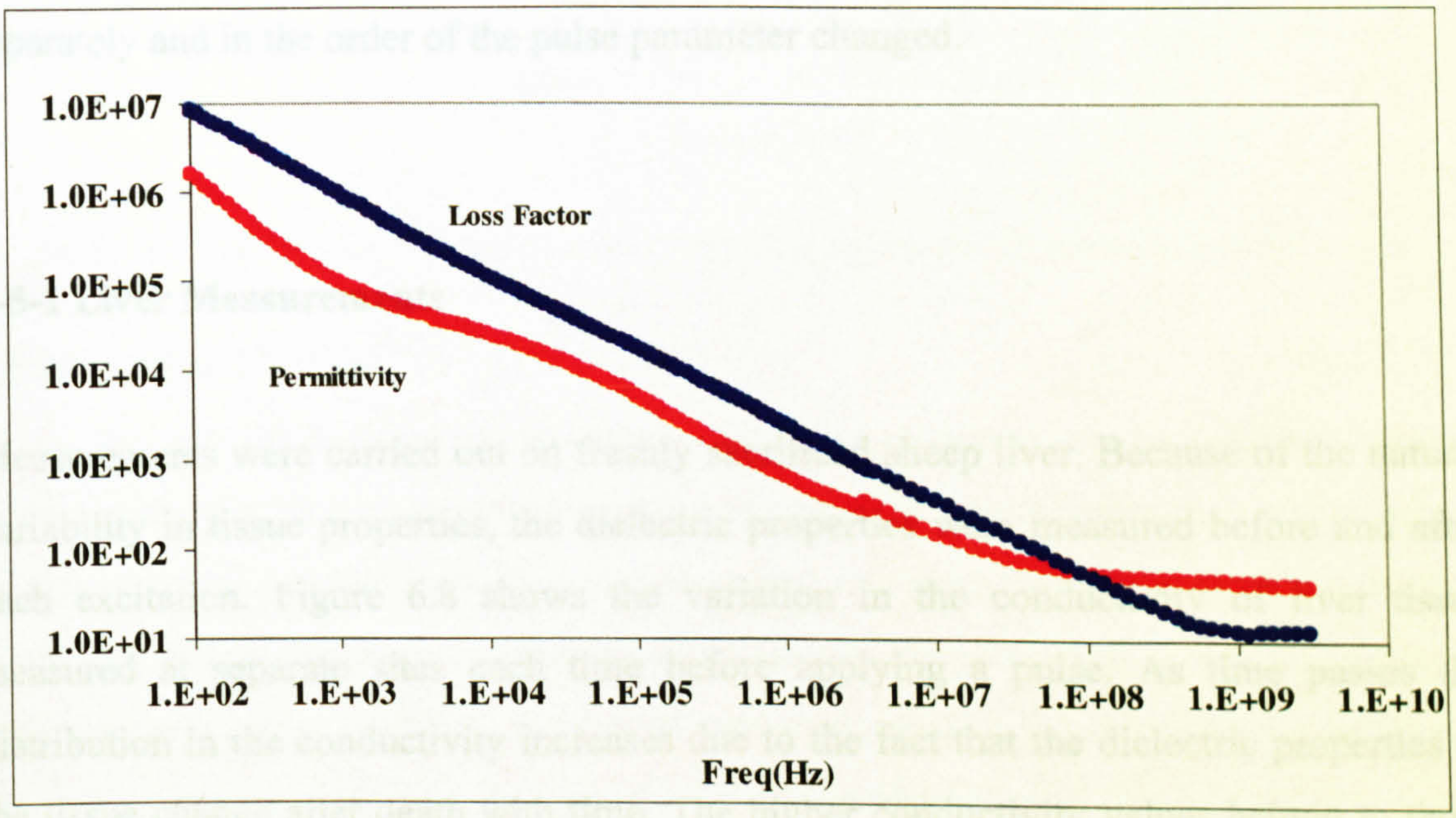

Figure 6.7

Figure 6.7: Complex permittivity of sheep liver measured by network analyser (conical probe) and impedance analyser (2mm parallel plate probe) using corrected Lead inductance

6-5 Results and observations

The pulse protocol in this project required different combinations of pulse parameters to be used experimentally. It is very difficult to change all the pulse parameters at the same time and perform the measurements. Therefore, each time, one of the pulse parameters was changed and the others kept constant at some certain values. The effect of changing each pulse parameter was then studied. Here the results are presented for each tissue separately and in the order of the pulse parameter changed.

6-5-1 Liver Measurements

Measurements were carried out on freshly sacrificed sheep liver. Because of the natural variability in tissue properties, the dielectric properties were measured before and after each excitation. Figure 6.8 shows the variation in the conductivity of liver tissue measured at separate sites each time before applying a pulse. As time passes the distribution in the conductivity increases due to the fact that the dielectric properties of the tissue change after death with time. The higher conductivity values belong to those measurements, which were carried out towards the end of the measurement period.

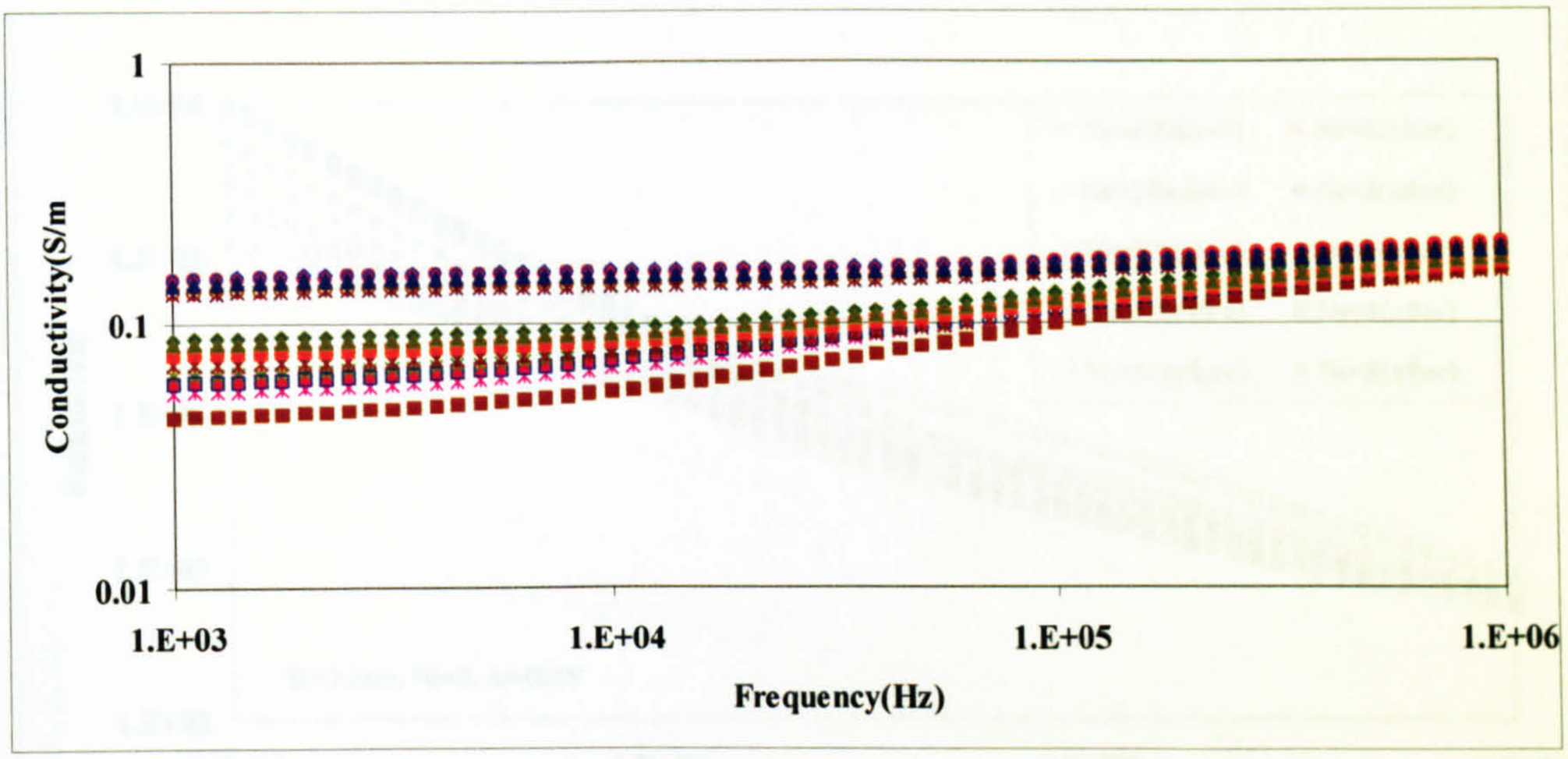

Figure 6.8 Conductivity of sheep liver before applying electric pulses, measured at different sites

Effect of pulse sequence

In the first attempt in liver measurements, the pulse sequence was changed while other pulse parameters were kept constant at certain values. Applying more than one sequence of pulses makes a strong impact on the tissue and it is predicted that a complete damage to the membrane occurs as the number of sequences are increased. A train of relatively high intensity pulses (400V, 2.5 ms) was used to emphasise the effect on the tissue and the corresponding change in the permittivity and conductivity of tissue in the frequency range of 1 kHz to 1 MHz. In this frequency range, the dielectric spectrum originates from the polarisation of cell membranes. Electroporation of the membrane caused by the high intensity pulses affects its polarisation capacity and hence the dielectric spectrum of the tissue.

Figures 6.9a and 6.9b show the changes in the conductivity and permittivity of sheep liver before and after applying electric pulses of different pulse sequence with the same pulse length, number and amplitude. Each measurements is paired with a "before" and "after". For the high number of sequences, a clicking noise was heard, suggesting some arcing, and the temperature rose. So the change in conductivity observed is partly due to rise in the temperature.

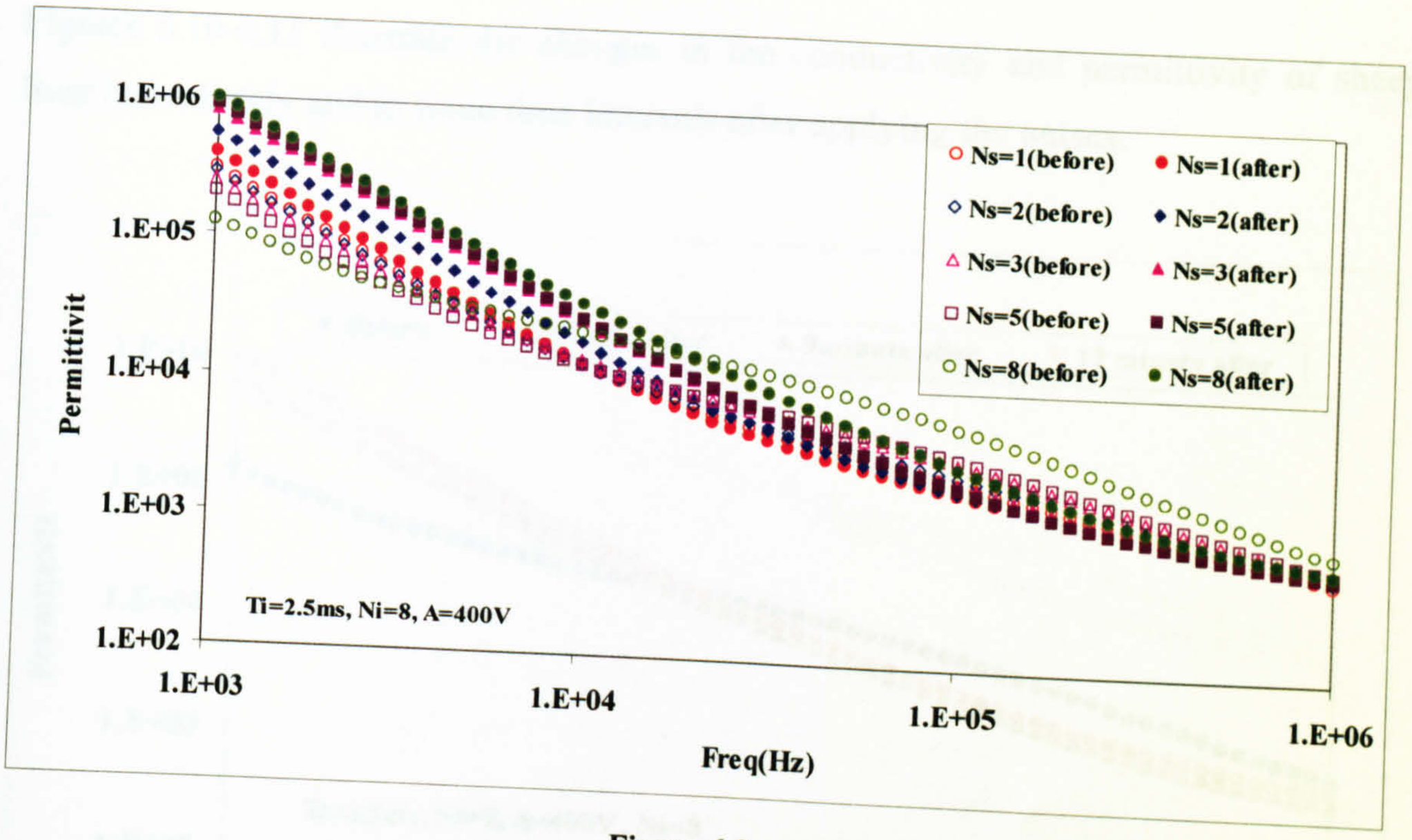

Figure 6.9a

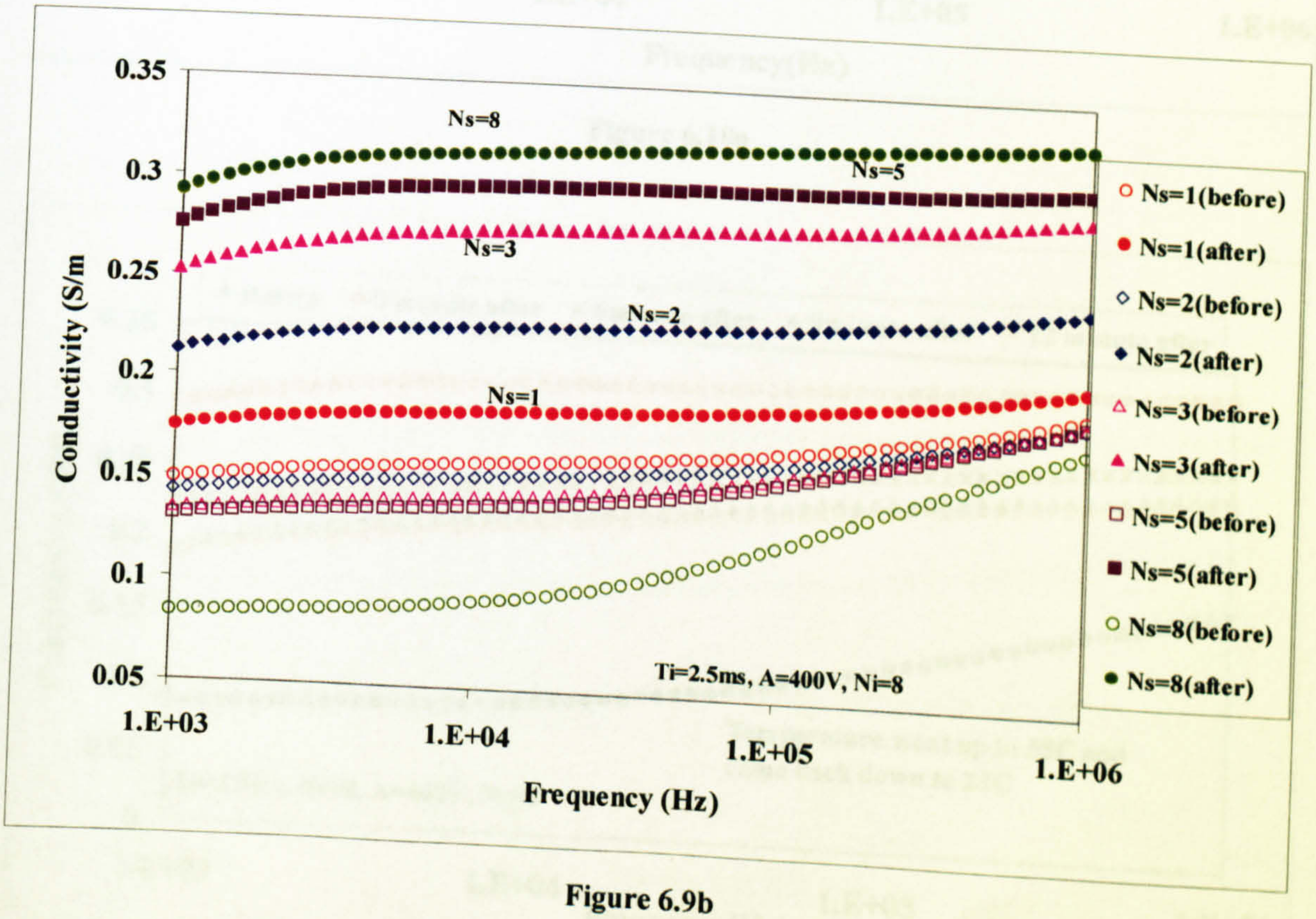

Figure 6.9b

Figure 6.9: a Permittivity **b** Conductivity of Lamb liver before and after applying pulses with various pulse sequences. Pulse width (Ti)=2.5ms, Pulse number (Ni)=8 and Pulse amplitude (A)=400V

Figures 6.10-6.11 illustrate the changes in the conductivity and permittivity of sheep liver immediately and in some time intervals after applying the pulses.

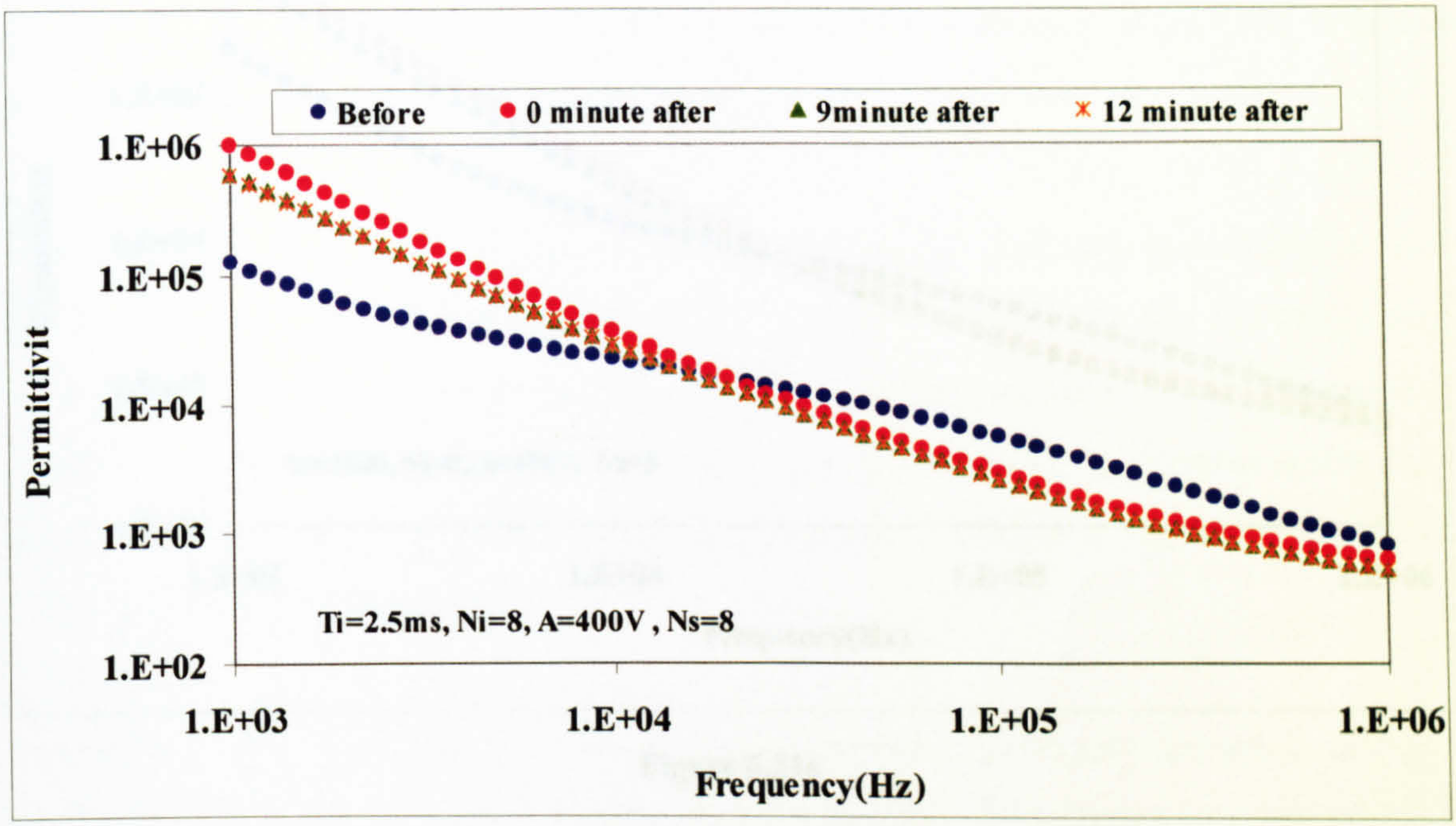

Figure 6.10a

Figure 6.10b

Figure 6.10: a Permittivity **b** Conductivity of sheep liver before and at various intervals after applying electric pulses (Ns=8)

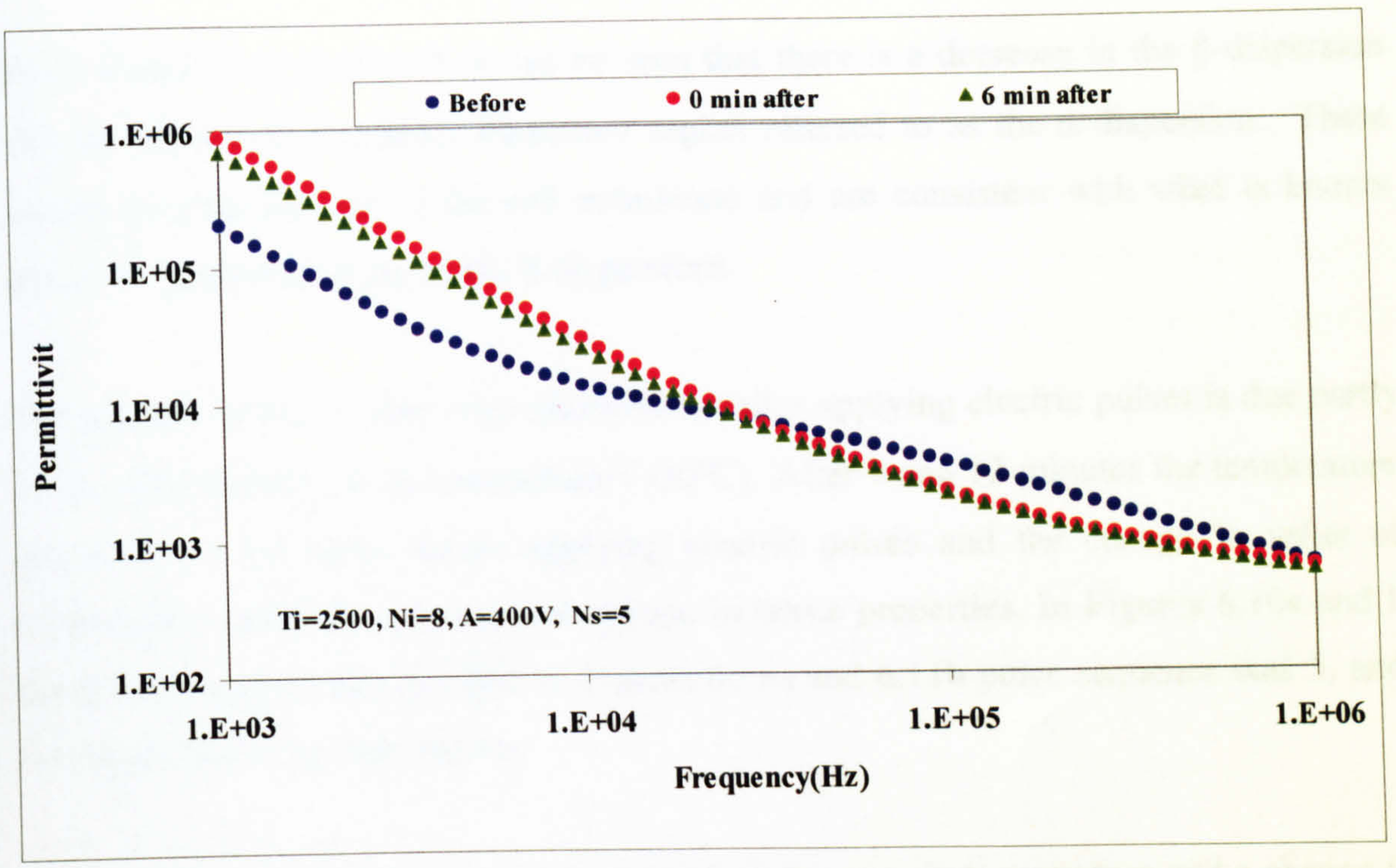

Figure 6.11a

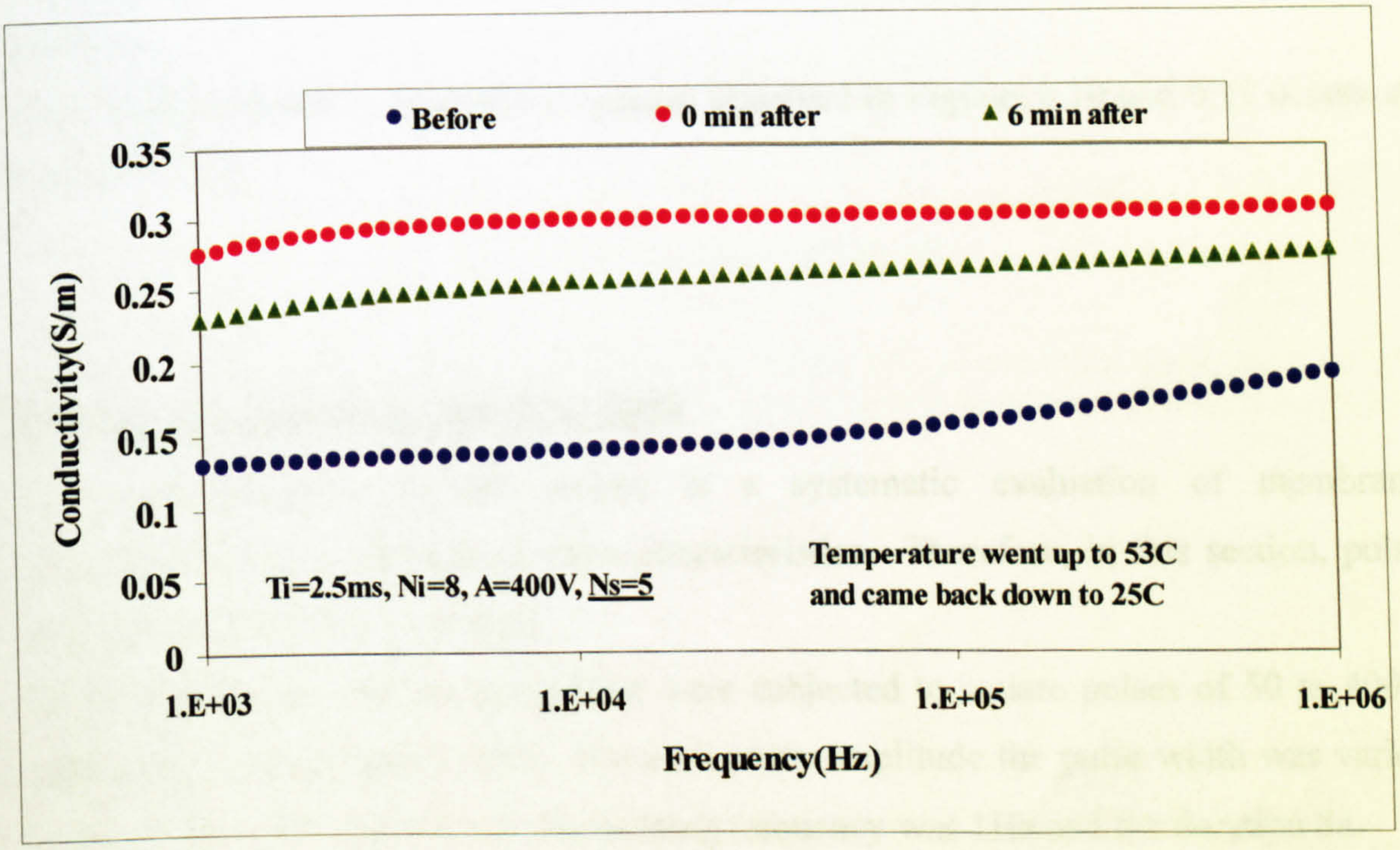

Figure 6.11b

Figure 6.11: a Permittivity **b** Conductivity of sheep liver before and at some intervals after applying pulses, with Ns=5

From Figures 6.10 and 6.11, it can be seen that there is a decrease in the β-dispersion and an increase in the lower frequency region referred to as the α-dispersion. These results indicate damage to the cell membrane and are consistent with what is known about the properties of the α and β dispersions.

The increase in the conductivity immediately after applying electric pulses is due partly to the considerable rise in temperature (~30°C). After 9 and 12 minutes the temperature was back to the value before applying electric pulses and the change in value of conductivity indicates a permanent change in tissue properties. In Figures 6.10a and b the pulse sequence was 8 while in Figures 6.11a and 6.11b pulse sequence was 5, and the temperature rise was smaller.

In summary the high intensity pulses caused an increase in temperature and a change in the dielectric properties. Measurements carried out after a 15 minutes interval, when the temperature effect had subsided showed that the effect of membrane electroporation remains.

The largest variation in dielectric properties observed in Figures 6.10 and 6.11 occurs at around 10 kHz.

Effect of pulse amplitude and pulse width

The main objective of the project is a systematic evaluation of membrane electroporation as a function of pulse characteristics. Therefore, in this section, pulse amplitude and width were varied.

Samples of freshly excised sheep liver were subjected to square pulses of 50 to 400V amplitude, in increments of 50V. For each pulse amplitude the pulse width was varied to 0.1, 0.5, 1, 1.5, 2 and 2.5 ms. The pulsing frequency was 1Hz and the duration 8s.

Because of the natural variability in tissue properties, the dielectric properties were measured before and after each excitation at each site separately.

The percentage difference in conductivity before and after applying pulses at 10 kHz has been used as a measure of the effect on the tissue. Figure 6.12 shows the %Increase in the conductivity of sheep liver at 10 kHz before and after pulse excitation as a function of pulse amplitude (with pulse width as parameter). Figure 6.13 shows the Average of the response of all pulses at each amplitude.

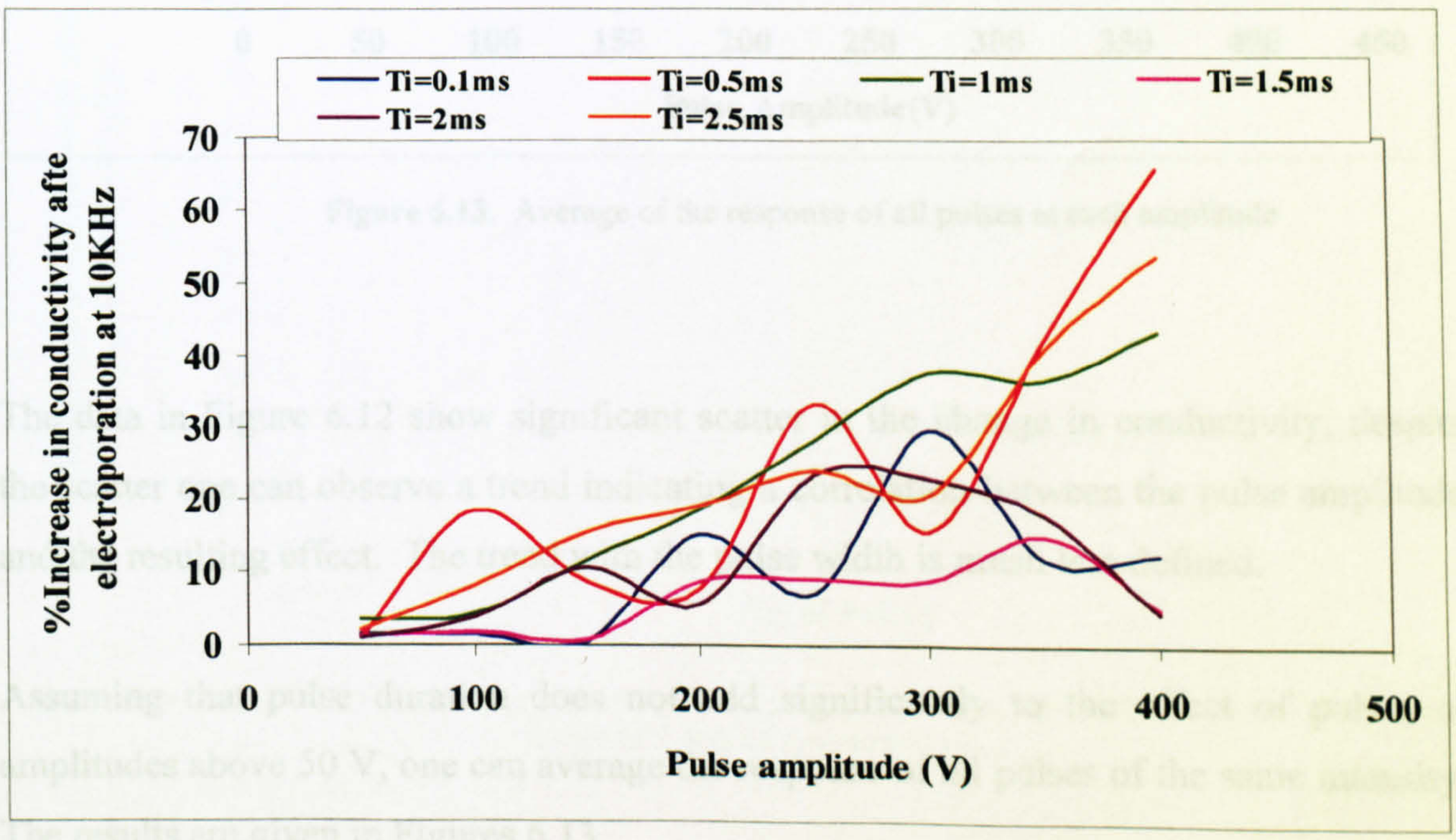

Figure 6.12: %Increase in the conductivity of sheep liver at 10 kHz before and after pulse excitation as a function of pulse amplitude (with pulse width as parameter)

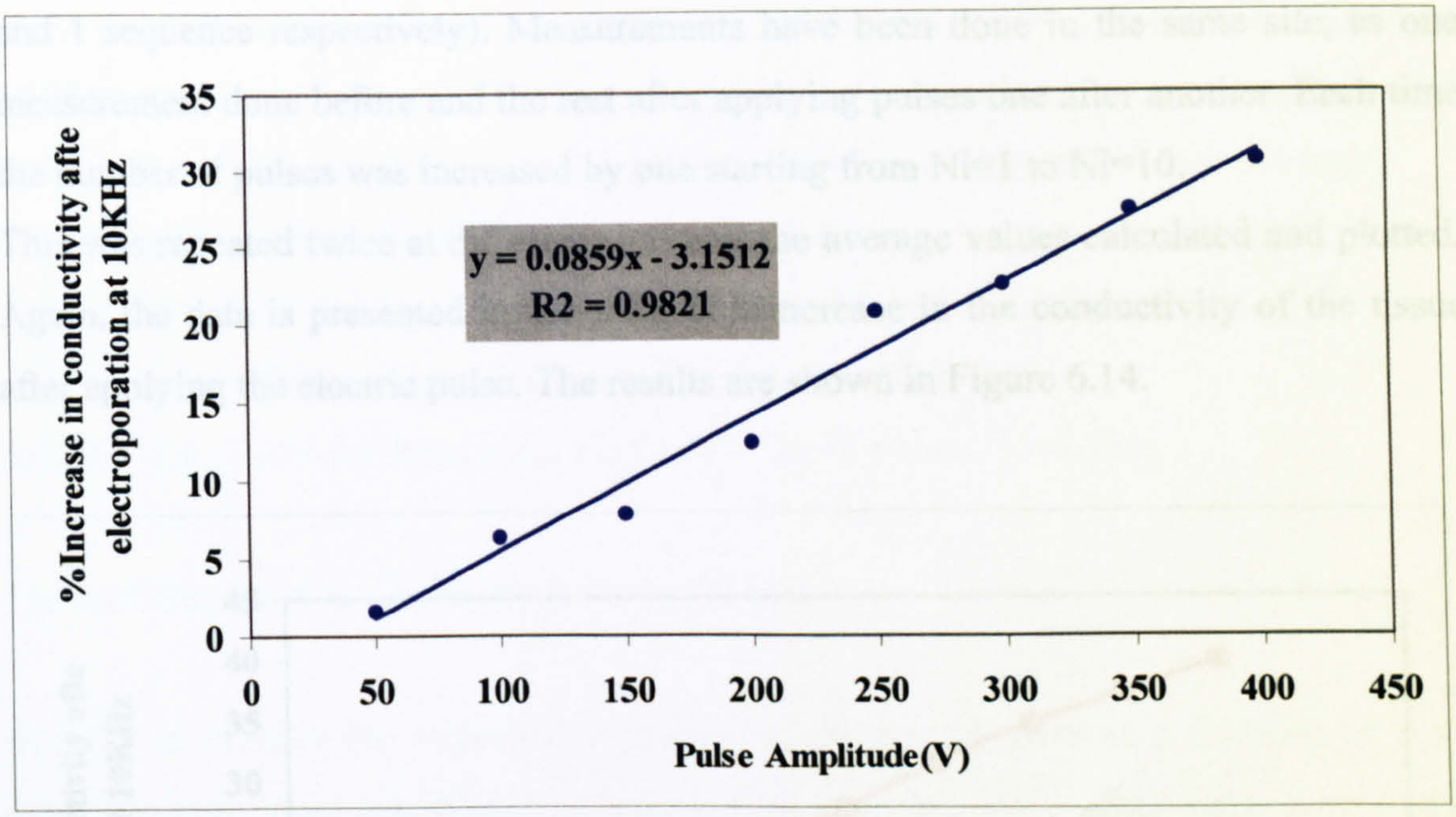

Figure 6.13. Average of the response of all pulses at each amplitude

The data in Figure 6.12 show significant scatter in the change in conductivity, despite the scatter one can observe a trend indicating a correlation between the pulse amplitude and the resulting effect. The trend with the pulse width is mush less defined.

Assuming that pulse duration does not add significantly to the effect of pulses of amplitudes above 50 V, one can average the response of all pulses of the same intensity. The results are given in Figures 6.13.

However, when the effect of all the pulses are pooled for each pulse intensity, a good correlation is observed (Figure 6.13).

Effect of pulse number

In this section the aim was to investigate the effect of increasing the number of pulses in the amount of electroporation produced in the tissue. To keep the number of variables down, pulse width, amplitude and number of sequences were kept constant (1ms, 400 V

and 1 sequence respectively). Measurements have been done in the same site, as one measurement done before and the rest after applying pulses one after another. Each time the number of pulses was increased by one starting from Ni=1 to Ni=10.
This was repeated twice at different sites and the average values calculated and plotted. Again, the data is presented in the form of %increase in the conductivity of the tissue after applying the electric pulse. The results are shown in Figure 6.14.

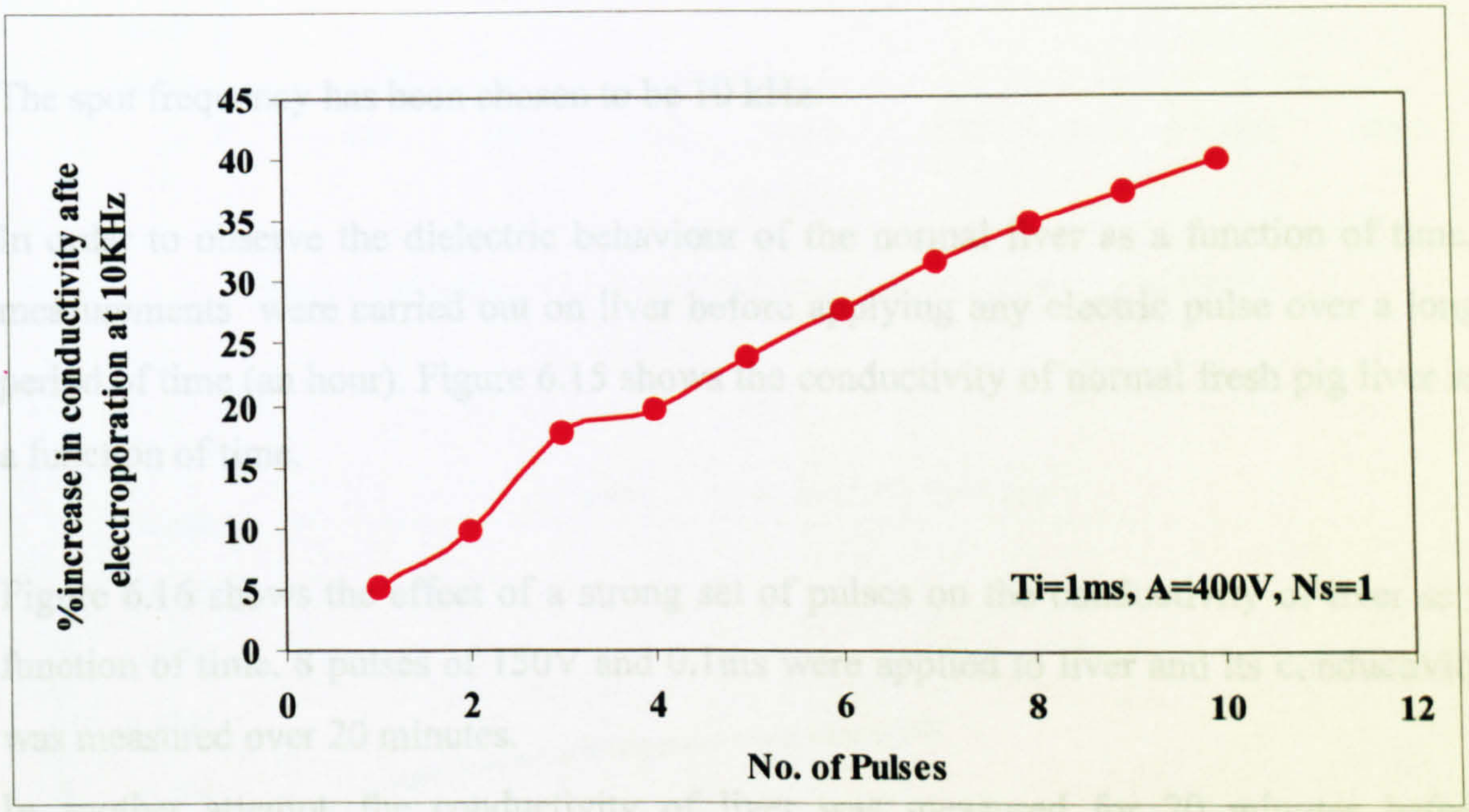

Figure 6.14 Effect of increasing the number of pulses in the electroporation of liver tissue (Average of 2 sets of measurements)

Liver electroporation as a function of time

An experimental set-up was developed for measurement at a spot frequency as a function of time. Ideally one would want to synchronise the start of the pulse train and the time series impedance measurement. The main problem was that the fastest impedance measurement is longer than the widest excitation pulse. However, the possible resealing effect may be recorded by measuring the dielectric properties of the tissue at a spot frequency over a period of time after applying the electric pulse.
In this part of the project, sheep liver was not available and pig liver was used instead.

In order to see any resealing or total damage effect, pulses of 0.1msec with amplitudes of 70 or 150V were chosen. The figures originated from personal communications with other partners in the project who work on the in-vivo electroporation of the tissues.
For reversible permeabilisation in-vivo the threshold is:
A=360V/cm (72 V for 2mm apart electrodes), Ni=8Pulses, Ti=0.1ms.
And for irreversible permeabilisation in vivo, the threshold is:
A=650V/cm (130V for 2mm apart electrodes), Ni=8 pulses, Ti=0.1ms.

The spot frequency has been chosen to be 10 kHz.

In order to observe the dielectric behaviour of the normal liver as a function of time, measurements were carried out on liver before applying any electric pulse over a long period of time (an hour). Figure 6.15 shows the conductivity of normal fresh pig liver as a function of time.

Figure 6.16 shows the effect of a strong set of pulses on the conductivity of liver as a function of time. 8 pulses of 150V and 0.1ms were applied to liver and its conductivity was measured over 20 minutes.
In another attempt, the conductivity of liver was measured for 20 minutes before applying any pulses. Then 2, 4, 6 and 8 pulses of 70V and 0.1ms were applied to the liver in 20-minute intervals. The result is shown in Figure 6.17.

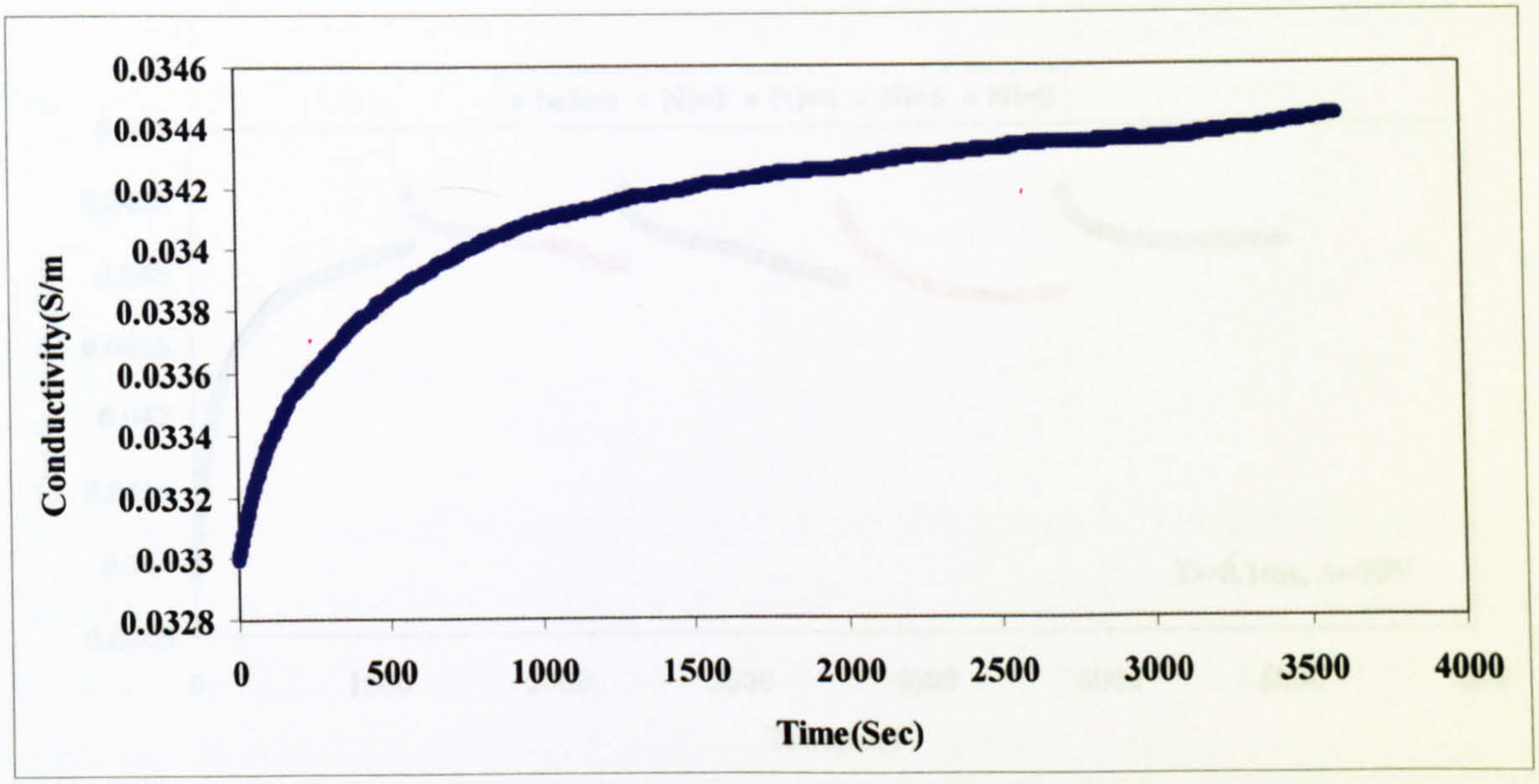

Figure 6.15 Conductivity of normal fresh pig liver as a function of time

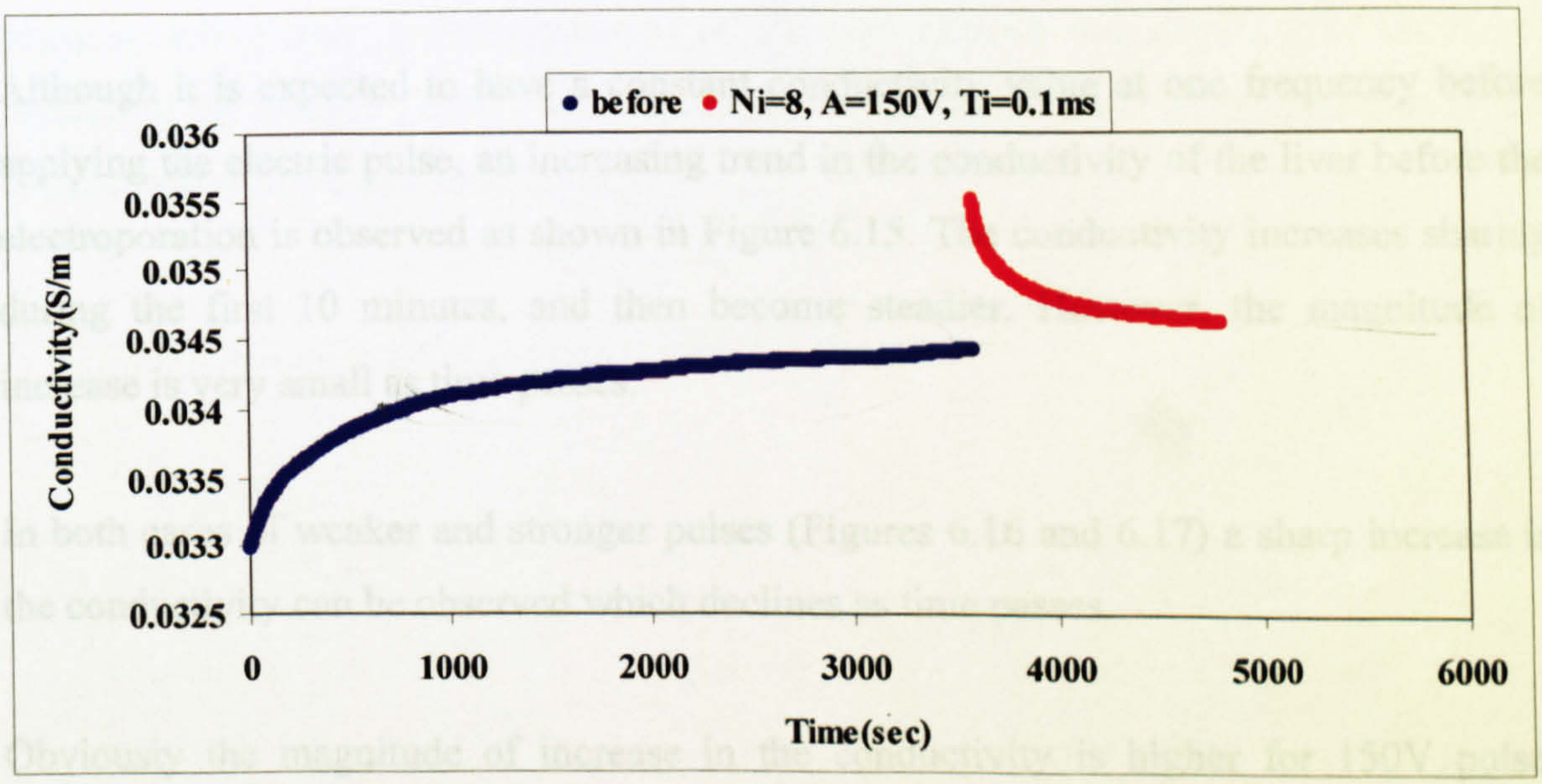

Figure 6.16 Conductivity of pig liver before and 20 minutes after applying electric pulses

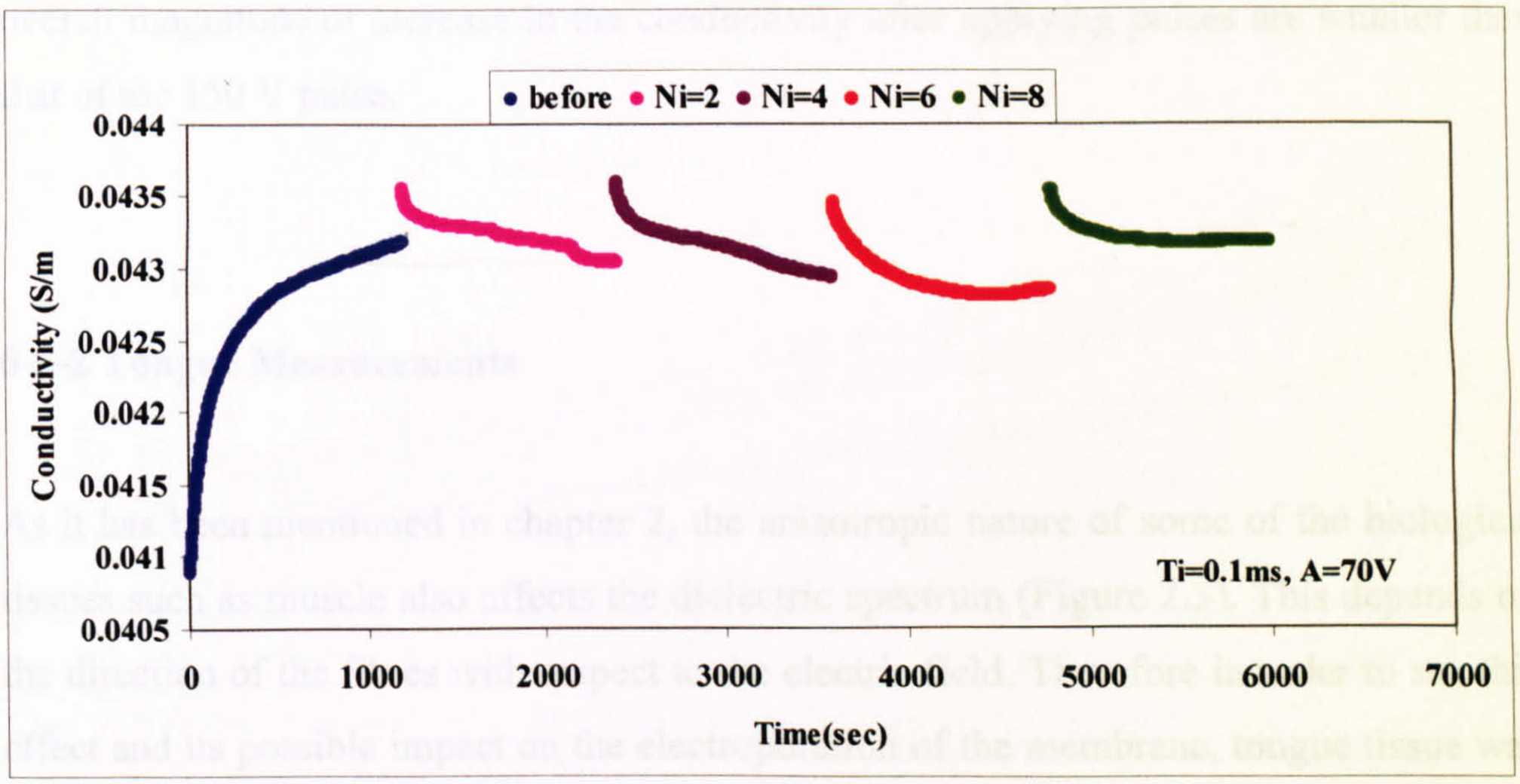

Figure 6.17 Conductivity of pig liver before and after applying electric pulses in 20 minute intervals

Although it is expected to have a constant conductivity value at one frequency before applying the electric pulse, an increasing trend in the conductivity of the liver before the electroporation is observed as shown in Figure 6.15. The conductivity increases sharply during the first 10 minutes, and then become steadier. However, the magnitude of increase is very small as time passes.

In both cases of weaker and stronger pulses (Figures 6.16 and 6.17) a sharp increase in the conductivity can be observed which declines as time passes.

Obviously the magnitude of increase in the conductivity is higher for 150V pulses (Figure 6.16). In the case of pulses of 150V, even after 20 minutes, the conductivity doesn't reach its original value (before electroporation).

In the case of 70V pulses (Figure 6.17) the same trend of increase and then gradual decrease in the conductivity can be observed after applying electric pulses. However, in this case different sets of pulses have been applied in 20 minutes intervals. The conductivity reaches its original value or less after 20 minutes in each case, but the

overall magnitude of increase in the conductivity after applying pulses are smaller than that of the 150 V pulse.

6-5-2 Tongue Measurements

As it has been mentioned in chapter 2, the anisotropic nature of some of the biological tissues such as muscle also affects the dielectric spectrum (Figure 2.5). This depends on the direction of the fibres with respect to the electric field. Therefore in order to see this effect and its possible impact on the electroporation of the membrane, tongue tissue was chosen to measure in two different directions, cross and parallel to the electric field. Figures 6.18a, and 6.18b show the distribution of sheep tongue conductivities before applying any electric pulse, measured at different sites in two direction of cross and parallel to the electric field. Figure 6.18c shows the comparison of the averages of the conductivities in the two directions.

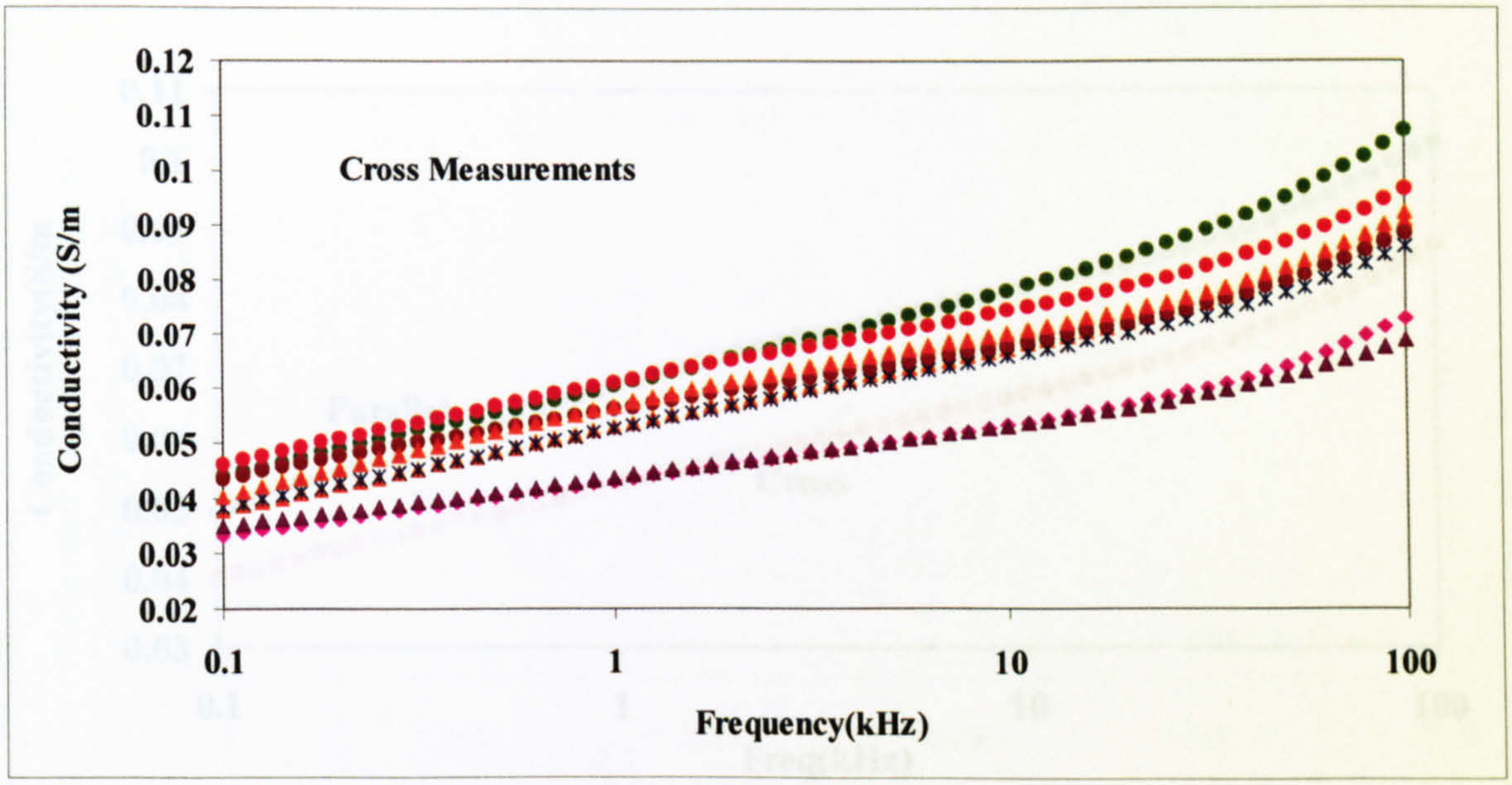

Figure 6.18a

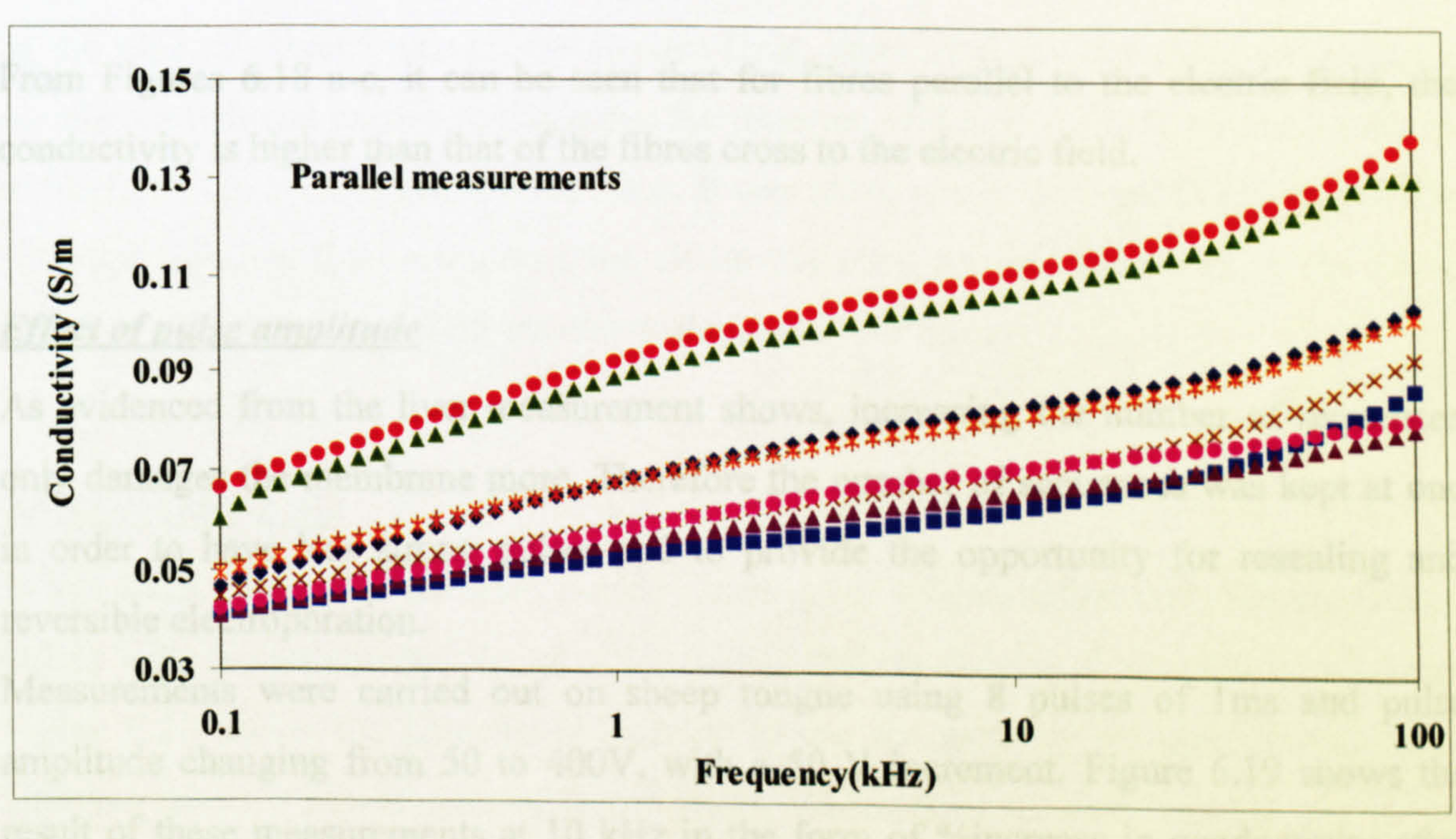

Figure 6.18b

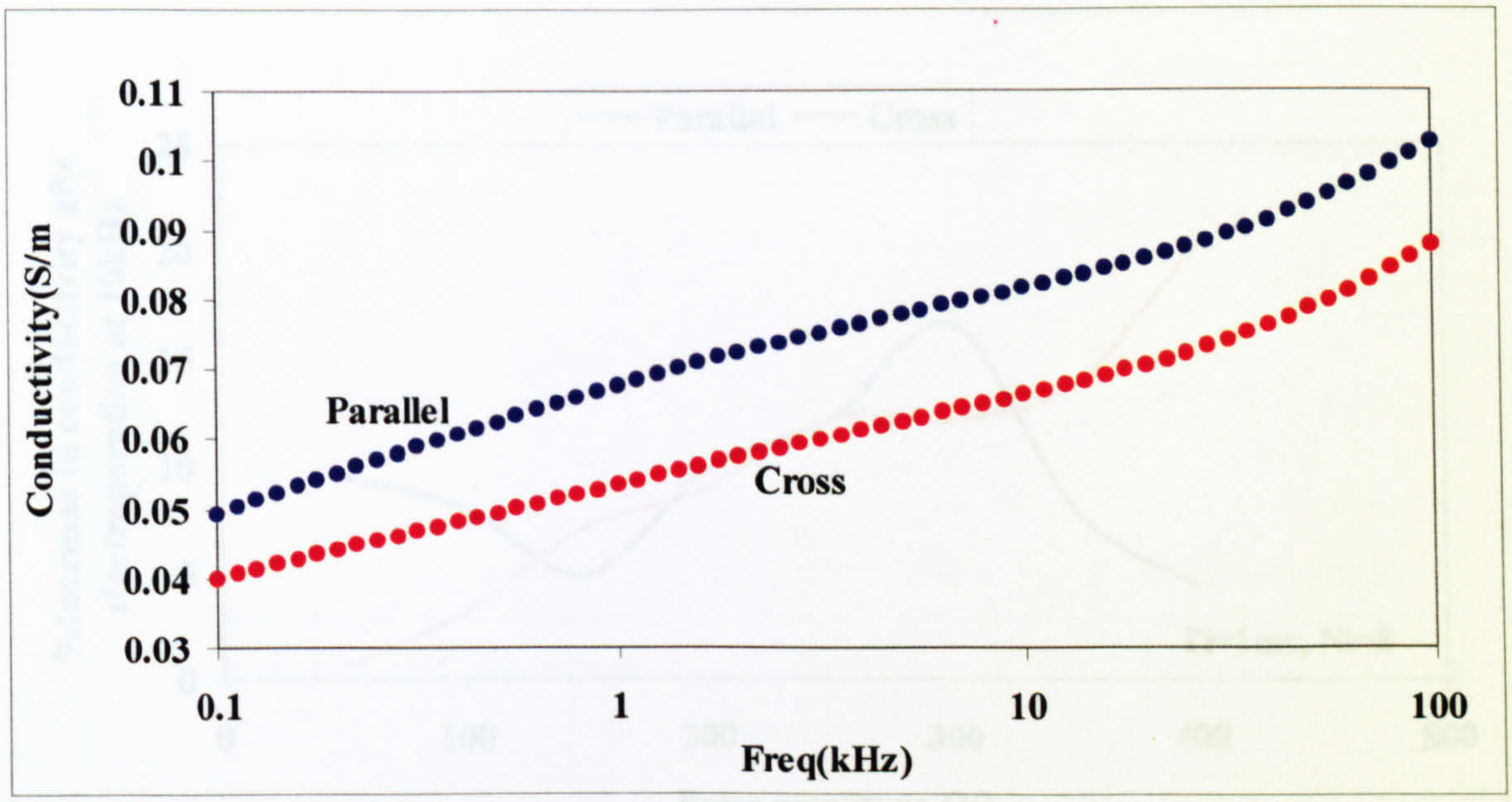

Figure 6.18c

Figure 6.18: Conductivity of sheep tongue before applying electric pulses **a:** cross to the electric field **b:** parallel to the electric field and **c:** comparison of the averages in the two directions

From Figures 6.18 a-c, it can be seen that for fibres parallel to the electric field, the conductivity is higher than that of the fibres cross to the electric field.

Effect of pulse amplitude

As evidenced from the liver measurement shows, increasing the number of sequences only damages the membrane more. Therefore the number of sequences was kept at one in order to have less strong pulses and to provide the opportunity for resealing and reversible electroporation.

Measurements were carried out on sheep tongue using 8 pulses of 1ms and pulse amplitude changing from 50 to 400V, with a 50 V increment. Figure 6.19 shows the result of these measurements at 10 kHz in the form of %increase in conductivity after electroporation. Measurements in both directions are presented.

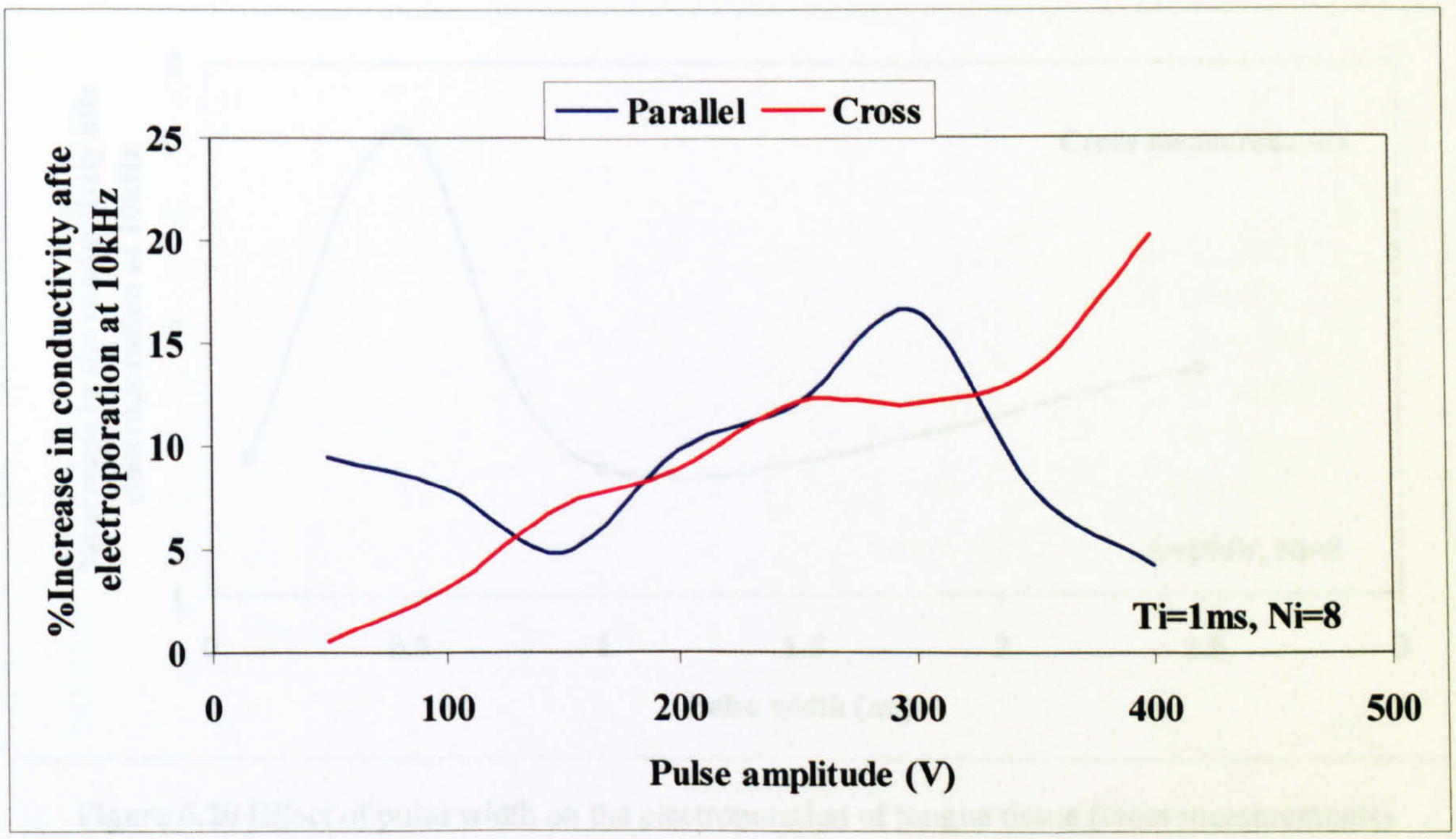

Figure 6.19 % Increases in the conductivity of sheep tongue at 10 kHz before and after pulse excitation as a function of pulse amplitude

In the case of fibres cross to the electric field, there is a general trend indicating a correlation between pulse amplitude and the resulting effect. In the case of fibres parallel to the field, the trend is not very obvious. It was always very difficult to get the parallel situation right, as this meant that the electrodes must be inserted cross to the fibres which could produce a certain amount of damage to the tissue

Effect of pulse width

In this stage, measurements were carried out on sheep tongue before and after applying 8 pulses with the amplitude kept at 100V and the width varying from of 0.1 to 2.5-ms. Figure 6.20 shows the percentage increase in the conductivity of sheep tongue after applying electric pulses with different width. Measurements were carried out in the direction cross to the electric field.

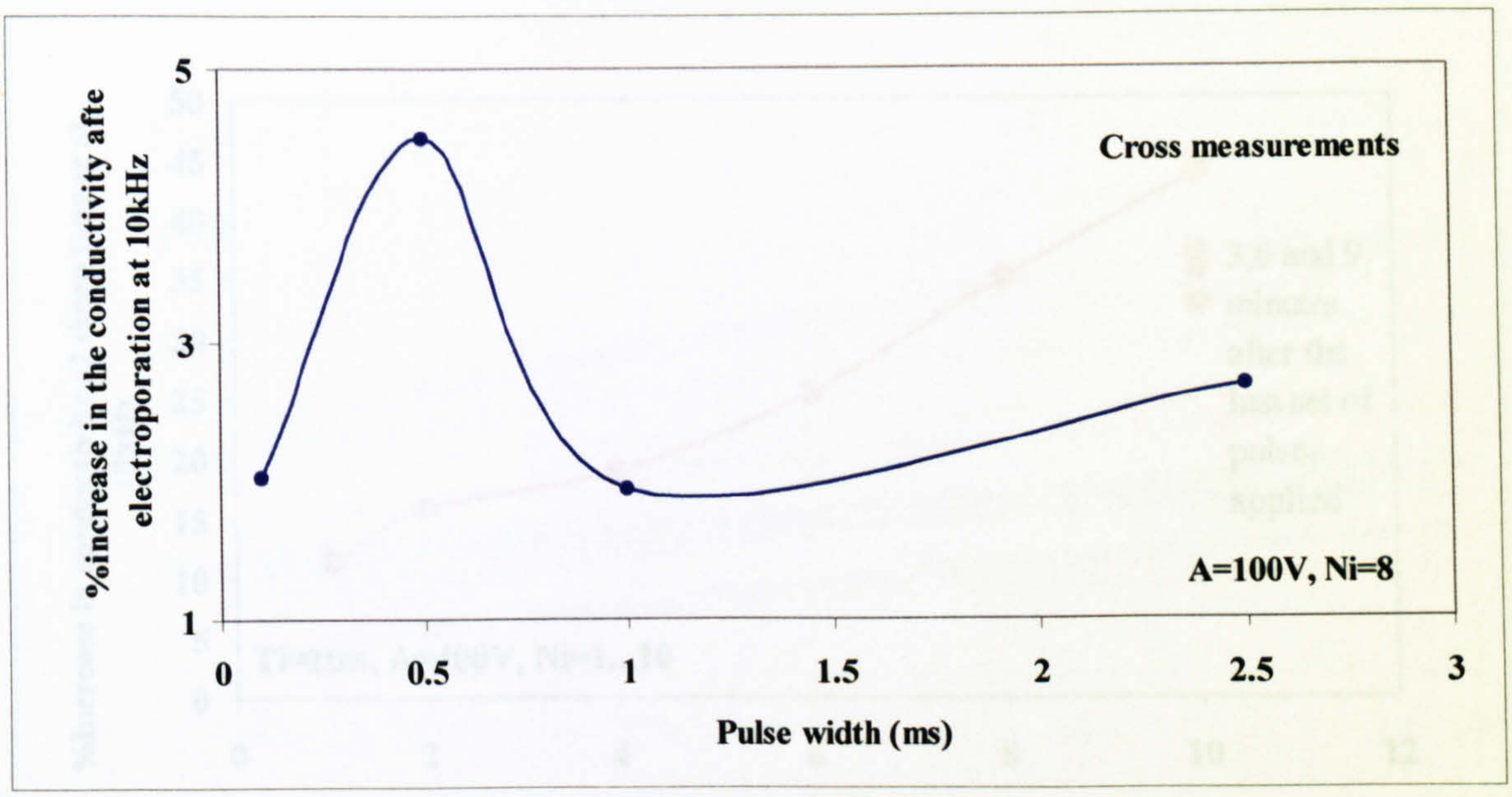

Figure 6.20 Effect of pulse width on the electroporation of tongue tissue (cross measurements)

Ignoring the 0.5ms pulse it can be seen from figure 6.20 that, there is a general increase in the amount of electroporation produced in the tongue tissue as the pulse width increases.

Effect of pulse number

The effect of increasing the number of pulses on the amount of electroporation produced in the tongue tissue is studied in this stage. To keep the number of variables down, pulse width, amplitude and number of sequences were constant (1ms, 400 V and 1 sequence). Measurements were done in the same site; one measurement done before applying any pulses and the rest after applying pulses one after another. Each time the number of pulses was increased by 2 steps starting from Ni=1 to Ni=10.

Again, the data is presented in the form of %increase in the conductivity of the tissue after applying the electric pulse. In three time intervals (3,6 and 9 minutes) after the last set of pulses (Ni=10) was applied, measurements were repeated to see any existing resealing effect. The results are shown in Figure 6.21.

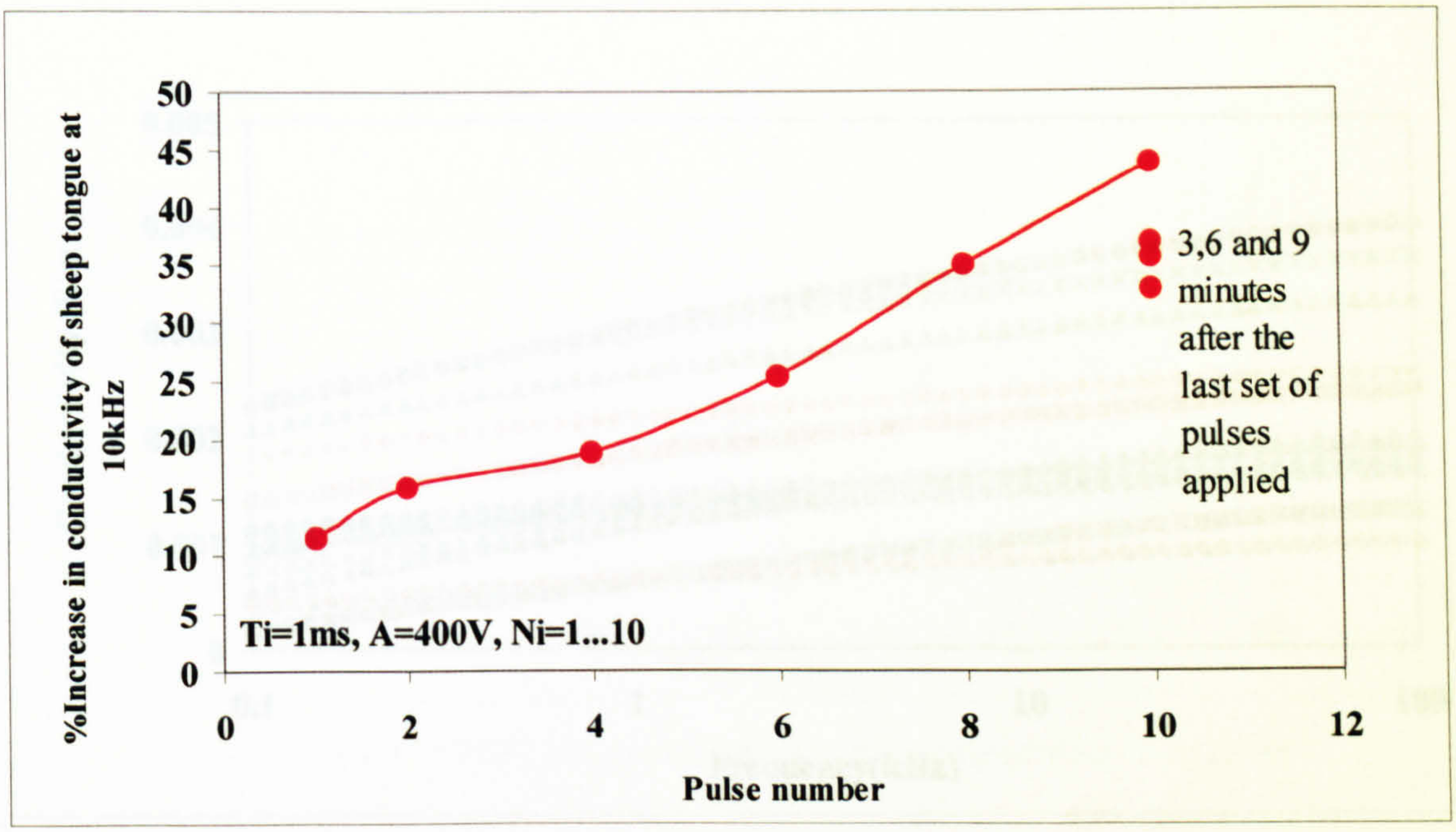

Figure 6.21 Effect of increasing the number of pulses in the electroporation of tongue tissue

After 3 minutes, the conductivity dropped to its value at half way between the 8 and 10 pulses and after 9 minutes, the conductivity was less than what it was before applying 8 pulses. No significant change was observed when more measurements were done after 9 minute. This could mean that some degree of closure had happened, but there had also been some permanent damage to the membrane, which could not be recovered.

6-5-3 Fat measurements

Similar to liver and tongue, because of the natural variability in tissue properties, the dielectric properties of fat were measured before and after each excitation. Figure 6.22 shows the variation in the conductivity of fat tissue measured at separate sites.

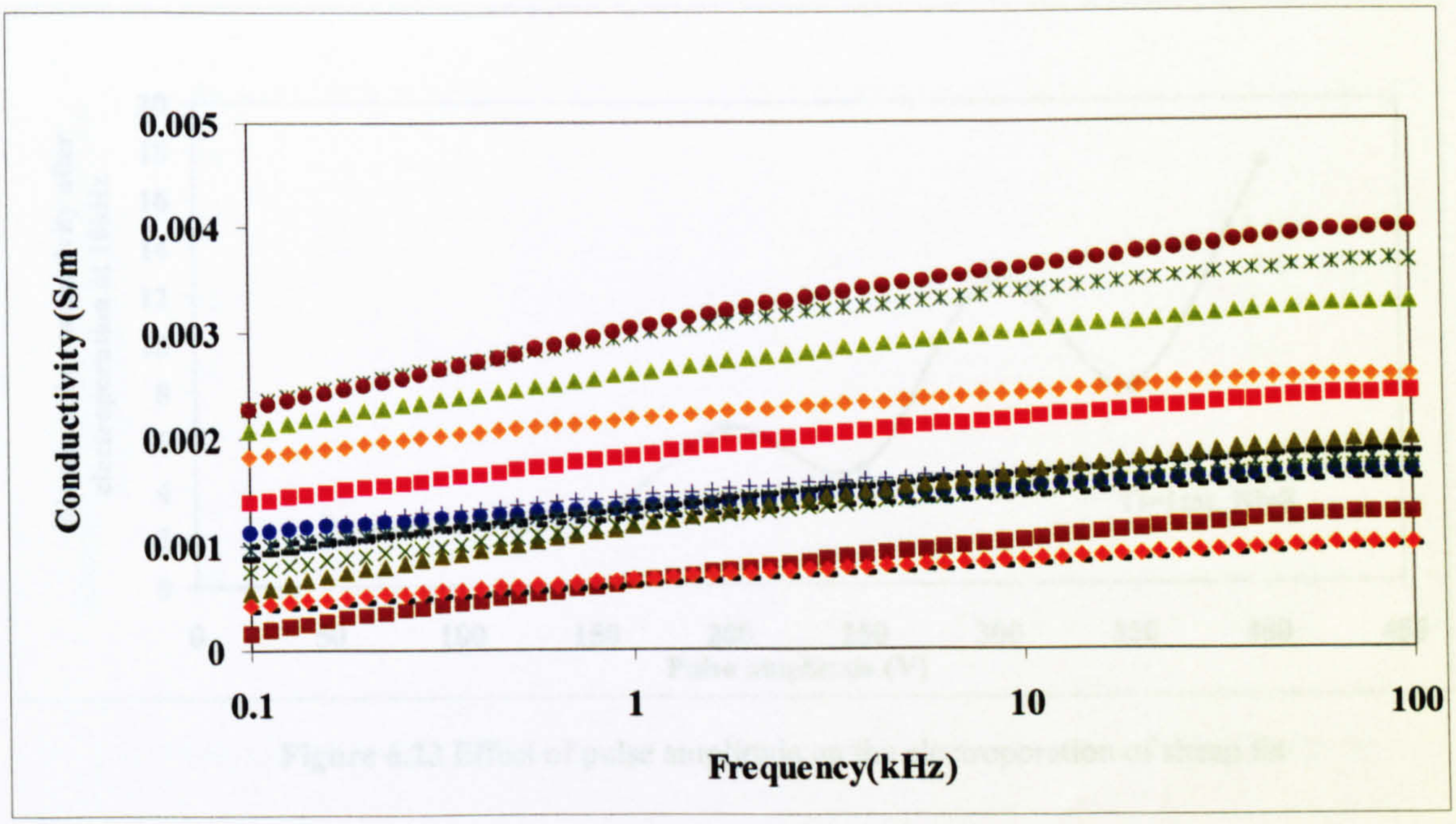

Figure 6.22 Distribution of conductivity of sheep fat before applying electric field

Effect of pulse amplitude

Since the effect of changing the pulse width was much less defined in the electroporation of liver and tongue tissue, it was decided to keep the pulse width constant and change only the pulse amplitude for the fat measurements. Measurements were carried out on sheep fat about 2 hours after the sacrifice of the animal, using 8 pulses of 0.1ms and the pulse amplitude changing from 50 to 400V, with a 50 V increment.

In order to increase the accuracy of results, measurements were repeated three times and the average of the three is presented in Figure 6.23.

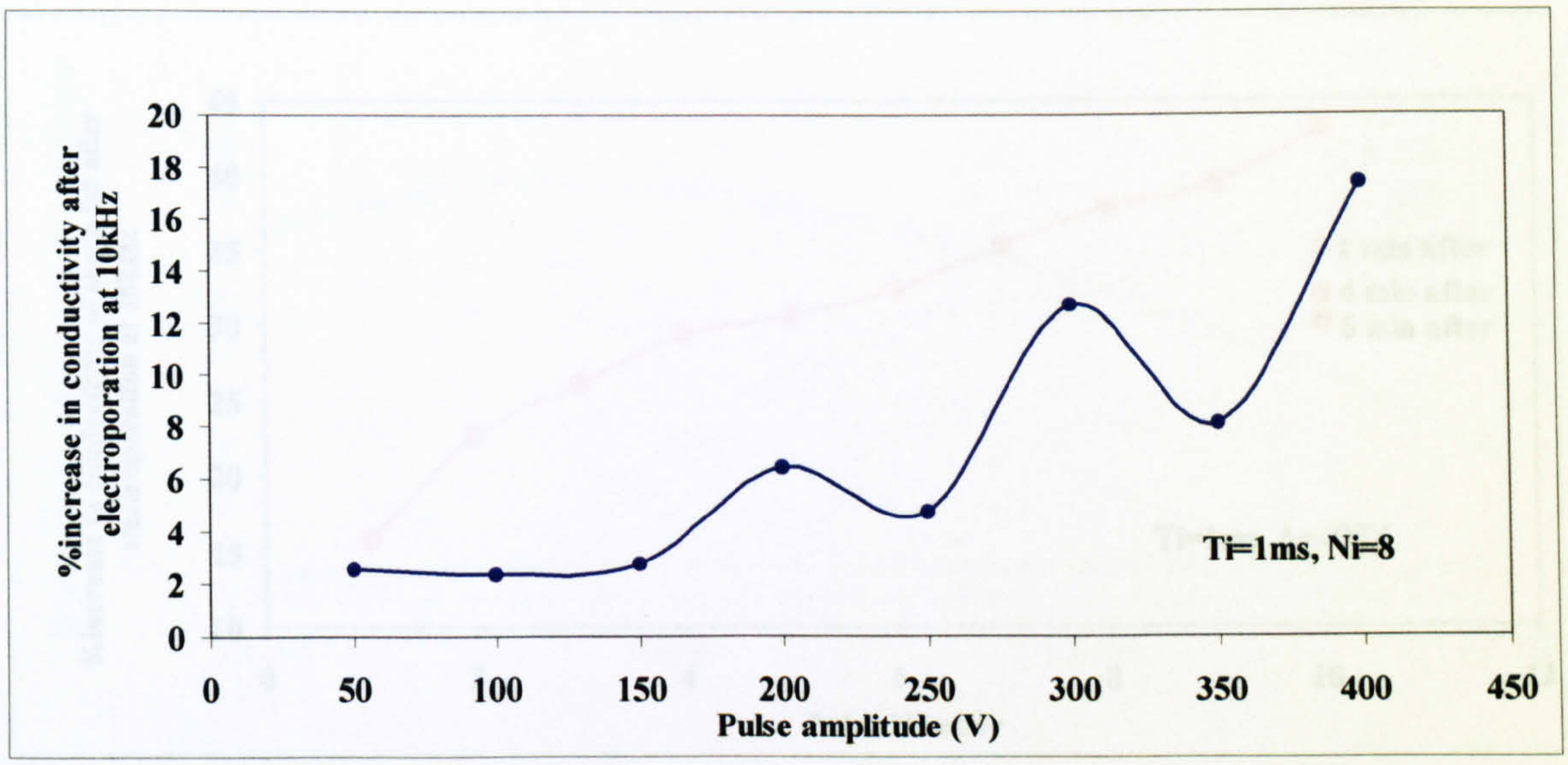

Figure 6.23 Effect of pulse amplitude on the electroporation of sheep fat

It can be seen from Figure 6.23 that although some scattering can be observed, there is an increasing trend in the conductivity of fat tissue as the pulse amplitude increases.

Effect of pulse number

In this section, the effect of increasing the number of pulses on the amount of electroporation produced in the fat tissue was studied. The pulse width, amplitude and number of sequences were kept constant (1ms, 400 V and 1 sequence). Measurements were carried out in the same site. One measurement done before applying any pulses and the rest after applying pulses one after another. Each time the number of pulses was increased by one step starting from Ni=1 to Ni=10. Two sets of measurements were carried out for more accurate results and the average values were calculated.

Again, the data are presented in the form of %increase in the conductivity of the tissue after applying the electric pulses. In three time intervals (1,4 and 6 minutes) after the last set of pulses (Ni=10) was applied, measurements were repeated to see any existing resealing effect. The results are shown in Figure 6.24.

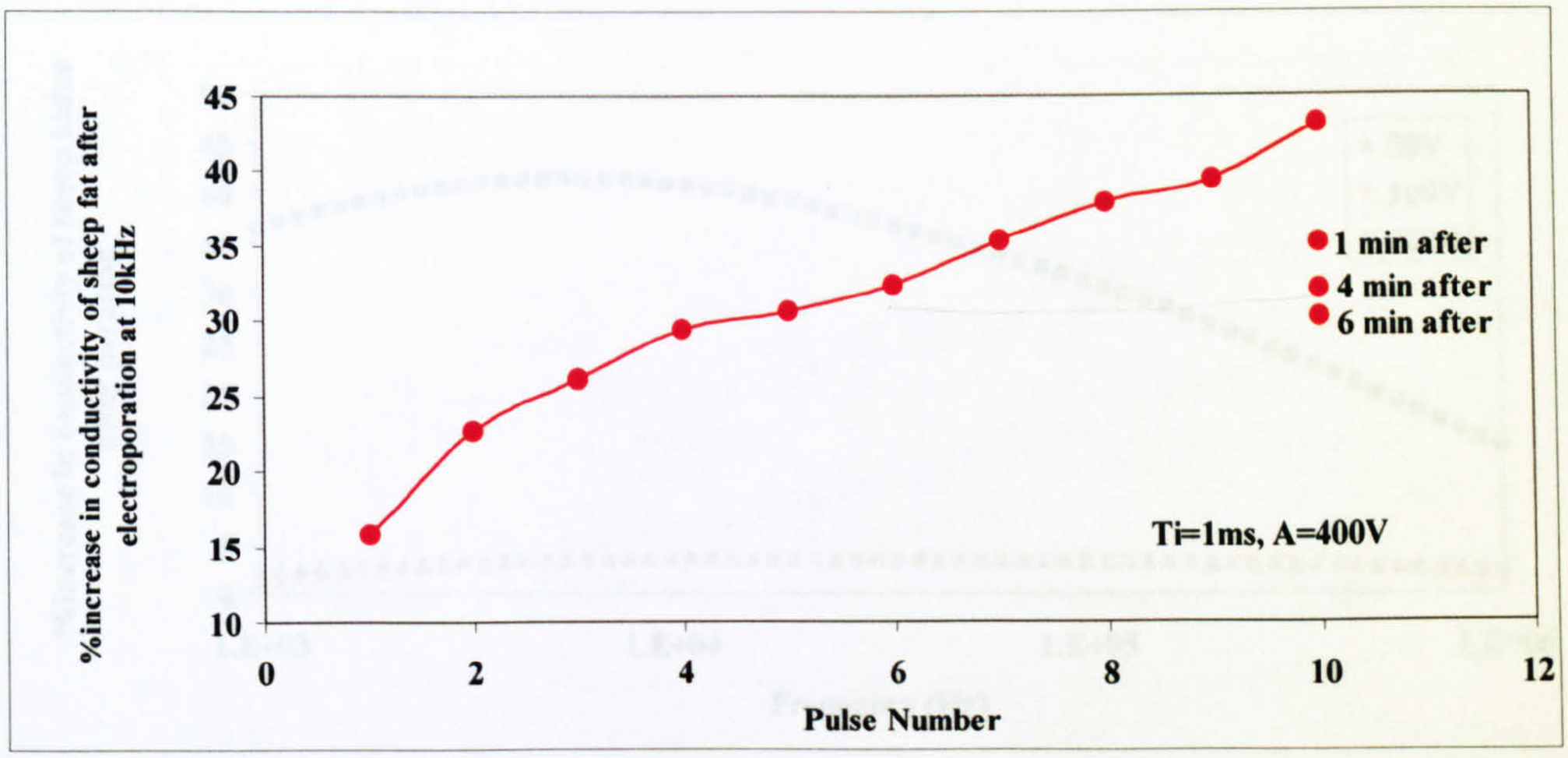

Figure 6.24 Effect of increasing the pulse number on the electroporation of sheep fat

After 1 minute, the conductivity dropped to less than what it was before applying the last pulse. At 4 minutes after the last pulse, the conductivity was less than what it was before applying 6 pulses. Finally after 6 minutes the conductivity dropped to a value less than what it was before applying 5 pulses. No significant change was observed when more measurements done after 6 minutes. This could mean that some degree of closure had happened, but there was also some permanent damage to the membrane, which could not be recovered.

6-5-4 Kidney measurements

Three sets of 8 pulses of 2.5ms and 50, 100 and 400 V respectively were applied to sheep kidney. Figure 6.25 shows the result. Also, Figures 6.26a and 6.26b show the dielectric spectrum of sheep kidney before and after applying 8 pulses of 2.5ms and 400V.

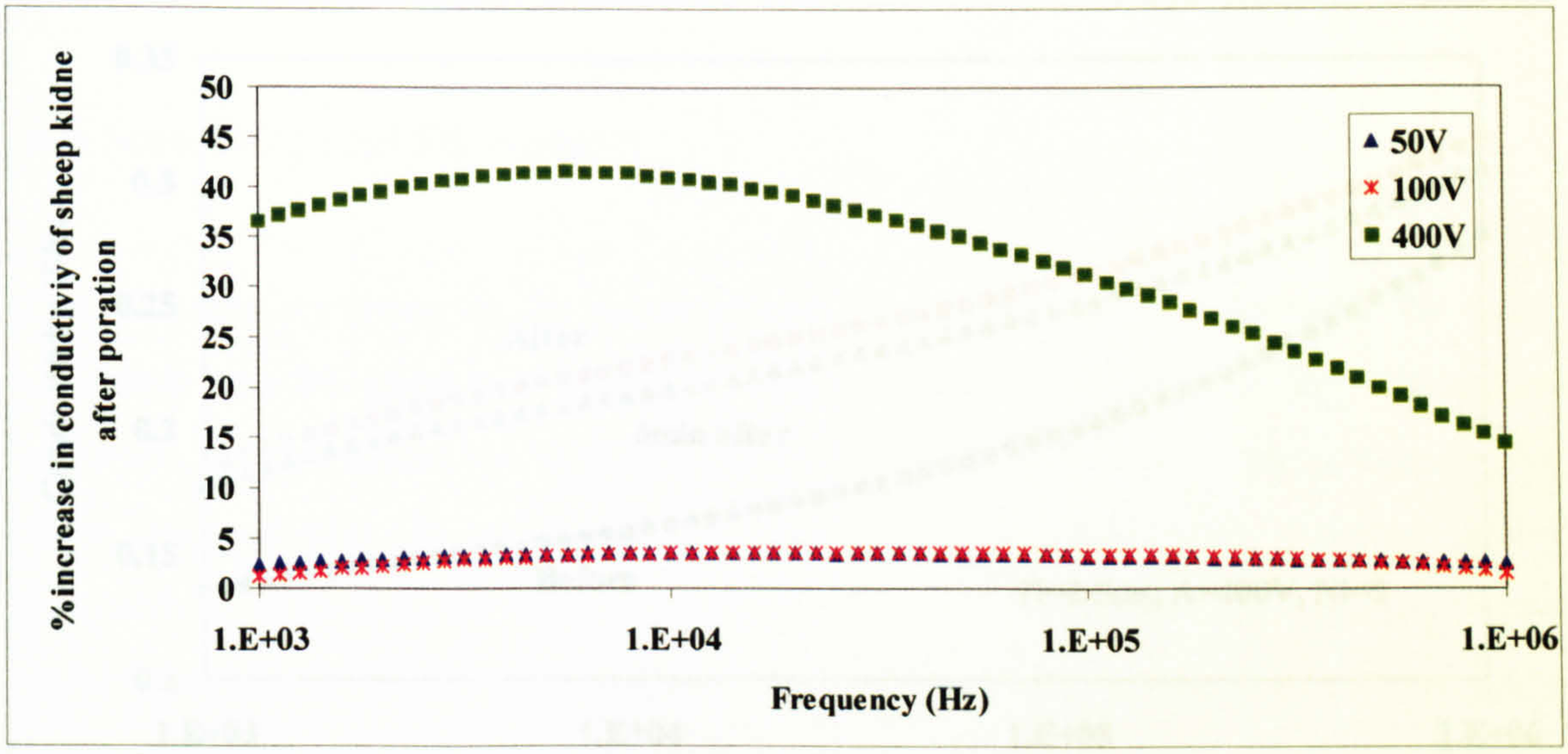

Figure 6.25 %Increase in the conductivity of sheep kidney after applying pulses of different amplitude

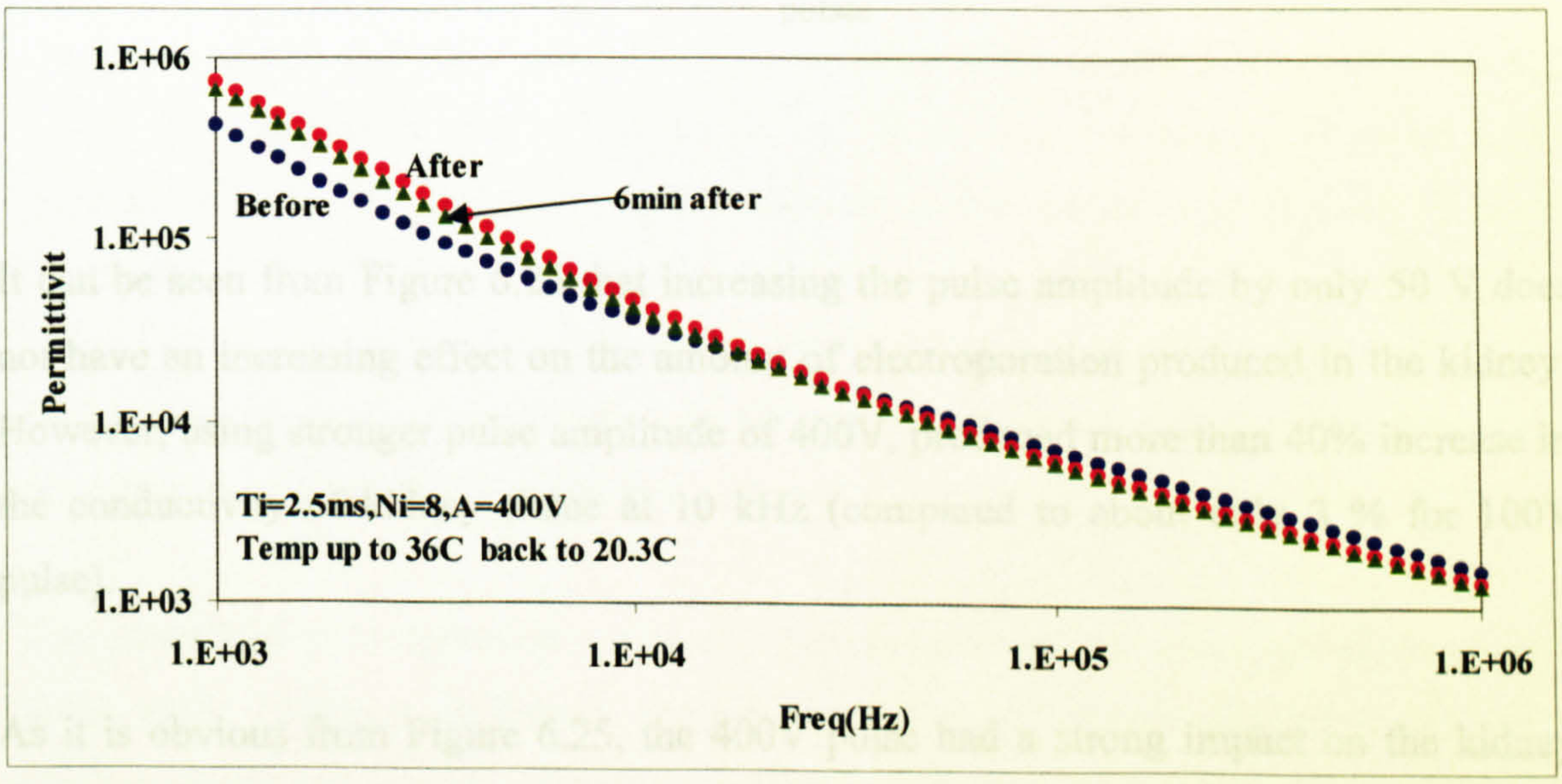

Figure 6.26a

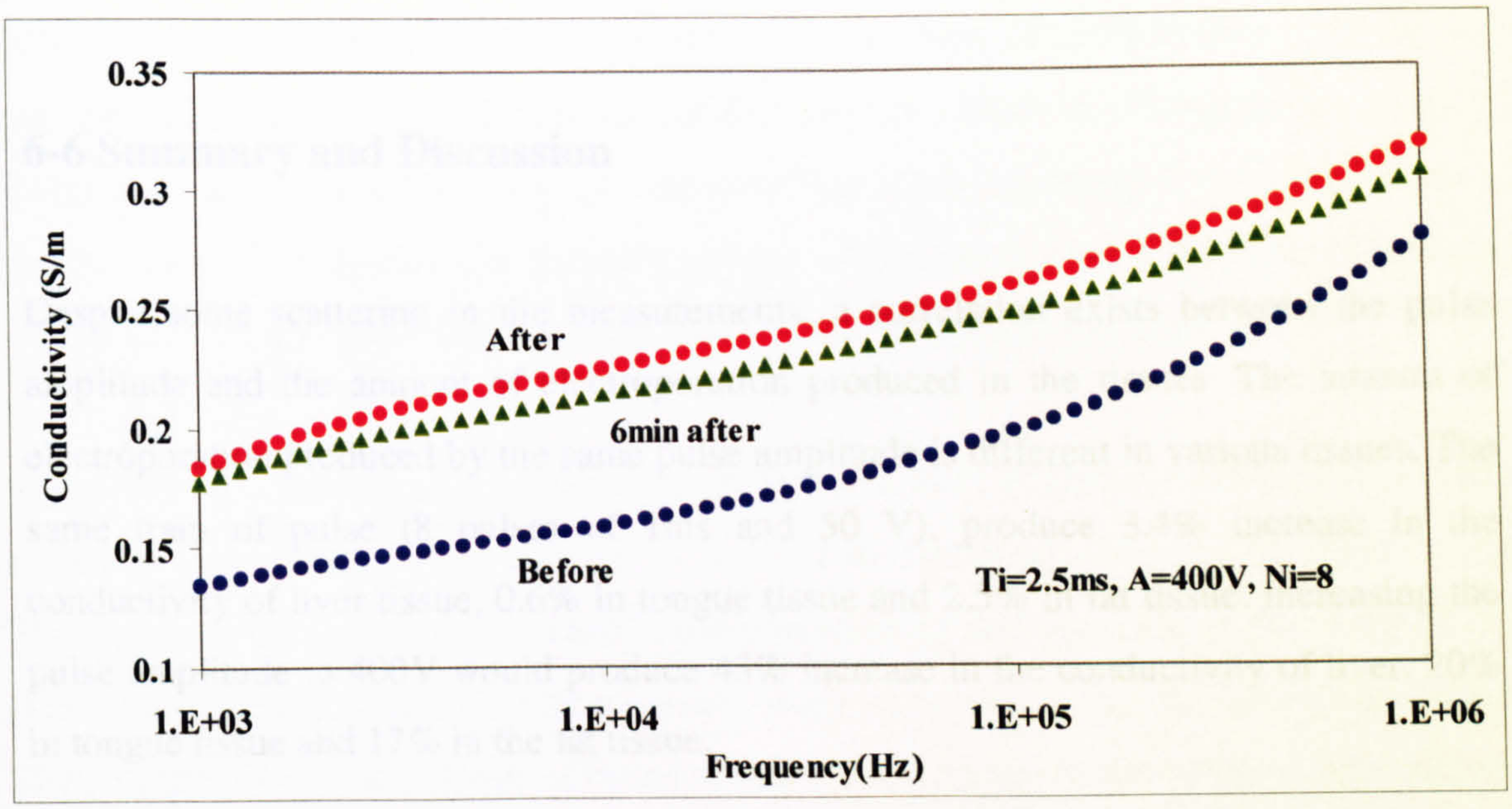

Figure 6.26b

Figure 6.26: a Permittivity **b** Conductivity of sheep kidney before and after applying electric pulses

It can be seen from Figure 6.25 that increasing the pulse amplitude by only 50 V does not have an increasing effect on the amount of electroporation produced in the kidney. However, using stronger pulse amplitude of 400V, produced more than 40% increase in the conductivity of kidney tissue at 10 kHz (compared to about only 3 % for 100V pulse).

As it is obvious from Figure 6.25, the 400V pulse had a strong impact on the kidney tissue. This can be seen clearly in Figures 6.26a and 6.26b, that show the dielectric spectrum of sheep kidney before and after applying 8 pulses of 2.5ms and 400V. A decrease in the β-dispersion and an increase in the α-dispersion can be observed.

The increase in the conductivity immediately after applying electric pulses is due partly to the considerable rise in temperature. After 6 minutes the temperature was back to the value before applying electric pulses and the change in value of conductivity indicate a permanent change in tissue.

6-6 Summary and Discussion

Despite some scattering in the measurements, a correlation exists between the pulse amplitude and the amount of electroporation produced in the tissues. The amount of electroporation produced by the same pulse amplitude is different in various tissues. The same train of pulse (8 pulses of 1ms and 50 V), produce 3.4% increase in the conductivity of liver tissue, 0.6% in tongue tissue and 2.5% in fat tissue. Increasing the pulse amplitude to 400V would produce 43% increase in the conductivity of liver, 20% in tongue tissue and 17% in the fat tissue.

The same pulses will produce more electroporation when applied in the order of increasing the number of pulses.
One pulse of 1ms and 400V, produces 5.2% increase in the conductivity of liver tissue, 11.4% in tongue tissue and 16% in fat tissue. Increasing the number of pulses to 8 gradually by one step will produce 35% increase in the conductivity of liver, 35% in tongue and 38% in fat tissue.

Different amounts of electroporation can be achieved when pulses are applied in one go or with gradual increase in the number.

The amount of electroporation produced in tissues showed no strong correlation with pulse width. However, this needs more investigation as previous studies for in vivo electroporation of muscle tissues and cell permeabilisation [9,10] reported that increasing the pulse duration will tend to increase the degree of perturbation of the affected membrane area.

All the tissues showed some degree of resealing depending on the strength of the pulses applied. In the case of tongue tissue the conductivity value dropped by 11% at 9 minutes after applying a train of pulses of the same amplitude and width with increasing order of number of pulses. In the same situation for fat, the conductivity dropped 13% at 6minutes after applying the last pulse.

When measuring the conductivity of liver as a function of time before applying any electric pulse, a gradual increase in conductivity is observed. Although the scale of increase in the conductivity is very small, but the trend continues even after 1 hour of measurement. This increase in the conductivity of normal liver as a function of time can be due to some chemical reactions between the electrodes and the liver.

In the case of measuring the conductivity before and after applying electric pulses over a period of time, it can not be concluded whether an electroporation has occurred or not. This is due to the very little increase in the conductivity and the scale of the changes. However, comparing the two sets of results one can conclude that for the weaker pulses of 70V there is a general trend of increase and then decrease in the value of conductivity while for the stronger pulse (150V), the conductivity increases and doesn't come back to the original value.

In the case of tongue measurements, it can be seen that for fibres parallel to the electric field, the conductivity is higher than that of the fibres cross to the electric field. One interpretation would be that this is due to the amount of polarisation occurring in the cellular membrane and the strength of the β dispersion in each case. The more polarisation occurs when the direction of the fibres are cross to that of the electric field, therefore causing stronger β dispersion and lower conductivity compared to the parallel case.

However, the amount of difference in the conductivity of the sheep tongue in two directions is very small, and this could be due to the natural variation of the dielectric properties of biological tissue. It was very difficult to get exactly parallel or cross directions and the tongue fibres were very delicate. Using the 2mm parallel plate probes could cause such disturbance in the tissue that the difference in the two directions could not be spotted very well.

In general, from these results, it is not possible to conclude that the direction of the tissue in respect to the electric field has any effect on the amount of electroporation produced in the tissue. However, it may be easier to detect the effect (if any exists) by

conducting measurements on harder types of muscle such as calf muscle (this was planned but the foot and mouth epidemic in UK prevented the plan at the time).

It was also noted that the frequency region where the electroporation effects appear at a maximum is around 10 kHz.

References for chapter 6

[1] Weaver J C, 1995, "Electroporation in cells and tissues: A biophysical phenomenon due to electromagnetic fields", *Radio Science,* **30** 205-221.

[2] Weaver J C and Chizmadzhev Yu A, 1996, "Theory of electroporation: A review", *Bioelectrochemistry and Bioenergetic* **41** 135-160.

[3] Neumann E, 2000, "Electrooptical and conductometrical relaxation techniques and the crossmembrane transport of genetic polyelectrodes", Proceedings of 3rd International Conference on Bioelectromagnetism, Oct 2000, Bled, Slovenia.

[4] Sale A J H and Hamilton W A, 1968, " Effects of high electric fields on micro-organisms, III Lysis of erythrocytes and protoplasts", *Biochim. Biophys. Acta* **163** 37-43.

[5] Neumann E, 1989 The relaxation hysteresis of membrane electroporation in : "Electroporation and Electrofusion in Cell Biology", Neumann E, Sowers A and Jordan C, Plenum Press , New York..

[6] Neumann E, 1988, "The electroporation hysteresis", *Ferroelectrics.* **86** 325-333

[7] Neumann E, Schaefer-Ridder M, Wang Y and Hofschneider P H, 1982, "Gene transfer into mouse lyoma cells by electroporation in high electric fields", *EMBO J.* **1** 841-845.

[8] Miklavcic D, Beravs K, Semrov D, Cemazar M, Demsar F and Sersa G, 1998, "The importance of electric field distribution for effective in vivo electroporation of tissues", *Biophysical Journal*, **74** 2152-2158.

[9] Gehl J, Sorensen T H, Nielsen K, Raskmark P, Nielsen S L, Skovsgaard T and Mir

L M, 1999, " In vivo electroporation of skeletal muscle: threshold, efficacy and relation to electric field distribution", *Biochem. Biophys. Acta.* **1428** 233-240.

[10] Gehl J and Mir L, 1999, "Determination of optimal parameters for in vivo gene transfer by electroporation, using a rapid in vivo test for cell permeabilisation", *Biochem.Biophys. Research Communications.* **261** 377-380.

Chapter 7- Conclusion and Future work

In each of the three main projects presented in this thesis, various aspects of the interaction mechanisms of electromagnetic radiation with biological tissues were studied in details.

At the fundamental level, the relationship between the tissue water and the dielectric properties was studied. The parameters of the γ dispersion were quantified and their correlation with the water content of the tissue was established. Also, the effect of general growth procedures on the dielectric properties of different tissues was studied. The results showed a correlation between the tissue water and composition and the dielectric properties of the tissues.

Also at the fundamental level, the effect of physiological changes on the dielectric properties of tissues was studied in the site of cellular membrane. The variation in the β dispersion due to the changes in the conditions of cellular membrane was demonstrated. Evidences of increase in the conductivity of tissues due to the applied electric pulses were also observed.

At the applied level, the use of dielectric spectroscopy in order to obtain information about the composition of biological material was investigated. The fact considered was that the spectrum of dielectric properties over a two to three decade range of frequencies can tell us something unique about the material. The dielectric spectrum of foodstuff above 1GHz were considered, and the dielectric parameters correlate with water content. This provides a means of performing some compositional analysis *(γ- dispersion).*

This chapter contains the conclusions of the works carried out throughout this project. It also contains suggestions for possible future work, which could be done based on the results obtained here.

The conclusions are presented in the order in which the work is presented in this thesis.

The outcome of the dielectric measurements of standard liquids in chapter 3 indicated that the techniques used throughout this project are accurate and the produced results are within approximately 1-2% agreement with literature data.
The reproducibility of the measurements was typically better than 1% at most frequencies for all the standard liquids used.

The aim of the first main project mentioned in chapter 4, was to find the extent in which dielectric spectroscopy can be used in the determination of added water and other composition variables in pork products. The results presented in this chapter showed that using the combination of dielectric spectroscopy and principal component analysis and regression can predict the composition of pork products. The main interest in this study however was added water, which it has been shown that can be determined to within approximately ±4% for completely blind samples. This value should be seen in the context of legislation, which requires that products be labelled to indicate the added water content to the nearest 5%. Including the protein content in the calibration data improved the results of predicting the calculated added water. The reason that including protein improves the calibration is that the major factor in the calculation of added water is the nitrogen content.
It is also concluded that the accuracy of the prediction of added water depends on the accuracy of its calculation when using chemical analysis data.
Although this project showed that the combination of dielectric spectroscopy and Principal Component Analysis and Regression is able to predict the amount of added water and other components, the main assumption was that the model is linear. This is a simplistic assumption and it is suggested that a future idea of work would be to use other analytical approaches which can make a non-linear model if required such as Artificial Neural Network.

The interest behind the project presented in chapter 5 originated from the question of to what extent the variation in the dielectric properties needs to be taken into consideration in the assessment of the exposure of children and adult to electromagnetic radiation. However, another purpose of the study was to provide a database of the dielectric

properties of rodent tissue as a function of age. The results obtained in this project indicated that among head tissues, brain, skin and skull exhibit the largest decrease in the permittivity and conductivity as the animal gets older, while the corresponding changes for the abdominal tissues are less prominent. Skull has the highest percentage decrease in the conductivity (42.45%) at 900MHz when the animal ages from 30 to 70 days old. This value is well above the variability in the measurement of the conductivity of skull at the same frequency (7.67%). The results of the fitting procedure show that the Cole-Cole expression is a good description of the dielectric behaviour of tissue water.

The dielectric properties of each tissue at microwave frequencies can be calculated from the parameters in Table 5.6 and used for the provision of dosimetry in lifetime exposure animal experiments. It is also interesting to anticipate what the projection of these results would mean for the assessment of the exposure of children to electromagnetic radiation compared to adults.

To incorporate the dielectric results obtained in this project in numerical studies and to compare the exposure assessment for a young and adult rat is one of the future pieces of work planned. It is also intended to expand the measurements to the medium frequency range (~300kHz - 300MHz) of the spectrum where the site of β dispersion is located.

The results presented in chapter 6 show a general variation in the dielectric properties of all studied tissues due to the inhomogeneous nature of the tissues. Although the scale of variation is very small, any changes in the dielectric properties occurring due to the applied electric pulses must be considered if larger than the natural variation in dielectric properties. However, since this study was comparative, natural variation does not effect the results.

Generally one can conclude that despite some scattering in the measurements, a correlation exists between the pulse amplitude and the amount of electroporation produced in the tissues. It is also true to say that the amount of electroporation produced by the same pulse amplitude is different in various tissues.

Another general conclusion from this project is that different amounts of electroporation can be achieved when pulses are applied in one go or with gradual increase in the number.

One more general conclusion could be that increasing the field strength tends to increase the area of the membrane, which is permeabilised.
No strong correlation was observed between the amount of electroporation produced in tissues and the pulse width. However, this needs more investigation to examine the suggestions by previous work that increasing the pulse duration tends to increase the degree of perturbation of the affected membrane area.

General biophysical conclusions can be drawn from the dielectric measurements of tongue tissue at different directions to the electric field. For fibres parallel to the electric field, the conductivity is higher than that of fibres cross to the electric field. This is due to the fact that more polarisation occurs when the direction of the fibres is cross to that of the electric field, therefore causing stronger β dispersion and lower conductivity compared to the parallel case. However, from the results obtained in this project one can not conclude that the direction of the tissue in respect to the electric field has any effect on the amount of electroporation produced in the tissue. It may be easier to detect the effect (if any exists) by doing measurements on other types of tissues with fibres in different directions.

The data obtained in this project for different pulse parameters can be used in future experiments in order to obtain more precise values of the pulse amplitude and number that would produce total reversible or irreversible effects on the membrane.

The results of investigation about dielectric behaviour of biological tissues at various conditions presented in this thesis provides useful information for better understanding of the interaction mechanisms of electromagnetic radiation and biological tissues.
These data can be used both in dosimetry studies and also as a base for future research in similar fields.

APPENDIX 1

Calculation of added water in meat products:

Proximate analysis can be carried out on meat samples for total water content (oven drying), Fat (Werner Schmidt), Ash, Protein (Total Nitrogen by Kjeldahl), and salt (NaCl). After adjustment for additives the added water content is calculated from these values assuming a Nitrogen factor of 3.5 (i.e. 3.5 % of untreated pork comprises protein nitrogen).

% Added Water = 100 – (%Meat Content + % Salt + % Additives)

Additives can be carbohydrates and nitrate / nitrites etc, although in the case of added nitrates & nitrites the level of addition will generally not make any significant differences to the % Added Water.

$$\% \text{ Meat Content} = \frac{\% \text{ Nitrogen due to meat} \times 100}{\text{Nitrogen Factor}} + \% \text{ Fat from the meat}$$

% Total Nitrogen = % Protein/6.25

% Carbohydrate = 100 – (%Ash + % Fat + % Moisture + % Protein)

% Nitrogen due to Carbohydrate = % Carbohydrate x 0.02

The factor 0.02 is derived by assuming that any carbohydrate has a nitrogen level of 2 percent.

% Nitrogen due to meat = % Total Nitrogen - % carbohydrate nitrogen

Nitrogen Factor = 3.5 (Pork)